Luís Miguel Fortuna Rodrigues Martelo

Spectral and Transport Properties of Low-Dimensional Mott-Hubbard Insulators and Electronic Conductors

Thesis associated with the Ph.D. Project entitled "Relation between magnetic effects and the electron-electron interaction in low-dimensional systems"

A dissertion submitted for the degree of Ph.D.
in Physics (Solid State)
at the University of Évora

Évora - 1999

To my parents, Rosa and Luís.

22/XII/99

Contents

Preface

Part of the work presented in this thesis was carried out at the Physics Department of the University of Évora (Portugal), under the supervision of Professor José Carmelo. The first year of the Ph.D. studies was spent at the *Institut de Physique Théorique of the Universty of Fribourg* (Switzerland), under the supervision of Professor Dionys Baeriswyl. I would like to thank both of them for their constant help and for having contributed in a very significant way to my insight and intuition in Physics. With both of them I have learned many important tools in theoretical physics. I also would like to express my sincere gratitude for the hospitality of the *Institut de Physique Théorique-Universté de Fribourg.*

I aknowledge also Professor Michael Dzierzawa, who introduced me to the Variational Monte Carlo techniques, during my stay at the University of Fribourg, and to Professor Pedro Sacramento for having produced and provided Figs. (2.2)-(2.5) and (5.2)-(5.8) and for useful physical discussions. I also thank Professor João Lopes dos Santos for many stimulating discussions.

I thank also the constant support of my parents, brothers, other relatives, friends and colleagues, and in particular the support of Amélia Maria.

I want to aknowlegde Mrs. Rosalina Neves, the librarian of the Faculty of Sciences of the University of Porto, for her efficiency and disponibility in sending me by surface mail all the articles that I have requested.

This work had the financial supported from *Fundação para a Ciência e a Tecnologia* (Portugal) through the Grant Praxis XXI/BD/3797/94.

Part of the work presented in this dissertation can be found in the following articles and preprints

1 - M. Dzierzawa, D. Baeriswyl, and L. M. Martelo, *"Variational wave functions for the Mott-Hubbard transtion"*, Helv. Phys. Acta **70**, 124-140 (1997).

2 - L. M. Martelo, M. Dzierzawa, L.Siffert, and D. Baeriswyl, *"Mott-Hubbard transition and antiferromagnetism in the honeycomb latttice"*, Z. Phys. B **103**, 335-338 (1997).

3 - J. M. P. Carmelo, L. M. Martelo, T. Prosen, and D. K. Campbell, *"Conservation laws, spectral weights, and inverse photoemission in the 1D Hubbard model"* (submitted to Phys. Rev. Lett., 1999).

4 - J. M. P. Carmelo, J. M. E. Guerra, and L. M. Martelo, *"Complete set of critical theories of the 1D Hubbard model"* (preprint, 1999).

Work published during the Ph.D. studies but not used in this dissertation

1 - I. R. Pimentel, F. Carvalho Dias, L. M. Martelo, and R. Orbach, *"Magnetic properties of weakly doped antiferromagnets"* Phys. Rev. B **60**, 12 329-12 334 (1999).

Chapter 1

Introduction

1.1 The general problem

The main goal of this thesis is the study of the many-electron problem in low-dimensional quantum liquids.

In three-dimensional systems (3D) the electron-electron interaction can be treated with success by mean-field approximations, band theory or the Fermi-Liquid Theory [1, 2, 3, 4, 5]. The one-particle spectral function of a Fermi Liquid (FL) contains a coherent peak (the quasi-particle peak), which is well-defined for energies close to the Fermi level, followed by an incoherent structure at higher energies. Thus, the low-energy properties are essentially determined by the quasi-particle coherent part of the spectral function.

In low-dimensinal systems, the effects of the electronic correlations are qualitatively different and change completely the nature of the quantum problem relatively to the corresponding non-interacting problem. There exists a class of one-dimensional (1D) systems which are exactly solvable by the Bethe ansatz (BA) technique [6]. These systems show a completely incoherent one-particle spectral function and belong an universality class of $1D$ quantum liquids which was named Luttinger Liquid (LL) [7].

There are many open questions in what the problem of strongly correlated electronic systems is concerned. On the analytical side, this follows from the lack of exact solutions and of controlled approximations and from the difficulty in extracting physical information from the BA solution. On the numerical side, the problem arises both from the smallness of the systems that can be treated exactly and from the fermionic "sign" problem.

The motivation of this thesis is a better understanding of the physical properties of low-dimensional materials where the effects of electronic correlations are expected to be particularly important. We will consider the Hubbard model [8, 9, 10], which is the simplest and standard model for the study of the effect of electronic correlations in a discrete lattice. The model contains two parame-

ters, the hopping kinetic integral t, which gives the probability amplitude for one electron to hop to a nearest neighbour site and the on-site Coulomb electronic repulsion integral U. We denote electronic density of the model by n. It is such that $0 \leq n \leq 2$. In the strong coupling limit, i.e. when $U \gg t$, the model can be mapped into the $t-J$ model [11], where J is the antiferromagnetic (AF) exchange coupling between adjacent sites and is given, in second order perturbation theory, by $J = 4t^2/U$.

In Chapters 2-5 of this work we will consider mainly the 1D Hubbard model. We will study its one-particle spectral properties, which distinguish the LL and FL like behaviours. The main motivation for this study is the recent and renewed experimental interest on the one-electron spectral properties of quasi 1D conductors and insulators [12, 13, 14, 15].

The symmetries of the model are easier to be identified within the pseudoparticle operational representation [16]. This basis is also often the most suitable for the extraction of the physical information contained in these symmetries. In this thesis we use symmetries of the 1D Hubbard model to extract important information on the energy dependence of the one-particle spectral function and associated density of states. These studies include energies in the range of the upper-Hubbard-band (UHB) [17] For instance, we find that the energy dependence of the one-particle density of states just above the UHB bottom edge is, for densities below half-filling, of power-law LL type. Since the experimental observation of the UHB requires inverse photoemission measurements, we suggest new experiments to be compared with our theoretical predictions.

Luttinger Liquids show unusual properties relatively to FL's [18], such as (i) supression of the FL characteristic step at the Fermi level energy in the one-particle density of states, which in a LL is replaced by a power-law singularity with positive exponent and (ii) spin-charge separation, the original degrees of freedom of the electrons are decoupled into charge and spin elementary excitations called holons and spinons, respectively [19].

On the other hand, in Chapters 6-7, we will study charge transport properties associated with the metal-insulator transition, which is one of the most interesting and intricate phenomenon in the many-body theory. Materials can be *grosso modo* divided in conductors (metals) and insulators. An electronic system can, in principle, exhibit a transition from a conducting phase to an insulating phase by tuning some characteristic parameter. The metal-insulator transition [20, 21, 22, 23, 24] is still not completely understood, despite the progresses that has been done during the last decades. Namely the development of new techniques for treating 1D many-fermion models, the application of renormalization group scaling theory and the advances in the limit of large dimensions.

It should be mentioned that a sharp qualitative distinction between a conductor and an insulator can only be made at temperature $T = 0K$. Thus, the metal-insulator transtion is actually a *quantum phase transition*, i.e. a funda-

mental change in the ground state of the system [25], for which less is known if we compare with the achieved understanding of classical phase transitions. Even the search for an order paramter for the metal-insulator transition has not revealed fruitful and its consideration in terms of a Landau theory has only been recently been suggested [26]. The main reason of this slow progress is that several mechanisms such as electronic correlations (Mott transition [27]), disorder effects (Anderson transition [28]), Fermi surface magnetic instabilities (Slater transition [29]), phononic effects (Peierls transition [30]), band structure effects, structural transitions, pressure, temperature or doping can induce a metal-insulator transition and be present at the same time.

The question whether the metal-insulator transition is a discontinuous first-order or a continuous second-order depends crucially on the mechanism which drives the transition. The Anderson metal-insulator transition occurs at a critical value of disorder that localizes electrons through quantum interference giving rise to a continuous second-order transtion at $T = 0K$ (amorphous alloys and doped semiconductors are experimental examples). The Mott metal-insulator transition usually gives rise to a discontinuous first-order transition at non-zero temperature. This is mainly due to the fact that strongly correlated systems have structural transitions coincident with the Mott transition driving the transition to be of first-order. This is the case of the typical strongly correlated compound V_2O_3 [31, 32]. An interesting compound is the also strongly electronic correlated chalcogenide doped compound $NiS_{2-x}Se_x$, where a continuous transition at very low temperatures is observed by tuning the applied pressure, without the presence of a structural transition [33]. The main reason for the slow progress in the understanding of the Mott transition is of course the diffilculty of mastering the problem of strong correlations. In addition, the pure Mott transition is often masked by an antiferromagnetic instability of the metallic phase.

The metal-insulator transition produced by electron correlations, when treated within the framework of the Hubbard model, is known as the Mott-Hubbard transition. In this thesis, we will study the Mott-Hubbard transition at $T = 0K$ and at half filling $n = 1$ by means of variational wavefunctions.

The metal-insulator transition is a key issue of general interest. In particular, the understanding of a doped Mott insulator is of great importance in the theory of high-temperature superconductors [34, 35] and more recently in the understanding of the properties of novel two-dimensional electronic systems in the presence of both interaction and disorder [36].

We will also study the dielectric susceptibility for interacting electronic systems. This quantity is finite in the insulating phase and diverges at the metal-insulator transition and therefore, it can be used in the description of metal-insulator transitions. The divergence of the dielectric susceptibilty at the metal-insulator transition is observed experimentally, e.g. in the phosphorus-doped silicon $Si : P$ [37].

1.2 Recent experimental studies

Our main motivation for the theoretical study of the one-particle spectral properties of the 1D Hubbard model is the renewed interest on the spectral properties of quasi 1D materials. For an excellent review of the characterization of these materials see Ref. [38]. It is worthwhile to mention here some of the recent experimental studies.

There are several experimental studies which confirm the occurence in these low-dimensional materials of the supression of the density of states at the the Fermi surface. This effect is predicted theoretically by the LL theory [7] and is controlled by the electron-electron interactions.

Dardel *et al.* [39] have considered two transition metals. The blue bronze $K_{0.3}MoO_3$ and the tetrachalcogenide $(TaSe_4)_2I$. These materials exhibit a metal-insulator transition associated with the formation of a charge density wave (CDW) at the critical Peierls temperatures $T_P = 180K$ and $T_P = 263K$, respectively. High-resolution photoemission experiments performed at temperatures just above the Peierls transition confirmed the supression of states at the Fermi level. The corresponding photoemission spectra are shown in Fig. 1.1. In a later work, Dardel *et al.* [40] have considered the two blue bronze transition metal $K_{0.3}MoO_3$ and $Rb_{0.3}MoO_3$. The latter material also shows a metal-insulator transition at $T_P = 180K$ which is associated with the formation of a CDW and the openinng of a gap in the energy spectrum. The spectral function is modified over an energy range one order of magnitude larger than that expected from the opening of a Peierls gap. A transfer of spectral weight from the vicinity of the Fermi level to higher binding energies was also observed. These results had led the authors to claim that besides the electron-phonon coupling, the electron-electron interaction is also important in these materials.

Hwu *et al.* [41] and Coluzza *et al.* [42] performed high-energy resolution photoemission in the chalcogenide transition metals $(TaSe_4)_2I$ and in the quasi 1D crystals $TaTe_4$, $NbTe_4$ and $(NbSe_4)_3I$, respectively. They also confirmed the supression of the spectral intensity at the Fermi level and indicated electronic correlations as the main mechanism behind that effect.

Dardel *et al.* [43] have also performed high-energy resolution photoemission in quasi-1D organic Bechgaard salts such as the tetramethyltetraselenafulvalene $(TMTSF)_2X$, with $X = ClO_4, PF_6$. For $X = PF_6$ this material shows a metal-insulator transition associated with the formation of a spin density wave (SDW) at $T = 12K$. At temperature $T = 50K$, a LL power-law behaviour at the Fermi level was observed and the exponent of the density of states obtained was larger than 1. We note within the 1D Hubbard model that exponent cannot be larger than 1/8. In order to explain this large value for the critical exponent, the authors suggested that one should include strong long-range interactions in the 1D Hubbard model to full explain these materials.

Nakamura [44] performed high-resolution photoemission in the compound

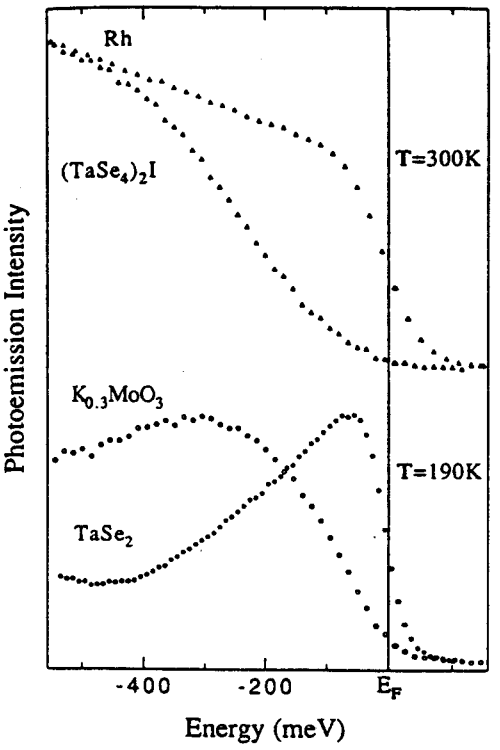

Figure 1.1: Photoemision spectra of the 1D transition metals $K_{0.3}MoO_3$ and $(TaSe_4)_2I$ for temperatures above the Peierls transition. The spectra of the 2D cpompound $TaSe_2$ and of the 3D Rh are also shown at the same temperatures (from Ref. [39]).
Comparison between the data of the quasi 1D materials and higher dimensional materials reveals a qualitative difference in what the spectra weight at the Fermi level is concerned.

$BaVS_3$ had also found that in the metallic phase ($T > 70K$) the spectra near the Fermi level show a power-law behaviour, being the exponent larger than $1/8$ ($<\sim$ 1). More recently, Denlinger *et al.* [15] used angle-resolved photoemission spectroscopy (ARPES) in the quasi 1D metal $Li_{0.9}Mo_6O_{17}$. These authors observed the same effects as the above studies.

In what concerns the observation of spin-charge separation, we can mention the ARPES in the 1D copper-oxide chain compound $SrCuO_2$ [12]. This study revealed clearly the existence of two distinct bands. This was interpreted as a direct observation of spin-charge separation (see Fig. 1.2). The observed spectra were understood quantitatively by means of exact diagonalization for the 1D $t-J$ model. For this compound the AF exchange interaction has been determined as $J = 0.18\ eV$ and $J = 0.23\ eV$ by uniform susceptibility and optical obsorption measurements, respectively. The hopping parameter was considered to be $t \simeq 0.6\ eV$, by taking the ratio $t/J = 3$, which was observed in other cuprates. The

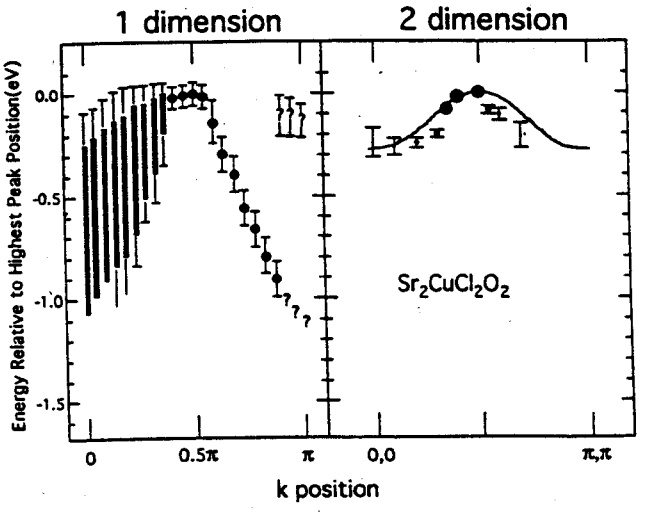

Figure 1.2: E vs. k for the 1D material $SrCuO_2$ and the 2D material $Sr_2CuCl_2O_2$ (from Ref. [12]).

two observed bands had approximately the energy dispersion 0.3 eV and 1.2 eV, respectively, and were identified with the spinon and the holon bands, respectively, whose energy scales are given by J and t, respectively.

Recent and sofisticate ARPES performed at room temperature in the 1D Mott-Hubbard insulator NaV_2O_5 for a large range of energies below the Fermi level, provided important features of the one-particle excitations of this material [13]. The strongly correlated electrons are located in the V $3d$ orbitals which are believed to be half filled (valence $3d^1$). The AF exchange interaction has been estimated to be $J = 0.05$ eV from magnetic susceptibility measurements. For vanadium oxides the effective on-site Coulomb repulsion is expected to be $U = 2 - 4$ eV. This leads to the value $t = 0.15 - 0.25$ eV (from the relationship $J = 4t^2/U$), which corresponds to a dispersion width of $2t = 0.3 - 0.5$ eV. This energy width is identified with the energy scale of the holon band. Actually, for the V $3d$ band a dispersional width of $0.06 - 0.12$ eV was observed. This is smaller but of the same order as the estimated $2t$ value. The binding energy of the V $3d$ band exhibited a clear momentum-dependent modulation with the periodicity of π, which implies an effective doubling of the unit cell. This feature can be explained either due to short-range AF correlations or to spin-Peierls order. However, since the experiments were performed at room temperature, i.e. in the paramagnetic phase well above the spin-Peierls transition temperature and since the AF shadow band was quite strong, the authors considered the possibility that this feature was a signature of the holon band. This was based on analytical results both from the 1D Hubbard model in the $U \to \infty$ limit and from the $t - J$ model. The spectral data did not identified any signature of the spinon band. Kobayashi *et al.* [14] have also performed ARPES in the insulating but "more conductive"

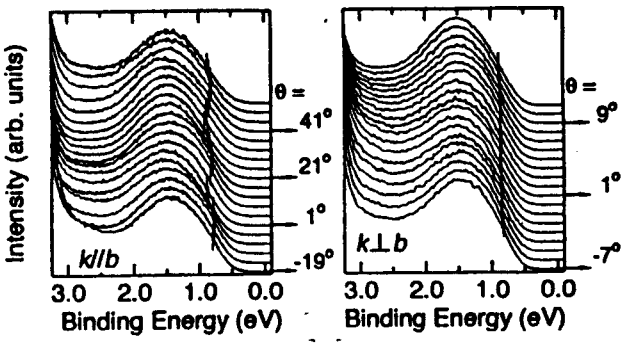

Figure 1.3: Spectra for $k \parallel$ to b axis and $k \perp$ to b in the V $3d$ band region for the compound NaV_2O_5 (from Ref. [13]).

compound $Na_{0.96}V_2O_5$. The agreement between the experimental results and the one-particle spectral function of the 1D $t-J$ model at finite temperatures, obtained by exact diagonalization, led the authors to consider their results as evidence for spin-charge separation. (For excellent reviews on the Bechgaard salts and their properties, namely the LL type behaviour and the plausibility of spin-charge separation in these materials, see Refs. [45, 46].)

Despite the above experimental results, the existence of pure LL's in Nature is not accepted by the whole community. On the other hand, there is limited theoretical information on spectral properties of 1D many-electron systems at finite energy scales. The main theoretical available tools - bosonization [47, 7] and conformal-field theory [48] - only provide the one-particle spectral porperties for energy values in the vicinity of the Fermi level. In order to further clarify this issue, it is also important to have a theoretical description of the one-electron spectral properties for finite energies above the Fermi level. This is one of the problems studied in this thesis.

This thesis is organized as follows. In Chapter 2, the Hubbard model is introduced and the pseudoparticle operational representation for the 1D Hubbard model is presented. A review of conformal-field theory is presented in Chapter 3. In Chapter 4, the conformal invariance and the conservation laws of the 1D Hubbard model are explored. Following symmetries of the model, the behaviour of correlation functions at finite energies is investigated. The formalism developed in the previous chapters is used in Chapter 5 to study the one-particle spectral propeties of the 1D Hubbard model. In Chapter 6 variational wave functions are used to describe the metal-insulator transition at half filling as function of the on-site interaction U. This studies considers the two-dimensional honeycomb Hubbard model and both the hypercubic and hyperdiamond Hubbard models. The dielectric suspectibility for interacting electronic systems is studied in Chapter 7, in order to porperly describe the insulating phase. Finally, in Chapter 8 the conclusions of this thesis are presented.

Bibliography

[1] L. D. Landau, Sov. Phys. JETP **3**, 920 (1957).

[2] L. D. Landau, Sov. Phys. JETP **5**, 101 (1957).

[3] L. D. Landau, Sov. Phys. JETP **8**, 70 (1958).

[4] D. Pines and P. Nozières, *The Theory of Quantum Liquids: Normal Fermi Liquids*, (Addison-Wesley, Second Edition, 1989).

[5] G. Baym and C. J. Pethick, *Landau Fermi-Liquid Theory, Concepts and Applications*, (John Wiley & Sons, New York, 1991).

[6] This Ansatz was introduced for the first time for the isotropic Heisenberg chain by H. Bethe, Z. Phys. **71**, 205 (1931).

[7] F. D. M. Haldane, J. Phys. C **14**, 2585 (1981)

[8] J. Hubbard, Proc. Roy. Soc. London **A276**, 238 (1963).

[9] J. Kanamori, Prog. Theor. Phys. **30**, 275 (1963).

[10] M. C. Gutzwiller, Phys. Rev. Lett. **10**, 159 (1963).

[11] Many authors have performed this transformation, see, e.g., J. E. Hirsch, Phys. Rev. Lett. **54**, 1317 (1985).

[12] C. Kim *et al.*, Phys. Rev. Lett. **77**, 4054 (1996).

[13] K. Kobayashi *et al.*, Phys. Rev. Lett. **80**, 3141 (1998).

[14] K. Kobayashi *et al.*, Phys. Rev. Lett. **82**, 803 (1999).

[15] J. D. Denlinger *et al.*, Phys. Rev. Lett. **82**, 2540 (1999).

[16] J. M. P. Carmelo and N. M. R. Peres, Phys. Rev. B **56**, 3717 (1997), and references therein.

[17] H. Eskes and A. M. Oleś, Phys. Rev. Lett. **73**, 1279 (1994).

[18] J. Voit, Rep. Prog. Phys. **57**, 977 (1994).

[19] E. H. Lieb and F. Y. Wu, Phys. Rev. Lett. **20**, 1445 (1968).

[20] D. Belitz, and T. R. Kirkpatrick, Rev. Mod. Phys. **66**, 261 (1994).

[21] *Metal-Insulator Transitions Revisited* (edited by P. P. Edwards, and C. N. R. Rao, Taylor and Francis, 1995).

[22] F. Gebhard, (Habilitationsschrift, *Modelle und Methoden für den Mott-Übergang*, Philips Universität Marburg, 1995) and references therein.

[23] E. Abrahams, and G. Kotliar, Science **274**, 1853 (1996).

[24] A. Georges, G. Kotliar, W. Krauth, and M. J. Rozenberg, Rev. Mod. Phys. **68**, 13 (1996).

[25] S. L. Sondhi, S. M. Girvin, J. P. Carini, and D. Shahar, Rev. Mod. Phys. **69**, 315 (1997).

[26] T. R. Kirkpatrick, and D. Belitz, Phys. Rev. Lett. **73**, 862 (1994).

[27] N. F. Mott, Proc. Phys. Soc. **A62**, 416 (1949); *ibid.*, *Metal-Insulator Transitions*, (Taylor and Francis, London 1990).

[28] P. W. Anderson, Phys. Rev. **109**, 1948 (1958).

[29] J. C. Slater, Phys. Rev. **82**, 538 (1951).

[30] R. E. Peierls, *Quantum Theory of Solids*, (Claredon Press, Oxford, 1955).

[31] D. B. McWhan *et al.*, Phys. Rev. Lett. **27**, 941 (1971); D. B. McWhan *et al.*, Phys. Rev. B **7**, 9224 (1973).

[32] S. Carter *et al.*, Phys. Rev. Lett. **67**, 3440 (1991).

[33] A. Husmann *et al.*, Science, **274**, 1874 (1996) and references therein.

[34] P. W. Anderson, in *Frontiers and Borderlines in Many-Particle Physics*, (edited by R. A. Broglia, and J. R. Schrieffer, North-Holland, Amsterdam, p. 1, 1988).

[35] E. Dagotto, Rev. Mod. Phys. **66**, 763 (1994).

[36] A. M. Goldman, and N. Marković, Physics Today (November 1998, p. 39), and references therein.

[37] T. F. Rohsenbaum *et al.*, Phys. Rev. B **27**, 7509 (1983).

[38] N. M. R. Peres, *The Many-Electron Problem in Novel Low-Dimensional Materials*, (PhD. Thesis, University of Évora, 1999). Also available in cond-mat/9802240.

[39] B. Dardel *et al.*, Phys. Rev. Lett. **67**, 3144 (1991).

[40] B. Dardel *et al.*, Europhys. Lett. **19**, 525 (1992).

[41] Y. Hwu *et al.*, Phys. Rev. B **46**, 13624 (1992).

[42] C. Coluzza *et al.*, Phys. Rev. B **47**, 6625 (1993).

[43] B. Dardel *et al.*, Europhys. Lett. **24**, 687 (1993).

[44] M. Nakamura *et al.*, Phys. Rev. B **49**, 16191 (1994).

[45] C. Bourbounais and D. Jérome, Science **281**, 1155 (1998).

[46] V. Vescoli *et al.*, Science **281**, 1181 (1998).

[47] J. Sólyom, Adv. Phys. **28**, 201 (1979).

[48] For an important collection of relevant articles, see, *Fields, Strings and Critical Phenomena*, (Les Houches 1988, Edited by E. Brézin and J. Zinn-Justin, North-Holland, 1990).

Chapter 2

The Hubbard Model

2.1 The Hamiltonian for interacting electrons

Our study of the electronic correlations requires the introdution of a suitable Hamiltonian describing interacting electrons in a lattice. We first make the Born-Oppenheimer [1] approximation, which assumes that ions are considered static relatively to the electronic degrees of freedom. The relevant electrons are those of the outer shells and we describe the system by one band. In view of this, the electronic Hamiltonian is given by [2]

$$\hat{H} = \sum_{ij,\sigma} (-t_{ij})\, c^{\dagger}_{i\sigma} c_{j\sigma} + \sum_{ijkl,\sigma\sigma'} V_{ijkl}\, c^{\dagger}_{i\sigma} c^{\dagger}_{j\sigma'} c_{k\sigma'} c_{l\sigma}, \tag{2.1}$$

where $c^{\dagger}_{i\sigma}(c_{i\sigma})$ is the operator that creates (annihilates) one electron in an atomic orbital centered at the lattice site $\mathbf{R}_i$ with spin projection $\sigma = \uparrow, \downarrow$. The hopping integrals are given by

$$t_{ij} = -\int d\mathbf{r}\, \varphi^{\star}(\mathbf{r} - \mathbf{R}_i) \left[-\frac{(\hbar\nabla)^2}{2m} + V(\mathbf{r}) \right] \varphi(\mathbf{r} - \mathbf{R}_j) \tag{2.2}$$

and the electron-electron Coulomb interaction integrals read

$$V_{ijkl} = \int d\mathbf{r} \int d\mathbf{r}'\, \varphi^{\star}(\mathbf{r} - \mathbf{R}_i)\varphi^{\star}(\mathbf{r}' - \mathbf{R}_j) \left[\frac{e^2}{|\mathbf{r} - \mathbf{r}'|} \right] \varphi(\mathbf{r}' - \mathbf{R}_k)\varphi(\mathbf{r} - \mathbf{R}_l), \tag{2.3}$$

where m and $(-e)$ are the electron mass and charge, respectively, $V(\mathbf{r})$ is the lattice potential and $\varphi(\mathbf{r} - \mathbf{R}_i)$ are the Wannier wave functions centered at the lattice site $\mathbf{R}_i$. The hopping integral t_{ij} gives the probability amplitude of an electron to hop from the atomic orbital centered at $\mathbf{R}_j$ to the one centered at $\mathbf{R}_i$. One can classify the hopping integrals according to the distance between lattice sites as t, t', t'',... for nearest, next nearest, third nearest,... neighbours, respectively.

The Hubbard model [2, 3, 4] is defined by taking only the interaction which corresponds to configurations where two electrons are at the same atomic orbital We denote V_{iiii} by U. This approximation can be justified by screening effects [2, 5]. For the kinetic term, the simplest approximation corresponds to take only hopping processes between nearest neighbours (i.e. the tight-binding approximation). Thus, the "simplest" physical model for the description of interacting electrons in a discrete lattice is given by

$$\hat{H}_H = \hat{T} + U\hat{D}, \tag{2.4}$$

where

$$\hat{T} = -t \sum_{<i,j>,\sigma} \left(c^{\dagger}_{i\sigma} c_{j\sigma} + h.c. \right) \tag{2.5}$$

is the kinetic operator,

$$\hat{D} = \sum_{i=1}^{L} \hat{n}_{i\uparrow} \hat{n}_{i\downarrow} \tag{2.6}$$

is the double ocupancy operator, t is the hopping integral between nearest neighbours, L is the number of sites of the system, $< i, j >$ denotes that the sum runs over nearest neighbours pairs, and $\hat{n}_{i\sigma} = c^{\dagger}_{i\sigma} c_{i\sigma}$. Although the Hubbard model (2.4) is formally simple, it still represents a highly non-trivial problem in the many-body theory.

2.2 The $SO(4)$ symmetry and s-wave pairing

The two-dimensional (2D) Hubbard model has been widely used in an attempt to describe the anomalous properties of the high-T_c superconductors. However, it is not clear whether these properties can be described within the framework of electronic correlations only In this section we find from the use of symmetry that there is no s-wave superconductivity at momentum $\mathbf{k} = \mathbf{Q} = (\pi, ..., \pi)$ in the Hubbard model for any bipartite lattice and dimension.

The $SO(4)$ symmetry of the model was discovered by C. N. Yang [6]. The details of the associate irreducible representation were studied by C. N. Yang and S. C. Zhang [7]. The $SO(4)$ algebra contains the usual $SU(2)$ spin algebra and also the $SU(2)$ η-spin algebra which is related to the charge degrees of freedom. In order to study the $SO(4)$ symmetry of the Hubbard model, it is convenient to rewrite the Hamiltonian (2.4) as follows

$$\hat{H}_{SO(4)} = -t \sum_{\langle ij \rangle,\sigma} \left(c^{\dagger}_{i\sigma} c_{j\sigma} + h.c. \right) + U \sum_{i} \left(c^{\dagger}_{i\uparrow} c_{i\uparrow} - \frac{1}{2} \right) \left(c^{\dagger}_{i\downarrow} c_{i\downarrow} - \frac{1}{2} \right). \tag{2.7}$$

The Hamiltonian (2.7) is invariant under the particle-hole transformation $c^{\dagger}_{i,\sigma} \rightarrow (-1)^i c_{i,\sigma}$ and also under the spin flip transformation $c^{\dagger}_{i,\sigma} \rightarrow c^{\dagger}_{i,-\sigma}$. These two symmetries are associated with the $SU(2)$ η-spin algebra, whose generators are

$$\begin{aligned} \hat{S}^c_z &= -\frac{1}{2}(L - \hat{N}) \\ \hat{S}^c_+ &= \sum_j (-1)^j c^{\dagger}_{j\downarrow} c^{\dagger}_{j\uparrow} \\ \hat{S}^c_- &= \sum_j (-1)^j c_{j\uparrow} c_{j\downarrow}, \end{aligned} \tag{2.8}$$

and with the $SU(2)$ spin algebra, whose generators are

$$\begin{aligned} \hat{S}^s_z &= -\frac{1}{2}(\hat{N}_\uparrow - \hat{N}_\downarrow) \\ \hat{S}^s_+ &= \sum_j c^{\dagger}_{j\downarrow} c_{j\uparrow} \\ \hat{S}^s_- &= \sum_j c^{\dagger}_{j\uparrow} c_{j\downarrow}, \end{aligned} \tag{2.9}$$

respectiely. Here $\hat{N} = \sum_\sigma \hat{N}_\sigma$ is the electron number operator and $\hat{N}_\sigma = \sum_j c^{\dagger}_{j\sigma} c_{j\sigma}$ is the number operator of electrons with spin projection $\sigma = \uparrow, \downarrow$. In equations (2.8) and (2.9) we used the notation $\eta \equiv S^c$ for η-spin and $S \equiv S^s$ for spin.

Let $|\psi\rangle$ be an energy eigenstate of the model (2.7). If $\hat{S}^\alpha_+ |\psi\rangle = 0$ then $|\psi\rangle$ is a lowest-weight state (LWS) of the $SU(2)$ S^α algebra, here $\alpha = c, s$. All the six operators (2.8)- (2.9) commute with the Hamiltonian (2.7). The two corresponding $SU(2)$ algebras are independent, i.e the generators of η-spin algebra commute with the generators of the spin algebra.

In order to further clarify the physical contents of the $SO(4)$ symmetry, let $|\psi\rangle$ be an energy eigenstate with N electrons, magnetization $1/2(N_\uparrow - N_\downarrow)$ and momentum $\mathbf{P}$. We consider the momentum representation of the above raising operators

$$\begin{aligned} \hat{S}^c_+ &= \sum_{\mathbf{k}} c^{\dagger}_{-\mathbf{k}+\mathbf{Q},\downarrow} c^{\dagger}_{\mathbf{k}\uparrow} \\ \hat{S}^s_+ &= \sum_{\mathbf{k}} c^{\dagger}_{\mathbf{k}\downarrow} c_{\mathbf{k}\uparrow}, \end{aligned} \tag{2.10}$$

where $\mathbf{Q} = (\pi, ..., \pi)$ is the antiferromagnetic wave vector. The energy eigenstate $\frac{1}{\sqrt{L}} \hat{S}^c_+ |\psi\rangle$ has $N+2$ electrons, momentum $\mathbf{P} + \mathbf{Q}$ and the same magnetization as $|\psi\rangle$, whereas the energy eigenstate $\frac{1}{\sqrt{L}} \hat{S}^s_+ |\psi\rangle$ has magnetization $1/2(N_\uparrow - N_\downarrow) - 1$ and the same number of electrons and momentum as $|\psi\rangle$.

The $SO(4)$ symmetry provides relevant information on the energies spectrum and the energy eigenstates of the Hubbard model for bipartite lattices and in any dimension. It can be used to classify all energy eigenstates according with the representation of the $SO(4)$ group [8]. The operator $(\hat{\mathbf{S}}^{\alpha})^2$ has eigenvalue $S^{\alpha}(S^{\alpha}+1)$ and commutes with all generators of the $SU(2)$ spin and η-spin algebras and also with the Hamitonian (2.7). Therefore, the quantum numbers $(S^c)^2$, S^c_z, $(S^s)^2$ and S^s_z can be used to classify the energy eigensates.

The $SO(4)$ symmetry implies the validity of the following theorem [9]: if the expectation value $< \sum_{\mathbf{k}} c^{\dagger}_{-\mathbf{k}\downarrow} c^{\dagger}_{\mathbf{k}\uparrow} > \neq 0$ in the ground state (GS) if the GS is superconducting, there is necessarily a triplet of collective modes with energy $0, \pm(U-2\mu)$, where μ is the chemical potential. These colectives modes correspond to the usual Goldstone mode and to two massive modes and couple directly to external charge disturbances of wave vector $\mathbf{Q}$. If the Hubbard model were the suitable model for the description of the physics of the high-T_c superconductors [10], then one should experimentally observe sharp resonances in the superconducting phase.

Let us now show that the $SO(4)$ symmetry implies the absence of s-wave η-pairing superconductivity in the Hubbard model for bipartite lattices in any dimension, all values of $U > 0$ and fillings. Let us consider the on-site s-wave pairing operator

$$\hat{O}^{\dagger}(i) = c^{\dagger}_{i\downarrow} c^{\dagger}_{i\uparrow}, \tag{2.11}$$

whose Fourier transform is given by

$$\begin{aligned} \hat{O}^{\dagger}(\mathbf{k}) &= \frac{1}{\sqrt{L}} \sum_{i=1}^{L} e^{-\mathbf{k}.\mathbf{R}_i} \hat{O}^{\dagger}(i) \\ &= \frac{1}{\sqrt{L}} \sum_{\mathbf{k}'} c^{\dagger}_{-\mathbf{k}'+\mathbf{k},\downarrow} c^{\dagger}_{\mathbf{k}',\uparrow}, \end{aligned} \tag{2.12}$$

where $\mathbf{k}$ is the total momentum of the electron pair. For $\mathbf{k} = 0$ the operator (2.12) is the usual s-wave Cooper-pair operator, whereas for $\mathbf{k} = \mathbf{Q}$ it represents the s-wave η-pairing operator.

Let us consider the time-ordered Green's function

$$G_s(i,j;t) = -i\langle 0|\mathcal{T}\hat{O}(i,t)\hat{O}^{\dagger}(j,0)|0\rangle \tag{2.13}$$

where $|0\rangle$ is the GS and $\mathcal{T}$ is the time-ordering operator. The Fourier transform of the function (2.13) is defined as

$$G(\mathbf{k},\mathbf{k}';t) = \frac{1}{L} \sum_{i,j=1}^{L} e^{-\mathbf{k}.\mathbf{R}_i} e^{\mathbf{k}'.\mathbf{R}_j} G(i,j;t)\,. \tag{2.14}$$

From the translational invariance of the system and using Eq. (2.12) we find

$$G(\mathbf{k},t) = -i\langle 0|\mathcal{T}\hat{O}(\mathbf{k},t)\hat{O}^\dagger(\mathbf{k},0)|0\rangle. \tag{2.15}$$

The Fourier transform to frequency space leads to

$$\begin{aligned} G(\mathbf{k},\omega) &= \int_{-\infty}^{\infty} dt\; e^{i\omega t} G(\mathbf{k},t) \\ &= \frac{1}{2\pi}\sum_{|n\rangle}\left[\frac{|\langle n|\hat{O}_s^\dagger(\mathbf{k})|0\rangle|^2}{\omega-(E_n-E_0)+i\epsilon} - \frac{|\langle n|\hat{O}_s(\mathbf{k})|0\rangle|^2}{\omega+(E_n-E_0)-i\epsilon}\right] \\ &= \frac{1}{2\pi}\sum_{|n\rangle}\left[\frac{|\langle n|\hat{O}_s^\dagger(\mathbf{k})|0\rangle|^2}{\omega-(E_n-E_0)+i\epsilon}\right], \end{aligned} \tag{2.16}$$

where $\{|n\rangle\}$ is a complete set of energy eigenstates of energies E_n, E_0 is the GS energy and $\epsilon \to 0^+$.

Let us consider the spectral function associated with the creation of one η-pair of electrons in the GS

$$\begin{aligned} \rho(\mathbf{k},\omega) &= -2\ \mathrm{Im}\ G(\mathbf{k},\omega) \\ &= \sum_{|n\rangle} |\langle n|\hat{O}_s^\dagger(\mathbf{k})|0\rangle|^2 \delta(\omega-(E_n-E_0))\,. \end{aligned} \tag{2.17}$$

The complete set of energy eigenstates includes the the state $|\eta\rangle$ such that

$$\begin{aligned} |\eta\rangle &= \frac{1}{\sqrt{L}}\hat{S}_+^c|0\rangle \\ &= \frac{1}{\sqrt{L}}\sum_{\mathbf{k}} c^\dagger_{-\mathbf{k}+\mathbf{Q},\downarrow} c^\dagger_{\mathbf{k}\uparrow}|0\rangle. \end{aligned} \tag{2.18}$$

At momentum $\mathbf{k} = \mathbf{Q}$ the operator (2.12) reads

$$\begin{aligned} \hat{O}^\dagger(\mathbf{Q}) &= \frac{1}{\sqrt{L}}\sum_{\mathbf{k}'} c^\dagger_{-\mathbf{k}'+\mathbf{Q},\downarrow} c^\dagger_{\mathbf{k}',\uparrow} \\ &\equiv \frac{1}{\sqrt{L}}\hat{S}_+^c \end{aligned} \tag{2.19}$$

and the spectral function becomes

$$\rho(\mathbf{Q},\omega) = \delta(\omega-(E_\eta-E_0)). \tag{2.20}$$

Here E_η is the energy of the state $|\eta\rangle$. It follows that at momentum $\mathbf{k} = \mathbf{Q}$ the spectral function is completely coherent.

Let us evaluate the energy of the electron η-pair for the Hubbard model in a magnetic field H and chemical potential μ

$$\hat{H} = \hat{H}_{SO(4)} + \sum_{\alpha} \mu_{\alpha} 2\hat{S}_z^{\alpha}, \tag{2.21}$$

where $\mu_c = \mu$ and $\mu_s = \mu_0 H$ (μ_0 is the Bohr magneton). The energy of the electron η-pair is given by

$$\begin{aligned} E_\eta &= \langle \eta | \hat{H} | \eta \rangle \\ &= E_0 + 2\mu \left(1 - \frac{1}{2}(L-N)\right). \end{aligned} \tag{2.22}$$

The electron η-pair propagates coherently in the system with energy $2\mu(1 - 1/2(L-N))$ and without any scattering, just like a free particle. We emphasize that in the absence of an incoherent part there is no superconductivity.

This result agrees with the general believe that the on-site s-wave pairing is suppressed in the Hubbard model due to the on-site Coulomb repulsion $U > 0$. This was strongly suggested by numerical Monte Carlo simulations [11, 12] and variational studies [13, 14]. Here it was exactly shown that such a supression is total at momentum $\mathbf{k} = \mathbf{Q}$.

It was also shown in the literature [15] that at half filling the extended s-wave electron pairing is not possible and that away from half filling the existence of extended s-wave electron pairing is only allowed if and only if the on-site s-wave electron pairing occurs. We mean by extended s-wave that the two electrons are in adjacent sites. Thus, our results imply the absence of extended s-wave η-pairing (i.e. at momentum $\mathbf{k} = \mathbf{Q}$) superconductivity in the Hubbard model for bipartite lattices in any dimension, all values of $U > 0$ and filling factors.

A similar procedure can be also carried out for the d-wave pairing operator. In 2D it is given by

$$\hat{O}_d^{\dagger}(i) = \frac{1}{4} \sum_{j=1}^{z} \gamma(j) \, (c_{i\downarrow}^{\dagger} c_{j\uparrow}^{\dagger} - c_{i\uparrow}^{\dagger} c_{j\downarrow}^{\dagger}), \tag{2.23}$$

where j is an adjacent site of i, $\gamma(j) = 1(-1)$ for horizontal (vertical) bonds and z is the coordination number. The d-wave Green's function is not completely coherent at $\mathbf{k} = \mathbf{Q}$, allowing for d-wave η-pairing superconductivity.

All these results agree with numerical Monte Carlo simulations [11, 12] and variational studies [13, 14] which strongly suggested the suppression of both s-wave and extended s-wave pairing and that the d-wave pairing is slightly enhanced.

Whether the 2D Hubbard model is a suitable starting point for the description of the properties of the high-T_c superconductors, including the possibility that the electron pairing mechanism could be the exchange of antiferromagnetic spin

fluctuations, which could give rise to d-wave pairing [16, 17, 18, 19, 20, 21, 22, 23, 24], remains an open question.

2.3 The 1D Hubbard model

2.3.1 The Bethe ansatz solution

In this section we consider that the 1D Hubbard model (2.7) is defined in a chain with a number of sites L and with L large and even. For simplicity, we consider electronic densities $0 < n \leq 1$ and spin densities $0 < m \leq n$, where $n = N/L$ is the electronic density and $m = [N_\uparrow - N_\downarrow]/L$ is the spin density. We define $2k_F = \pi N/L$, $k_{F\sigma} = \pi N_\sigma/L$ and $u = U/4$.

The 1D Hubbard model can be exactly solved [25, 26] by the Bethe ansatz (BA) technique [27]. However, the energy eigen-functions are not easy to treat, what renders the calculation of correlation functions a hard task (an exception is the limit $U \rightarrow \infty$ [28]). In spite of the progresses that have been achieved in the last decades, many aspects of the finite-energy physics of the model remain open issues. The pseudoparticle operational representation [49] of the model has actually given important physical insight.

We start by presenting a brief description of the BA solution (for pedagogical reviews see [29, 30, 31, 32, 33, 34, 35]). Importantly, the BA solution only refers to the Hilbert subspace spanned by the set of LWS's of both the spin and η-spin $SU(2)$ algebras. Fortunately, the use of these algebras allows the extraction of the energy of the non-LWS's from the BA energy of the LWS's. of the same S^α tower.

The BA solution gives the energy spectrum in terms of a set of numbers named rapidities $\{k_j, \Lambda_\mu\}$, which are the solutions of the following equations [26]

$$e^{ik_jL} = \prod_{\mu=1}^{N_\downarrow} \frac{\sin k_j - \Lambda_\mu + iu}{\sin k_j - \Lambda_\mu - iu} \tag{2.24}$$

$$\prod_{j=1}^{N} \frac{\Lambda_\mu - \sin k_j + iu}{\Lambda_\mu - \sin k_j - iu} = -\prod_{\nu=1}^{N_\downarrow} \frac{\Lambda_\mu - \Lambda_\nu + iu}{\Lambda_\mu - \Lambda_\nu - iu}. \tag{2.25}$$

The rapidities can be purely real or complex, i.e with finite real and imaginary parts. In order to describe the BA complex rapidities in the thermodynamic limit $L \rightarrow \infty$, Takahashi reformulated the original solution conjecturating the form of these rapidities [36]. This conjecture contains the so-called string hypothesis, which has an accuracy $\mathcal{O}(e^{-\epsilon L})$, where ϵ is some positive number. The string hypothesis is valid in the limit $L \rightarrow \infty$. This leads to a reformulation of Eqs.(2.24) and (2.25) in terms of three "types" of real parts of the rapidities , $\{k_j, \Lambda_\mu^n, \Lambda_\mu^{'n}\}$, which obey the following coupled equations

$$k_j L \;=\; 2\pi I_j - \sum_{n=1}^{\infty}\sum_{\mu=1}^{M_n} 2\tan^{-1}\left(\frac{\sin k_j - \Lambda_\mu^n}{u}\right) - \sum_{n=1}^{\infty}\sum_{\mu=1}^{M_n'} 2\tan^{-1}\left(\frac{\sin k_j - \Lambda_\mu'^n}{u}\right) \tag{2.26}$$

$$L\left(\sin^{-1}(\Lambda_\mu'^n + iu) + \sin^{-1}(\Lambda_\mu'^n - iu)\right) \;=$$

$$= 2\pi J_\mu'^n + \sum_{j=1}^{N-2M'} 2\tan^{-1}\left(\frac{\Lambda_\mu'^n - \sin k_j}{u}\right) + \sum_{m=1}^{\infty}\sum_{\nu=1}^{M_m'} \Theta_{n,m}\left(\frac{\Lambda_\mu'^n - \Lambda_\nu'^m}{u}\right) \tag{2.27}$$

$$\sum_{j=1}^{N-2M'} 2\tan^{-1}\left(\frac{\Lambda_\mu'^n - \sin k_j}{u}\right) \;=\; 2\pi J_\mu^n + \sum_{m=1}^{\infty}\sum_{\nu=1}^{M_m} \Theta_{n,m}\left(\frac{\Lambda_\mu^n - \Lambda_\nu^m}{u}\right). \tag{2.28}$$

The function $\Theta_{n,m}(x)$ is defined in Eq. (A2.10) of Appendix A2. Within equations (2.26)-(2.27) all the energy eigenstates described by the BA solution, i.e. which are LWS's of both the spin and η-spin $SU(2)$ algebras, are specified by the numbers I_j, J_μ^n and $J_\mu'^n$. These numbers satisfy the following conditions

$$I_j = \begin{cases} \text{integer}, & \text{for } (\sum_{i=1}^{\infty}(M_i + M_i')) \text{ even} \\ \text{half}-\text{odd integer}, & \text{for } (\sum_{i=1}^{\infty}(M_i + M_i')) \text{ odd} \end{cases} \tag{2.29}$$

$$J_\mu'^n = \begin{cases} \text{integer}, & \text{for } (L - (N + M_n')) \text{ odd} \\ \text{half}-\text{odd integer}, & \text{for } (L - (N + M_n')) \text{ odd} \end{cases} \tag{2.30}$$

$$J_\mu^n = \begin{cases} \text{integer}, & \text{for } (N + M_n) \text{ even} \\ \text{half}-\text{odd integer}, & \text{for } (N + M_n) \text{ odd} \end{cases} \tag{2.31}$$

and also

$$|I_j| \;<\; \frac{1}{2}\, L \tag{2.32}$$

$$|J_\mu'^n| \;<\; \frac{1}{2}\,(L - N + 2M' - \sum_{m=1}^{\infty}[n + m - |n - m| - \delta_{n,m}]\, M_m') \tag{2.33}$$

$$|J_\mu^n| \;<\; \frac{1}{2}\,(N - 2M' - \sum_{m=1}^{\infty}[n + m - |n - m| - \delta_{n,m}]\, M_m) \tag{2.34}$$

where

$$M' \;=\; \sum_{n=1}^{\infty} n M_n'. \tag{2.35}$$

The number of down spins and up spins are given by

$$N_{\downarrow} = \sum_{n=1}^{\infty} nM_n + M' \tag{2.36}$$

and

$$N_{\uparrow} = N - N_{\downarrow}, \tag{2.37}$$

respectively. The total energy and momentum are given by

$$E_{SO(4)} = -2t \sum_{j=1}^{N-2M'} (\cos k_j) + 4t \sum_{n=1}^{\infty} \sum_{\mu=1}^{M'_n} \mathrm{Re}\sqrt{1-(\Lambda'^{n}_{\mu} - niu)^2} - \frac{UN}{2} + \frac{UL}{4} \tag{2.38}$$

and

$$P = \frac{2\pi}{L} \left(\sum_{j=1}^{N-2M'} I_j - \sum_{n=1}^{\infty} \sum_{\mu=1}^{M'_n} J'^{n}_{\mu} \right), \tag{2.39}$$

respectively.

2.3.2 The pseudoparticle representation

The low-energy pseudoparticle representation of the 1D Hubbard model has been extensively described in the literature [37]-[49]. On the other hand, the generalization of that basis for the whole Hilbert space is still in progress. In that representation one describes the 1D Hubbard model by a set of pseudoparticle bands labelled by $\alpha = c, s$ and $\gamma = 0, 1, ..., L/2$ for $\alpha = c$ and $\gamma = 0, 1, ..., L/2 - 1$ for $\alpha = s$. The label α is related to the original charge and spin ($\alpha = s$) degrees of freedom of the model and the label γ corresponds to both real rapidities ($\gamma = 0$) and complex rapidities ($\gamma > 0$). The pseudoparticle creation and annihilation operators obey anticommution relations

$$\left\{ b^{\dagger}_{q,\alpha,\gamma}, b_{q',\alpha',\gamma'} \right\} = \delta_{q,q'} \delta_{\alpha,\alpha'} \delta_{\gamma,\gamma'} \ , \tag{2.40}$$

being all the remaining anticommutators zero. Each eigenstate is characterized by the number $N_{\alpha,\gamma}$ of pseudoparticles associated with the number operator $\hat{N}_{\alpha,\gamma}$ such that

$$\hat{N}_{\alpha,\gamma}|\psi\rangle = N_{\alpha,\gamma}|\psi\rangle. \tag{2.41}$$

Here $|\psi\rangle$ is any LWS of the $SU(2)$ S^{α} algebra. A α, γ pseudoparticle particle with $\gamma > 0$ is called heavy pseudoparticle. The pseudoparticle number operator reads

$$\hat{N}_{\alpha,\gamma} = \sum_{q} \hat{N}_{\alpha,\gamma}(q) = b^{\dagger}_{q,\alpha,\gamma}\, b_{q,\alpha,\gamma}. \tag{2.42}$$

It is convenient to change the notation of the quantum numbers I_j, $J^{'n}_{\mu}$ and J^{n}_{μ} given by Eqs. (2.29)-(2.31) of Takahashi formulation [36], as follows

$$I_j \equiv I^{c,0}_j \tag{2.43}$$

$$J^{'\gamma}_j \equiv I^{c,\gamma>0}_j \tag{2.44}$$

$$J^{\gamma+1}_j \equiv I^{s,\gamma}_j . \tag{2.45}$$

The numbers $N-2M^{'}$, $M^{'}_{n}$ and M_n of Takahashi formulation [36] are directly related to the pseudoparticle numbers $N_{\alpha,\gamma}$ by

$$N-2M^{'} \equiv N_{c,0} \tag{2.46}$$

$$M^{'}_{\gamma} \equiv N_{c,\gamma>0} \tag{2.47}$$

$$M_{\gamma+1} \equiv N_{s,\gamma}. \tag{2.48}$$

We emphasize that Eqs. (2.26)-(2.28) refer to "occupied" j values of the quantum numbers $I^{\alpha,\gamma}_j$, such that $N_{\alpha,\gamma} = \sum_j$. On the other hand, it is convenient to rather define j in a broader domain including both occupied and non-occupied $I^{\alpha,\gamma}_j$ values. In this case we have that $d_{F_{\alpha,\gamma}} = \sum_j$, where

$$d_{F\alpha,\gamma} = N_{\alpha,\gamma} + N^{h}_{\alpha,\gamma} \tag{2.49}$$

and $N^{h}_{\alpha,\gamma}$ gives the number of pseudoholes in each α,γ band and the numbers $I^{\alpha,\gamma}_j$ are equally spaced and are such that

$$I^{\alpha,\gamma}_{j+1} - I^{\alpha,\gamma}_{j} = 1 . \tag{2.50}$$

This allows us to introduce the discrete pseudoparticle momentum (pseudomomentum)

$$q_j = \frac{2\pi}{L} I^{\alpha,\gamma}_j. \tag{2.51}$$

where $j = 1, 2, 3, ..., d_{F_{\alpha,\gamma}}$. Here $d_{F_{\alpha,\gamma}}$ is the Fock dimension of the α,γ pseudoparticle band, which gives the total number of pseudomomentum available values in the corresponding pseudoparticle band.

The restrictions of the quantum numbers I_j, $J^{'n}_{\mu}$ and J^{n}_{μ} (2.32)-(2.34) combined with the relations (2.46)-(2.48) allows us to obtain an expression of the Fock dimensions, which are then given by

$$d_{F_{c,0}} = L \tag{2.52}$$

$$d_{F_{c,\gamma>0}} = L - N_{c,0} + N_{c,\gamma} - \sum_{\gamma'>0} [\gamma + \gamma' - |\gamma - \gamma'|] \; N_{c,\gamma'} \tag{2.53}$$

$$d_{F_{s,\gamma}} = N_{c,0} - 2N_{s,0} + N_{s,\gamma} - 2\sum_{\gamma'>0} N_{s,\gamma'} - \sum_{\gamma'>0} [\gamma + \gamma' - |\gamma - \gamma'|] \; N_{s,\gamma'}. \tag{2.54}$$

It follows from Eqs. (2.49), (2.52) and (2.54) that the number of $\alpha, 0$ pseudoholes is given by

$$N^h_{c,0} = L - N_{c,0} \tag{2.55}$$

and

$$N^h_{s,0} = N_{c,0} - 2N_{s,0} - 2\sum_{\gamma>0} N_{s,\gamma}. \tag{2.56}$$

The use of Eqs. (2.55) and (2.56) permits rewritting the Fock dimension expressions (2.52)-(2.54) as follows

$$d_{F_{\alpha,\gamma}} = N^h_{\alpha,0} + N_{\alpha,\gamma} - \sum_{\gamma'>0} [\gamma + \gamma' - |\gamma - \gamma'|] \; N_{\alpha,\gamma'}. \tag{2.57}$$

The quantum numbers $I^{\alpha,\gamma}_j$ are consecutive integers or half-odd integers for $\bar{N}_{\alpha,\gamma}$ odd and even, respectively. The parity of these numbers, Eqs. (2.29)-(2.31), is the same as the below r.h.s. numbers

$$\begin{aligned} \bar{N}_{c,0} &\rightarrow N_{s,0} + \sum_{\alpha,\gamma>0} N_{\alpha,\gamma} \\ \bar{N}_{c,\gamma>0} &\rightarrow 1 + L - N + N_{c,\gamma} \\ \bar{N}_{s,\gamma} &\rightarrow 1 + N - N_{s,\gamma}. \end{aligned} \tag{2.58}$$

The pseudomomentum of the α, γ band is such that $q^{(-1)}_{\alpha,\gamma} \leq q \leq q^{(+1)}_{\alpha,\gamma}$. For $\alpha, \gamma \equiv c, 0$ the limits of the pseudo-Brillouin zones are given by

$$q^{(\pm 1)}_{c,0} = \pm\pi \left[1 - \frac{1}{L}\right] \tag{2.59}$$

for $\bar{N}_{c,0}$ even and

$$q^{(+1)}_{c,0} = \pi, \quad q^{(-1)}_{c,0} = -\pi \left[1 - \frac{2}{L}\right] \tag{2.60}$$

or

$$q_{c,0}^{(+1)} = \pi\left[1 - \frac{2}{L}\right], \quad q_{c,0}^{(-1)} = -\pi \tag{2.61}$$

for $\bar{N}_{c,0}$ odd. For the remaining α, γ bands the limits of the pseudo-Brillouin zones are symmetric and read

$$q_{\alpha,\gamma}^{(\pm 1)} = \pm\frac{\pi}{L}\left[d_{F\alpha,\gamma} - 1\right]. \tag{2.62}$$

The real part of the rapidities, $\{k_j, \Lambda_\mu^n, \Lambda_\mu'^n\}$, are given in the pseudoparticle representation by the real functions

$$K(q_j) \equiv k_j\,, \tag{2.63}$$

$$R_{c,\gamma>0}(q_j) \equiv \frac{\Lambda_j'^{\gamma}}{u}\,, \tag{2.64}$$

and

$$R_{s,\gamma}(q_j) \equiv \frac{\Lambda_j^{1+\gamma}}{u}, \tag{2.65}$$

respectively. Following equations (2.26), (2.27) and (2.28), the functions (2.63)-(2.65) are the solutions of the following functional equations

$$\begin{aligned} K(q) &= q - \frac{2}{N_a}\sum_{\gamma=0}\sum_{q'} N_{s,\gamma}(q')\tan^{-1}\Big(\frac{R_{c,0}(q) - R_{s,\gamma}(q')}{1+\gamma}\Big) \\ &- \frac{2}{N_a}\sum_{\gamma=1}\sum_{q'} N_{c,\gamma}(q')\tan^{-1}\Big(\frac{R_{c,0}(q) - R_{c,\gamma}(q')}{\gamma}\Big)\,, \end{aligned} \tag{2.66}$$

$$\begin{aligned} 2Re\sin^{-1}\Big(u(R_{c,\gamma}(q) - i\gamma)\Big) &= q + \frac{2}{N_a}\sum_{q'} N_{c,0}(q')\tan^{-1}\Big(\frac{R_{c,\gamma}(q) - R_{c,0}(q')}{\gamma}\Big) \\ &+ \frac{1}{N_a}\sum_{\gamma'=1}\sum_{q'} N_{c,\gamma'}(q')\Theta_{\gamma,\gamma'}\Big(R_{c,\gamma}(q) - R_{c,\gamma'}(q')\Big), \end{aligned} \tag{2.67}$$

and

$$\begin{aligned} 0 &= q - \frac{2}{N_a}\sum_{q'} N_{c,0}(q')\tan^{-1}\Big(\frac{R_{s,\gamma}(q) - R_{c,0}(q')}{1+\gamma}\Big) \\ &+ \frac{1}{N_a}\sum_{\gamma'=0}\sum_{q'} N_{s,\gamma'}(q')\Theta_{1+\gamma,1+\gamma'}\Big(R_{s,\gamma}(q) - R_{s,\gamma'}(q')\Big)\,. \end{aligned} \tag{2.68}$$

where $N_{\alpha,\gamma}(q)$ is the pseudomomentum distribution function which specifies the energy eigenstates and the function $\Theta_{\gamma,\gamma'}(x)$ is defined by Eq. (A2.10) of Appendix A2. For each energy eigenstate the distribution $N_{\alpha,\gamma}(q)$ has different values. The pseudomomentum distribution function $N_{\alpha,\gamma}(q)$ is such that

$$\hat{N}_{\alpha,\gamma}(q)|\psi\rangle \;=\; N_{\alpha,\gamma}(q)|\psi\rangle\,; \tag{2.69}$$

where $|\psi\rangle$ is any S^α LWS. Equations (2.66)-(2.68) provide the real part of the BA rapidities as functionals of the distribution $N_{\alpha,\gamma}(q)$.

It is convenient to introduce the rapidity function

$$R_{c,0}(q) \;=\; \frac{\sin K(q)}{u}. \tag{2.70}$$

One can associate the real part of the rapidities with the operators $\hat{R}_{\alpha,\gamma}(q)$ such that

$$\hat{R}_{\alpha,\gamma}(q)|\psi\rangle \;=\; R_{\alpha,\gamma}(q)|\psi\rangle \tag{2.71}$$

where $|\psi\rangle$ is any S^α LWS. From the use Eqs. (2.66)-(2.68), we find that the real part of the rapidities has the following values at the limits of the pseudo-Brillouin zones

$$K(q_{c,0}^{(\pm 1)}) \;=\; \pm\pi, \quad R_{c,0}(q_{c,0}^{(\pm 1)}) \;=\; 0 \tag{2.72}$$

$$R_{\alpha,\gamma}(q_{\alpha,\gamma}^{(\pm 1)}) \;=\; \pm\infty \quad \text{for } \alpha,\gamma \neq \mathrm{c},0. \tag{2.73}$$

In the continuum limit, the energy spectrum (2.38) is given in the pseudoparticle representation by

$$\begin{aligned} E_{SO(4)} \;=\; & -2t\frac{L}{2\pi}\int_{-q_{c,0}^{(-1)}}^{q_{c,0}^{(+1)}} dq\; N_{c,0}(q)\cos K(q) + \\ & +4t\frac{L}{2\pi}\sum_{\gamma>0}\int_{-q_{c,\gamma}^{(-1)}}^{q_{c,\gamma}^{(+1)}} dq\; N_{c,\gamma}(q)\mathrm{Re}\sqrt{1-u^2(R_{c,\gamma}(q)-i\gamma)^2} + \\ & +\; U\left[\frac{L}{4}-\frac{N_{c,0}}{2}-\sum_{\gamma>0}\gamma N_{c,\gamma}\right]. \end{aligned} \tag{2.74}$$

2.3.3 The pseudoparticle perturbation theory

We introduce now the pseudoparticle perturbation theory [49]. The GS pseudomomentum distributions read

$$
\begin{aligned}
N^0_{\alpha,0}(q) &= \Theta\left(q^{+1}_{F_{\alpha,0}} - q\right), \qquad 0 < q < q^{(+1)}_{\alpha,0};\\
N^0_{\alpha,0}(q) &= \Theta\left(q - q^{-1}_{F_{\alpha,0}}\right), \qquad q^{-1}_{F_{\alpha,0}} < q \leq 0;\\
N^0_{\alpha,\gamma}(q) &= 0, \qquad \gamma > 0.
\end{aligned}
\tag{2.75}
$$

where the GS pseudo-Fermi points are given by

$$
\begin{aligned}
q^{(\pm 1)}_{F_{\alpha,0}} &= \pm q_{F_{\alpha,0}} + \mathcal{O}\left(\frac{1}{L}\right),\\
q^{(\pm 1)}_{F_{\alpha,\gamma}} &= 0, \qquad \gamma > 0
\end{aligned}
\tag{2.76}
$$

and

$$
q_{F_{\alpha,0}} = \frac{\pi N_{\alpha,0}}{L} \tag{2.77}
$$

with

$$
\begin{aligned}
q^0_{F_{c,0}} &= 2k_F\\
q^0_{F_{s,0}} &= k_{F\downarrow}
\end{aligned}
\tag{2.78}
$$

The following parameters play an important role in the theory

$$
Q^{(\pm)} = K^{(0)}(q^{(\pm)}_{Fc,0}) \tag{2.79}
$$

$$
r^{(\pm)}_{\alpha,\gamma} = R^{(0)}_{\alpha,\gamma}(q^{(\pm)}_{F\alpha,\gamma}). \tag{2.80}
$$

where $K^{(0)}(q)$ and $R^{(0)}_{\alpha,\gamma}(q)$ are the real parts of the rapidities for a given reference state.

Let us consider the pseudomomentum distribution operator normal ordered relatively to the GS

$$
: \hat{N}_{\alpha,\gamma}(q) : = \hat{N}_{\alpha,\gamma}(q) - N^0_{\alpha,\gamma}(q), \tag{2.81}
$$

which satisfies the eigenvalue equation

$$
: \hat{N}_{\alpha,\gamma}(q) : |\psi\rangle = \delta N_{\alpha,\gamma}(q)|\psi\rangle \tag{2.82}
$$

where deviation $\delta N_{\alpha,\gamma}(q)$ relatively to GS is assumed to be small. The pseudoparticleperturbation theory consists in expanding the rapidities and the energy spectrum in terms of the deviations $\delta N_{\alpha,\gamma}(q)$. In the case of the real part of the rapidities this leads to

$$R_{\alpha,\gamma}(q) = R^{(0)}_{\alpha,\gamma}(q) + R^{(1)}_{\alpha,\gamma}(q) + R^{(2)}_{\alpha,\gamma}(q) + ... \quad (2.83)$$

where $R^{(0)}_{\alpha,\gamma}(q)$ is the GS eigenvalue of the rapidity operator $R_{\alpha,\gamma}(q)$ and $R^{(n)}_{\alpha,\gamma}(q)$ is the term of the order of $\mathcal{O}((\delta N_{\alpha,\gamma}(q))^n)$. On the other hand, the change in the energy spectrum relatively to the GS is given by

$$\begin{aligned} \Delta E_{SO(4)} &= E_{SO(4)} - E^0_{SO(4)} \\ &= \sum_{j=1}^{\infty} \Delta E^{(j)}_{SO(4)}. \end{aligned} \quad (2.84)$$

The first-order term reads

$$\Delta E^{(1)}_{SO(4)} = \sum_{q,\alpha,\gamma} \epsilon^0_{\alpha,\gamma}(q)\delta N_{\alpha,\gamma}(q), \quad (2.85)$$

where the pseudoparticle bands $\epsilon^0_{\alpha,\gamma}(q)$ are given by

$$\epsilon^0_{c,0}(q) = -\frac{U}{2} - 2t\cos K^{(0)}(q) + 2t\int_{Q^{(-)}}^{Q^{(+)}} dk\ \bar{\Phi}_{c,0;c,0}\left(\frac{\sin k}{u}, R^{(0)}_{c,0}(q)\right)\sin k, \quad (2.86)$$

$$\begin{aligned} \epsilon^0_{c,\gamma>0}(q) &= -\gamma U + 4t\mathrm{Re}\sqrt{1-u^2(R_{c,\gamma}(q)+i\gamma)^2} \\ &\quad +2t\int_{Q^{(-)}}^{Q^{(+)}} dk\ \bar{\Phi}_{c,0;c,\gamma}\left(\frac{\sin k}{u}, R^{(0)}_{c,\gamma}(q)\right)\sin k \end{aligned} \quad (2.87)$$

and

$$\epsilon^0_{s,\gamma}(q) = 2t\int_{Q^{(-)}}^{Q^{(+)}} dk\ \bar{\Phi}_{c,0;s,\gamma}\left(\frac{\sin k}{u}, \frac{R^{(0)}_{s,\gamma}(q)}{u}\right)\sin k, \quad (2.88)$$

where the phase shifts $\bar{\Phi}_{\alpha,\gamma;\alpha',\gamma'}$ are defined by the coupled integral equations (A2.1)-(A2.9) of Appendix A2. The band expressions (2.86)-(2.88) for $\gamma = 0$ simplify at zero magnetic field $H = 0$ and in the limit $U \gg t$ [38] and read

$$\epsilon^0_{c,0}(q) \approx -\frac{U}{2} - 2t\left\{\cos(q) + \frac{4t}{U}\ln 2\left[\sin^2(q) + \frac{1}{2}\left(1 - \frac{\sin(2\pi n)}{2\pi n}\right)\right]\right\}, \quad U \gg t \quad (2.89)$$

and

$$\epsilon^0_{s,0}(q) \approx -W_s\cos\left(\frac{q}{n}\right), \quad U \gg t, \quad (2.90)$$

where

$$W_s = \frac{\pi}{2}\,\frac{4t^2}{U}\,n\left(1-\frac{\sin(2\pi n)}{2\pi n}\right). \tag{2.91}$$

The pseudoparticle group velocities are given by

$$v_{\alpha,\gamma}(q) \;=\; \frac{d\epsilon^0_{\alpha,\gamma}(q)}{dq}. \tag{2.92}$$

The second-order energy term reads

$$\Delta E^{(2)}_{SO(4)} \;=\; \frac{1}{L}\sum_{q,\alpha,\gamma}\sum_{q',\alpha',\gamma'}\frac{1}{2}f_{\alpha,\gamma;\alpha',\gamma'}(q,q')\delta N_{\alpha,\gamma}(q)\;\delta N_{\alpha',\gamma'}(q') \tag{2.93}$$

where the Landau f-functions are given by

$$\begin{aligned} f_{\alpha,\gamma;\alpha',\gamma'}(q,q') \;&=\; 2\pi v_{\alpha,\gamma}(q)\Phi_{\alpha,\gamma;\alpha',\gamma'}(q,q') + 2\pi v_{\alpha',\gamma'}(q')\Phi_{\alpha',\gamma';\alpha,\gamma}(q',q) \\ &+\; 2\pi\sum_{j=\pm 1}\sum_{\alpha''}\sum_{\gamma''}\theta(N_{\alpha'',\gamma''})v_{\alpha'',\gamma''}\Phi_{\alpha'',\gamma'';\alpha,\gamma}(jq_{F_{\alpha'',\gamma''}},q) \\ &\times\; \Phi_{\alpha'',\gamma'';\alpha',\gamma'}(jq_{F_{\alpha'',\gamma''}},q'), \end{aligned} \tag{2.94}$$

and the functions $\Phi_{\alpha,\gamma;\alpha',\gamma'}(q,q')$ are the two-pseudoparticle forward-scattering phase shifts. They measure the phase shift occurring in the phase of the α',γ' pseudoparticle at pseudomomentum q' due to a zero-momentum forward-scattering collision with the α,γ pseudoparticle at pseudomomentum q. The phase shifts are given by

$$\Phi_{\alpha,\gamma;\alpha',\gamma'}(q,q') \;=\; \bar{\Phi}_{\alpha,\gamma;\alpha',\gamma'}(R^{(0)}_{\alpha,\gamma}(q),R^{(0)}_{\alpha',\gamma'}(q')), \tag{2.95}$$

where the functions $\bar{\Phi}_{\alpha,\gamma;\alpha',\gamma'}(r,r')$ are the solutions of the integral equations of Appendix A2.

Note that in what concerns the energy spectrum, the 1D Hubbard model has in the pseudoparticle representation a Fermi-Liquid type energy functional [50, 51]. The original non-perturbative electronic problem (the spectral function of the 1D Hubbard model is completely incoherent), becomes perturbative in the pseudoparticle basis.

From equation (2.84) we can write the 1D Hubbard model in the pseudoparticle operational representation as follows

$$:\hat{H}_{SO(4)} := \hat{H}_{SO(4)} - E^0_{SO(4)} = \sum_{j=1}^{\infty}\hat{H}^{(j)}_{SO(4)}, \tag{2.96}$$

where the first-order and second-order pseudoparticle-scattering terms are given by

$$\hat{H}^{(1)}_{SO(4)} = \sum_{q,\alpha,\gamma} \epsilon^0_{\alpha,\gamma}(q) : \hat{N}_{\alpha,\gamma}(q) : \tag{2.97}$$

and

$$\hat{H}^{(2)}_{SO(4)} = \frac{1}{L} \sum_{q,\alpha,\gamma} \sum_{q',\alpha',\gamma'} \frac{1}{2} f_{\alpha,\gamma;\alpha',\gamma'}(q,q') : \hat{N}_{\alpha,\gamma}(q) : : \hat{N}_{\alpha',\gamma'}(q') : \tag{2.98}$$

respectively. Note that in this basus, the Hamiltonian pseudoparticle interacting terms of (2.96) are all of zero-momentum forward scattering type.

From the studies of Ref.[49], the pseudoparticle bands have finite energy widths which are given by

$$\begin{aligned} \Delta\epsilon^0_{c,0} &= 4t \\ \Delta\epsilon^0_{\alpha,\gamma} &= |\epsilon^0_{\alpha,\gamma}(0)|\,, \qquad \alpha,\gamma \neq c,0. \end{aligned} \tag{2.99}$$

On the other hand, the width of the pseudomomentum bands is for all α,γ bands given by

$$\Delta q_{\alpha,\gamma} = \sum_{\iota=\pm 1} \iota q^{(\iota)}_{\alpha,\gamma} = 2q_{\alpha,\gamma} - \frac{2\pi}{L}\,. \tag{2.100}$$

where the pseudo-Brillouin limits $q^{(\iota=\pm 1)}_{\alpha,\gamma}$ are given by Eqs. (2.59)-(2.62) and the parameters $q_{\alpha,\gamma}$ reads

$$\begin{aligned} q_{c,0} &= \pi \\ q_{\alpha,\gamma} &= \frac{\pi d_{F_{\alpha,\gamma}}}{L}\,, \qquad \alpha,\gamma \neq c,0. \end{aligned} \tag{2.101}$$

Note that the $c,0$ pseudoparticle band has the same momentum and energy widths as the $U = 0$ electronic band.

2.3.4 The non-LWS's and the α-Yang particles

As we have mentioned and was shown in Refs. [52, 53, 54], the energy eigenstates of the 1D Hubbard model which span the Hilbert subspace associated with the BA solution are LWS's of both the $SU(2)$ spin and η-spin algebras. The complete set of energy eigenstates can be obtained by acting onto these LWS's the spin and η-spin $SU(2)$ raising operators. In terms of the pseudoparticle representation, this can be achieved by the introduction of a quantum number $\beta = \pm 1/2$ which labels the pseudoholes of the $\alpha,0$ bands [49]. Alternatively to this β representation, we use here an equivalent representation which describes the non-LWS's by the

creation onto the LWS's of *c-Yang particles* and *s-Yang particles* with elementary operators given by

$$\begin{aligned} d^{\dagger}_{q_\alpha} &= \frac{\hat{S}^{\alpha}_{+}}{\sqrt{-2\hat{S}^{\alpha}_{z}}} \\ d_{q_\alpha} &= \frac{\hat{S}^{\alpha}_{-}}{\sqrt{-2\hat{S}^{\alpha}_{z}}}, \end{aligned} \tag{2.102}$$

where $q_c = \pi$ and $q_s = 0$. These operators obey the following commution relations

$$\left[d_{q_\alpha}, d^{\dagger}_{q'_\alpha}\right] = \delta_{\alpha,\alpha'}. \tag{2.103}$$

The number operator $\hat{\mathcal{N}}_\alpha = d^{\dagger}_{q_\alpha} d_{q_\alpha}$ commutes with the Hamiltonian and counts the number of α-Yang particles. The number $\mathcal{N}_\alpha$ is conserved and given by

$$\mathcal{N}_\alpha = S^\alpha + S^\alpha_z, \tag{2.104}$$

and such that $0 \leq \mathcal{N}_\alpha \leq 2S^\alpha$. We notice that for the S^α LWS's the number of α-Yang particles is zero, i.e $\mathcal{N}_\alpha = 0$. The number $\mathcal{N}_\alpha$ is maximum for the S^α highest-weight states (HWS's).

The momentum operator is given by (see Eq. 2.39)

$$\hat{P} = \sum_{q} \sum_{\alpha,\gamma=0} q C_{\alpha,\gamma} \hat{N}_{\alpha,\gamma}(q) + \pi \sum_{\gamma>0} (1+\gamma) \hat{N}_{c,\gamma} + \hat{\mathcal{N}}_c, \tag{2.105}$$

where

$$\begin{aligned} C_{c,0} &= C_{s,\gamma} = 1 \\ C_{c,\gamma>0} &= -1. \end{aligned} \tag{2.106}$$

Note that the eigenvalue of the momentum term, $\pi \sum_{\gamma>0} \left[(1+\gamma)\hat{N}_{c,\gamma} + \hat{\mathcal{N}}_c\right]$, is always a multiple of $\pm\pi$.

2.3.5 The ground state in terms of left and right occupations

Let us introduce the quantum number $\iota = sgn(q)$, which refers to right ($\iota = 1$) and left ($\iota = -1$) α, γ pseudoparticles. We also introduce the operator $\hat{N}_{\alpha,\gamma,\iota}$ which counts the number of ι pseudoparticles in each α, γ pseudoparticle band and the corresponding eigenvalue $N_{\alpha,\gamma,\iota}$.

The GS is the state of minimal energy at fixed $N_\uparrow$ and $N_\downarrow$ electron numbers. Following equations (2.75), it has the pseudoparticle numbers $N_{c,0} = N$, $N_{s,0} = N_\downarrow$, $N_{\alpha,\gamma} = 0$ for $\gamma > 0$ and $\mathcal{N}_\alpha = 0$. And either $J_{\alpha,0} = \frac{1}{2}\sum_\iota \iota N_{\alpha,0,\iota} = 0$ or $J_{\alpha,0} = \frac{1}{2}\sum_\iota \iota N_{\alpha,0,\iota} = \pm\frac{1}{2}$. Relatively to the electronic and pseudoparticle vacuum, which we denote here by $|V\rangle$, it follows from Eq. (2.75) that the GS has the following form

$$|GS\rangle = \prod_{\alpha,\iota}\prod_{\iota\kappa<0} b^\dagger_{\kappa,\alpha,0,\iota}|V\rangle\,, \tag{2.107}$$

where the pseudomomentum κ is defined relatively to the GS pseudo-Fermi points. It follows Eqs. (2.75) for $N^0_{\alpha,\gamma}(\kappa)$ that the GS pseudomomentum distribution $N^0_{\alpha,\gamma,\iota}(\kappa)$ reads

$$\begin{aligned} N^0_{\alpha,0,\iota}(\kappa) &= \Theta\big(-\iota\kappa\big) \\ N^0_{\alpha,\gamma,\iota}(\kappa) &= 0\,, \qquad \gamma > 0. \end{aligned} \tag{2.108}$$

The limits of the pseudo-Brillouin zones, Eqs. (2.60)-(2.62), can be written as

$$q^{(\pm 1)}_{\alpha,\gamma} = \pm q_{\alpha,\gamma} + \mathcal{O}\left(\frac{1}{L}\right) \tag{2.109}$$

where the pseudo-Brillouin parameters $q_{\alpha,\gamma}$ are given in Eq. (2.101). For the GS, the pseudo-Brillouin parameters are given by

$$\begin{aligned} q^0_{c,0} &= \pi \\ q^0_{s,0} &= k_{F\uparrow} \\ q^0_{c,\gamma>0} &= \pi - 2k_F \\ q^0_{s,\gamma>0} &= k_{F\uparrow} - k_{F\downarrow}. \end{aligned} \tag{2.110}$$

The GS occupancy of the $\epsilon^0_{\alpha,\gamma}(q)$ pseudoparticle bands is sketched in Fig. 2.1 for magnetic field $H = 0$ and finite U. At zero magnetic field we have that $k_{F\uparrow} = k_{F\downarrow} = k_F$ and the $s,0$ band is filled and the $s,\gamma > 0$ bands collapse into one point.

The width of the $s,0$ band is given by $W_s = |\epsilon^0_{s,0}(0)|$ and can be obtained numerically. It is plotted as function of n in Fig. 2.2.

The parameter $\Delta_c = -2\epsilon^0_{c,0}(\pi)$ plays an important role in the one-particle quantities of Chapter 5. It is a function of U and n and is given asymptotically by

$$\Delta_c = \begin{cases} U - 4t\,, & n = 0 \\ \Delta_{MH}\,, & n = 1 \end{cases} \tag{2.111}$$

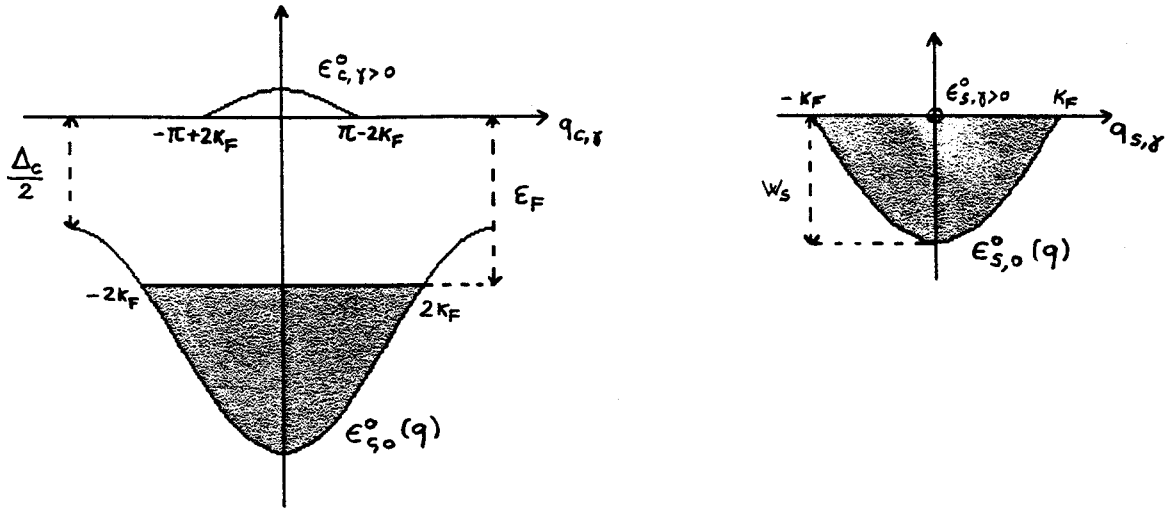

Figure 2.1: Sketch of the ground state occupancy of the $\epsilon^0_{\alpha,\gamma}(q)$ pseudoparticle bands for $H = 0$ and finite U.

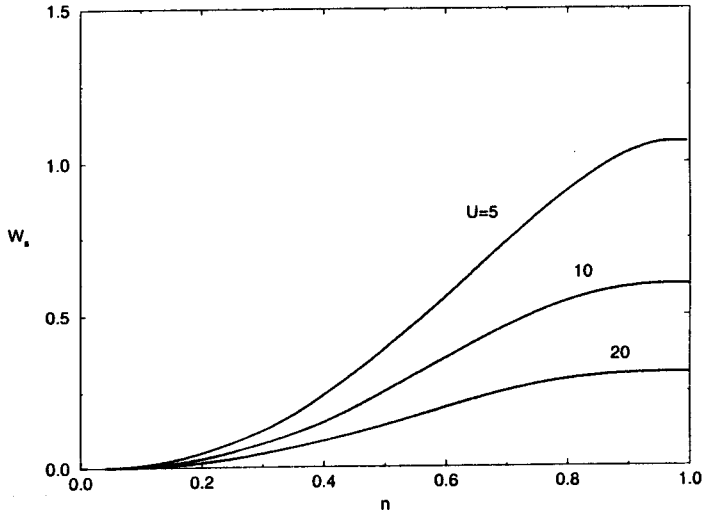

Figure 2.2: Width of the $s, 0$ band as function of n for different values of U (in units of t).

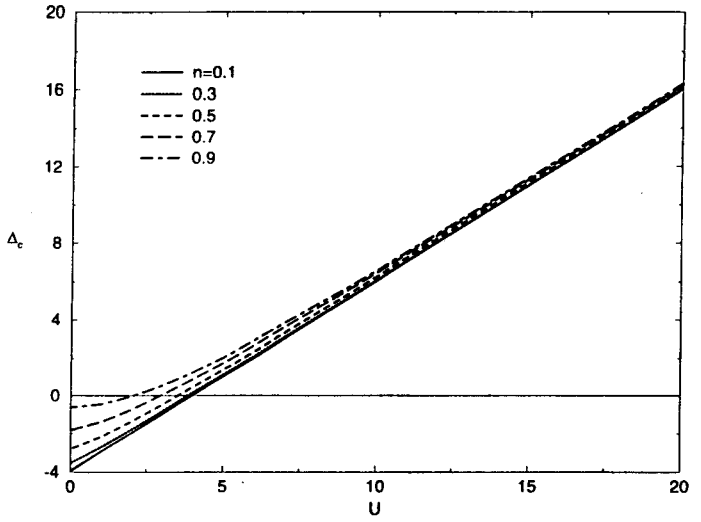

Figure 2.3: The parameter Δ_c as function of U (in units of t) for different densities n.

where Δ_{MH} is the Mott-Hubbard gap of the 1D Hubbard model at half-filling ($\Delta_{MH} = 0$ for $U = 0$ and $\Delta_{MH} \rightarrow U - 4t$ for $U \rightarrow \infty$). The parameter Δ_c can be obtained numerically and is plotted as function of U in Fig. 2.3. It has negatives values for $U < U^{\star}$. Here the parameter $U^{\star}$ is defined by equation $\Delta_c(U^{\star}, n) = 0$ and is a decreasing function of n such that $U^{\star} = 4t$ for $n = 0$ and $U^{\star} = 0$ for $n = 1$. The parameter $U^{\star}$ is plotted as a function of n in Fig. 2.4. Since the one-electron spectral function studied in Chapter 5 has nearly no spectral weight for $U < U^{\star}$, for simplicity in our study we consider $U > U^{\star}$.

Finally, we note that at $H = 0$, the Fermi energy is given by $\epsilon_F = -\epsilon^0_{c,0}(2k_F)$ and is plotted as function of U in Figs. 2.5.

2.3.6 The topological momentum shift mechanism

The fact that the numbers $I^{\alpha,\gamma}_j$ can be either consecutive integers or half-odd integers for different Hamiltonian eigenstates leads to the concept of α,γ topological momentum shift. The change in the integer or half-odd integer character of some of the numbers $I^{\alpha,\gamma}_j$, associated with the transition between two states, shifts *all* the occupied pseudomomenta. The α,γ topological momentum shift operators shift all the pseudomomenta of the corresponding α,γ band by $\pm\frac{\pi}{L}$. Creation or annihilation of pseudoparticles requires the occurrence of such topological momentum shifts. Therefore, in addition to the pseudoparticle operators, the pseudoparticle representation also includes topological momentum shift operators. The corresponding α,γ unitary generator is such that

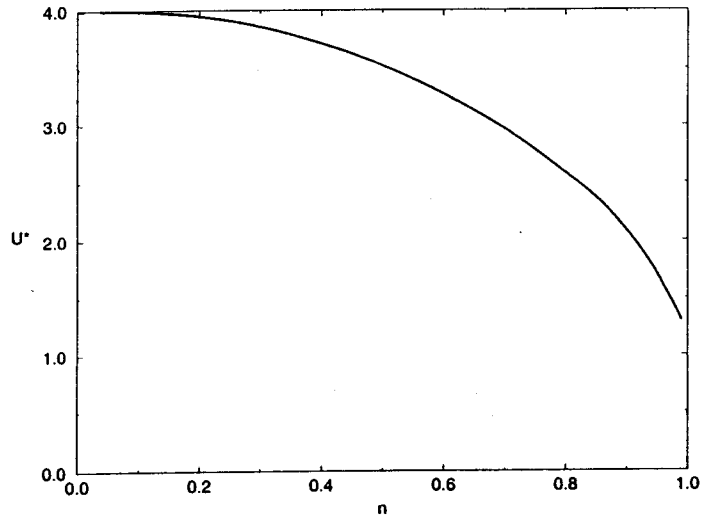

Figure 2.4: The parameter $U^\star$ (in units of t) as function of the density n.

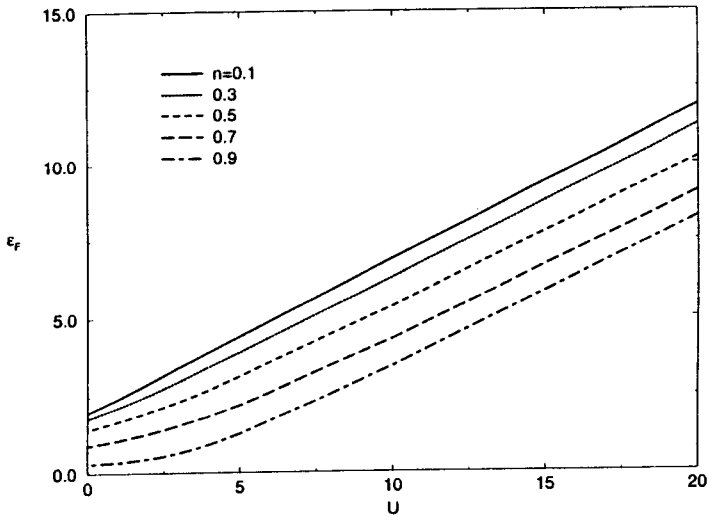

Figure 2.5: The Fermi energy ϵ_F (in units of t) as function of U for different densities n.

$$U^{\pm 1}_{\alpha,\gamma}\, b^{\dagger}_{q,\alpha,\gamma} = b^{\dagger}_{q\pm\frac{\pi}{L},\alpha,\gamma}\, U^{\pm 1}_{\alpha,\gamma} \tag{2.112}$$

and reads [49]

$$U^{\pm 1}_{\alpha,\gamma} = \exp\left[\sum_{q} b^{\dagger}_{q\mp\frac{\pi}{L},\alpha,\gamma} b_{q,\alpha,\gamma}\right] . \tag{2.113}$$

2.3.7 Relation between the electronic numbers and the numbers of pseudoparticle and α-Yang particles

In general, the relation between the electronic and pseudoparticle operators is not known. In the present quantum problem the number of σ electrons is a good quantum number. Using equations (2.36),(2.37) and (2.46)-(2.48), we find that the electronic numbers N and N_σ can be expressed in terms of the pseudoparticle numbers $N_{\alpha,\gamma}$ and the α-Yang particles numbers $\mathcal{N}_\alpha$ as follows

$$\begin{aligned} N &= N_{c,0} + \sum_{\gamma>0} 2\gamma N_{c,\gamma} + 2\mathcal{N}_c \\ N_\uparrow - N_\downarrow &= N_{c,0} - 2N_{s,0} - \sum_{\gamma>0} 2(1+\gamma) N_{s,\gamma} - 2\mathcal{N}_s . \end{aligned} \tag{2.114}$$

Combining the sum rules (2.114) with Eqs. (2.55) and (2.56), we find the following relations

$$\begin{aligned} N &= L - N^h_{c,0} + \sum_{\gamma>0} 2\gamma N_{c,\gamma} + 2\mathcal{N}_c \\ N_\uparrow - N_\downarrow &= N^h_{s,0} - \sum_{\gamma>0} 2\gamma N_{s,\gamma} - 2\mathcal{N}_s . \end{aligned} \tag{2.115}$$

Let us consider small changes in the σ electron, α,γ pseudoparticle and α-Yang particle numbers relatively to the corresponding GS numbers. In order to clarify the electronic character of α,γ pseudoparticles and α-Yang particles, we find from Eqs. (2.115) the following relations

$$\begin{aligned} \Delta N &= -\Delta N^h_{c,0} + \sum_{\gamma>0} 2\gamma \Delta N_{c,\gamma} + 2\Delta\mathcal{N}_c \\ \Delta(N_\uparrow - N_\downarrow) &= \Delta N^h_{s,0} - \sum_{\gamma>0} 2\gamma \Delta N_{s,\gamma} - 2\Delta\mathcal{N}_s . \end{aligned} \tag{2.116}$$

For large U the number of doubly occupied sites, $D = \langle \hat{D} \rangle$, becomes a good quantum number. The change in this number reads

$$\Delta D = \sum_{\gamma>0} \gamma \Delta N_{c,\gamma} + \Delta \mathcal{N}_c. \tag{2.117}$$

We emphasize that at at zero magnetic field the $c,0$ and $s,0$ pseudoholes describe the holons and spinons, respectively [48]. It follows that the numbers $\Delta N^h_{c,0}$ and $\Delta N^h_{s,0}$ refers to changes in the numbers of holons and spinons, respectively.

In order to relate the changes in the holon and spinon numbers and the changes in the electronic numbers, we consider in Eqs. (2.116) $\Delta N_{\alpha,\gamma} = 0$ for $\gamma > 0$ and $\Delta \mathcal{N}_\alpha = 0$ and find

$$\begin{aligned} \Delta N &= -\Delta N^h_{c,0} \\ \Delta(N_\uparrow - N_\downarrow) &= \Delta N^h_{s,0} \\ \Delta D &= 0, \qquad U \gg t. \end{aligned} \tag{2.118}$$

It follows that holons and spinons are one-electron objects.

In order to relate the changes in the number of c-Yang particles to the changes in the electronic numbers, we consider in Eqs. (2.116) $\Delta N^h_{\alpha,0} = 0$, $\Delta N_{\alpha,\gamma} = 0$ and $\Delta \mathcal{N}_s = 0$ and find

$$\begin{aligned} \Delta N &= 2\Delta \mathcal{N}_c \\ \Delta(N_\uparrow - N_\downarrow) &= 0 \\ \Delta D &= \Delta \mathcal{N}_c, \qquad U \gg t. \end{aligned} \tag{2.119}$$

As expected, one c-Yang particle is a two-electron object and for large U its creation is associated with a change in the double occupancy by one.

In the case of the changes in the numbers of s-Yang particles, we consider in the Eqs. (2.116) $\Delta N^h_{\alpha,0} = 0$, $\Delta N_{\alpha,\gamma} = 0$ for $\gamma = 0$ and $\Delta \mathcal{N}_c = 0$ and find

$$\begin{aligned} \Delta N &= 0 \\ \Delta(N_\uparrow - N_\downarrow) &= -2\Delta \mathcal{N}_s \\ \Delta D &= 0, \qquad U \gg t. \end{aligned} \tag{2.120}$$

As expected, one s-Yang particle is a two-electron object and its creation is associated with a change the magnetization of the system by (-1).

In waht concerns the changes in the numbers of heavy c,γ pseudoparticles, we consider in Eqs. (2.116) $\Delta N^h_{\alpha,0} = 0$, $\Delta N_{s,\gamma} = 0$ and $\Delta \mathcal{N}_\alpha = 0$ and find

$$\begin{aligned} \Delta N &= 2\gamma \Delta N_{c,\gamma} \\ \Delta(N_\uparrow - N_\downarrow) &= 0 \\ \Delta D &= \gamma \Delta N_{c,\gamma}, \qquad U \gg t. \end{aligned} \tag{2.121}$$

One heavy c,γ pseudoparticle is a 2γ-electron object and for large U its creation is associated with a change of γ in the double occupancy.

Finally, in order to relate the changes in the numbers of heavy s,γ pseudoparticles to the changes in the electronic numbers, we consider in Eqs. (2.116) $\Delta N^{h}_{\alpha,0} = 0$, $\Delta N_{c,\gamma} = 0$ and $\Delta \mathcal{N}_{\alpha} = 0$ and find

$$\begin{aligned} \Delta N &= 0 \\ \Delta(N_{\uparrow} - N_{\downarrow}) &= -2\gamma \Delta N_{s,\gamma} \\ \Delta D &= 0, \qquad U \gg t . \end{aligned} \tag{2.122}$$

We thus conclude that one heavy s,γ pseudoparticle is a γ-electron object and its creation is associated with a number γ of spin-flips processes.

Appendix A2

In this appendix we present the coupled integral equations whose solutions provides the functions $\bar{\Phi}_{\alpha,\gamma;\alpha',\gamma'}$ of Eq. (2.95). These equations are given by [49]

$$\bar{\Phi}_{c,0;c,0}(r,r') = \frac{1}{\pi}\int_{r_{s,0}^{(-)}}^{r_{s,0}^{(+)}} dr'' \frac{\bar{\Phi}_{s,0;c,0}(r'',r')}{1+(r-r'')^2}, \tag{A2.1}$$

$$\bar{\Phi}_{c,0;c,\gamma}(r,r') = -\frac{1}{\pi}\tan^{-1}(\frac{r-r'}{\gamma}) + \frac{1}{\pi}\int_{r_{s,0}^{(-)}}^{r_{s,0}^{(+)}} dr'' \frac{\bar{\Phi}_{s,0;c,\gamma}(r'',r')}{1+(r-r'')^2}, \tag{A2.2}$$

$$\bar{\Phi}_{c,0;s,\gamma}(r,r') = -\frac{1}{\pi}\tan^{-1}(\frac{r-r'}{1+\gamma}) + \frac{1}{\pi}\int_{r_{s,0}^{(-)}}^{r_{s,0}^{(+)}} dr'' \frac{\bar{\Phi}_{s,0;s,\gamma}(r'',r')}{1+(r-r'')^2}, \tag{A2.3}$$

$$\bar{\Phi}_{c,\gamma;c,0}(r,r') = \frac{1}{\pi}\tan^{-1}(\frac{r-r'}{\gamma}) - \frac{1}{\pi}\int_{r_{c,0}^{(-)}}^{r_{c,0}^{(+)}} dr'' \frac{\bar{\Phi}_{c,0;c,0}(r'',r')}{\gamma[1+(\frac{r-r''}{\gamma})^2]}, \tag{A2.4}$$

$$\bar{\Phi}_{c,\gamma;c,\gamma'}(r,r') = \frac{1}{2\pi}\Theta_{\gamma,\gamma'}\big(r-r'\big) - \frac{1}{\pi}\int_{r_{c,0}^{(-)}}^{r_{c,0}^{(+)}} dr'' \frac{\bar{\Phi}_{c,0;c,\gamma'}(r'',r')}{\gamma[1+(\frac{r-r''}{\gamma})^2]}, \tag{A2.5}$$

$$\bar{\Phi}_{c,\gamma;s,\gamma'}(r,r') = -\frac{1}{\pi}\int_{r_{c,0}^{(-)}}^{r_{c,0}^{(+)}} dr'' \frac{\bar{\Phi}_{c,0;s,\gamma'}(r'',r')}{\gamma[1+(\frac{r-r''}{\gamma})^2]}, \tag{A2.6}$$

$$\begin{aligned}\bar{\Phi}_{s,\gamma;c,0}(r,r') &= -\frac{1}{\pi}\tan^{-1}(\frac{r-r'}{1+\gamma}) + \frac{1}{\pi}\int_{r_{c,0}^{(-)}}^{r_{c,0}^{(+)}} dr'' \frac{\bar{\Phi}_{c,0;c;0}(r'',r')}{(1+\gamma)[1+(\frac{r-r''}{1+\gamma})^2]} \\ &- \int_{r_{s,0}^{(-)}}^{r_{s,0}^{(+)}} dr'' \bar{\Phi}_{s,0;c,0}(r'',r') \frac{\Theta_{1+\gamma,1}^{[1]}\big(r-r''\big)}{2\pi},\end{aligned} \tag{A2.7}$$

$$\begin{aligned}\bar{\Phi}_{s,\gamma;c,\gamma'}(r,r') &= \frac{1}{\pi}\int_{r_{c,0}^{(-)}}^{r_{c,0}^{(+)}} dr'' \frac{\bar{\Phi}_{c,0;c;\gamma'}(r'',r')}{(1+\gamma)[1+(\frac{r-r''}{1+\gamma})^2]} \\ &- \int_{r_{s,0}^{(-)}}^{r_{s,0}^{(+)}} dr'' \bar{\Phi}_{s,0;c,\gamma'}(r'',r') \frac{\Theta_{1+\gamma,1}^{[1]}\big(r-r''\big)}{2\pi},\end{aligned} \tag{A2.8}$$

$$\begin{aligned}\bar{\Phi}_{s,\gamma;s,\gamma'}(r,r') &= \frac{\Theta_{1+\gamma,1+\gamma'}\big(r-r'\big)}{2\pi} + \frac{1}{\pi}\int_{r_{c,0}^{(-)}}^{r_{c,0}^{(+)}} dr'' \frac{\bar{\Phi}_{c,0;s;\gamma'}(r'',r')}{(1+\gamma)[1+(\frac{r-r''}{1+\gamma})^2]} \\ &- \int_{r_{s,0}^{(-)}}^{r_{s,0}^{(+)}} dr'' \bar{\Phi}_{s,0;s,\gamma'}(r'',r') \frac{\Theta_{1+\gamma,1}^{[1]}\big(r-r''\big)}{2\pi},\end{aligned} \tag{A2.9}$$

where

$$\begin{aligned}\Theta_{\gamma,\gamma'}(x) &= \Theta_{\gamma',\gamma}(x) = \delta_{\gamma,\gamma'}\{2\tan^{-1}\Big(\frac{x}{2\gamma}\Big) + \sum_{l=1}^{\gamma-1} 4\tan^{-1}\Big(\frac{x}{2l}\Big)\} \\ &+ (1-\delta_{\gamma,\gamma'})\{2\tan^{-1}\Big(\frac{x}{|\gamma-\gamma'|}\Big) + 2\tan^{-1}\Big(\frac{x}{\gamma+\gamma'}\Big) \\ &+ \sum_{l=1}^{\frac{\gamma+\gamma'-|\gamma-\gamma'|}{2}-1} 4\tan^{-1}\Big(\frac{x}{|\gamma-\gamma'|+2l}\Big)\} \qquad \text{(A2.10)}\end{aligned}$$

and

$$\begin{aligned}\Theta^{[1]}_{\gamma,\gamma'}(x) &= \Theta^{[1]}_{\gamma',\gamma}(x) = \frac{d\Theta_{\gamma,\gamma'}(x)}{dx} \\ &= \delta_{\gamma,\gamma'}\{\frac{1}{\gamma[1+(\frac{x}{2\gamma})^2]} + \sum_{l=1}^{\gamma-1}\frac{2}{l[1+(\frac{x}{2l})^2]}\} \\ &+ (1-\delta_{\gamma,\gamma'})\{\frac{2}{|\gamma-\gamma'|[1+(\frac{x}{|\gamma-\gamma'|})^2]} + \frac{2}{(\gamma+\gamma')[1+(\frac{x}{\gamma+\gamma'})^2]} \\ &+ \sum_{l=1}^{\frac{\gamma+\gamma'-|\gamma-\gamma'|}{2}-1}\frac{4}{(|\gamma-\gamma'|+2l)[1+(\frac{x}{|\gamma-\gamma'|+2l})^2]}\}. \qquad \text{(A2.11)}\end{aligned}$$

For $\gamma = 0$ Eqs. (A2.7) and (A2.9) can be rewritten as

$$\bar{\Phi}_{s,0;c,0}(r,r') = -\frac{1}{\pi}\tan^{-1}(r-r') + \int_{r_{s,0}^{(-)}}^{r_{s,0}^{(+)}} dr'' G(r,r'')\bar{\Phi}_{s,0;c,0}(r'',r') \ , \qquad \text{(A2.12)}$$

and

$$\begin{aligned}\bar{\Phi}_{s,0;s,0}(r,r') &= \frac{1}{\pi}\tan^{-1}(\frac{r-r'}{2}) - \frac{1}{\pi^2}\int_{r_{c,0}^{(-)}}^{r_{c,0}^{(+)}} dr''\frac{\tan^{-1}(r''-r')}{1+(r-r'')^2} \\ &+ \int_{r_{s,0}^{(-)}}^{r_{s,0}^{(+)}} dr'' G(r,r'')\bar{\Phi}_{s,0;s,0}(r'',r') \ , \qquad \text{(A2.13)}\end{aligned}$$

and the kernel $G(r,r')$ reads

$$G(r,r') = -\frac{1}{2\pi}\left[\frac{1}{1+((r-r')/2)^2}\right]\left[1-\frac{1}{2}\left(t(r)+t(r')+\frac{l(r)-l(r')}{r-r'}\right)\right], \qquad \text{(A2.14)}$$

with

$$t(r) = \frac{1}{\pi}\left[\tan^{-1}(r + r_{c,0}^{(+)}) - \tan^{-1}(r + r_{c,0}^{(-)})\right] , \tag{A2.15}$$

and

$$l(r) = \frac{1}{\pi}\left[\ln(1 + (r + r_{c,0}^{(+)})^2) - \ln(1 + (r + r_{c,0}^{(-)})^2)\right] . \tag{A2.16}$$

Bibliography

[1] N. W. Ashcroft and N. Mermin, *Solid State Physics*, (Saunders College Publishing, Fort Worth, 1976).

[2] J. Hubbard, Proc. Roy. Soc. London **A276**, 238 (1963).

[3] J. Kanamori, Prog. Theor. Phys. **30**, 275 (1963).

[4] M. C. Gutzwiller, Phys. Rev. Lett. **10**, 159 (1963).

[5] S. Mazumdar and A. P. N. Bloch Phys. Rev. Lett. **50**, 207 (1983).

[6] C. N. Yang, Phys. Rev. Lett. **63**, 2144 (1989).

[7] C. N. Yang and S. C. Zhang, Mod. Phys. Lett. B **4**, 759 (1990).

[8] S. C. Zhang, Int. J. Mod. Phys. B **5**, 153 (1991).

[9] S. C. Zhang, Phys. Rev. Lett. **65**, 120 (1990).

[10] P. W. Anderson, Science **235**, 1196 (1987).

[11] S. R. White *et al.*, Phys. Rev. B **39**, 839 (1989).

[12] S. R. White *et al.*, Phys. Rev. B **40**, 506 (1989).

[13] C. Gros, R. Joynt and T. M. Rice, Z. Phys. B **68**, 425 (1987).

[14] C. Gros, Ann. Phys. (N.Y.) **189**, 53 (1989).

[15] S. C. Zhang, Phys. Rev. B **42**, 1012 (1990).

[16] N. E. Bickers, D. J. Scalapino and R. T. Scalettar, Int. J. Mod. Phys. B **1**, 687 (1987).

[17] J. R. Schrieffer, X. G. Wen and S. C. Zhang, Phys. Rev. Lett. **60**, 944 (1988).

[18] J. R. Schrieffer, X. G. Wen and S. C. Zhang, Phys. Rev. B **39**, 11663 (1989).

[19] N. E. Bickers, D. J. Scalapino and S. R. White, Phys. Rev. Lett. **62**, 961 (1989).

[20] T. Moriya, Y. Takahashi and K. Ueda, J. Phys. Soc. Jpn. **59**, 2905 (1990).

[21] T. Moriya, Y. Takahashi and K. Ueda, Physica. C **185**, 114 (1991).

[22] P. Monthoux and D. Pines, Phys. Rev. Lett. **69**, 961 (1992).

[23] Z. X. Shen, W. E. Spicer, D. M. King, D. S. Desseau and B. O. Wells, Science **267**, 343 (1995), and references therein.

[24] D. J. Scalapino, *The Structure of Two Different Pairing Interactions* (1995).

[25] C. N. Yang, Phys. Rev. Lett. **19**, 1312 (1967).

[26] E. H. Lieb, and F. Y. Wu, Phys. Rev. Lett. **20**, 1445 (1968).

[27] This Ansatz was introduced for the first time for the isotropic Heisenberg chain by H. Bethe, Z. Phys. **71**, 205 (1931).

[28] K. Penc, K. Hallberg, F. Mila and H. Shiba, Phys. Rev. B **55**, 15475 (1997).

[29] M. Gaudin, *La Fonction d'Onde de Bethe*, (Masson, Paris, 1983).

[30] B. Sutherland, *An Introduction to the Bethe Ansatz*, in *Exactly Solvable Problems in Condensed Matter and Relativistic Field Theory*, (Lectures Notes in Physics **242**, Springer-Verlag, Berlin, 1985).

[31] D. Baeriswyl, *Bethe Ansatz for the One-Dimensional Hubbard Model*, in *Le Modèle de Hubbard* (Troisième Cycle de la Physique en Suisse Romande, 1991).

[32] V. E. Korepin, N. M. Bogolioubov and A. G. Izergin, *Quantum Inverse Scattering Method and Correlation Functions*, (Cambridge University Press, Cambridge, 1993).

[33] J. Voit, Rep. Prog. Phys. **57**, 977 (1994).

[34] H. J. Schulz, *Fermi Liquids and Non-Fermi Liquids* (1995) (cond-mat/9503150 v2).

[35] N. M. R. Peres, *The Many-Electron Problem in Novel Low-Dimensional Materials*, (PhD. Thesis, University of Évora, 1999). Available in cond-mat/9802240.

[36] M. Takahashi, Prog. Theor. Phys. **47**, 69 (1972).

[37] J. M. P. Carmelo, and A. A. Ovchinnikov, J. Phys.: Condens. Matter. **3**, 757 (1991).

[38] J. M. P. Carmelo, P. Horsh, P. A. bares and A. A. Ovchinnikov, Phys. Rev B, **44**, 9967 (1991).

[39] J. M. P. Carmelo and P. Horsh, Phys. Rev. Lett. **68**, 871 (1992).

[40] J. M. P. Carmelo, P. Horsh and A. A. Ovchinnikov, Phys. Rev. B **45**, 7899 (1992).

[41] J. M. P. Carmelo, P. Horsh and A. A. Ovchinnikov, Phys. Rev. B **46**, 14728 (1992).

[42] J. M. P. Carmelo and A. H. Castro Neto, Phys. Rev. Lett. **70**, 1904 (1993).

[43] J. M. P. Carmelo, P. Horsh, D. K. Campbell and A. H. Castro Neto, Phys. Rev. B **48**, 4200 (1993).

[44] J. M. P. Carmelo, A. H. Castro Neto and D. K. Campbell, Phys. Rev. B **50**, 3667 (1994).

[45] J. M. P. Carmelo, A. H. Castro Neto and D. K. Campbell, Phys. Rev. B **50**, 3683 (1994);

[46] J. M. P. Carmelo, A. H. Castro Neto and D. K. Campbell, Phys. Rev. Lett. **73**, 926 (1994).

[47] J. M. P. Carmelo and N. M. R. Peres, Phys. Rev. B **51**, 7481 (1995).

[48] J. M. P. Carmelo and N. M. R. Peres, Nuc. Phys. B **458**, 579 (1996).

[49] J. M. P. Carmelo and N. M. R. Peres, Phys. Rev. B **56**, 3717 (1997).

[50] D. Pines and P. Nozières, *The Theory of Quantum Liquids: Normal Fermi Liquids*, (Addison-Wesley, Second Edition, 1989).

[51] G. Baym and C. J. Pethick, *Landau Fermi-Liquid Theory, Concepts and Applications*, (John Wiley & Sons, New York, 1991).

[52] F. H. L. Eßler, V. E. Korepin, and K. Schoutens, Phys. Rev. Lett. **67**, 3848 (1991).

[53] F. H. L. Eßler, V. E. Korepin, and K. Schoutens, Nuc. Phys. B **372**, 559 (1992).

[54] F. H. L. Eßler, V. E. Korepin, and K. Schoutens, Nuc. Phys. B **384**, 431 (1992).

Chapter 3

Basic Ideas on Conformal Invariance

3.1 Introduction

Conformal invariance is a very successful symbiosis between quantum-field theory and statistical mechanics which had and will continue to have a tremendous impact in several branches of physics. For instance, conformal-field theory (CFT) [1, 2, 3, 4, 5, 6, 7, 8, 9, 10] was recentely applied to the study of the quantum Hall effect [11, 12] and of 1D quantum impurities [13]. Combined with the BA solutions of integrable electronic models [14, 15, 16, 17], it has also provided the critical exponents for the low-energy correlation functions of these models [18, 19, 20, 21].

In this thesis we will use conformal-field theory of multicomponent systems [19] in the study of the correlation functions of 1D Hubbard model. Futhermore, we will find that for each occupied α, γ pseudoparticle branch there is a Virasoro algebra associated with such conformal-field theory.

In this chapter we give a brief introduction to conformal invariance of one-component systems. In order to introduce the concept of conformal invariance, we start by considering the simpler yet related concept of scale invariance. The degrees of freedom of an interactive system are correlated over a typical distance named the correlation length ξ. In a second-order phase transition this correlation length diverges at the critical point, when compared to some characteristic length scale of the system, e.g. the lattice spacing a ($\xi/a \rightarrow \infty$). The system loses memory of the details of the lattice structure and scale invariance is used to extract important information on the critical behaviour of the system.

Correlations between the different degrees of freedom of the system are characterized by suitable correlation functions. Among the correlation functions, some are particularly important since for large distances they behave near the critical point as power laws

$$\langle \phi(\mathbf{r})\phi(\mathbf{r}')\rangle \;=\; \frac{1}{|\mathbf{r}-\mathbf{r}'|^{2x}} \tag{3.1}$$

where $\phi(\mathbf{r})$ is a field operator at the point $\mathbf{r}$ and $|\mathbf{r}-\mathbf{r}'| \to \infty$. A scaling transformation is defined by globally rescaling all the distances by a rigid factor λ and by multiplying the field operators by a suitable factor as follows

$$\begin{aligned} \mathbf{r} &\to \lambda\mathbf{r} \\ \phi(\mathbf{r}) &\to \phi'(\mathbf{r}) = \lambda^x \phi(\lambda\mathbf{r}). \end{aligned} \tag{3.2}$$

where the exponent x is the same as the one of expression (3.1). The correlation function (3.1) is invariant under a global scaling transformation, i.e.

$$\langle \phi'(\mathbf{r})\phi'(0)\rangle \;=\; \frac{1}{|\mathbf{r}|^{2x}}. \tag{3.3}$$

The field $\phi(\mathbf{r})$ and the exponent x are named scale operator and scale dimension of the field, respectively. The scaling hypothesis states that, near a critical point, the field operator $\phi(\mathbf{r})$ is a homogeneous function whose degree is the exponent x [see Eq. (3.2)]. The scaling hypothesis is justified within the framework of the Renormalization Group [22].

3.2 Conformal invariance

The previous scaling transformation deals with a global rescaling of the system distances. A conformal transformation is more general and deals with a *local* rescaling of the system.

A central theorem in conformal-field theory [23] states that if a system is translational and rotational invariant (at least in the continuum limit), scale invariant at a given critical point and has short-range interactions, then it exhibits conformal invariance in the considered critical point.

Conformal invariance is specially useful in two-dimensional systems (one space x and one time t dimensions), since for these systems the algebra associated with conformal transformations is infinite dimensional (i.e. it has an infinite number of generators). This happens because in two-dimensional space the equations that give the conformal transformations are equivalent to the Cauchy-Riemann equations, whose solutions are the holomorphic and antiholomorphic complex functions [9]. Thus, it is convenient to study conformal invariance in the complex plane. It is worth to refer that a conformal transformation conserves the angles of intersection between two curves in the complex plane [24].

Let us consider a system described by the usual space and Minkowski time coordinates (x,t). In order to use the machinery of complex functions it is convenient to consider the Euclidean space instead of the original Minkowski space.

These two spaces are related by a simple Wick's rotation in the time coordinate. We introduce the following variables

$$\begin{cases} z = x + iv\tau \\ \bar{z} = x - iv\tau \end{cases} \tag{3.4}$$

where v is the "light-velocity" and τ is the Euclidean time ($\tau = -it$).

For a conformal-invariant system there exists a set of correlation functions that behave near the conformal critical point, in the long-range limit, as follows

$$\langle 0|\phi(z,\bar{z})\phi(z',\bar{z}')|0\rangle = \frac{1}{(z-z')^{2h}} \frac{1}{(\bar{z}-\bar{z}')^{2\bar{h}}} \tag{3.5}$$

where $|0\rangle$ is the vacuum of the theory, $(z-z') \to \infty$ and $(\bar{z}-\bar{z}') \to \infty$.

We consider now a generic conformal transformation defined by

$$\begin{cases} z \to \omega(z) \\ \bar{z} \to \bar{w}(\bar{z}), \end{cases} \tag{3.6}$$

where the complex functions $\omega(z)$ and $\bar{\omega}(\bar{z})$ must be analytical. The two components of the above transformation are called holomorphic and antiholomorphic, respectively.

The field-operator transformation law for global scaling, Eq. (3.2), suggests the following generalization for local conformal transformations

$$\phi(z,\bar{z}) \to \phi'(z,\bar{z}) = \left(\frac{\partial w}{\partial z}\right)^{h} \left(\frac{\partial \bar{w}}{\partial \bar{z}}\right)^{\bar{h}} \phi(w,\bar{w}). \tag{3.7}$$

If the vacuum state is invariant under a conformal transformation, the relation for correlation functions before and after this conformal transformation is performed is given by

$$\langle 0|\phi(z,\bar{z})\phi(z',\bar{z}')|0\rangle = \left(\frac{\partial w}{\partial z}\right)^{h} \left(\frac{\partial w'}{\partial z'}\right)^{h} \left(\frac{\partial \bar{w}}{\partial \bar{z}}\right)^{\bar{h}} \left(\frac{\partial \bar{w}'}{\partial \bar{z}'}\right)^{\bar{h}} \langle 0|\phi(w,\bar{w})\phi(w',\bar{w}')|0\rangle . \tag{3.8}$$

To find out for which conformal transformations the relation (3.8) is fulfilled, we consider the infinitesimal conformal transformations defined by

$$\begin{cases} z \to w(z) = z + \epsilon_n z^{j+1} \\ \bar{z} \to \bar{w}(\bar{z}) = \bar{z} + \bar{\epsilon}_n \bar{z}^{j+1} \end{cases} \tag{3.9}$$

where $\epsilon_j, \bar{\epsilon}_j \to 0^+$. For instance, $j = 0$ corresponds to an infinitesimal scale dilation, $j = 1$ to an infinitesimal rotation and $j = -1$ to an infinitesimal space-time translation of the system. We also impose that correlation functions are invariant under infinitesimal conformal transformations, i.e.

$$\langle 0|\phi(\omega,\bar{\omega})\phi(\omega',\bar{\omega}')|0\rangle = \frac{1}{(\omega-\omega')^{2h}}\frac{1}{(\bar{\omega}-\bar{\omega}')^{2\bar{h}}} \tag{3.10}$$

in the long-range limit. It is straightforward to show that the relation (3.8) is only fulfilled for $n = 0, \pm 1$. Therefore, correlation functions are only invariant for infinitesimal transformations $\omega(z) = z+\epsilon_{-1}+\epsilon_0 z+\epsilon_1 z^2$. Only these transformations leave the vacuum state invariant (see, e.g. Ref. [9]).

The field $\phi(z,\bar{z})$ is called a *primary field* of the theory and the corresponding exponents $(h,\bar{h})$ are called *conformal dimensions*. The primary fields play a crucial role since they determine the physical correlations functions of the system. The conformal dimensions determine the *critical exponents* of the physical correlation functions and characterize the critical points of the system.

3.3 Evaluation of conformal dimensions

In order to evaluate the conformal dimensions $(h,\bar{h})$ of a primary field $\phi(z,\bar{z})$, one makes a finite-size analysis of the system. This is made by placing the system in a periodic box of length L. This causes a change in the energy spectrum of the system and a gap of order $(1/L)$ arises. It is convenient to define the following variables

$$\begin{cases} z = ix + v\tau \\ \bar{z} = ix - v\tau \end{cases} \tag{3.11}$$

where $\tau = -it$ is the Euclidean time with $t \in]-\infty,\infty[$ and the space coordinate belongs the domain $x \in [0,L[$. The suitable conformal transformation is now defined by

$$\begin{cases} z \rightarrow w(z) = e^{2\pi z/L} \\ \bar{z} \rightarrow \bar{w}(\bar{z}) = e^{2\pi\bar{z}/L}. \end{cases} \tag{3.12}$$

The above conformal transformation maps the cylinder defined by the complex coordinates $(z,\bar{z})$ onto the full complex plane defined by the coordinates $(w,\bar{w})$. The vacuum state of the system changes from $|0\rangle_L$ in the cylinder to $|0\rangle_P$ in the full complex plane. The correlation function in the cylinder and in the full complex plane satisfies the following relation [see Eq. (3.7)]

$$\begin{aligned} {}_L\langle 0|\phi(z,\bar{z})\phi(z',\bar{z}')|0\rangle_L &= \left(\frac{\partial w}{\partial z}\right)^h \left(\frac{\partial w'}{\partial z'}\right)^h \left(\frac{\partial \bar{w}}{\partial \bar{z}}\right)^{\bar{h}} \left(\frac{\partial \bar{w}'}{\partial \bar{z}'}\right)^{\bar{h}} \times \\ &\times {}_P\langle 0|\phi(w,\bar{w})\phi(w',\bar{w}')|0\rangle_P, \end{aligned} \tag{3.13}$$

where the correlation function in the full complex plane is given by expression (3.10). Using the conformal transformation (3.12), the correlation function in the cylinder reads

$$_L\langle 0|\phi(z,\bar{z})\phi(z',\bar{z}')|0\rangle_L = \left[\frac{\pi/L}{\sinh(2\pi(z-z')/L)}\right]^{2h} \cdot \left[\frac{\pi/L}{\sinh(2\pi(\bar{z}-\bar{z}')/L)}\right]^{2\bar{h}} \tag{3.14}$$

which for $x > x'$ can be expanded as

$$\begin{aligned}\langle 0|\phi(z,\bar{z})\phi(z',\bar{z}')|0\rangle_L &= \sum_{N,\bar{N}=0}^{\infty} a_N a_{\bar{N}}\, e^{-i(2\pi/L)(h-\bar{h}+N-\bar{N})(x-x')} \times \\ &\quad \times e^{i(2\pi/L)(h+\bar{h}+N+\bar{N})v(t-t')}\end{aligned} \tag{3.15}$$

where $a_N = \Gamma(h+\bar{h}+N)/[\Gamma(h+\bar{h})N!]$. On the other hand, the Lehman spectral representation for the correlation function yields

$$\langle 0|\phi(z,\bar{z})\phi(z',\bar{z}')|0\rangle_L = \sum_{|Q\rangle} e^{-i(P_Q^L-P_0^L)(x-x')}.e^{i(E_Q^L-E_0^L)(t-t')}|\langle 0|\phi(0,0)|Q\rangle_L|^2 \tag{3.16}$$

where one has used a complete set of intermediate eigenstates $|Q\rangle_L$ of the Hamiltonian and momentum operator, whose eigenvalues for the finite system are E_Q^L and P_Q^L, respectively.

Comparison of expressions (3.15) and (3.16) gives the finite-size expressions from which the conformal dimensions can be extracted

$$\begin{cases} E_Q^L - E_0^L &= \frac{2\pi}{L}v(h+\bar{h}+N+\bar{N}) \\ P_Q^L - P_0^L &= \frac{2\pi}{L}(h-\bar{h}+N-\bar{N}). \end{cases} \tag{3.17}$$

Therefore, to each primary field $\phi(z,\bar{z})$ of conformal dimensions $(h,\bar{h})$ it corresponds an infinite number of states $|Q\rangle$ labelled by the numbers $(N,\bar{N})$ with energy and momentum E_Q^L and P_Q^L, respectively. The state that corresponds to the smallest gap (i.e. $N=\bar{N}=0$) must be non-degenerate and is called a highest-weight state (HWS) of the associated Virasoro algebra and will be denoted by $|h,\bar{h}\rangle$. The conformal dimensions are thus given by the finite-size difference between energy and momentum of the first excited state relatively to the vacuum state of the system. This highly non-trivial result is one of the most powerful ones in conformal-field theory.

3.4 Representation of the conformal group

The group associated with conformal transformations is represented by the underlying algebra: the Virasoro algebra. The generators of that algebra are denoted by L_j and $\bar{L}_j$ (with $j = 0, \pm 1, \pm 2, ...$) and are such that

$$\begin{cases} L_j & : \quad z \rightarrow z + \epsilon_j z^{j+1} \\ \bar{L}_j & : \quad \bar{z} \rightarrow \bar{z} + \bar{\epsilon}_j \bar{z}^{j+1} . \end{cases} \tag{3.18}$$

The Virasoro generators obey the following commution relations

$$\begin{aligned} [L_j, L_l] &= (j-l)L_{j+l} + \frac{\mathcal{C}}{12} j(j^2-1)\delta_{j+l,0} \\ \left[\bar{L}_j, \bar{L}_l\right] &= (j-l)\bar{L}_{j+l} + \frac{\mathcal{C}}{12} j(j^2-1)\delta_{j+l,0} \\ \left[L_j, \bar{L}_l\right] &= 0 \end{aligned} \tag{3.19}$$

where $\mathcal{C}$ is the so called conformal anomaly (or central charge), which arises from the normal ordering procedure relatively to the vacuum of the theory. This anomaly does not appear in the corresponding classical Virasoro algebra.

We construct now the irreducible representation of the Virasoro algebra. For simplicity, we first consider only the holomorphic part. As usual, we first search for the HWS in the Hilbert space of the considered system. The HWS's are eigenstates of the generator L_0 whose eigenvalue is precisely the corresponding conformal dimension h. The HWS's are annihilated by the generators $L_{j>0}$ and the generators $L_{j<0}$ when acting on them construct a tower of states, i.e.

$$\begin{aligned} L_0|h\rangle &= h|h\rangle , \\ L_{j>0}|h\rangle &= 0 , \\ L_{j<0}|h\rangle &= |h+j\rangle . \end{aligned} \tag{3.20}$$

A tower-state $|h+j\rangle$ is also an eigenstate of the generator L_0 of eigenvalue $(h+j)$. We consider now both the holomorphic and the antiholomorphic components. It can be shown [9] that the Virasoro algebras HWS $|h, \bar{h}\rangle$ is obtained by applying onto the corresponding vacuum the primary field $\phi(z, \bar{z})$ with conformal dimensions $(h, \bar{h})$ as follows

$$|h, \bar{h}\rangle = \lim_{z, \bar{z} \rightarrow 0} \phi(z, \bar{z})|0\rangle. \tag{3.21}$$

Finally, it is worth to mention that the long-range asymptotics behaviour of primary-field correlation functions (3.5), can be obtained either from the Ward identities of the theory [9] or by considering the following evolution law for the primary fields [23]

$$\phi(z, \bar{z}) = e^{zL_{-1}} e^{\bar{z}\bar{L}_1} \phi(0, 0). \tag{3.22}$$

Bibliography

[1] A. A. Belavin, A. M. Polyakov, and A. B. Zamolodchikov, J. Stat. Phys. **34**, 763 (1984)

[2] A. A. Belavin, A. M. Polyakov, and A. B. Zamolodchikov, Nucl. Phys. B **241**, 333 (1984).

[3] H. W. Blöte, John L. Cardy, and M. P. Nightingale, Phys. Rev. Lett. **56**, 742 (1985).

[4] Ian Affleck, Phys. Rev. Lett. **56**, 746 (1985).

[5] J. Cardy, Nuc. Phys. B **270**, 186 (1986).

[6] For an important collection of relevant articles, see, *Fields, Strings and Critical Phenomena*, (Les Houches 1988) edited by E. Brézin and J. Zinn-Justin (North-Holland, 1990).

[7] H. Saleur, Phys. Rep. **184**, 177 (1989).

[8] C. Itzykson, and J.-M. Drouffe, *Statistical Field Theory - Vol. 2*, (Cambridge University Press, New York, 1989).

[9] D. Boyanovsky, and C. M. Naon, Rev. Nuo. Cim. **13**, N. 2 (1990).

[10] W. M. Koo, and H. Saleur, Nucl. Phys. B **426**, 459 (1994).

[11] A. W. W. Ludwig and I. Affleck, Nucl. Phys. B **428**, 545 (1994).

[12] P. Fendley, A. W. W. Ludwig, and H. Saleur, Nucl. Phys. B **45A**, 29 (1996).

[13] F. Lesage, H. Saleur, and S. Skorik, Phys. Rev. Lett. **76**, 3388 (1996).

[14] H. A. Bethe, Z. Phys. **71**, 205 (1931).

[15] C. N. Yang, Phys. Rev. Lett. **19**, 1312 (1967).

[16] E. H. Lieb, and F. Y. Wu, Phys. Rev. Lett. **20**, 1445 (1968).

[17] V. E. Korepin, N. M. Bogoliubov, and A. G. Izergin, *Quantum Inverse Scattering Method and Correlation Functions* (Cambridge University Press, 1993).

[18] N. M. Bogoliubov, A. G. Izergin, and N. Yu. Reshetikhin, J. Phys. A **20**, 5361 (1987).

[19] A. G. Izergin, V. E. Korepin, and N. Yu. Reshetikhin, J. Phys. A: Math. Gen. **22**, 2615 (1989).

[20] H. Frahm, and V. E. Korepin, Phys. Rev. B **42** 10553 (1990).

[21] H. Frahm, and V. E. Korepin, Phys. Rev. B **43** 5653 (1991).

[22] R. Shankar, Rev. of Mod. Phys. **66**, 129 (1994);

[23] P. Christe and M. Henkel, *Introduction to Conformal Invariance and its Applications to Critical Phenomena*, (Springer-Verlag, Berlin, 1993).

[24] See, e.g. M. Schottenloher, *A Mathematical Introduction to Conformal Field Theory*, (Springer-Verlag, Berlin, 1997).

Chapter 4

Conformal Invariance and Conservation Laws in the 1D Hubbard Model

4.1 Introduction

Main goal of this chapter is to introduce the theoretical tools necessary for the study of one-electron spectral functions properties of the 1D Hubbard Model presented in Chapter 2. By allowing the study of finite-energy correlation function associated with the creation of α-Yang particles, the critical theory introduced in this chapter is a generalization for finie energies of the low-energy approach of Refs. [1, 2]. Fortunately, the one-particle spectral function upper-Hubbard-band is determined by excitations involving the creation of one c-Yang particle, one holon and one spinon.

However, the validity of the of the conformal-field theories (CFT's) studied in this chapter is restricted to small yet finite densities of $\gamma > 0$ pseudoparticles $n_{\alpha,\gamma} \equiv N_{\alpha,\gamma}/L$. Importantly, we find that the Fourier transforms of the general (x,t) correlation function expressions provide, in some limits, the correct expressions, valid for vanishing small densities $n_{\alpha,\gamma}$ of $\gamma > 0$ pseudoparticles.

Although the addition to the system of $\gamma > 0$ pseudoparticles is not a dominant process in what the one-electron upper-Hubbar-band is concerned, the theory here presented also describes the creation of $\gamma > 0$ pseudoparticles.

The finite-energy behaviour of correlation functions of (1+1) dimensional solvable many-electron systems defined in a discrete lattice remains as an important challenge. Previous studies of Frahm and Korepin on the 1D Hubbard model [1, 2] refer only to the asymptotic behaviour of correlation functions at low-energy.

In this chapter we combine the pseudoparticle operational basis with the conservation laws associated with the integrability of the 1D Hubbard model and extract valuable information on the finite-energy asymptotic behaviour of corre-

lation functions.

4.2 The conservation laws in the pseudoparticle basis

As mentioned in previous sections, the 1D Hubbard model is solvable by the BA technique [3, 4, 5]. Shastry [6] has studied the relationship between the BA solvability and the concept of "integrability", (by analogy to the conservation laws of integrable classical systems). He has shown that in the thermodynamic limit, $L \rightarrow \infty$, there is an infinite number of commuting operators corresponding to the expected conservation laws.

We find below that the symmetries associated with this infinite set of conservation laws, when expressed in the pseudoparticle operational representation, provides valuable information on the model correlation functions.

The 1D Hubbard model in a magnetic field H and chemical potential μ reads

$$\hat{H} = \hat{H}_{SO(4)} + \sum_{\alpha} \mu_{\alpha} 2\hat{S}_{z}^{\alpha} \; , \tag{4.1}$$

where $\hat{H}_{SO(4)}$ is given by Eq. (2.7), $\mu_c = \mu$, $\mu_s = \mu_0 H$ (μ_0 is the Bohr magneton) and $\hat{S}_{z}^{c}$ and $\hat{S}_{z}^{s}$ are the diagonal generators of the η-spin $SU(2)$ and spin $SU(2)$ algebras given in Eqs. (2.8) and (2.9), respectively.

There remain important open issues regarding the nature, number, and utility of the conservation laws in the 1D Hubbard model. First, what is the total number of conservation laws ? For large but finite L, the number of conservation laws found in Ref. [7] is $L+1$, including the electron number and the magnetization. This number appears insufficient to ensure the integrability of the model, which by analogy to classical mechanics ought to require a *minimum* number of commuting conservation laws equal to the number of degrees of freedom, which is $2L$. Second, what are the physical implications of the conservation laws and how can they be used ?

In this chapter we provide insights into both these open issues by showing that the pseudoparticle representation allows one to write down explicit expressions for a total of $2L+4$ independent conservation laws. Further, although one cannot in general find explicit expressions for the extra conservation laws in terms of the original electron operators, we show in a particular limit that the $L+3$ conservation laws beyond those found in [6, 7] are *non-local* when expressed in terms of the electron operators, thus explaining why they were not previously found.

The solvability of the 1D Hubbard model is restricted to the Hilbert subspace spanned by the LWS's of the spin and η-spin algebras [8]. However, the use of the $SO(4)$ algebra reveals that the model is integrable in the whole Hilbert space.

The conservation laws of Refs. [6, 7] are closely related to that integrability – the total number of pseudoparticle branches of the BA operator basis of Ref. [9] is $L+1$ and equals the number of these independent conservation laws. These branches are labelled by the pseudoparticle quantum numbers α, γ with $\alpha = c, s$ and $\gamma = 0, 1, 2, ..., \frac{L}{2}$ and $\gamma = 0, 1, 2, ..., \frac{L}{2} - 1$ for c and s, respectively. (These pseudoparticles are well-defined objects when L is large and the string hypothesis becomes valid [8]).

Based on both the anticommuting α, γ pseudoparticle and the commuting α-Yang particle characters and on the completeness of the corresponding basis, we find that the set of $L+3$ *charge* commuting operators $\hat{\mathcal{N}}_\alpha$ and $\hat{N}_{\alpha,\gamma}$ correspond to independent conservation laws. Importantly, the α, γ pseudoparticles obey *independent* right ($\iota = +1$) and left ($\iota = -1$) conservation laws, with $\iota = sgn(q)$. This introduces the conserved number operators $\hat{N}_{\alpha,\gamma,\iota}$. It follows that the $L+4$ charge and *current* operators

$$\hat{\mathcal{N}}_\alpha\,, \qquad \hat{N}_{\alpha,\gamma} = \sum_\iota \hat{N}_{\alpha,\gamma,\iota}\,; \tag{4.2}$$

$$\hat{J}_{\alpha,\gamma} = \frac{1}{2}\sum_\iota \iota \hat{N}_{\alpha,\gamma,\iota}\,, \tag{4.3}$$

refer to independent conservation laws and commute with the Hamiltonian and among themselves, i.e. $[\hat{H}_{SO(4)}, \hat{\mathcal{N}}_\alpha] = [\hat{H}_{SO(4)}, \hat{N}_{\alpha,\gamma}] = [\hat{H}_{SO(4)}, \hat{J}_{\alpha,\gamma}] = 0$ and also $[\hat{N}_{\alpha,\gamma}, \hat{N}_{\alpha',\gamma'}] = 0$, $[\hat{J}_{\alpha,\gamma}, \hat{J}_{\alpha',\gamma'}] = 0$, $[\hat{N}_{\alpha,\gamma}, \hat{J}_{\alpha',\gamma'}] = 0$, and $\hat{\mathcal{N}}_\alpha$ also commutes with all these operators. Thus, in the pseudoparticle basis we see explicitly that the total number of conservation laws is indeed greater than the $2L$ needed to ensure "integrability".

In general, the transformation between electronic and pseudoparticle states is not known. Therefore, we do not expect simple expressions and there is not an obvious one-to-one correspondence with the operators in Eqs. (4.2) and (4.3). Out of the additional $L+3$ conservation laws beyond those found in Refs. [6, 7], two of them are essentially trivial and are the *non-local* operators $\hat{\mathbf{S}}^\alpha.\hat{\mathbf{S}}^\alpha$ with eigenvalue $S^\alpha[S^\alpha+1]$. The other new laws are also non-local in the electron representation, a result that we can establish both numerically for small chains and analytically in the limit $U/t \to 0$. In this limit the $L+1$ commuting operators of Ref. [7] become diagonal in the k momentum basis and can be expressed as a sum of two terms, corresponding to right-moving ($\nu = +1$) and left-moving ($\nu = -1$) *electrons*. For instance, the number of particles, the Hamiltonian, and the first non-trivial commuting operator [7] can be written as

$$\hat{N} = \sum_\nu \hat{N}_\nu, \tag{4.4}$$

$$\hat{H} = \sum_\nu \hat{H}_\nu \tag{4.5}$$

and

$$\hat{j} = \sum_{\nu} \hat{j}_{\nu}, \tag{4.6}$$

respectively. Importantly, for each $\nu = \pm 1$ component, the operator is conserved independently. Thus, in addition to the three operators $\hat{N}$, $\hat{H}$, and $\hat{j}$, we can define three independent operators $\hat{N}^{-} \equiv \sum_{\nu} \nu \hat{N}_{\nu}$, $\hat{H}^{-} \equiv \sum_{\nu} \nu \hat{H}_{\nu}$, and $\hat{j}^{-} \equiv \sum_{\nu} \nu \hat{j}_{\nu}$ that are also conserved. Using Fourier transforms to re-express these operators in terms of the electron operators in coordinate space, $c^{\dagger}_{j\sigma}$ and $c_{j\sigma}$, we find that

$$\hat{N}^{-} = \frac{i}{\pi} \sum_{j,j',\sigma} \frac{[1-(-1)^{|j-j'|}]}{(j-j')} c^{\dagger}_{j\sigma} c_{j'\sigma} \,, \tag{4.7}$$

$$\hat{H}^{-} = -\frac{it}{\pi} \sum_{j,j',\sigma} [1+(-1)^{|j-j'|}] \sum_{l=\pm 1} \frac{1}{(j-j'+l)} c^{\dagger}_{j\sigma} c_{j'\sigma} \tag{4.8}$$

and

$$\hat{j}^{-} = \frac{it^2}{\pi} \sum_{j,j',\sigma} [1-(-1)^{|j-j'|}] \sum_{l=\pm 1} \frac{l}{(j-j'+2l)} c^{\dagger}_{j\sigma} c_{j'\sigma} \tag{4.9}$$

which are the first three of the new, independent conservation laws (for $U/t \rightarrow 0$). Applying similar manipulations to the other operators in Ref. [7], we can find the expressions for the remainder of the $L+1$ new conservation laws. In contrast to the *local* operators of Refs. [7] (i.e. whose expressions involve a single j summation), the new laws are *non-local*. At finite values of U we do not have explicit expressions for the non-local conservation laws in terms of electron operators.

In terms of the pseudoparticles, the conservation laws simply fix the occupation numbers $[\{\mathcal{N}_{\alpha}\}, \{N_{\alpha,\gamma}\}, \{J_{\alpha,\gamma}\}]$ and all energy eigenstates can be specified (albeit not uniquely) by giving the values of these numbers.

4.3 Compact reference states and the Hamiltonian at critical points

We now introduce the convenient concept of compact reference states (CRS's), which are special reference states among all the eigenstates of the model.

A canonical ensemble is characterized by constant electron numbers $N_{\uparrow}$ and $N_{\downarrow}$. Each canonical ensemble can be divided into a set of *sub-canonical ensembles* associated with different constant values of the pseudoparticle numbers. The relation between a canonical ensemble and a sub-canonical ensemble is obtained from the sum rules that relate the electronic numbers with the pseudoparticle numbers, Eqs. (2.114).

As we have seen in Chapter 2, in the pseudoparticle representation the GS corresponds to a compact filled Fermi sea of $\alpha, 0$ pseudoparticle. Its pseudomomentum occupancy corresponds to a symmetric ($J_{\alpha,0} = 0$) or quasi-symmetric ($J_{\alpha,0} = \pm\frac{1}{2}$) distribution. Following equations (2.75) the GS is such that $N_{\alpha,\gamma} = 0$ for $\gamma > 0$ and $\mathcal{N}_\alpha = 0$. The transitions from the GS to excited states obey and are restricted by the sum rules (2.114). These transitions are specified by the corresponding changes in the generalized charge numbers $\Delta N_{\alpha,\gamma}$, the generalized current numbers $\Delta J_{\alpha,\gamma}$ and the numbers $\mathcal{N}_\alpha$. Among these transtions, we consider the GS - CRS transitions, which involve small densities of pseudoparticle-pseudohole processes $\Delta n_{\alpha,\gamma} \equiv \Delta N_{\alpha,\gamma}/L$ and $n_\alpha \equiv \mathcal{N}_\alpha/L$.

In general, both the pseudomomentum width and energy width of the α, γ pseudoparticle bands are finite. Therefore, for each sub-canonical ensemble corresponding to a CRS of fixed $N_{\alpha,\gamma}$ and $\mathcal{N}_\alpha$ numbers there are two alternative choices of CRS's α, γ pseudomomentum occupancies which we label with the quantum number $\lambda = \pm 1$. When $\lambda = +1(\text{or } -1)$ the CRS has a pseudomomentum occupancy which corresponds to a compact α, γ pseudoparticle (or pseudohole) filled Fermi sea around $q_{\alpha,\gamma} = 0$. Note that the GS- $\alpha, 0$ occupancies correspond always to $\lambda = +1$.

The alternative $\lambda = +1$ and $\lambda = -1$ CRS's α, γ occupancies are two extreme cases. For instance, one could start from a $\lambda = +1$ CRS α, γ occupancy and, by sucessive elementary α, γ pseudoparticle - pseudohole processes, arrive to the corresponding $\lambda = -1$ CRS α, γ occupancy (or vice-versa). Importantly, the critical theory studied in this thesis corresponds to Hilbert subspaces spanned by the CRS's and the tower states obtained by a *small density* of α, γ pseudoparticle-pseudohole processes of low-energy and small-momentum relative to the initial CRS. Thus, we will not consider the whole tower of Hamiltonian eigenstates. This means that we decouple the two Hilbert subspaces associated with both extremes $\lambda = 1$ and $\lambda = -1$, of the α, γ tower of states and that the intermediate tower states are out of the Hilbert subspaces of the critical theory presented here.

The GS - CRS transitions are such that for each α, γ band the final state has either $\lambda = +1$ or $\lambda = -1$ CRS occupancy. Therefore, the $\lambda = \pm 1$ values are always alternative and the expressions does not include λ summations. On the other hand, for the electronic densities and spin densities considered in the present study, the GS - CRS transitions to $\alpha, 0$ LWS's involve, in general, a large number of pseudoparticles. Therefore, for $\gamma = 0$ we consider $\lambda = +1$ only.

For $\lambda = 1(\text{or } -1)$, the compact α, γ pseudoparticle (or pseudohole) CRS occupancy corresponds to pseudomomenta

$$q \in [q^{(-1)}_{F_{\alpha,\gamma,\lambda=\pm 1}}, q^{(+1)}_{F_{\alpha,\gamma,\lambda=\pm 1}}], \tag{4.10}$$

where

$$q^{(\pm 1)}_{F_{\alpha,\gamma,\lambda}} = \pm q_{F\alpha,\gamma,\lambda} + \mathcal{O}\left(\frac{1}{L}\right), \tag{4.11}$$

and

$$q_{F\alpha,\gamma,+1} = \frac{\pi N_{\alpha,\gamma}}{L}\,; \qquad q_{F\alpha,\gamma,-1} = \frac{\pi N^{h}_{\alpha,\gamma}}{L} \tag{4.12}$$

are the $\lambda = +1$ or $\lambda = -1$ CRS's pseudo-Fermi points of the α, γ occupied band.

In the case of the critical theory here studied, which corresponds to Hilbert subspaces spanned by energy eigenstates generated from a small density of α, γ pseudoparticle - pseudohole processes around the CRS's compact occupancies, there is an extra conservation law associated with the quantum number λ. In this case we can call $\alpha, \gamma, \lambda, \iota$ pseudoparticles the α, γ, ι pseudoparticles whose occupancies in the CRS is of $\lambda = +1$ or $\lambda = -1$ type. This allows us to introduce the pseudoparticle number $N_{\alpha,\gamma,\lambda,\iota}$ and the corresponding operator $\hat{N}_{\alpha,\gamma,\lambda,\iota}$.

Let us introduce the $\alpha, \gamma, \lambda, \iota$ pseudoparticle operators which obey the following anticommutation relations

$$\left\{ b^{\dagger}_{\kappa,\alpha,\gamma,\lambda,\iota}, b_{\kappa',\alpha',\gamma',\lambda',\iota'} \right\} = \delta_{\kappa,\kappa'}\delta_{\alpha,\alpha'}\delta_{\gamma,\gamma'}\delta_{\lambda,\lambda'}\delta_{\iota,\iota'}\,. \tag{4.13}$$

where the pseudomomentum κ is given by

$$\kappa = \begin{cases} q - q^{(+1)}_{F_{\alpha,\gamma,\lambda}}, & \text{for} \quad 0 < q < q^{(+1)}_{\alpha,\gamma,\lambda}, \quad \iota = +1 \\ \\ q - q^{(-1)}_{F_{\alpha,\gamma,\lambda}}, & \text{for} \quad q^{(-1)}_{\alpha,\gamma,\lambda} < q < 0, \quad \iota = -1. \end{cases} \tag{4.14}$$

Moreover, we can write

$$\hat{N}_{\alpha,\gamma,\lambda,\iota} = \sum_{\kappa} \hat{N}_{\alpha,\gamma,\lambda,\iota}(\kappa)\,, \tag{4.15}$$

where the operator $\hat{N}_{\alpha,\gamma,\lambda,\iota}(\kappa)$ reads

$$\hat{N}_{\alpha,\gamma,\lambda,\iota}(\kappa) = b^{\dagger}_{\kappa,\alpha,\gamma,\lambda,\iota} b_{\kappa,\alpha,\gamma,\lambda,\iota}\,. \tag{4.16}$$

The topological momentum shift operator, Eq. (2.113), can be rewritten in terms of κ and ι summations as

$$U^{\pm 1}_{\alpha,\gamma,\lambda} = \exp[\sum_{\kappa,\iota} b^{\dagger}_{\kappa \mp \frac{\pi}{L},\alpha,\gamma,\lambda,\iota} b_{\kappa,\alpha,\gamma,\lambda,\iota}]\,. \tag{4.17}$$

As for the GS, Eq. (2.107), we can generate a CRS from the vacuum $|V\rangle$ by application onto it of pseudoparticle generators. A CRS is then a generalization of the GS such that

$$|CRS\rangle \;=\; \prod_{\alpha,\gamma,\iota} [U^{l_{\alpha,\gamma,\lambda}}_{\alpha,\gamma}]^{j_{\alpha,\gamma}} \left[\prod_{\iota\lambda\kappa < \Delta q^{(\iota)}_{F_{\alpha,\gamma,\lambda}}} b^{\dagger}_{\kappa,\alpha,\gamma,\lambda,\iota} \right] |V\rangle\,, \tag{4.18}$$

where the productory refers to occupied α, γ branches only, $j_{\alpha,\gamma} = 0, 1$ is defined as

$$j_{\alpha,\gamma} = \frac{1-(-1)^{\Delta\bar{N}_{\alpha,\gamma}}}{2}, \tag{4.19}$$

and $\Delta\bar{N}_{\alpha,\gamma}$ are the changes in the $\bar{N}_{\alpha,\gamma}$ numbers associated with the GS - CRS transition. We emphasize that when $j_{\alpha,\gamma} = 0$ the corresponding topological momentum shift operator factor reduces to the identity operator and there is no α,γ pseudomomentum shift. The number $l_{\alpha,\gamma}$ of expression (4.18) is either $l_{\alpha,\gamma} = +1$ or $l_{\alpha,\gamma} = -1$, depending on whether the GS - CRS transition shifts the α,γ pseudomomentum Fermi sea to the right or to the left, respectively.

In the case of $\gamma > 0$ bands the number $l_{\alpha,\gamma,\lambda}$ is uniquely defined by the property that the limits of the α,γ pseudo-Brillouin zones are symmetric for all the state occupancies. It is straightforward to show that this is only fulfilled either for $l_{\alpha,\gamma,\lambda=+1}$ or $l_{\alpha,\gamma,\lambda=-1}$.

The CRS pseudo-Fermi occupancies defined in Eqs. (4.11)-(4.12) correspond to current numbers such that $J_{\alpha,\gamma} = 0$ or $J_{\alpha,\gamma} = \pm\frac{1}{2}$. Following conservation laws associated with the $N_{\alpha,\gamma,\lambda,\iota}$ numbers, we can define a CRS in a more general way as a reference state for the family of states with the same values of pseudoparticle numbers $N_{\alpha,\gamma,\lambda,\iota}$ and numbers $\mathcal{N}_\alpha$. Such state has independent compact pseudoparticle momentum occupancies for right ($\iota = +1$) and left ($\iota = -1$) pseudoparticles. In this general case the CRS pseudo-Fermi points are of the form

$$q^{(\pm 1)}_{F_{\alpha,\gamma,\lambda}} = q_{F\alpha,\gamma,\lambda,\iota} + \mathcal{O}\left(\frac{1}{L}\right), \tag{4.20}$$

where

$$q_{F\alpha,\gamma,+1,\iota} = \iota\,\frac{\pi N_{\alpha,\gamma,\iota}}{L}; \qquad q_{F\alpha,\gamma,-1,\iota} = \iota\,\frac{\pi N^h_{\alpha,\gamma,\iota}}{L}, \tag{4.21}$$

and $N^h_{\alpha,\gamma,\iota}$ is the number of ι pseudoholes in the α,γ band.

Following the α,γ generalized charge conservation laws, Eq. (4.2), we can decouple the Hubbard Hamiltonian (4.1) into two terms. Expressing the diagonal generators of the η-spin and spin $SU(2)$ algebras in terms of the electronic numbers and writing the chemical potential as $\mu_c = \mu = -\epsilon^0_{c,0}(q^0_{F_{c,0,1}}) - 1/2\epsilon^0_{s,0}(q^0_{F_{s,0,1}})$ and the magnetic field as $\mu_s = \mu_0 H = -\epsilon^0_{s,0}(q^0_{F_{s,0,1}})$ [9], the Hubbard Hamiltonian in a chemical potential and magnetic field, Eq. (4.1), can be rewritten as

$$\hat{H} = \hat{H}_0 + \hat{H}_{CL} \tag{4.22}$$

where $\hat{H}_0$ contains the α,γ generalized charge operators $\hat{N}_{\alpha,\gamma}$ and $\hat{\mathcal{N}}_\alpha$ of Eq. (4.2) and is given by

$$\hat{H}_0 = \sum_\alpha \left[2\mu_\alpha[\sum_{\gamma>0}(\delta_{\alpha,s}+\gamma)\hat{N}_{\alpha,\gamma}] + \hat{\mathcal{N}}_\alpha\right] + \sum_{\alpha,\gamma>0}\mu_{\alpha,\gamma,\lambda}\hat{N}_{\alpha,\gamma} \tag{4.23}$$

and

$$\hat{H}_{CL} = \hat{H}_{SO(4)} - \sum_{\alpha,\gamma} \mu_{\alpha,\gamma,\lambda} \hat{N}_{\alpha,\gamma} - \mu_c L \tag{4.24}$$

where

$$\mu_{\alpha,\gamma,\lambda} = \epsilon^0_{\alpha,\gamma}(q^0_{F\alpha,\gamma,\lambda}). \tag{4.25}$$

The pseudo-Fermi points $q^0_{F_{\alpha,\gamma,\lambda}}$ are those of the initial GS and are given by Eq. (2.110). The quantity $\mu_{\alpha,\gamma,\lambda}$ represents the energy associated with increasing the number of α,γ pseudoparticles by one.

Since the Hamiltonians $\hat{H}_{SO(4)}$, $\hat{H}$, $\hat{H}_{CL}$ and $\hat{H}_0$ commute with each other, all eigenstates of $\hat{H}_{SO(4)}$ (which we denote by $|\psi\rangle$) are also eigenstates of $\hat{H}$, $\hat{H}_{CL}$ and $\hat{H}_0$. In particular,

$$\hat{H}_0|\psi\rangle = \omega_0|\psi\rangle, \tag{4.26}$$

where

$$\omega_0 = \sum_{\alpha} \left[2\mu_\alpha [\sum_{\gamma>0} (\delta_{\alpha,s} + \gamma) N_{\alpha,\gamma}] + \mathcal{N}_\alpha \right] + \sum_{\alpha,\gamma>0} \mu_{\alpha,\gamma} N_{\alpha,\gamma}, \tag{4.27}$$

can be shown to be the excitation energy of a GS - CRS transition, i.e.

$$\omega_0 = \langle CRS|\hat{H}|CRS\rangle - \langle GS|\hat{H}|GS\rangle \tag{4.28}$$

where $\hat{H}$ is the full Hamiltonian, Eqs. (4.1) and (4.22), and the CRS $N_{\alpha,\gamma}$ and $\mathcal{N}_\alpha$ numbers are the ones which apperar in the energy ω_0, Eq. (4.27).

Following the α,γ generalized current conservation laws $\hat{J}_{\alpha,\gamma}$, Eq. (4.3, we decouple the total momentum operator (2.105) as follows

$$\hat{P} = \hat{P}_0 + \hat{P}_{CL} \tag{4.29}$$

where

$$\hat{P}_0 = \sum_{\alpha,\gamma} 2C_{\alpha,\gamma} q^0_{F_{\alpha,\gamma,\lambda}} : \hat{J}_{\alpha,\gamma} : + \pi \sum_{\gamma>0} [(1+\gamma)\hat{N}_{c,\gamma} + \hat{\mathcal{N}}_c] \tag{4.30}$$

and

$$\hat{P}_{CL} = \sum_{q,\alpha,\gamma} C_{\alpha,\gamma} q \hat{N}_{\alpha,\gamma}(q) - 2C_{\alpha,\gamma} q^0_{F_{\alpha,\gamma,\lambda}} : \hat{J}_{\alpha,\gamma} : . \tag{4.31}$$

The quantity $C_{\alpha,\gamma} q^0_{F_{\alpha,\gamma,\lambda}}$ represents the momentum associated with the variation of the current number $J_{\alpha,\gamma}$ by 1/2. The operators $\hat{P}$, $\hat{P}_0$ and $\hat{P}_{CL}$ commute with each other. This means that all these momentum operators have the same momentum eigenstates, the corresponding eigenvalues being in general different. In particular

$$\hat{P}_0|\psi\rangle = k_0|\psi\rangle \tag{4.32}$$

where

$$k_0 = \sum_{\alpha,\gamma} 2C_{\alpha,\gamma} q^0_{F_{\alpha,\gamma,\lambda}} \Delta J_{\alpha,\gamma} + \pi \sum_{\gamma>0} [(1+\gamma)N_{c,\gamma} + \mathcal{N}_c], \tag{4.33}$$

can be shown to be the excitation momentum of a GS - CRS transition, i.e.

$$k_0 = \langle CRS|\hat{P}|CRS\rangle - \langle GS|\hat{P}|GS\rangle \tag{4.34}$$

where $\hat{P}$ is the operator (4.29) and the CRS numbers are the ones of Eq. (4.33).

Importantly, one restrict our study to CRS's such that the Hamiltonians $\hat{H}$ and $\hat{H}_{CL}$ have the same GS. Fortunately, these CRS's and associated tower of states span the Hilbert space subspaces which determine and control the leading-order terms of the correlation functions expressions [10]. For the case of the $c, \gamma > 0$ (or $s, \gamma > 0$) bands this is always true for $\lambda = -1$ (or $\lambda = +1$) CRS occupancies. In the case of $\lambda = +1$ and $\lambda = -1$ CRS occupancies in $c, \gamma > 0$ and $s, \gamma > 0$ bands, respectively, $\hat{H}$ and $\hat{H}_{CL}$ have also the same GS if we define these Hamiltonians in the same particular Hilbert subspaces of fixed excitation momentum.

Since in the ome-electron stuidies of Chapter 5 the dominant excitations involve the creation of c-Yang particles but no creation of the $\gamma > 0$ pseudoparticles, in this thesis we do not further discuss the questions concerning these restrictions in the choice of $\lambda = +1$ or $\lambda = -1$ CRS occupancies.

4.4 Finite-size analysis and critical exponents

In this section we study the critical theory associated with the low-energy and small-momentum Hilbert subspace of $\hat{H}_{CL}$ and $\hat{P}_{CL}$. We start by restricting our study to CRS's with small yet finite densities $n_{\alpha,\gamma}$ of $\gamma > 0$ pseudoparticle. On the other hand, the theory here presented applies both to vanishing and finite densities n_α of α-Yang particles.

In this case the conformal invariance of $\hat{H}_{CL}$ and $\hat{P}_{CL}$ provides information on the finite-energy and finite-momentum physics of the original 1D Hubbard model, as we find below.

Let us construct the low-energy Hamiltonian associated with $\hat{H}_{CL}$. By combining Eqs. (4.24) and (4.25) with Eqs. (2.96) and (2.97), the Hamiltonian (4.24) can be written in normal order relatively to the GS as

$$:\hat{H}_{CL} := \hat{H}_{CL} - E_{GS} = \sum_{j=1}^{\infty} \hat{H}^{(j)}_{CL}, \tag{4.35}$$

where the first-order pseudoparticle-scattering term is given by

$$\hat{H}_{CL}^{(1)} = \sum_{q,\alpha,\gamma} [\epsilon^0_{\alpha,\gamma}(q) - \epsilon^0_{\alpha,\gamma}(q^0_{F\alpha,\gamma,\lambda})] : \hat{N}_{\alpha,\gamma}(q) : , \tag{4.36}$$

and

$$\hat{H}_{CL}^{(j)} = \hat{H}^{(j)} ; \qquad j > 1 , \tag{4.37}$$

where $\hat{H}^{(j)}$ are the Hamiltonians of Eq. (2.96).

The critical-point low-energy Hamiltonian is obtained by linearization of the pseudoparticle bands $\epsilon^0_{\alpha,\gamma}(q) - \epsilon^0_{\alpha,\gamma}(q_{F\alpha,\gamma,\lambda})$ of Eq.(4.36) around the pseudo-Fermi points and by considering only in the Hamiltonian (4.35) the first-order and second-order pseudoparticle scattering terms. We emphasize that consideration of higher-order scattering terms in the Hamiltonian (4.35) leads to energy contributions of third and higher-order in the density of excited pseudoparticles. Since the critical theory here presented refers only to energy contributions of first-order and second-order in the density of pseudoparticles involved in the GS - CRS transitions, these Hamiltonian terms are irrelevant for our study and are not considered here.

Furthermore, we also replace the full Landau f-functions of Eq. (2.98) by their values at the pseudo-Fermi points. The GS normal ordered Hamiltonian at the critical point, which we denote by $: \hat{H}_c :$, is then given by

$$\begin{aligned} : \hat{H}_c : \; &= \sum_{\kappa,\alpha,\gamma,\iota} \iota\kappa v_{\alpha,\gamma,\lambda} : \hat{N}_{\alpha,\gamma,\lambda,\iota}(\kappa) : \\ &+ \frac{1}{L} \sum_{\kappa,\kappa'} \sum_{\alpha,\alpha'} \sum_{\gamma,\gamma'} \sum_{\iota} \frac{1}{2} [f^1_{\alpha,\gamma,\lambda;\alpha',\gamma',\lambda'} : \hat{N}_{\alpha,\gamma,\lambda,\iota}(\kappa) :: \hat{N}_{\alpha',\gamma',\lambda',\iota}(\kappa') : \\ &+ f^{-1}_{\alpha,\gamma,\lambda;\alpha',\gamma',\lambda'} : \hat{N}_{\alpha,\gamma,\lambda,\iota}(\kappa) :: \hat{N}_{\alpha',\gamma',\lambda',-\iota}(\kappa') :] , \end{aligned} \tag{4.38}$$

where

$$v_{\alpha,\gamma,\lambda} \equiv v_{\alpha,\gamma}(q_{F_{\alpha,\gamma,\lambda}}) \tag{4.39}$$

is such that

$$\frac{v_{\alpha,\gamma,\lambda}}{|v_{\alpha,\gamma,\lambda}|} = C_{\alpha,\gamma} . \tag{4.40}$$

The constant $C_{\alpha,\gamma}$ is given in Eq. (2.106). Moreover,

$$f^l_{\alpha,\gamma,\lambda;\alpha',\gamma',\lambda'} = f_{\alpha,\gamma;\alpha',\gamma'}(q_{F_{\alpha,\gamma,\lambda}}, lq_{F_{\alpha',\gamma',\lambda'}}) , \tag{4.41}$$

where $l = \pm 1$, $q_{F_{\alpha,\gamma,\lambda}}$ is given by Eq. (4.12) and the Landau f-functions read

$$
\begin{aligned}
f_{\alpha,\gamma;\alpha',\gamma'}(q,q') &= 2\pi v_{\alpha,\gamma}(q)\Phi_{\alpha,\gamma;\alpha',\gamma'}(q,q') + 2\pi v_{\alpha',\gamma'}(q')\Phi_{\alpha',\gamma';\alpha,\gamma}(q',q) \\
&+ 2\pi \sum_{j=\pm 1}\sum_{\alpha''}\sum_{\gamma''}\theta(N_{\alpha'',\gamma''})\lambda'' v_{\alpha'',\gamma'',\lambda''}\Phi_{\alpha'',\gamma'';\alpha,\gamma}(jq_{F_{\alpha'',\gamma'',\lambda''}},q) \\
&\times \Phi_{\alpha'',\gamma'';\alpha',\gamma'}(jq_{F_{\alpha'',\gamma'',\lambda''}},q') \,. \qquad (4.42)
\end{aligned}
$$

Here the functions $\Phi_{\alpha,\gamma;\alpha',\gamma'}(q,q')$ are the two-pseudoparticle forward-scattering phase shifts. defined in Appendix A2 of Chapter 2.

On the other hand, the GS normal ordered momentum operator is at the critical point given by

$$
\begin{aligned}
:\hat{P}_c: &= :\hat{P}_{CL}: \\
&= \sum_{\kappa,\alpha,\gamma,\iota} C_{\alpha,\gamma\kappa} :\hat{N}_{\alpha,\gamma,\lambda,\iota}(\kappa): \,. \qquad (4.43)
\end{aligned}
$$

When acting on the suitable Hilbert subspaces, the Hamiltonian (4.38) and momentum (4.43) fully define the critical theory here studied.

We will show now that the quantum problem $:\hat{H}_c:$, Eq. (4.38), is conformal invariant. Let us rewrite the f-function expression (4.42) in terms of two-pseudoparticle phase shifts. It is convenient to introduce the following Landau parameters

$$
\mathcal{F}^{j}_{\alpha,\gamma,\lambda;\alpha',\gamma',\lambda'} = \delta_{\alpha,\alpha'}\delta_{\gamma,\gamma'}\lambda v_{\alpha,\gamma,\lambda} + \frac{1}{2\pi}\sum_{l=\pm 1}[l]^{j} f^{l}_{\alpha,\gamma,\lambda;\alpha',\gamma',\lambda'} \,, \qquad (4.44)
$$

where $j = 0, 1$. The use of Eq. (4.42) reveals that the Landau-parameters expression involves exclusively the two-pseudoparticle phase shifts and velocities (4.39) and reads

$$
\mathcal{F}^{j}_{\alpha,\gamma,\lambda;\alpha',\gamma',\lambda'} = \sum_{\alpha'',\gamma''}\theta(N_{\alpha'',\gamma''})\lambda'' v_{\alpha'',\gamma'',\lambda''}\xi^{j}_{\alpha'',\gamma'',\lambda'';\alpha,\gamma,\lambda}\xi^{j}_{\alpha'',\gamma'',\lambda'';\alpha',\gamma',\lambda'} \,, \qquad (4.45)
$$

where $\xi^{j}_{\alpha,\gamma,\lambda;\alpha',\gamma',\lambda'}$ (with $j = 0, 1$) are the following combinations of two-pseudoparticle phase shifts

$$
\xi^{j}_{\alpha,\gamma,\lambda;\alpha',\gamma',\lambda'} = \delta_{\alpha,\alpha'}\delta_{\gamma,\gamma'} + \lambda\sum_{l=\pm 1}[l]^{j}\Phi_{\alpha,\gamma;\alpha',\gamma'}(q_{F_{\alpha,\gamma,\lambda}}, lq_{F_{\alpha',\gamma',\lambda'}}) \,. \qquad (4.46)
$$

These are studied in detail in Appendix A4.

In Appendix B4 it is shown that the use of expressions (4.44)-(4.46) in the critical Hamiltonian (4.38) leads to the following expression for the excitation energy measured relatively to the GS

$$\Delta E = \frac{2\pi}{L}\sum_{\alpha,\gamma}\theta(N_{\alpha,\gamma})\lambda v_{\alpha,\gamma,\lambda}\{[\Gamma^0_{\alpha,\gamma,\lambda}]^2 + [\Gamma^1_{\alpha,\gamma,\lambda}]^2 + \sum_{\iota} N^{ph}_{\alpha,\gamma,\lambda,\iota}\} + \\ + \mathcal{O}\left(\frac{1}{L}\right). \quad (4.47)$$

We note that only when the CRS densities of α, γ pseudoparticles are finite the velocities $v_{\alpha,\gamma,\lambda}$ of expression (4.47) are also finite and the spectrum (4.47) is conformal invariant. The critical theory associated with vanishing small densities of α, γ pseudoparticles is not conformal invariant. In the latter case the critical spectrum is not of the form (4.47) and was studied in Ref. [11].

In Appendix B4 we also arrive to the expression of the excitation momentum relatively to the GS

$$\Delta P = \frac{2\pi}{L}\sum_{\alpha,\gamma}\theta(N_{\alpha,\gamma})\lambda C_{\alpha,\gamma}[\Delta N_{\alpha,\gamma,\lambda}\Delta J_{\alpha,\gamma,\lambda} + \sum_{\iota}\iota N^{ph}_{\alpha,\gamma,\lambda,\iota}]. \quad (4.48)$$

The quantities $\Gamma^0_{\alpha,\gamma,\lambda}$ and $\Gamma^1_{\alpha,\gamma,\lambda}$ are given by

$$\Gamma^0_{\alpha,\gamma,\lambda} = \sum_{\alpha',\gamma'}\theta(N_{\alpha',\gamma'})\xi^0_{\alpha,\gamma,\lambda;\alpha',\gamma',\lambda'}\frac{\Delta N_{\alpha',\gamma',\lambda'}}{2}, \quad (4.49)$$

and

$$\Gamma^1_{\alpha,\gamma,\lambda} = \sum_{\alpha',\gamma'}\theta(N_{\alpha',\gamma'})\xi^1_{\alpha,\gamma,\lambda;\alpha',\gamma',\lambda'}\Delta J_{\alpha',\gamma',\lambda'}, \quad (4.50)$$

respectively, and $N^{ph}_{\alpha,\gamma,\lambda,\iota}$ measures the number of small-momentum and low-energy $\alpha, \gamma, \lambda, \iota$ pseudoparticle - pseudohole processes around the initial CRS's. These processes generate the tower states.

Due to the integer or half-odd integer character of the pseudomomentum numbers $I^{\alpha,\gamma}_j$, Eq. (2.45), the numbers $\Delta J_{\alpha,\gamma,\lambda}$ are integers or half-odd integers depending on the parities of the numbers $\Delta N_{\alpha,\gamma,\lambda}$ as follows

$$\Delta J_{c,0,+1} = \left[\sum_{\alpha,\gamma}\frac{\Delta N_{\alpha,\gamma,\lambda}}{2}\right] \text{ mod } 1, \quad (4.51)$$

$$\Delta J_{\alpha,\gamma,+1} = \left[\frac{\Delta N_{c,0,+1}}{2}\right] \text{ mod } 1, \quad (4.52)$$

and

$$\Delta J_{\alpha,\gamma,-1} = \left[\frac{\Delta N_{\alpha,\gamma,-1}}{2}\right] \text{ mod } 1, \quad (4.53)$$

where the second expression refers to all values of $\alpha, \gamma, +1$ except $c, 0, +1$.

A central result is that Eqs. (4.47) and (4.48) can be rewritten as

$$\Delta E = \frac{2\pi}{L} \sum_{\alpha,\gamma,\iota} \theta(N_{\alpha,\gamma}) \lambda C_{\alpha,\gamma} |v_{\alpha,\gamma,\lambda}| \left[h^{\iota}_{\alpha,\gamma,\lambda} + N^{ph}_{\alpha,\gamma,\lambda,\iota} \right] + \mathcal{O}\left(\frac{1}{L}\right) \tag{4.54}$$

and

$$\Delta P = \frac{2\pi}{L} \sum_{\alpha,\gamma,\iota} \theta(N_{\alpha,\gamma}) \iota \lambda C_{\alpha,\gamma} \left[h^{\iota}_{\alpha,\gamma,\lambda} + N^{ph}_{\alpha,\gamma,\lambda,\iota} \right], \tag{4.55}$$

respectively. This finite-size analysis is of the type considered in multicomponent CFT [12] and can be interpretated as a product of Virasoro algebras.

Comparing Eqs. (4.47)-(4.48) and (4.54)-(4.55), we obtain expressions for the conformal dimensions of the theory as functions of the parameters $\xi^{j}_{\alpha,\gamma,\lambda;\alpha',\gamma',\lambda'}$. These conformal dimensions are given by

$$2h^{\iota}_{\alpha,\gamma,\lambda} = [\Gamma^{0}_{\alpha,\gamma,\lambda}]^2 + [\Gamma^{1}_{\alpha,\gamma,\lambda}]^2 + \iota \Delta N_{\alpha,\gamma,\lambda} \Delta J_{\alpha,\gamma,\lambda} \, . \tag{4.56}$$

The conformal dimensions $h^{\iota}_{\alpha,\gamma,\lambda}$ are functions of the numbers $\Delta N_{\alpha,\gamma,\lambda}$, which characterized the GS - CRS transition and of these conformal dimensions involve interacting terms which are combinations of two-pseudoparticle forward scattering phase shifts at the α, γ pseudo-Fermi surfaces. In Appendix A4 we present simplified expressions for the parameters $\xi^{j}_{\alpha,\gamma,\lambda;\alpha',\gamma',\lambda'}$, Eq. (4.46), which control the interaction dependence of these dimensions.

4.5 The α, γ Virasoro algebras

In this section we express the generators of the α, γ Virasoro algebras in the $\alpha, \gamma, \lambda, \iota$-pseudoparticle operator basis. From the CFT introduced in Chapter 3, it is known that at the critical point a solvable interacting model with short-range interactions can be mapped onto a continuum quantum field theory, which is translational, rotational and scale invariant [13].

The use of the pseudoparticle conservation laws will show that the $\hat{H}_{CL}$ and $\hat{P}_{CL}$ critical theory is associated with the existence of 1D Hubbard-model critical points corresponding to finite energies ω_0 and momenta k_0 of Eqs. (4.27) and (4.33). These correspond to low-energy $(\omega - \omega_0)$ and small momentum $(k - k_0)$ continuum-field theories. The existence of critical points around finite energies ω_0 is a property of solvable interacting discrete lattice models. In the case of solvable interacting continuum models there are only the usual $\omega_0 = 0$ critical points [14].

In the study of the critical spectra (4.47), (4.48), (4.54), and (4.55) normal order was taken relatively to the GS (the CFT vacuum). The corresponding energy spectrum provides the conformal dimensions of the theory. On the other hand, in the study of the α, γ Virasoro algebras we will use as reference state the

final CRS's (HWS's or LWS's of these algebras). Normal order relatively to the final CRS's will be denoted by ::. (The excited tower-states of each α, γ Virasoro algebras correspond to pseudoparticle-pseudohole processes around the CRS's.)

Normal ordered relatively to the final CRS's the Hamiltonian (4.38) and momentum operator (4.43) simply read

$$:: \hat{H}_c :: = \sum_{\kappa,\alpha,\gamma,\iota} \theta(N_{\alpha,\gamma}) \iota \kappa v_{\alpha,\gamma,\lambda} :: \hat{N}_{\alpha,\gamma,\lambda,\iota}(\kappa) :: , \tag{4.57}$$

$$:: \hat{P}_c :: = \sum_{\kappa,\alpha,\gamma,\iota} \theta(N_{\alpha,\gamma}) \kappa C_{\alpha,\gamma} :: \hat{N}_{\alpha,\gamma,\lambda,\iota}(\kappa) :: , \tag{4.58}$$

respectively, with the pseudomomentum κ, Eq. (4.14), defined relatively to the pseudo-Fermi points of the reference CRS, Eqs. (4.20)-(4.21). We emphasize that the Hamiltonian (4.57) is of non interacting character. Moreover, CRS normal ordering is equivalent to consider $\omega_0 = 0$ and $k_0 = 0$.

Criticality is approached as $\omega \to 0$ (and $\kappa \to 0$) and the Hamiltonian $\hat{H}_c$ is mapped onto a continuum field theory. This corresponds to a low-energy $(\omega - \omega_0)$ and small-momentum $(k - k_0)$ theory for the original Hubbard model. We can map the model $\hat{H}_c$ onto the following massless fermionic Dirac Lagrangean density

$$\hat{\mathcal{L}} = \sum_{\alpha,\gamma,\iota} \theta(N_{\alpha,\gamma}) \hat{\mathcal{L}}_{\alpha,\gamma,\lambda,\iota} , \tag{4.59}$$

where the $\hat{\mathcal{L}}_{\alpha,\gamma,\lambda,\iota}$ Lagrangean-density components read

$$\begin{aligned} \hat{\mathcal{L}}_{\alpha,\gamma,\lambda,\iota} &= \frac{1}{2} \psi^{\dagger}_{\alpha,\gamma,\lambda,\iota}(x,t) i \left[\frac{\partial}{\partial t} + \iota v_{\alpha,\gamma,\lambda} \frac{\partial}{\partial x} \right] \psi_{\alpha,\gamma,\lambda,\iota}(x,t) \\ &- \frac{1}{2} \left\{ \left[\frac{\partial}{\partial t} + \iota v_{\alpha,\gamma,\lambda} \frac{\partial}{\partial x} \right] \psi^{\dagger}_{\alpha,\gamma,\lambda,\iota}(x,t) \right\} i \psi_{\alpha,\gamma,\lambda,\iota}(x,t) . \end{aligned} \tag{4.60}$$

The quantum numbers α, γ, λ, and ι play here the role of colors of the fields. (In the above expressions the normal order is taken with respect to the suitable CRS.) It follows from Eq. (4.13) that the fermionic fields obey anticommutation relations

$$\left\{ \psi^{\dagger}_{\alpha,\gamma,\lambda,\iota}(x,t), \psi_{\alpha',\gamma',\lambda',\iota'}(x',t') \right\} = \delta_{\alpha,\alpha'} \delta_{\gamma,\gamma'} \delta_{\lambda,\lambda'} \delta_{\iota,\iota'} \delta(x - x') \delta(t - t') . \tag{4.61}$$

In Appendix C4 we show that the energy-momentum tensor associated with the critical point quantum problem (4.59) decouples into a number $\mathcal{N}_{VA}$ of tensors, where

$$\mathcal{N}_{VA} = \sum_{\alpha,\gamma} \theta(N_{\alpha,\gamma,\lambda}) , \tag{4.62}$$

is the number of CRS occupied α, γ bands. This is a generalization of the usual critical theory without $\gamma > 0$ pseudoparticle and α-Yang particle occupancy where $\mathcal{N}_{VA} = 2$ [15, 16]. Each of the tensors acts in the corresponding orthogonal α, γ Hilbert subspace. The Lorentz invariance of each α, γ Hilbert subspace confirms and justifies that the complete critical theory is simply given by the product of a number $\mathcal{N}_{VA}$ of Virasoro algebras, each one with conformal anomaly $\mathcal{C}_{\alpha,\gamma} = 1$. Each of these α, γ gapless excitation branches corresponds to independent Minkowski spaces with common space and time but with different "light velocities" $v_{\alpha,\gamma,\lambda}$. This agrees with the form of the energy spectrum, Eq. (4.54).

The α, γ Virasoro algebra generators are related to the tensor $\hat{T}^{\alpha,\gamma,\lambda}_{\iota,\iota}(x^\iota)$ defined and studied in Appendix C4. They are the coefficients of the following tensor expansion [13]

$$\hat{T}^{\alpha,\gamma,\lambda}_{\iota,\iota}(x^\iota) = \frac{2\pi}{L^2} \sum_j L^{\alpha,\gamma,\lambda,\iota}_{\iota\lambda j} e^{-i\iota\lambda\frac{2\pi}{L}jx^\iota} , \tag{4.63}$$

where $x^\iota = t + \iota x$ and $j = 0, \pm 1, \pm 2, ...$

Let us consider the following expansions of the pseudoparticle fields

$$\psi_{\alpha,\gamma,\lambda,\iota}(x^{-\iota}) = \frac{1}{\sqrt{L}} \sum_\kappa b_{\kappa,\alpha,\gamma,\lambda,\iota} e^{-i\frac{2\pi}{L}\kappa x^{-\iota}} , \tag{4.64}$$

$$\psi^\dagger_{\alpha,\gamma,\lambda,\iota}(x^{-\iota}) = \frac{1}{\sqrt{L}} \sum_\kappa b^\dagger_{-\kappa,\alpha,\gamma,\lambda,\iota} e^{-i\frac{2\pi}{L}\kappa x^{-\iota}} . \tag{4.65}$$

Inserting the above fields in Eq. (C4.8), it is straightforward to find that the generators of the α, γ Virasoro algebra are given by

$$L^{\alpha,\gamma,\lambda,\iota}_{-j} = \sum_\kappa \iota\lambda\left(\kappa + \frac{1}{2}\iota\lambda\frac{2\pi}{L}j\right) :: b^\dagger_{\kappa+\iota\lambda\frac{2\pi}{L}j;\alpha,\gamma,\lambda,\iota} b_{\kappa,\alpha,\gamma,\lambda,\iota} :: + \frac{1}{8}\delta_{j,0} . \tag{4.66}$$

The case $j = 0$ is special, the generator $L^{\alpha,\gamma,\lambda,\iota}_0$ containing an extra $1/8$ term. This follows from the imposition that the norm of the states should be the same when calculated from the generator commutation relations and directly from the generator expressions (see Appendix D4).

In order to extract the conformal dimensions, which correspond to the interacting part of the Hamiltonian at the critical point, we consider the operators $L^{\alpha,\gamma,\lambda,\iota}_0$ normal ordered relatively to the GS. This state is the reference vacuum of the CFT. The CRS normal ordered generator $L^{\alpha,\gamma,\lambda,\iota}_0$ and the corresponding GS normal-ordered operator $: L^{\alpha,\gamma,\lambda,\iota}_0 :$ read

$$L^{\alpha,\gamma,\lambda,\iota}_0 = \iota\lambda \sum_\kappa \kappa :: \hat{N}_{\alpha,\gamma,\lambda,\iota}(\kappa) :: + \frac{1}{8} , \tag{4.67}$$

and

$$: \hat{L}_0^{\alpha,\gamma,\lambda} := \iota\lambda \sum_{\kappa} \kappa : \hat{N}_{\alpha,\gamma,\lambda,\iota}(\kappa) : + \frac{1}{2} \sum_{j=0,1} [\hat{\Gamma}^j_{\alpha,\gamma,\lambda}]^2 \tag{4.68}$$

respectively, where

$$\hat{\Gamma}^0_{\alpha,\gamma,\lambda} = \frac{1}{2} \sum_{\alpha',\gamma'} \theta(N_{\alpha',\gamma'}) \xi^0_{\alpha,\gamma,\lambda;\alpha',\gamma',\lambda'} : \hat{N}_{\alpha',\gamma',\lambda'} : , \tag{4.69}$$

and

$$\hat{\Gamma}^1_{\alpha,\gamma,\lambda} = \sum_{\alpha',\gamma'} \theta(N_{\alpha',\gamma'}) \xi^1_{\alpha,\gamma,\lambda;\alpha',\gamma',\lambda'} : \hat{J}_{\alpha',\gamma',\lambda'} : , \tag{4.70}$$

are the operators whose eigenvalues are given in Eqs. (4.49) and (4.50), respectively.

Equations (4.66) and (4.67) provide the Virasoro algebra generators in the pseudoparticle basis. Note that the generators $L_j^{\alpha,\gamma,\lambda,+1}$ and $L_j^{\alpha,\gamma,\lambda,-1}$ are the operators usually written as $L_j^{\alpha,\gamma,\lambda}$ and $\overline{L}_j^{\alpha,\gamma,\lambda}$, respectively (see the notation of Refs. [17, 13]).

The commutation relations between the generators of the Virasoro algebras are found to be

$$\left[L_j^{\alpha,\gamma,\lambda,\iota}, L_l^{\alpha',\gamma',\lambda',\iota'}\right] = \delta_{\alpha,\alpha'}\delta_{\gamma,\gamma'}\delta_{\lambda,\lambda'}\delta_{\iota,\iota'}\left[(j-l)L_{j+l}^{\alpha,\gamma,\lambda,\iota} + \frac{1}{12}j(j^2-1)\delta_{j+l,0}\right] . \tag{4.71}$$

In Eq. (4.71) we used units such that $2\pi/L \equiv 1$. The commutation relations confirms that each α,γ Virasoro algebra has conformal anomaly $\mathcal{C}_{\alpha,\gamma} = 1$ [18, 19, 20, 21, 17, 13, 22] and that the complete critical theory is a product of $\mathcal{N}_{VA}$ (Eq. 4.62) α,γ Virasoro algebras.

The eigenstates involving α,γ pseudoparticle - pseudohole processes can be obtained by acting the above non-diagonal generators onto the HWS's or LWS's of the Virasoro algebras. When acting onto these CRS's the $j \neq 0$ operators $L_j^{\alpha,\gamma,\lambda,\iota}$ create a number $|j|$ of pseudoparticle - pseudohole pairs describing the low-energy and small-momentum physics around the CRS.

A CRS is an eigenstate of the operators $: L_0^{\alpha,\gamma,\lambda,\iota} :$ whose eigenvalue is the corresponding conformal dimension $h^{\iota}_{\alpha,\gamma,\lambda}$, Eq. 4.56),

$$: L_0^{\alpha,\gamma,\lambda,\iota} : |CRS\rangle = h^{\iota}_{\alpha,\gamma,\lambda}|CRS\rangle . \tag{4.72}$$

On the other hand, when acting onto the CRS the generator $L_{j\neq 0}^{\alpha,\gamma,\lambda,\iota}$ yields

$$L_j^{\alpha,\gamma,\lambda,\iota}|CRS\rangle = \left\{ \begin{array}{cc} |\alpha,\gamma,\lambda,\iota,j\rangle, & sgn(j) = -\lambda\iota \\ 0, & sgn(j) = \lambda\iota , \end{array} \right. \tag{4.73}$$

where $|\alpha,\gamma,\lambda,\iota,j\rangle$ is a tower-state and $|j|$ is given by

$$|j| \equiv N^{ph}_{\alpha,\gamma,\lambda,\iota} \,. \tag{4.74}$$

Here $N^{ph}_{\alpha,\gamma,\lambda,\iota}$ is the number of pseudoparticle - pseudohole processes. The excited tower states, $|\alpha,\gamma,\lambda,\iota,j\rangle$, are also eigenstates of : $L_0^{\alpha,\gamma,\lambda,\iota}$: such that

$$: L_0^{\alpha,\gamma,\lambda,\iota} : |\alpha,\gamma,\lambda,\iota,j\rangle = \Delta^{\iota}_{\alpha,\gamma,\lambda}|\alpha,\gamma,\lambda,\iota,j\rangle \,, \tag{4.75}$$

where the eigenvalue reads

$$\Delta^{\iota}_{\alpha,\gamma,\lambda} = h^{\iota}_{\alpha,\gamma,\lambda} + N^{ph}_{\alpha,\gamma,\lambda,\iota} \,. \tag{4.76}$$

These states are eigenstates of both the Hamiltonian $\hat{H}_{CL}$ and of the original Hubbard Hamiltonian. Upon suitable normalization, they belong the set of orthonormal Hamiltonian eigenstates of the following general form

$$|\psi;\alpha,\gamma,\lambda,\iota,j\rangle = b^{\dagger}_{\kappa=\lambda\iota\frac{2\pi}{L}|j|,\alpha,\gamma,\lambda,\iota} b_{\kappa=0,\alpha,\gamma,\lambda,\iota}|CRS\rangle \,, \tag{4.77}$$

where the pseudomomentum κ, Eq. (4.14), was measured relatively to the CRS pseudo-Fermi points. We note that for $N^{ph}_{\alpha,\gamma,\lambda,\iota} = |j| > 1$ there are many other orthonormal Hamiltonian eigenstates with the same eigenvalue, $N^{ph}_{\alpha,\gamma,\lambda,\iota}$, but which are not of form (4.77). However, the generators of these eigenstates (relatively to the CRS) can also be written in terms of the operators (4.66). For instance, the energy eigenstate

$$|\psi; N^{ph}_{\alpha,\gamma,\lambda,\iota} = 2\rangle = b^{\dagger}_{\kappa=\lambda\iota\frac{2\pi}{L},\alpha,\gamma,\lambda,\iota} b_{\kappa=-\lambda\iota\frac{2\pi}{L},\alpha,\gamma,\lambda,\iota}|CRS\rangle \,, \tag{4.78}$$

is not of the general form (4.77). Its generator can be written as a linear combination of the operators $L^{\alpha,\gamma,\lambda,\iota}_{j=-2\lambda\iota}$ and $(L^{\alpha,\gamma,\lambda,\iota}_{j=-\lambda\iota})^2$. The generators of energy eigenstates with pseudoparticle - processes in several $\alpha,\gamma,\lambda,\iota$ branches can also be expressed in terms of the operators (4.66).

4.6 Correlation functions

Let $\phi_\vartheta(x,t)$ represent a physical field. In the case of one-particle and two-particle physical fields the relevant primary fields and associated CRS's are such that $\sum_{\alpha,\gamma>0} N_{\alpha,\gamma} + \sum_\alpha \mathcal{N}_\alpha = 0,1$. This means that for such physical fields the corresponding densities of $\gamma > 0$ pseudoparticles, $n_{\alpha,\gamma}$, are vanishing small.

On the other hand, the CFT here presented applies to the situation when the $\gamma > 0$ densities $n_{\alpha,\gamma}$ are small but finite, yet the density n_α of α-Yang particles can be either vanishing small or finite. The corresponding CRS's and primary fields are relevant for physical fields of $(\sum_{\alpha,\gamma} N_{\alpha,\gamma} + \sum_\alpha \mathcal{N}_\alpha)$ -particle character.

However, the general correlation function expressions evaluated from the finite-density $n_{\alpha,\gamma}$ CFT's here presented will be shown to be useful for the calculation

of correlation functions of physical fields associated with vanishing small densities $n_{\alpha,\gamma}$.

The space x dependence of the physical fields associated with $\hat{P}$ and $\hat{P}_{CL}$ and the time t dependence associated with the quantum problems $\hat{H}$ and $\hat{H}_{CL}$ are in the Heisenberg representation given by

$$\phi_\vartheta(x,t) = e^{-i\hat{H}t}e^{i\hat{P}x}\phi_\vartheta(0,0)e^{-i\hat{P}x}e^{i\hat{H}t}\,, \tag{4.79}$$

and

$$\phi^{CL}_\vartheta(x,t) = e^{-i\hat{H}_{CL}t}e^{i\hat{P}_{CL}x}\phi_\vartheta(0,0)e^{-i\hat{P}_{CL}x}e^{i\hat{H}_{CL}t}\,, \tag{4.80}$$

respectively.

We now consider the Hilbert subspace spanned by the set of all Hamiltonian eigenstates, $|\psi(\nu)\rangle$, with fixed $N_{\alpha,\gamma}$ and $\mathcal{N}_\alpha$ numbers.

We note that for the original Hubbard model the different sets of $\{N_{\alpha,\gamma},\mathcal{N}_\alpha\}$ numbers associated with a given physical field correspond to CRS's of different energy ω_0, Eq. (4.27). Therefore, here we fix the numbers $N_{\alpha,\gamma}$ and $\mathcal{N}_\alpha$, what is equivalent to consider the correlation-function behaviour in the vicinity of the corresponding finite-energy value ω_0.

The correlation function for the physical field is given by

$$\begin{aligned}\langle GS|\phi_\vartheta(x,t)\phi_\vartheta(0,0)|GS\rangle &= \sum_\nu \langle GS|\phi_\vartheta(x,t)|\psi(\nu)\rangle\langle\psi(\nu)|\phi_\vartheta(0,0)|GS\rangle \\ &= e^{i(\omega_0 t - k_0 x)}\langle GS|\phi^{CL}_\vartheta(x,t)\phi^{CL}_\vartheta(0,0)|GS\rangle\end{aligned} \tag{4.81}$$

where we have used the space-time evolution laws (4.79) and (4.80), the decoupling of $\hat{H}$ (4.22) and $\hat{P}$ (4.29), the commutation relations $[\hat{H}_{CL},\hat{H}_0] = [\hat{P}_{CL},\hat{P}_0] = [\hat{H}_{CL},\hat{P}_0] = 0$, and the facts that for $\hat{H}_0$ and $\hat{P}_0$ the GS has eigenvalue zero and the final states have all the same eigenvalue ω_0 (4.27) and k_0 (4.33), respectively.

On the other hand, the correlation function of $\hat{H}_{CL}$ consist of a sum of terms (see Appendix E4)

$$\langle GS|\phi^{CL}_\vartheta(x,t)\phi^{CL}_\vartheta(0,0)|GS\rangle = \frac{1}{\prod_{\alpha,\gamma,\iota}(x-\iota v_{\alpha,\gamma,\lambda}t)^{2\Delta^\iota_{\alpha,\gamma,\lambda}}}\,, \tag{4.82}$$

where $\Delta^\iota_{\alpha,\gamma,\lambda} = h^\iota_{\alpha,\gamma,\lambda} + N^{ph}_{\alpha,\gamma,\iota}$, are dimensions given by Eq. (4.76). Out of the terms of general form (4.82), the leading term in the asymptotic expansion of the correlation function of $\phi^{CL}_\vartheta(x,t)$ decays with critical exponents with the corresponding fixed values for charge numbers $\Delta N_{\alpha,\gamma}$ and $\mathcal{N}_\alpha$ by minimizing with respect to the current numbers $\Delta J_{\alpha,\gamma}$ using the restrictions (4.51)-(4.53).

Finally, by inserting the function (4.82) in the r.h.s. of Eq. (4.81), we arrive to the main result of this section. The correlation functions of the original Hubbard model consist of a sum of terms of the form

$$\chi_\vartheta(x,t) = \langle GS|\phi_\vartheta(x,t)\phi_\vartheta(0,0)|GS\rangle = \frac{e^{i(\omega_0 t - k_0 x)}}{\prod_{\alpha,\gamma,\iota}(x - \iota v_{\alpha,\gamma,\lambda} t)^{2\Delta^\iota_{\alpha,\gamma,\lambda}}}\,, \tag{4.83}$$

the leading term in the asymptotic expansion being directly connected to the leading term of the function (4.82) by relation (4.81).

In order to derive the expressions for the correlation functions in the k and ω space, we evaluate the Fourier transform

$$\chi_\vartheta(k,\omega) = \int_{-\infty}^{\infty} dx \int_{-\infty}^{\infty} dt\; e^{i(kx-\omega t)}\chi_\vartheta(x,t). \tag{4.84}$$

We calculate the function (4.84) for $k = k_0$, what provides general expressions for $Im\chi_\vartheta(k_0,\omega)$ and $Re\chi_\vartheta(k_0,\omega)$. We also evaluate expressions for the following functions

$$D_\vartheta(\omega) \;=\; \sum_k Im\chi_\vartheta(k,\omega) \tag{4.85}$$

and

$$N_\vartheta(k) \;=\; \sum_\omega Im\chi_\vartheta(k,\omega). \tag{4.86}$$

As for the simpler case of Refs. [23, 24], we find for small positive energy $(\omega - \omega_0)$ the following general expressions

$$Im\chi_\vartheta(k_0,\omega) \propto \left(\omega - \omega_0\right)^{\varsigma_\vartheta}, \tag{4.87}$$

$$Re\chi_\vartheta(k_0,\omega) \propto \left(\omega - \omega_0\right)^{\varsigma_\vartheta}, \tag{4.88}$$

when $\varsigma_\vartheta \neq 0$ and $Re\chi_\vartheta(k_0,\omega) \propto -\ln(\omega - \omega_0)$ when $\varsigma_\vartheta = 0$, and

$$D_\vartheta(\omega) \propto \left(\omega - \omega_0\right)^{1+\varsigma_\vartheta}. \tag{4.89}$$

For small momenta $(k - k_0)$ we find

$$N_\vartheta(k) \propto |k - k_0|^{1+\varsigma_\vartheta}. \tag{4.90}$$

The critical exponent of expressions (4.87)-(4.90) is an exclusive function of the anomalous dimensions $\Delta^\iota_{\alpha,\gamma,\lambda}$, Eq. (4.76), and read

$$\varsigma_\vartheta = -2 + 2\sum_{\alpha,\gamma,\iota} \Delta^\iota_{\alpha,\gamma,\lambda}\,. \tag{4.91}$$

The correlation function expressions (4.83)-(4.90) are valid for physical fields whose final CRS's have small finite occupancies for the $\gamma > 0$ pseudoparticles.

However, in the case of the one-particle correlation functions studied in the Chapter 5, the CRS's occupancies are for the $\gamma > 0$ pseudoparticles either zero or vanishing small. In the latter case, the corresponding $\gamma > 0$ pseudoparticle bands cannot be linearized at the pseudo-Fermi points. These energy bands are quadratic at low-energy and the corresponding spectrum is not conformal invariant.

Fortunately, the critical theory associated with multicomponent systems with both linear and non-linear pseudoparticle bands was studied in Ref. [11]. Importantly, following the results of that reference, in spite of the fact that the critical spectrum of these multicomponent systems is not conformal invariant, the critical theory is still controlled by the anomalous dimensions $\Delta^{\iota}_{\alpha,\gamma,\lambda}$, Eq. (4.76). Moreover, while expressions (4.83) and (4.89) are not valid in the limit of vanishing occupancy for the $\gamma > 0$ pseudoparticles, the expressions (4.87), (4.88) and (4.90) provide the correct result in that limit. On the other and, the theory here presented provides the correct expressions for both vanishing small and finite densities n_{α} of α-Yang particles.

It follows that the critical theory here discussed provides correct correlation function expressions for $\chi_{\vartheta}(k,\omega)$ at $k = k_0$ and ω in the vicinity of ω_0 even in the limit of vanishing small density of $\gamma > 0$ pseudoparticles. Also the general expressions for $N_{\vartheta}(k)$, Eq. (4.90), remain valid in that limit. Obviously, the suitable anomalous dimensions $\Delta^{\iota}_{\alpha,\gamma,\lambda}$ involve in this case vanishing small values for $\gamma > 0$ pseudoparticle densities.

Finally, in the case that the physical fields and corresponding CRS's do not involve the $\gamma > 0$ pseudoparticle occupancies, the theory here presented is fully equivalent to the theory introduced in Ref. [11]. In the simple case that there is neither $\gamma > 0$ pseudoparticle nor α-Yang particle occupancy, the approach here discussed reduces to the usual two-component CFT of Ref. [1, 2]. However, in the case that the physical fields involve CRS's with both $\alpha, 0$ pseudoparticles and α-Yang particle occupancies, the theory here studied goes beyond the low-energy theory of Ref. [1, 2]. In contrast to the approach of that reference, which only provides low-energy expressions for correlation functions, the theory here presented provides correlation function expressions for energies in the vicinity of the finite energies ω_0, with the ω_0 expression, Eq. (4.27), simplifying to

$$\omega_0 = \sum_{\alpha} 2\mu_{\alpha}\mathcal{N}_{\alpha}. \tag{4.92}$$

For instance, the upper-Hubbard-band of the one-electron spectral function studied in Chapter 5 is dominated by CRS's with no $\gamma > 0$ pseudoparticle occupancy and $\mathcal{N}_c = 1$, what leads to $\omega_0 = 2\mu_c = 2\mu = 2\epsilon_F$. This finite-energy problem cannot be studied within the low-energy critical theory of Ref. [1, 2] .

Appendix A4

In this appendix we study in detail the parameters $\xi^{j}_{\alpha,\gamma,\lambda;\alpha',\gamma',\lambda'}$, Eq. (4.46), which control the expressions of the dimensions, Eq.(4.76) and correlation-functions critical exponents. In order to obtain the following equations, we use the phase shift coupled equations (Eqs. A2.1-A2.9). We note that the parameters $\xi^{j}_{\alpha,\gamma,\lambda;\alpha',\gamma',\lambda'}$ are defined at the GS pseudo-Fermi points. This implies for the rapidities of the heavy pseudoparticle that

$$r^{(\pm)}_{\alpha,\gamma>0,\lambda} = R^{(0)}(q^{(\pm)}_{F_{\alpha,\gamma>0,\lambda}}) = \left\{ \begin{array}{ll} 0 & ,\lambda = 1 \\ \pm\infty & ,\lambda = -1\,. \end{array} \right. \tag{A4.1}$$

First we consider the parameters which account for the interaction between $\alpha, 0$ pseudoparticles

$$\xi^{j}_{\alpha,0,1;\alpha',0,1} \equiv \xi^{j}_{\alpha,\alpha'} \tag{A4.2}$$

where $\xi^{1}_{\alpha,\alpha'}$ are the entries of the so-called dressed charge matrix [27, 12, 28]

$$Z_1 = \left[\begin{array}{cc} \xi^{1}_{c,c} & \xi^{1}_{c,s} \\ \xi^{1}_{s,c} & \xi^{1}_{c,s} \end{array} \right], \tag{A4.3}$$

and $\xi^{0}_{\alpha,\alpha'}$ are the entries are the entries of matrix Z_0 such that

$$Z_0 = \left[[Z_1]^{-1} \right]^{T} = \left[\begin{array}{cc} \xi^{0}_{c,c} & \xi^{0}_{c,s} \\ \xi^{0}_{s,c} & \xi^{0}_{c,s} \end{array} \right]. \tag{A4.4}$$

The entries $\xi^{1}_{\alpha,\alpha'}$ are given by

$$\begin{aligned} \xi^{1}_{\alpha,\alpha'} &= \delta_{\alpha,\alpha'} + \sum_{l=\pm 1} l\Phi_{\alpha,0;\alpha',0}(q_{F_{\alpha,0,1}}, lq_{F_{\alpha',0,1}}) \\ &= \delta_{\alpha,\alpha'} + \sum_{l=\pm 1} l\bar{\Phi}_{\alpha,0;\alpha',0}(r_{\alpha,0,1}, lr_{\alpha',0,1})\,, \end{aligned} \tag{A4.5}$$

and can be written as $\xi^{1}_{\alpha,\alpha'} = \xi^{1}_{\alpha,\alpha'}(r_{\alpha,0})$, where function $\xi^{1}_{\alpha,\alpha'}(r)$ reads

$$\xi^{1}_{\alpha,\alpha'}(r) = \delta_{\alpha,\alpha'} + \sum_{l=\pm 1} l\bar{\Phi}_{\alpha,0;\alpha',0}(r, lr_{\alpha',0,1}). \tag{A4.6}$$

Using the phase shift Eqs. (A2.1)-(A2.9) we arrive to the following coupled integral equations for the functions (A4.6)

$$\xi^{1}_{c,c}(r) = 1 + \frac{1}{\pi}\int_{r^{(-)}_{s,0}}^{r^{(+)}_{s,0}} dr'\, \frac{\xi^{1}_{s,c}(r')}{1+(r-r')^2} \tag{A4.7}$$

$$\xi^1_{c,s}(r) \;=\; \frac{1}{\pi}\int_{r^{(-)}_{s,0}}^{r^{(+)}_{s,0}} dr' \;\frac{\xi^1_{s,s}(r')}{1+(r-r')^2} \tag{A4.8}$$

$$\xi^1_{s,c}(r) \;=\; t(r) + \int_{r^{(-)}_{s,0}}^{r^{(+)}_{s,0}} dr' \; G(r,r')\; \xi^1_{s,c}(r') \tag{A4.9}$$

$$\xi^1_{s,s}(r) \;=\; 1 + \int_{r^{(-)}_{s,0}}^{r^{(+)}_{s,0}} dr' \; G(r,r')\; \xi^1_{s,s}(r') \tag{A4.10}$$

We now consider the parameters associated with the interactions between $\alpha, 0$ pseudoparticle and heavy $\alpha, \gamma > 0$ pseudoparticles. After some algebra we find that they are of the form

$$\xi^j_{\alpha,0,1;\alpha',\gamma',\lambda'} = \delta_{\lambda',1}(1-j) g^0_{\alpha;\alpha',\gamma'} + \delta_{\lambda',-1} j g^1_{\alpha;\alpha'}\,, \tag{A4.11}$$

where $g^0_{\alpha;\alpha',\gamma'} \;=\; g^0_{\alpha;\alpha',\gamma'}(r_{\alpha,0})$ and the functions $g^0_{\alpha;\alpha',\gamma'}(r)$ satisfies the following coupled integral equations

$$\begin{aligned} g^0_{c;\alpha,\gamma}(r) \;&=\; -\frac{2}{\pi}\tan^{-1}\left(\frac{r}{\delta_{\alpha,s}+\gamma}\right) + \\ &\quad + \frac{1}{\pi}\int_{r^{(-)}_{s,0}}^{r^{(+)}_{s,0}} dr' \;\frac{g^0_{s;\alpha,\gamma}(r')}{1+(r-r')^2}, \end{aligned} \tag{A4.12}$$

$$\begin{aligned} g^0_{s;\alpha,\gamma}(r) \;&=\; \delta_{\alpha,s}\frac{2}{\pi}\left[\tan^{-1}\left(\frac{r}{\gamma}\right) + \tan^{-1}\left(\frac{r}{2+\gamma}\right)\right] - \\ &\quad -\frac{2}{\pi^2}\int_{r^{(-)}_{c,0}}^{r^{(+)}_{c,0}} dr' \;\frac{1}{1+(r-r')^2}\tan^{-1}\left(\frac{r'}{\delta_{\alpha,s}+\gamma}\right) + \\ &\quad + \int_{r^{(-)}_{s,0}}^{r^{(+)}_{s,0}} dr' \; G(r-r') g^0_{s;\alpha,\gamma}(r'), \end{aligned} \tag{A4.13}$$

and $g^1_{\alpha;\alpha'} = g^1_{\alpha;\alpha'}(r_{\alpha,0})$ is given by

$$g^1_{\alpha;\alpha'} \;=\; \xi^1_{\alpha,c} \;-\; 2\delta_{\alpha',s}\xi^1_{\alpha,\alpha'}. \tag{A4.14}$$

Let us now consider the parameters associated with the interactions between heavy $\alpha, \gamma > 0$ pseudoparticles and $\alpha, 0$ pseudoparticles. In this case we find the following expressions

$$\xi^j_{\alpha,\gamma,\lambda;\alpha',0,1} \;=\; \delta_{\lambda,1} j g^1_{\alpha,\gamma;\alpha'} \;+\; \delta_{\lambda,-1}(1-j) g^0_{\alpha;\alpha'} \tag{A4.15}$$

where

$$g^1_{\alpha,\gamma;\alpha'} = (\delta_{\alpha,s}-\delta_{\alpha,c})\frac{2}{\pi}\int_0^{r_{c,0}} dr' \frac{1}{(\delta_{\alpha,s}+\gamma)\left[1+\left(\frac{r'}{\delta_{\alpha,s}+\gamma}\right)^2\right]}\xi^1_{c,\alpha'}(r') -$$

$$-\delta_{\alpha,s}\frac{2}{\pi}\int_0^{r_{s,0}} dr' \left[\frac{1}{\gamma\left[1+\left(\frac{r'}{\gamma}\right)^2\right]} + \frac{1}{(2+\gamma)\left[1+\left(\frac{r'}{2+\gamma}\right)^2\right]}\right]\xi^1_{s,\alpha'}(r'), \tag{A4.16}$$

and

$$g^0_{\alpha;\alpha'} = \delta_{\alpha,\alpha'} + \delta_{\alpha,s}(\delta_{\alpha,\alpha'}-\delta_{\alpha,-\alpha'}) \tag{A4.17}$$

Finally, we consider the parameters associated with the interactions between heavy $\alpha,\gamma>0$ pseudoparticles. In this case we find after some algebra

$$\xi^j_{\alpha,\gamma,\lambda;\alpha',\gamma',\lambda'} = \delta_{\alpha,\alpha'}\left[\delta_{\gamma,\gamma'}\delta_{\lambda,\lambda'}\left[1-\delta_{\lambda,1}(j-\frac{1}{2})\right]\right] +$$

$$+\delta_{\alpha,\alpha'}\left[-\delta_{\lambda,\lambda'}\delta_{\lambda,-1}\frac{(-1)^j}{2}+\lambda\delta_{\lambda,-\lambda'}\left(\frac{1-\lambda}{2}-j\right)\right]\times$$

$$\times(2\delta_{\alpha,s}+\gamma+\gamma'-|\gamma-\gamma'|)+\delta_{\lambda,-\lambda'}\delta_{\lambda,1}j(g^1_{\alpha,\gamma;c}-2g^1_{\alpha,\gamma;s}). \tag{A4.18}$$

Appendix B4

In this appendix we present the finite-size analysis of the energy spectrum (4.47) and momentum spectrum (4.48) from the use of the Hamiltonian at the critical point (4.38) and momentum operator (4.43), respectively.

It follows from the pseudoparticle representation that the energy eigenstates of the Hamiltonian (4.38) are also eigenstates of the pseudoparticle number operators and obey the equation

$$: \hat{N}_{\alpha,\gamma,\lambda,\iota}(\kappa) : |\psi\rangle = \delta N_{\alpha,\gamma,\lambda,\iota}(\kappa)|\psi\rangle \, , \tag{B4.1}$$

where the eigenvalue deviations, $\delta N_{\alpha,\gamma,\lambda,\iota}(\kappa)$, equal either 1 or 0 for occupied and unoccupied pseudomomentum values, respectively.

The critical energy and momentum spectra associated with the Hamiltonian (4.38) and momentum operator (4.43), respectively, can be written as

$$\Delta E = \Delta E_1 + \Delta E_2 \, , \tag{B4.2}$$

and

$$\Delta P = \frac{L}{2\pi} \sum_{\alpha,\gamma,\iota} \int_{\kappa} d\kappa \, \kappa C_{\alpha,\gamma} \delta N_{\alpha,\gamma,\lambda,\iota}(\kappa) \, , \tag{B4.3}$$

respectively, where

$$\Delta E_1 = \frac{L}{2\pi} \sum_{\alpha,\gamma,\iota} \int_{\kappa} d\kappa \, \iota\kappa v_{\alpha,\gamma,\lambda} \delta N_{\alpha,\gamma,\lambda,\iota}(\kappa) \, , \tag{B4.4}$$

and

$$\begin{aligned} \Delta E_2 \; = \; & \frac{1}{L} \sum_{\alpha,\alpha'} \sum_{\gamma,\gamma'} \sum_{\iota} \frac{1}{2} \Big[f^{1}_{\alpha,\gamma,\lambda;\alpha',\gamma',\lambda'} \Delta N_{\alpha,\gamma,\lambda,\iota} \Delta N_{\alpha',\gamma',\lambda',\iota} \\ & + f^{-1}_{\alpha,\gamma,\lambda;\alpha',\gamma',\lambda'} : \Delta N_{\alpha,\gamma,\lambda,\iota} \Delta N_{\alpha',\gamma',\lambda',-\iota} \Big] \, . \end{aligned} \tag{B4.5}$$

To obtain these expressions we have used Eq. (B4.1), replaced κ summations by the κ integrals of Eqs. (B4.3) and (B4.4) which run over the whole domain of the pseudomomentum (4.14), and used the following sum rule

$$\Delta N_{\alpha,\gamma,\lambda,\iota} = \sum_{\kappa} \delta N_{\alpha,\gamma,\lambda,\iota}(\kappa) = \frac{L}{2\pi} \int_{\kappa} d\kappa \, \delta N_{\alpha,\gamma,\lambda,\iota}(\kappa) \, . \tag{B4.6}$$

In order to solve the integrals of Eqs. (B4.3) and (B4.4), we have to write the general expression of the deviation $\delta N_{\alpha,\gamma,\lambda,\iota}(\kappa)$ for the Hilbert subspace to which the critical Hamiltonian (4.38) and momentum (4.43) refer to. Based on

both the general Hamiltonian-eigenstate pseudoparticle representattion and on the critical-point Hilbert subspace definition, we find the following general deviation expression

$$\delta N_{\alpha,\gamma,\lambda,\iota}(\kappa) = \delta N^{CRS}_{\alpha,\gamma,\lambda,\iota}(\kappa) + \delta N^{ph}_{\alpha,\gamma,\lambda,\iota}(\kappa)\,, \tag{B4.7}$$

where the deviations $\delta N^{CRS}_{\alpha,\gamma,\lambda,\iota}(\kappa)$ and $\delta N^{ph}_{\alpha,\gamma,\lambda,\iota}(\kappa)$ describe the GS - CRS transition and pseudoparticle - pseudohole processes around that CRS, respectively, and obey the following normalization sum rules

$$\frac{L}{2\pi}\int_{\kappa} d\kappa\, \delta N^{CRS}_{\alpha,\gamma,\lambda,\iota}(\kappa) = \Delta N_{\alpha,\gamma,\lambda,\iota}\,, \tag{B4.8}$$

and

$$\frac{L}{2\pi}\int_{\kappa} d\kappa\, \delta N^{ph}_{\alpha,\gamma,\lambda,\iota}(\kappa) = 0\,, \tag{B4.9}$$

respectively. Their general form is

$$\delta N^{CRS}_{\alpha,\gamma,\lambda,\iota}(\kappa) = \sum_{l,l'=\pm 1} l\Theta\Big(l'\lambda\iota\Big)\Theta\Big(l\Delta\kappa_{\alpha,\gamma,\lambda,\iota}\Big)\Theta\Big(ll'\kappa\Big)\Theta\Big(l[\Delta\kappa_{\alpha,\gamma,\lambda,\iota} - l'\kappa]\Big)\,, \tag{B4.10}$$

where

$$\Delta\kappa_{\alpha,\gamma,\lambda,\iota} = \Delta q^{(\iota)}_{F_{\alpha,\gamma,\lambda}} = \frac{2\pi}{L}\left[\frac{\Delta N_{\alpha,\gamma,\lambda}}{2} + \iota D_{\alpha,\gamma,\lambda}\right]\,, \tag{B4.11}$$

and the number

$$\delta N^{ph}_{\alpha,\gamma,\lambda,\iota}(\kappa) = \frac{2\pi}{L}\sum_{l=1}^{N_{\alpha,\gamma,\lambda,\iota}}\sum_{j=1}^{N^{l}_{\alpha,\gamma,\lambda,\iota}}\left[-\delta(\kappa-\kappa_j) + \delta(\kappa-\kappa_j-\lambda\iota l\frac{2\pi}{L})\right]\,, \tag{B4.12}$$

is such that the total number of elementary pseudoparticle - pseudohole processes is given by

$$N^{ph}_{\alpha,\gamma,\lambda,\iota} = \sum_{l=1}^{N_{\alpha,\gamma,\lambda,\iota}} l\, N^{l}_{\alpha,\gamma,\lambda,\iota}\,. \tag{B4.13}$$

In these equations the numbers $N_{\alpha,\gamma,\lambda,\iota}$ are fixed and refer the CRS and associated tower states.

The evaluation of the integral of Eqs. (B4.3) and (B4.4) with the deviations defined by Eqs. (B4.7) and (B4.10) - (B4.12) leads to the following results

$$\frac{L}{2\pi}\int_{\kappa} d\kappa\,\kappa\delta N^{CRS}_{\alpha,\gamma,\lambda,\iota}(\kappa) = \frac{2\pi}{L}\frac{\lambda\iota}{2}\left[\frac{\Delta N_{\alpha,\gamma,\lambda}}{2} + \iota D_{\alpha,\gamma,\lambda}\right]^2\,, \tag{B4.14}$$

and

$$\frac{L}{2\pi}\int_{\kappa} d\kappa\, \kappa \delta N^{ph}_{\alpha,\gamma,\lambda,\iota}(\kappa) = \frac{2\pi}{L}\lambda_\iota N^{ph}_{\alpha,\gamma,\lambda,\iota}\,. \tag{B4.15}$$

The use of Eqs. (B4.14) and (B4.15) in the above momentum and energy expressions leads to the critical momentum spectrum, Eq. (4.48), and to the following expression for the energy (B4.4)

$$\Delta E_1 = \frac{2\pi}{L}\sum_{\alpha,\gamma}\theta(N_{\alpha,\gamma})\lambda v_{\alpha,\gamma,\lambda}\left\{\left[\frac{\Delta N_{\alpha,\gamma,\lambda}}{2}\right]^2 + [D_{\alpha,\gamma,\lambda}]^2 + \sum_{\iota} N^{ph}_{\alpha,\gamma,\lambda,\iota}\right\}, \tag{B4.16}$$

respectively.

Let us express the f-functions of Eq. (B4.5) in terms of the phase-shift quantities (4.46) by use of Eqs. (4.44) and (4.45). In that calculation we use the following equality

$$\begin{aligned}
&\sum_{l,l'=\pm 1}[l]^j \Phi_{\alpha,\gamma;\alpha',\gamma'}(q_{F_{\alpha,\gamma,\lambda}}, l' q_{F_{\alpha',\gamma',\lambda'}})\Phi_{\alpha,\gamma;\alpha',\gamma'}(q_{F_{\alpha,\gamma,\lambda}}, ll' q_{F_{\alpha',\gamma',\lambda'}}) \\
&= \sum_{l,l'=\pm 1}[l]^j[l']^j \Phi_{\alpha,\gamma;\alpha',\gamma'}(q_{F_{\alpha,\gamma,\lambda}}, l q_{F_{\alpha',\gamma',\lambda'}})\Phi_{\alpha,\gamma;\alpha',\gamma'}(q_{F_{\alpha,\gamma,\lambda}}, l' q_{F_{\alpha',\gamma',\lambda'}})\,; \qquad j = 0,1
\end{aligned} \tag{B4.17}$$

After some simple algebra, we arrive to

$$\begin{aligned}
\Delta E_2 \;=\; & \frac{2\pi}{L}\sum_{\alpha,\gamma}\theta(N_{\alpha,\gamma})\lambda v_{\alpha,\gamma,\lambda}\Bigg\{ -\left[\frac{\Delta N_{\alpha,\gamma,\lambda}}{2}\right]^2 - [D_{\alpha,\gamma,\lambda}]^2 \\
& + \left[\sum_{\alpha',\gamma'}\theta(N_{\alpha',\gamma'})\xi^1_{\alpha,\gamma;\alpha',\gamma'} D_{\alpha',\gamma',\lambda'}\right]^2 \\
& + \left[\sum_{\alpha',\gamma'}\theta(N_{\alpha',\gamma'})\xi^0_{\alpha,\gamma;\alpha',\gamma'}\frac{\Delta N_{\alpha',\gamma',\lambda'}}{2}\right]^2\Bigg\}.
\end{aligned} \tag{B4.18}$$

Finally, we follow Eq. (B4.2) and add the energies (B4.16) and (B4.18) to arrive to the critical-energy spectrum (or finite-size energy spectrum) (4.47). This energy can be simply rewritten in terms of the conformal dimensions $h^\iota_{\alpha,\gamma,\lambda}$, Eq. (4.54). For $\gamma = 0$ (and $\lambda = +1$) the conformal dimensions can be rewritten as

$$h^\iota_{\alpha,0,+1} = \bar{h}^\iota_\alpha + h^{int}_{\alpha,0,+1}\,, \tag{B4.19}$$

where the $\bar{h}^\iota_\alpha$ term refers to the usual $\alpha, 0, +1$ pseudoparticle expression [1, 2, 29]

$$2\bar{h}^{\iota}_{\alpha} = \Big(\sum_{\alpha'} \xi^{1}_{\alpha\alpha'} D_{\alpha',0,+1} + \iota \sum_{\alpha'} \xi^{0}_{\alpha\alpha'} \frac{\Delta N_{\alpha',0,+1}}{2}\Big)^{2}, \tag{B4.20}$$

which is nothing but the $2h^{\iota}_{\alpha,0} = [\Gamma^{0}_{\alpha,0} + \iota\Gamma^{1}_{\alpha,0}]^2$ expression. (Note that $\xi^{1}_{\alpha\alpha'}$ and $\xi^{0}_{\alpha\alpha'}$ are entries of matrices which are the transverse and the inverse, respectively, of the dressed-charge matrix [1, 2]). When the CRS includes $\gamma > 0$ heavy-pseudoparticle occupancy these couple to the $\alpha, 0, +1$ pseudoparticles what gives rise to the ι-independent term $h^{int}_{\alpha,0,+1}$ of the rhs of Eq. (B4.19). This is of the form

$$2h^{int}_{\alpha,0,+1} = W^{0}_{\alpha,0,+1}\Big(W^{0}_{\alpha,0,+1} + \sum_{\alpha'} \xi^{0}_{\alpha\alpha'} \Delta N_{\alpha',0,+1}\Big) + W^{1}_{\alpha,0,+1}\Big(W^{1}_{\alpha,0,+1} + 2\sum_{\alpha'} \xi^{1}_{\alpha\alpha'} \Delta J_{\alpha',0,+1}\Big), \tag{B4.21}$$

where

$$W^{0}_{\alpha,0,+1} = \sum_{\alpha',\gamma'>0} \xi^{0}_{\alpha,0,+1;\alpha',\gamma',\lambda'} \frac{N_{\alpha',\gamma',\lambda'}}{2}, \tag{B4.22}$$

$$W^{1}_{\alpha,0,+1} = \sum_{\alpha',\gamma'>0} \theta(N_{\alpha',\gamma'}) \xi^{1}_{\alpha,0,+1;\alpha',\gamma',\lambda'} \Delta J_{\alpha',\gamma',\lambda'}\,. \tag{B4.23}$$

Appendix C4

In this appendix we show that the energy-momentum tensor associated with the critical-point quantum problem (4.59) decouples into a number $\mathcal{N}_{VA}$ of tensors.

The Hamiltonian density corresponding to the Lagrangean density (4.60) can be written as

$$\hat{\mathcal{H}} = \sum_{\alpha,\gamma,\iota} \theta(N_{\alpha,\gamma}) \hat{\mathcal{H}}_{\alpha,\gamma,\lambda,\iota} \,, \tag{C4.1}$$

where

$$\hat{\mathcal{H}}_{\alpha,\gamma,\lambda,\iota} = -\frac{i}{2} \iota v_{\alpha,\gamma,\lambda} \left\{ \psi^{\dagger}_{\alpha,\gamma,\lambda,\iota}(x,t) \frac{\partial}{\partial x} \psi_{\alpha,\gamma,\lambda,\iota}(x,t) - \left[\frac{\partial}{\partial x} \psi^{\dagger}_{\alpha,\gamma,\lambda,\iota}(x,t) \right] \psi_{\alpha,\gamma,\lambda,\iota}(x,t) \right\} . \tag{C4.2}$$

We introduce now the light-cone combinations

$$x^{\iota}_{\alpha,\gamma,\lambda} = t + \iota \frac{x}{v_{\alpha,\gamma,\lambda}} \,, \tag{C4.3}$$

corresponding to the metrics

$$g_{\iota,\iota'} = \frac{\delta_{\iota,-\iota'}}{2} \,. \tag{C4.4}$$

In these variables the α, γ, ι Lagrangean density (4.60) reads

$$\hat{\mathcal{L}}_{\alpha,\gamma,\lambda,\iota} = i \left\{ \psi^{\dagger}_{\alpha,\gamma,\lambda,\iota} \partial^{\alpha,\gamma,\lambda}_{\iota} \psi_{\alpha,\gamma,\lambda,\iota} - \left[\partial^{\alpha,\gamma,\lambda}_{\iota} \psi^{\dagger}_{\alpha,\gamma,\lambda,\iota} \right] \psi_{\alpha,\gamma,\lambda,\iota} \right\} \,, \tag{C4.5}$$

where $\psi^{\dagger}_{\alpha,\gamma,\lambda,\iota} = \psi^{\dagger}_{\alpha,\gamma,\lambda,\iota}(x^{+1}_{\alpha,\gamma,\lambda}, x^{-1}_{\alpha,\gamma,\lambda})$ and $\psi_{\alpha,\gamma,\lambda,\iota} = \psi_{\alpha,\gamma,\lambda,\iota}(x^{+1}_{\alpha,\gamma,\lambda}, x^{-1}_{\alpha,\lambda,\gamma})$. We have here addopted the notation

$$\partial^{\alpha,\gamma,\lambda}_{\iota} = \frac{\partial}{\partial x^{\iota}_{\alpha,\gamma,\lambda}} \,. \tag{C4.6}$$

The classical equations of motion for the fields are

$$\partial^{\alpha,\gamma,\lambda}_{\iota} \psi_{\alpha,\gamma,\lambda,\iota} = 0 \,; \qquad \partial^{\alpha,\gamma,\lambda}_{\iota} \psi^{\dagger}_{\alpha,\gamma,\lambda,\iota} = 0 \,, \tag{C4.7}$$

which implies that the fields $\psi_{\alpha,\gamma,\lambda,\iota}$ and $\psi^{\dagger}_{\alpha,\gamma,\lambda,\iota}$ depend only on the $x^{-\iota}_{\alpha,\gamma,\lambda}$ variable, i.e. $\psi_{\alpha,\gamma,\lambda,\iota} = \psi_{\alpha,\gamma,\lambda,\iota}(x^{-\iota}_{\alpha,\gamma,\lambda})$ and $\psi^{\dagger}_{\alpha,\gamma,\lambda,\iota} = \psi^{\dagger}_{\alpha,\gamma,\lambda,\iota}(x^{-\iota}_{\alpha,\gamma,\lambda})$.

Using equations (C4.5) and (C4.7) it is straightforward to evaluate the expression for the CRS normal ordered energy-momentum tensor. It can be written as

$$\hat{T}_{\iota,\iota} = \sum_{\alpha,\gamma} \theta(N_{\alpha,\gamma}) \hat{T}^{\alpha,\gamma,\lambda}_{\iota,\iota} \,, \tag{C4.8}$$

where $T^{\alpha,\gamma,\lambda}_{\iota,\iota}$ is related to the $\hat{T}^{\alpha,\gamma,\lambda;\alpha',\gamma',\lambda'}_{\iota,\iota'}$ tensor components as follows

$$\hat{T}^{\alpha,\gamma,\lambda;\alpha',\gamma',\lambda'}_{\iota,\iota'} = 2\delta_{\alpha,\alpha'}\delta_{\gamma,\gamma'}\delta_{\lambda,\lambda'}g_{\iota,\iota'}T^{\alpha,\gamma,\lambda}_{\iota,\iota}\,, \tag{C4.9}$$

and reads

$$\hat{T}^{\alpha,\gamma,\lambda}_{\iota,\iota} = \frac{i}{2} : \left\{\psi^{\dagger}_{\alpha,\gamma,\lambda,\iota}\partial^{\alpha,\gamma,\lambda}_{-\iota}\psi_{\alpha,\gamma,\lambda,\iota} - \left[\partial^{\alpha,\gamma,\lambda}_{-\iota}\psi^{\dagger}_{\alpha,\gamma,\lambda,\iota}\right]\psi_{\alpha,\gamma,\lambda,\iota}\right\} : . \tag{C4.10}$$

Again, normal order is here relative to the reference CRS. It follows from Eq. (C4.9) that the α,γ,λ off-diagonal components of the tensor vanish.

Each component tensor $\hat{T}^{\alpha,\gamma,\lambda}_{\iota,\iota}$ refers to one independent α,γ,λ field theory and to one Hilbert subspace which is orthogonal to all remaining α',γ',λ' Hilbert subspaces associated with different components $\hat{T}^{\alpha',\gamma',\lambda'}_{\iota,\iota}$. Therefore, for each tensor component $\hat{T}^{\alpha,\gamma,\lambda}_{\iota,\iota}$ it corresponds one independent Minkowski space with light velocity $v_{\alpha,\gamma,\lambda}$. Each component tensor $\hat{T}^{\alpha,\gamma,\lambda}_{\iota,\iota}$ is associated with a α,γ Virasoro algebra.

Appendix D4

In this appendix the presence of the term 1/8 in the Virasoro algebra operator $L_0^{\alpha,\gamma,\lambda,\iota}$, expression, Eq. (4.67), is explained.

In order to correctly describe the Virasoro algebra associated with each α,γ pseudoparticle band, one has to take the normal order relatively to the corresponding CRS (HWS or LWS of that algebra). The Hilbert subspace representation of each of these algebras should describe an unitary theory, i.e. the metric in this subspace of states (spanned by the CRS and its tower states) must be positive definite. If $|\psi\rangle$ is a physical state, then $\langle\psi|\psi\rangle \geq 0$. If $\langle\psi|\psi\rangle = 0$, then $|\psi\rangle \equiv 0$ is a null state, which in an unitary theory vanishes identically. Therefore, all the states (CRS and tower states) of this Hilbert subspace should have have a positive norm.

For simplicity, we consider the Virasoro generator of a α,γ pseudoparticle branch for $\lambda = +1$ and $\iota = +1$

$$L_{-j} = \sum_{\kappa} \left(\kappa + \frac{1}{2}j\right) :: b^{\dagger}_{\kappa+j} b_{\kappa} :: + \varrho\,\delta_{j,0} \tag{D4.1}$$

where the generator L_0 must contain a shift ϱ (otherwise, $L_0|CRS\rangle = 0$). The commutation relation of these generators must satisfy the following equation

$$[L_j, L_l] = (j-l)L_{j+l} + \frac{\mathcal{C}}{12} j(j^2-1)\delta_{j+l,0} \tag{D4.2}$$

where $\mathcal{C}$ is the conformal anomaly of the corresponding α,γ theory.

Let us evaluate the norm of the excited tower states $L_{-j}|CRS\rangle$ (with $j > 0$). On the one hand, we use the commutation relation of the Virasoro operators and find

$$\begin{aligned} \langle CRS|L_j L_{-j}|CRS\rangle &= \langle CRS|[L_j, L_{-j}]|CRS\rangle \\ &= 2j\varrho + \frac{\mathcal{C}}{12} j(j^2-1). \end{aligned} \tag{D4.3}$$

On the other hand, we use the expression of the Virasoro operators and write

$$L_{-j}|CRS\rangle = \sum_{\kappa=0}^{-j+1} \left(\kappa + \frac{j}{2}\right) :: b^{\dagger}_{\kappa+j} b_{\kappa} :: |CRS\rangle \tag{D4.4}$$

what implies that

$$\begin{aligned} \langle CRS|L_j L_{-j}|CRS\rangle &= \sum_{\kappa=0}^{-j+1} \left(\kappa + \frac{j}{2}\right)^2 \\ &= \frac{1}{12} j(j^2-1) + \frac{j}{4}. \end{aligned} \tag{D4.5}$$

Consistency of the norm of the excited states requires then the condition

$$2j\varrho + \frac{C}{12}j(j^2-1) = \frac{1}{12}j(j^2-1) + \frac{j}{4}. \qquad \text{(D4.6)}$$

The cubic part of j implies a conformal anomaly $C = 1$ and the factor ϱ is constant and equals $1/8$. Only in this case we obtain the correct commutation relations between the Virasoro generators.

Appendix E4

In this appendix we introduce the primary-field pseudoparticle expressions and present the derivation of the long-range asymptotic behavior of two-point correlation functions for these fields.

It is convenient to consider the problem in complex variables in the Euclidean plane. Rather than the variables (C4.3), we use here the following definition

$$x^{\iota}_{\alpha,\gamma,\lambda} = \tau - i\iota\frac{x}{v_{\alpha,\gamma,\lambda}}\,, \tag{E4.1}$$

where τ is an Euclidean time.

Combining the pseudoparticle theory presented in previous sections with the CFT studies of Ref. [30], one can generalize the usual CFT primary fields expression to the present theory with the result

$$\phi^{CL}(x,t) = \left\{\prod_{\alpha,\gamma}\phi_{\alpha,\gamma,\lambda}(x^{+1}_{\alpha,\gamma,\lambda}, x^{-1}_{\alpha,\gamma,\lambda})\right\}\,, \tag{E4.2}$$

where we have the following evolution law

$$\phi_{\alpha,\gamma,\lambda}(x^{+1}_{\alpha,\gamma,\lambda}, x^{-1}_{\alpha,\gamma,\lambda}) = \prod_{\iota} e^{x^{\iota}_{\alpha,\gamma,\lambda}L^{\alpha,\gamma,\lambda,\iota}_{-\lambda\iota}}\phi_{\alpha,\gamma,\lambda}(0,0)\,. \tag{E4.3}$$

Here the exponential is to be represented by an operator series, $L^{\alpha,\gamma,\lambda,\iota}_{-\lambda\iota} = L^{\alpha,\gamma,\lambda,\iota}_{\mp 1}$ is the $j = -\lambda\iota = \mp 1$ generator defined by Eq. (4.66), and the fields,

$$\phi_{\alpha,\gamma,\lambda}(0,0) = \lim_{x^{+1}_{\alpha,\gamma,\lambda}, x^{-1}_{\alpha,\gamma,\lambda}\rightarrow 0}\phi_{\alpha,\gamma,\lambda}(x^{+1}_{\alpha,\gamma,\lambda}, x^{-1}_{\alpha,\gamma,\lambda})\,, \tag{E4.4}$$

are obtained below and are such that

$$\phi^{CL}(0,0) = \prod_{\alpha,\gamma}\phi_{\alpha,\gamma,\lambda}(0,0)\,. \tag{E4.5}$$

The primary fields (E4.2) transform the GS as

$$\phi^{CL}(x,t)|GS\rangle = \left\{\prod_{\alpha,\gamma,\iota} e^{x^{\iota}_{\alpha,\gamma,\lambda}L^{\alpha,\gamma,\lambda,\iota}_{-\lambda\iota}}\right\}|CRS\rangle\,, \tag{E4.6}$$

and thus the field (E4.5) corresponds to excitations which transform the CFT vacuum, i.e. the GS, onto the HWS's or LWS's of the Virasoro algebras [13],

$$|CRS\rangle = \phi^{CL}(0,0)|GS\rangle\,. \tag{E4.7}$$

From the use of Eqs. (2.107) and (4.18) it is possible to find the expression of the field operators $\phi_{\alpha,\gamma,\lambda}(0,0)$ explicitly. Equations (E4.2) and (E4.3) then provide the expressions of the primary fields $\phi^{CL}(x,t)$.

By using the pseudomomentum κ, Eq. (4.14), defined relatively to the GS, we find after some algebra

$$\phi_{\alpha,\gamma,\lambda}(0,0) = [U_{\alpha,\gamma}^{l_{\alpha,\gamma}}]^{j_{\alpha,\gamma}} \phi^{(1)}_{\alpha,\gamma,\lambda}(0,0)\ \phi^{(2)}_{\alpha,\gamma,\lambda}(0,0)\,. \tag{E4.8}$$

Here $U_{\alpha,\gamma}^{l_{\alpha,\gamma}}$ is the topological momentum shift operator (4.17) with $l_{\alpha,\gamma} = +1$ or $l_{\alpha,\gamma} = -1$ depending on whether the GS - CRS transition shifts the α,γ-pseudomomentum sea to the right or to the left, respectively, $j_{\alpha,\gamma} = 0, 1$ is given in Eq. (4.19), and the field $\phi^{(1)}_{\alpha,\gamma,\lambda}(0,0)$ reads

$$\phi^{(1)}_{\alpha,\gamma,\lambda}(0,0) = \prod_{\iota} \prod_{\iota\lambda\kappa\in\Delta\kappa_1} \left(\theta(\Delta N_{\alpha,\gamma,\lambda,\iota}) b^{\dagger}_{\kappa,\alpha,\gamma,\lambda,\iota} + \theta(-\Delta N_{\alpha,\gamma,\lambda,\iota}) b_{\kappa,\alpha,\gamma,\lambda,\iota}\right), \tag{E4.9}$$

where the domain $\Delta\kappa_1$ is either

$$\Delta\kappa_1 \in [0, \Delta q^{(\iota)}_{F_{\alpha,\gamma,\lambda}}]\,; \qquad \Delta q^{(\iota)}_{F_{\alpha,\gamma,\lambda}} > 0\,, \tag{E4.10}$$

or

$$\Delta\kappa_1 \in [\Delta q^{(\iota)}_{F_{\alpha,\gamma,\lambda}}, 0]\,; \qquad \Delta q^{(\iota)}_{F_{\alpha,\gamma,\lambda}} < 0\,. \tag{E4.11}$$

On the other hand, the field $\phi^{(2)}_{\alpha,\gamma,\lambda}(0,0)$ is given by

$$\phi^{2}_{\alpha,\gamma,\lambda}(0,0) = \delta_{\lambda,+1} + \delta_{\lambda,-1} \prod_{\iota} \prod_{-\iota\kappa\in\Delta\kappa_2} \left(\theta(\Delta d_{F_{\alpha,\gamma}}) b^{\dagger}_{\kappa,\alpha,\gamma,-1,\iota} + \theta(-\Delta d_{F_{\alpha,\gamma}}) b_{\kappa,\alpha,\gamma,-1,\iota}\right), \tag{E4.12}$$

where the domain $\Delta\kappa_2$ is either

$$\Delta\kappa_2 \in [(q^{(\iota)}_{\alpha,\gamma} - q^{(\iota)}_{F_{\alpha,\gamma,-1}}), (q^{(\iota)}_{\alpha,\gamma} - q^{(\iota)}_{F_{\alpha,\gamma,-1}} + \Delta q^{(\iota)}_{\alpha,\gamma})]\,, \qquad \Delta q^{(\iota)}_{\alpha,\gamma} > 0\,, \tag{E4.13}$$

or

$$\Delta\kappa_2 \in [(q^{(\iota)}_{\alpha,\gamma} - q^{(\iota)}_{F_{\alpha,\gamma,-1}}) + \Delta q^{(\iota)}_{\alpha,\gamma}, (q^{(\iota)}_{\alpha,\gamma} - q^{(\iota)}_{F_{\alpha,\gamma,-1}})]\,, \qquad \Delta q^{(\iota)}_{\alpha,\gamma} < 0\,. \tag{E4.14}$$

Following Eq. (E4.2), the two-point correlation function for a primary field can be written as

$$\langle GS|\phi^{CL}(x,t)\phi^{CL}(x',t')|GS\rangle = \prod_{\alpha,\gamma} \prod_{\alpha',\gamma'} \langle GS|\phi_{\alpha,\gamma,\lambda}(x^{+1}_{\alpha,\gamma,\lambda}, x^{-1}_{\alpha,\gamma,\lambda})\phi_{\alpha',\gamma',\lambda'}(y^{1}_{\alpha',\gamma',\lambda'}, y^{-1}_{\alpha',\gamma',\lambda'})|GS\rangle\,. \tag{E4.15}$$

We remind that GS is the vacuum of the CFT. The productories refer only to CRS occupied α,γ pseudoparticle bands.

From equation (E4.6) it follows the one-to-one correspondence between the primary fields and the CRS

$$|CRS\rangle = \left\{ \prod_{\alpha,\gamma,\iota} \lim_{y^{+1}_{\alpha,\gamma,\lambda}, y^{-1}_{\alpha,\gamma,\lambda} \to 0} \phi_{\alpha,\gamma,\lambda}(y^{+1}_{\alpha,\gamma,\lambda}, y^{-1}_{\alpha,\gamma,\lambda}) \right\} |GS\rangle \,. \tag{E4.16}$$

This expression is equivalent to Eq. (E4.7). In order to extract the long-range asymptotic behavior for the two-point correlation function, we consider the following projective map

$$x^{\iota}_{\alpha,\gamma,\lambda} = -\frac{1}{y^{\iota}_{\alpha,\gamma,\lambda}}\,, \tag{E4.17}$$

which transforms the fields as follows

$$\begin{aligned} \phi_{\alpha,\gamma,\lambda}(y^{+1}_{\alpha,\gamma,\lambda}, y^{-1}_{\alpha,\gamma,\lambda}) &= \prod_{\iota} \left(\frac{\partial x^{\iota}_{\alpha,\gamma,\lambda}}{\partial y^{\iota}_{\alpha,\gamma,\lambda}} \right)^{h^{\iota}_{\alpha,\gamma,\lambda}} \phi_{\alpha,\gamma,\lambda}(x^{+1}_{\alpha,\gamma,\lambda}, x^{-1}_{\alpha,\gamma,\lambda}) \\ &= \prod_{\iota} (x^{\iota}_{\alpha,\gamma,\lambda})^{2h^{\iota}_{\alpha,\gamma,\lambda}} \phi_{\alpha,\gamma,\lambda}(x^{+1}_{\alpha,\gamma,\lambda}, x^{-1}_{\alpha,\gamma,\lambda})\,. \end{aligned} \tag{E4.18}$$

One should notice that although the map interchanges the points at zero and at infinity it transforms the full complex plane into itself and so it does not change the theory. This map allows us to write

$$\begin{aligned} \langle GS|\, \phi^{CL}(x,t) &= \langle GS| \left\{ \prod_{\alpha,\gamma} \phi_{\alpha,\gamma,\lambda}(x^{+1}_{\alpha,\gamma,\lambda}, x^{-1}_{\alpha,\gamma,\lambda}) \right\} \\ &= \langle CRS| \left\{ \prod_{\alpha,\gamma,\iota} (x^{\iota}_{\alpha,\gamma,\lambda})^{-2:L^{\alpha,\gamma,\lambda,\iota}_{0}:} e^{(1/x^{\iota}_{\alpha,\gamma,\lambda}).L^{\alpha,\gamma,\lambda,\iota}_{\lambda\iota}} \right\}, \end{aligned} \tag{E4.19}$$

where now the operator series which represents the exponential is evaluated at infinity. As for the state (E4.16), from this relation it follows that

$$\langle CRS| = \langle GS| \left\{ \prod_{\alpha,\gamma,\iota} \lim_{x^{+1}_{\alpha,\gamma,\lambda}, x^{-1}_{\alpha,\gamma,\lambda} \to \infty} \phi_{\alpha,\gamma,\lambda}(x^{+1}_{\alpha,\gamma,\lambda}, x^{-1}_{\alpha,\gamma,\lambda}).(x^{\iota}_{\alpha,\gamma,\lambda})^{2h^{\iota}_{\alpha,\gamma,\lambda}} \right\}. \tag{E4.20}$$

In order to derive the asymptotic behavior of two-point correlation function defined by Eq. (E4.15) at $x' = t' = 0$, we use the orthonormality of the different CRS's and expressions (E4.6) and (E4.19). Expanding the Taylor series and noticing that

$$\langle CRS| \prod_{\alpha,\gamma,\iota} (L^{\alpha,\gamma,\lambda,\iota}_{\lambda\iota})^{n} (L^{\alpha,\gamma,\lambda,\iota}_{-\lambda\iota})^{m} |CRS\rangle = \prod_{\alpha,\gamma,\iota} \delta_{n+m} n! \frac{(2h^{\iota}_{\alpha,\gamma,\lambda} - 1 + n)!}{(2h^{\iota}_{\alpha,\gamma,\lambda} - 1)!}\,, \tag{E4.21}$$

we find that

$$\begin{aligned}
&\langle GS|\phi^{CL}(x,t)\phi^{CL}(0,0)|GS\rangle = \\
&= \lim_{y^1_{\alpha,\gamma,\lambda},y^{-1}_{\alpha,\gamma,\lambda}\to 0}\prod_{\alpha,\gamma}\delta_{\alpha,\alpha'}\delta_{\gamma,\gamma'}\delta_{\lambda,\lambda'}\langle GS|\phi_{\alpha,\gamma,\lambda}(x^{+1}_{\alpha,\gamma,\lambda},x^{-1}_{\alpha,\gamma,\lambda})\phi_{\alpha,\gamma,\lambda}(y^{1}_{\alpha,\gamma,\lambda},y^{-1}_{\alpha,\gamma,\lambda})|GS\rangle \\
&= \frac{1}{\prod_{\alpha,\gamma,\iota}(x^{\iota}_{\alpha,\gamma,\lambda})^{2h^{\iota}_{\alpha,\gamma,\lambda}}}\,. \qquad \text{(E4.22)}
\end{aligned}$$

This can be rewritten as

$$\langle GS|\phi_{\alpha,\gamma\lambda}(x,t)\phi_{\alpha,\gamma,\lambda}(0,0)|GS\rangle = \frac{1}{(x-\iota v_{\alpha,\gamma,\lambda}t)^{2h^{\iota}_{\alpha,\gamma,\lambda}}}\,. \qquad \text{(E4.23)}$$

where we have rotated the time coordinate from Euclidean time to real Minkowski time, $t = i\tau$.

Bibliography

[1] H. Frahm and V. E. Korepin, Phys. Rev. B **42** 10553 (1990).

[2] H. Frahm and V. E. Korepin, Phys. Rev. B **43**, 5653 (1991).

[3] C. N. Yang, Phys. Rev. Lett. **19**, 1312 (1967).

[4] E. H. Lieb and F. Y. Wu, Phys. Rev. Lett. **20**, 1445 (1968).

[5] M. Takahashi, Prog. Theor. Phys. **47**, 69 (1972).

[6] B. S. Shastry, Phys. Rev. Lett. **56**, 1529 (1986).

[7] E. Olmedilla and Miki Wadati, Phys. Rev. Lett. **60**, 1595 (1988).

[8] See, T. Deguchi, F. H. L. Essler, F. Gölmann, A. Klümper, V. E. Korepin, and K. Kusakabe, to appear in Phys. Rep. (1999), and references therein.

[9] J. M. P. Carmelo and N. M. R. Peres, Phys. Rev. B **56**, 3117 (1997).

[10] J. M. P. Carmelo, (submitted to Phys. Rev. B, 1999).

[11] J. M. P. Carmelo, J. M. E. Guerra, J. M. B. Lopes dos Santos and A. H. Castro Neto, Phys. Rev. Lett. **83**, 3892 (1999).

[12] A.G. Izergin, V.E. Korepin and N. Yu Reshetikhin, J. Phys. A: Math. Gen. **22**, 2615 (1989).

[13] D. Boyanovsky and C.M. Naon, Rev. Nuo. Cim. **13**, N. 2 (1990).

[14] A. H. Castro Neto, H. Q. Lin, Y.-H. Chen and J. M. P. Carmelo, Phys. Rev. B **50**, 14032 (1994).

[15] J. M. P. Carmelo and A. H. Castro Neto, Phys. Rev. Lett. **70**, 1904 (1993).

[16] J. M. P. Carmelo, A. H. Castro Neto and D. K. Campbell, Phys. Rev. B **50**, 3667 (1994).

[17] C. Itzykson and J.-M. Drouffe, *Statistical Field Theory - Vol. 2*, (Cambridge University Press, New York, 1989).

[18] A. A. Belavin, A. M. Polyakov and A. B. Zamolodchikov, J. Stat. Phys. **34**, 763 (1984).

[19] A. A. Belavin, A. M. Polyakov and A. B. Zamolodchikov, Nucl. Phys. B **241**, 333 (1984).

[20] H. W. Blöte, John L. Cardy and M. P. Nightingale, Phys. Rev. Lett. **56**, 742 (1985).

[21] Ian Affleck, Phys. Rev. Lett. **56**, 746 (1985).

[22] For an important collection of relevant articles, see, *Fields, Strings and Critical Phenomena*, (Les Houches 1988) edited by E. Brézin and J. Zinn-Justin (North-Holland, 1990).

[23] J. M. P. Carmelo, P. Horsch, D. K. Campbell and A. H. Castro Neto, Phys. Rev. B Rap. Comm. **48**, 4200 (1993).

[24] J. M. P. Carmelo, F. Guinea and P. D. Sacramento, Phys. Rev. B **55**, 7565 (1997).

[25] N. M. Bogoliubov, A. G. Izergin and N. Yu Reshetikhin, J. Phys. A **20**, 5361 (1987).

[26] W. Metzner and Carlo Di Castro. Phys. Rev. B **47**, 16107 (1993).

[27] F. Woynarovich, J. Phys. A: Math. Gen. **22**, 4243 (1989).

[28] H. Frahm and N.-C. Yu, J. Phys. A: Math. Gen. **23**, 2115 (1990).

[29] J. M. P. Carmelo, A. H. Castro Neto and D. K. Campbell, Phys. Rev. B **50**, 3683 (1994).

[30] P. Christe and M. Henkel, *Introduction to Conformal Invariance and its Applications to Critical Phenomena*, Springer-Verlag, Berlin, 1993.

Chapter 5

One-Particle Spectral Properties of the 1D Hubbard Model

5.1 Introduction

A general description of the one-particle spectral properties of the 1D Hubbard model for the whole range of energies and for the whole parameter space (on-site repulsion U and density n) is still an open problem of great physical importance.

The use of the BA solution of the model [1, 2, 3, 4, 5, 6, 7, 8, 9], the canonical transformation [10] and numerical Monte Carlo simulations [11] have provided important partial information on the one-electron spectral properties. However, many of these results are limited to particular limits, such as infinite U, half filling or low-excitation energy in the vicinity of the Fermi level. The one-particle spectral function of the related 1D Luttinger model was also investigated by means of bosonization techniques [12, 13].

The original BA solution of the 1D Hubbard model was given in terms of two coupled equations [14], associated with charge and spin excitations, the so-called *holons* and *spinons*, respectively. The excitation spectra of holons and spinons can be obtained from that solution [15] and an operational representation for the generators of these excitatinons was introduced in Refs. [16, 17]. As it was mentioned in Chapter 1, there has been a renewed interest on the one-particle spectral functions of quasi one-dimensional materials and experimental observation of holons and spinons has been claimed.

In this chapter we apply the formalism developed in previous chapters to study the one-particle spectral properties of the 1D Hubbard model. In particular, we obtain information on spectral properties at relevant threshold finite energies.

5.2 The lower- and the upper-Hubbard-bands

It is useful for the study of the density of states of the 1D Hubbard model to introduce the concepts of lower-Hubbard-band (LHB) and upper-Hubbard-band (UHB) which are widely used in the description of the physics of this model [10]. The density of states is the integral over all momenta of the one-particle spectral function. This function describes the removal or the addition of one electron from and to the system, respectively.

The LHB and UHB can be defined in terms of the changes of the average number of doubly occupied sites, $D = \langle \hat{D} \rangle$, where the operator $\hat{D}$ is given by Eq. (2.6). Let D_0 denote the GS average number of doubly occupied sites. At large U the number of doubly occupied sites becomes a good quantum number and the changes $\Delta D = D - D_0$ are given by Eq. (2.117). At large U the LHB is associated with two types of processes, (i) the removal of one electron from the system or (ii) the addition of one electron to an empty site. These processes correspond to $\Delta D = 0$. The situation (ii) can only happen for electronic densities $0 < n < 1$. On the other hand the UHB is associated with the addition of one electron to an occupied site, which corresponds to $\Delta D_0 = 1$. Thus, the UHB is expected to be located at an energy of the order of the on-site repulsion U, above the LHB.

The processes (i) and (ii) are associated with the parts of the density of states which we denote by $B(\omega)$ and $A_{LHB}(\omega)$, respectively, whereas the UHB is associated with the part of the density of states which we call $A_{UHB}(\omega)$. The functions $B(\omega)$ and $A(\omega) = A_{LHB}(\omega) + A_{UHB}(\omega)$ are defined as

$$B(\omega) = \sum_{k,\sigma} B_\sigma(k,\omega) \tag{5.1}$$

and

$$A(\omega) = \sum_{k,\sigma} A_\sigma(k,\omega)\,, \tag{5.2}$$

respectively, where the spectral functions $B_\sigma(k,\omega)$ and $A_\sigma(k,\omega)$ read

$$\begin{aligned} B_\sigma(k,\omega) &= \int_{\infty}^{\infty} dt\; e^{i\omega t} \langle GS | c^\dagger_{k\sigma}(t) c_{k\sigma}(0) | GS \rangle \\ &= \sum_f |\langle f, N-1 | c_{k\sigma} | GS, N \rangle|^2 \delta(\omega + (E_f^{N-1} - E_0^N)) \end{aligned} \tag{5.3}$$

and

$$\begin{aligned} A_\sigma(k,\omega) &= \int_{\infty}^{\infty} dt\; e^{i\omega t} \langle GS | c_{k\sigma}(t) c^\dagger_{k\sigma}(0) | GS \rangle \\ &= \sum_f |\langle f, N+1 | c^\dagger_{k\sigma} | GS, N \rangle|^2 \delta(\omega - (E_f^{N+1} - E_0^N))\,, \end{aligned} \tag{5.4}$$

respectively, where E_0^N is the GS energy of the system with N electrons and the final states $|f, N \mp 1\rangle$ are energy eigenstates of the system with $N \mp 1$ electrons and eigenenergy $E_f^{N\mp1}$. The functions (5.3) and (5.4) corresponds to changes in the electronic number $\Delta N = -1, \Delta N_\sigma = -1$ and $\Delta N = 1, \Delta N_\sigma = 1$, respectively. As in the case of the density of states, we can define the LHB and UHB spectral functions $A_{LHB}(k,\omega)$ and $A_{UHB}(k,\omega)$, respectively, with $A(k,\omega) = A_{LHB}(k,\omega) + A_{UHB}(k,\omega)$. The functions $B(\omega)$, $A_{LHB}(\omega)$ and $A_{UHB}(\omega)$ obey the following sum rule

$$\sum_\omega \left[B(\omega) + A_{LHB}(\omega) + A_{UHB}(\omega)\right] \;=\; 2L\,. \tag{5.5}$$

The corresponding spectral weights are given by

$$W_B \;=\; \sum_\omega B(\omega) \;=\; N\,, \tag{5.6}$$

$$W_{LHB} \;=\; \sum_\omega A_{LHB}(\omega) \;=\; 2(L-N) \;+\; N\mathcal{G}\,, \tag{5.7}$$

$$W_{UHB} \;=\; \sum_\omega A_{UHB}(\omega) \;=\; N\,(1 \;-\; \mathcal{G})\,, \tag{5.8}$$

where the funcion $\mathcal{G}$ is given by $\mathcal{G} = \delta_{U,0}$ for density $n = 1$. For densities $0 < n < 1$ it reads $\mathcal{G} = 1$ for $U = 0$ and for large U it was obtained by Eskes and Oleś [10] by means of the Ogata-Shiba wavefunction [18] and is given by

$$\mathcal{G} \;=\; \frac{4t}{U}\,\frac{\sin(\pi(1-n))}{\pi n}\,. \tag{5.9}$$

The spectral weights W_{LHB} and W_{UHB} are plotted in Fig. 5.1 in units of L for $U/t = 10, 20$ as function of the density n. Due to the electronic interactions, there is a transfer of spectral weight from the LHB to the UHB as U increases [19, 20, 10]. At large U the spectral weight of the UHB is a rapid increasing function of the density.

5.3 One-particle spectral functions

Although we are mostly interested in zero-magnetic field spectral properties, we start by considering that the magnetic field is finite and take the limit $H \to 0$ in the end of the calculations. Our finite magnetic-field results are valid for fields $0 \leq H < H_c$, where

$$H_c \;=\; \frac{t}{\mu_0}\Big\{\sqrt{1+u^2}\Big[1-\frac{2}{\pi}\cot^{-1}\left(\frac{\sqrt{1+u^2}}{u}\,\tan(\pi n)\right)\Big] - u2n - \eta_0\cos(\pi n)\Big\} \tag{5.10}$$

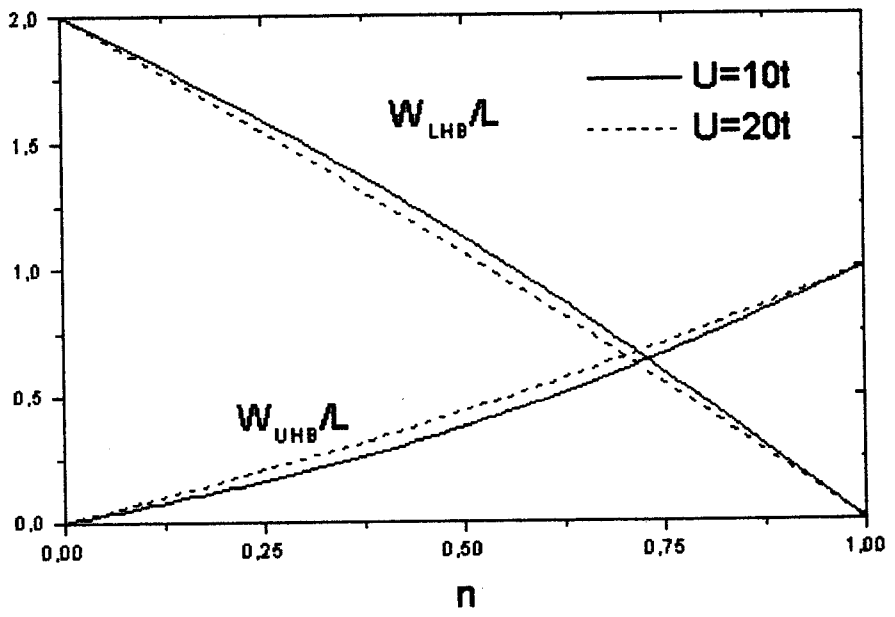

Figure 5.1: The spectral weights W_{LHB} and W_{UHB} in units of L as function of the density n for different values of U.

whith

$$\eta_0 = \frac{2}{\pi} \tan^{-1}\left(\frac{\sin(\pi n)}{u}\right), \tag{5.11}$$

is the critical magnetic field for fully polarized ferromagnetism [21].

We first consider the one-particle spectral function associated with the removal of one electron of momentum k and spin projection σ, which is given by Eq. (5.3).

In the case $\sigma = \uparrow$ we can evaluate the function (5.3) low ω and for $k = k_0$ with k_0 given in Table 5.1. There are four values of k_0 which correspond to four alternative final CRS's. For each of these CRS's there is a tower of states with the same values of the numbers $\Delta N^h_{\alpha,0}$, $N_{\alpha,\gamma>0}$, $\mathcal{N}_\alpha$ and $\Delta J_{\alpha,0}$. These numbers are given in Table 5.1 for the states belonging these four towers. For each k_0 value the low ω and $k = k_0$ expression of the spectral function (5.3) is controlled by the set of transitions to the corresponding CRS and associated tower of states. Table 5.1 also provides the numbers associated with the two towers of states which control the expression of the function (5.3) for $\sigma = \downarrow$, $k = k_0 = \pm k_{F\downarrow}$ and low-ω. The corresponding CRS's have momentum $k_0 = \pm k_{F\downarrow}$.

In the general case, it follows from Eq. (2.115) that the changes in the electronic numbers, ΔN and ΔN_σ, can be expressed in terms of the numbers $\Delta N^h_{\alpha,0}$, $\Delta N_{\alpha,\gamma>0} \equiv N_{\alpha,\gamma>0}$ and $\mathcal{N}_\alpha$ as

	$\Delta N^h_{c,0}$	$\Delta N^h_{s,0}$	$N_{\alpha,\gamma>0}$	$\mathcal{N}_\alpha$	$\Delta J_{c,0}$	$\Delta J_{s,0}$	ω_0	k_0
$B_\uparrow(k,\omega)$	1	-1	0	0	$\pm 1/2$	$\pm 1/2$	0	$\pm k_{F\uparrow}$
	1	-1	0	0	$\pm 1/2$	$\mp 1/2$	0	$\pm(2k_F + k_{F\downarrow})$
$B_\downarrow(k,\omega)$	1	1	0	0	0	$\pm 1/2$	0	$\pm k_{F\downarrow}$

Table 5.1: Relevant transitions for the function $B_\sigma(k,\omega)$.

$$\Delta N = -\Delta N^h_{c,0} + \sum_{\gamma>0} 2\gamma N_{c,\gamma} + 2\mathcal{N}_c \tag{5.12}$$

$$\Delta(N_\uparrow - N_\downarrow) = \Delta N^h_{s,0} - \sum_{\gamma>0} 2\gamma N_{s,\gamma} - 2\mathcal{N}_s. \tag{5.13}$$

For low ω and $k = k_0$ the ω dependence of the spectral function (5.3) is such that

$$B_\sigma(k,\omega) \propto Im\chi_\sigma(k,\omega) \tag{5.14}$$

where $\chi_\sigma(k,\omega)$ is the Fourier transform, Eq. (4.84), of the one-particle function

$$\chi_\sigma(x,t) = \langle GS|c^\dagger_j(t)c_i(0)|GS\rangle\,. \tag{5.15}$$

Here $x = R_j - R_i$, being R_j and R_i the lattice vectors of the sites labelled by j and i, respectively. The use of the results of Chapter 4 leads to Eq. (4.87) with $\vartheta = \sigma$ for the function (5.14). In the case $\sigma =\uparrow$ the exponents read

$$\varsigma^0_\uparrow = -2 + \frac{1}{2}\sum_\alpha \left[(\xi^0_{\alpha,c})^2 + (\xi^1_{\alpha,c} - \xi^1_{\alpha,s})^2\right] \tag{5.16}$$

$$\varsigma^+_\uparrow = -2 + \frac{1}{2}\sum_\alpha \left[(\xi^0_{\alpha,c})^2 + (\xi^1_{\alpha,c} + \xi^1_{\alpha,s})^2\right], \tag{5.17}$$

for $k_0 = \pm k_{F\uparrow}$ and $k_0 = \pm(2k_F + k_{F\downarrow})$, respectively. For $\sigma =\downarrow$ and $k = k_0 = \pm k_{F\downarrow}$ The function (5.14) is also of the form (4.87), with the critical exponent given by

$$\varsigma^0_\downarrow = -2 + \frac{1}{2}\sum_\alpha \left[(\xi^0_{\alpha,c} + \xi^0_{\alpha,s})^2 + (\xi^1_{\alpha,s})^2\right]. \tag{5.18}$$

We now consider the one-particle spectral function associated with the addition of one electron of momentum k and spin projection σ, which is given by Eq. (5.4). For low ω and $k = k_0$ the ω dependence of the spectral function (5.4) is such that

$$A_\sigma(k,\omega) \propto Im\chi^\dagger_\sigma(k,\omega) \tag{5.19}$$

where $\chi^\dagger_\sigma(k,\omega)$ is the Fourier transform of the one-particle correlation function

	$\Delta N^h_{c,0}$	$\Delta N^h_{s,0}$	$N_{\alpha,\gamma>0}$	$\mathcal{N}_\alpha$	$\Delta J_{c,0}$	$\Delta J_{s,0}$	ω_0	k_0
$A^{LHB}_\uparrow(k,\omega)$	-1	1	0	0	$\pm 1/2$	$\pm 1/2$	0	$\pm k_{F\uparrow}$
	-1	1	0	0	$\pm 1/2$	$\mp 1/2$	0	$\pm(2k_F + k_{F\downarrow})$
$A^{LHB}_\downarrow(k,\omega)$	-1	-1	0	0	0	$\pm 1/2$	0	$\pm k_{F\downarrow}$

Table 5.2: Relevant transitions for the function $A^{LHB}_\sigma(k,\omega)$.

$$\chi^\dagger_\sigma(x,t) \;=\; \langle GS|c_j(t)c^\dagger_i(0)|GS\rangle \tag{5.20}$$

where $x = R_j - R_i$ and R_j and R_i are the same as in Eq. (5.15).

We start by considering the spectral function $A^{LHB}_\sigma(k,\omega)$. In the case $\sigma =\uparrow$ we can evaluate the function (5.4) for low ω and $k = k_0$ with k_0 given in Table 5.2. There are four values of k_0 which correspond to four alternative final CRS's. For each of these CRS's there is a tower of states with the same values $\Delta N^h_{\alpha,0}$, $N_{\alpha,\gamma>0}$, $\mathcal{N}_\alpha$ and $\Delta J_{\alpha,0}$. These numbers are given in Table 5.2 for the states belonging these four towers. For each k_0 value the low ω and $k = k_0$ expression of the function (5.4) is controlled by the set of transitions to the corresponding CRS and associated tower of states. Table 5.2 also provides the numbers associated with the two towers of states which control the expression of the function (5.4) for $\sigma =\downarrow$, low ω and $k = k_0 = \pm k_{F\downarrow}$. The corresponding CRS's have momentum $k_0 = \pm k_{F\downarrow}$.

The use of the results of Chapter 4 reveals that the function (5.19) is for $k = k_0$ and low ω of the general form (4.87) with critical exponents $\varsigma^0_\uparrow$ given by Eq. (5.16) and $\varsigma^+_\uparrow$ given by Eq. (5.17) for $k_0 = \pm k_{F\uparrow}$ and $k_0 = \pm(2k_F + k_{F\downarrow})$, respectively. For $\sigma =\downarrow$ and $k = k_0 = \pm k_{F\downarrow}$, the function (5.19) has the same form for low ω with critical exponent $\varsigma^0_\downarrow$ given by Eq. (5.18). These results reveal that the ω dependence of the functions $B_\sigma(k_0,\omega)$ and $A^{LHB}_\sigma(k_0,\omega)$ is symmetric around the Fermi surface.

Let us now consider the function associated with the addition of one electron to the UHB, $A^{UHB}_\sigma(k,\omega)$. As this part of the spectral function corresponds to the UHB, the corresponding edge energy ω_0 is finite and originates from excitations of minimal energy ω_0 above the Fermi level.

According to Table 5.3 there are two main channels contibuting to the function $A^{UHB}_\sigma(k,\omega)$. In the limit $U \rightarrow \infty$ these two excitation channels compete at the excitation energy $2\epsilon_F$, for in that limit $\epsilon_{c,1}(0) \rightarrow 0$. We first analyze the first channel which involves the addition of one c-Yang particle to the system. This process costs precisely the energy $2\epsilon_F$. This excitation channel also involves the creation of one spinon and one holon. Th latter excitation provides a finite energy width to the UHB, whose lower edge is located at $\omega = 2\epsilon_F$. In the case $\sigma =\uparrow$ we can evaluate the function (5.4) for $k = k_0$ and low excitation energy $(\omega - \omega_0) > 0$ with k_0 and ω_0 given in Table 5.3. There are four values of k_0 which correspond to four alternative final CRS's. For each of these CRS's there is a tower of states

	$\Delta N^h_{c,0}$	$\Delta N^h_{s,0}$	$N_{c,1}$	$\mathcal{N}_c$	$\Delta J_{c,0}$	$\Delta J_{s,0}$	ω_0	k_0
$A^{UHB}_{\uparrow}(k,\omega)$	1	1	0	1	0	$\pm 1/2$	$2\epsilon_F$	$\pm\pi \pm k_{F\downarrow}$
$A^{UHB}_{\downarrow}(k,\omega)$	1	−1	0	1	$\pm 1/2$	$\pm 1/2$	$2\epsilon_F$	$\pm\pi \pm k_{F\uparrow}$
	1	−1	0	1	$\pm 1/2$	$\mp 1/2$	$2\epsilon_F$	$\pm\pi \pm (2k_F + k_{F\downarrow})$
$A^{UHB}_{\uparrow}(k,\omega)$	1	1	1	0	$\pm 1/2$	$\pm 1/2$	$2\epsilon_F + \epsilon_{c,1}(0)$	$\pm k_{F\uparrow}$
	1	1	1	0	$\pm 1/2$	$\mp 1/2$	$2\epsilon_F + \epsilon_{c,1}(0)$	$\pm(2k_F + k_{F\downarrow})$
$A^{UHB}_{\downarrow}(k,\omega)$	1	−1	1	0	0	$\pm 1/2$	$2\epsilon_F + \epsilon_{c,1}(0)$	$\pm k_{F\downarrow}$

Table 5.3: Relevant transitions for the function $A^{UHB}_{\sigma}(k,\omega)$. The pseudoparticle numbers $N_{\alpha,\gamma>0}$ and $\mathcal{N}_s$ which are not shown in the table are zero.

with the same values $\Delta N^h_{\alpha,0}$, $N_{\alpha,\gamma>0}$, $\mathcal{N}_\alpha$ and $\Delta J_{\alpha,0}$. These numbers are given in Table 5.3 for the states belonging these four tower of states. For each k_0 value the low $(\omega-\omega_0) > 0$ and $k = k_0$ expression of (5.4) is controlled by the set of transitions to the corresponding CRS and associated tower of states. Table 5.3 also provides the numbers associated with the eight towers of states which control the expression of the function (5.4) for $\sigma =\downarrow$, low $(\omega-\omega_0) > 0$ and $k = k_0 = \pm\pi \pm k_{F\uparrow}$ or $k = k_0 = \pm\pi \pm (2k_F + k_{F\downarrow})$. The corresponding CRS's have momentum $k_0 = \pm\pi \pm k_{F\uparrow}$ or $k = k_0 = \pm\pi \pm (2k_F + k_{F\downarrow})$.

The use of the results of Chapter 4 leads to the general expression (4.87) for the function (5.19) and low $(\omega-\omega_0) > 0$ energy, with critical exponents $\varsigma^0_{\downarrow}$ given by Eq. (5.18) for $k_0 = \pm\pi \pm k_{F\downarrow}$ and $\varsigma^0_{\uparrow}$ given by Eq. (5.16) or $\varsigma^+_{\uparrow}$ given by Eq. (5.17) for $k_0 = \pm(2k_F+k_{F\uparrow})$ or $k_0 = \pm\pi\pm(2k_F+k_{F\downarrow})$, respectively. Note that the functions $A^{LHB}_{\sigma}(k,\omega)$ and $A^{UHB}_{-\sigma}(k,\omega)$ have for low $\omega > 0$ and low $(\omega-\omega_0) > 0$, respectively, the same critical exponents, in what the c-Yang particle channel of the latter function is concerned.

Let us now analyze the second channel of $A^{UHB}_{\sigma}(k,\omega)$, which corresponds to the creation of one heavy $c,1$ pseudoparticle, one holon and one spinon. In the case of this channel, the function (5.19) is of the general form (4.87) for $\sigma =\uparrow$, $k = k_0 = \pm(2k_F + k_{F\downarrow})$ and low $(\omega - 2\epsilon_F - \epsilon_{c,1}(0))$, with the most divergent exponent corresponding to $\Delta J_{c,0} = -\Delta J_{s,0}$ and given by

$$\begin{aligned}\bar{\varsigma}_{\uparrow} &= -3/2 + \frac{1}{2}\sum_{\alpha}\left[(\xi^0_{\alpha,c}+\xi^0_{\alpha,s})^2 + (\xi^1_{\alpha,c}-\xi^1_{\alpha,s})^2\right] \\ &+ \frac{1}{2}\sum_{\alpha}\left[(g^0_{\alpha;c,1})^2 - 2g^0_{\alpha;c,1}(\xi^0_{\alpha,c}+\xi^0_{\alpha,s})\right] \\ &+ \frac{1}{2}\,(g^1_{c,1;c} - g^1_{c,1;s} + 1)^2 . \qquad (5.21)\end{aligned}$$

Following Table 5.3, the corresponding structure starts at energy $(2\epsilon_F+\epsilon_{c,1}(0))$. In the case $\sigma =\downarrow$, the function (5.19) is also of the general form (4.87) for $k_0 = \pm k_{F\downarrow}$ and low $(\omega - 2\epsilon_F - \epsilon_{c,1}(0))$, with the critical exponent given by

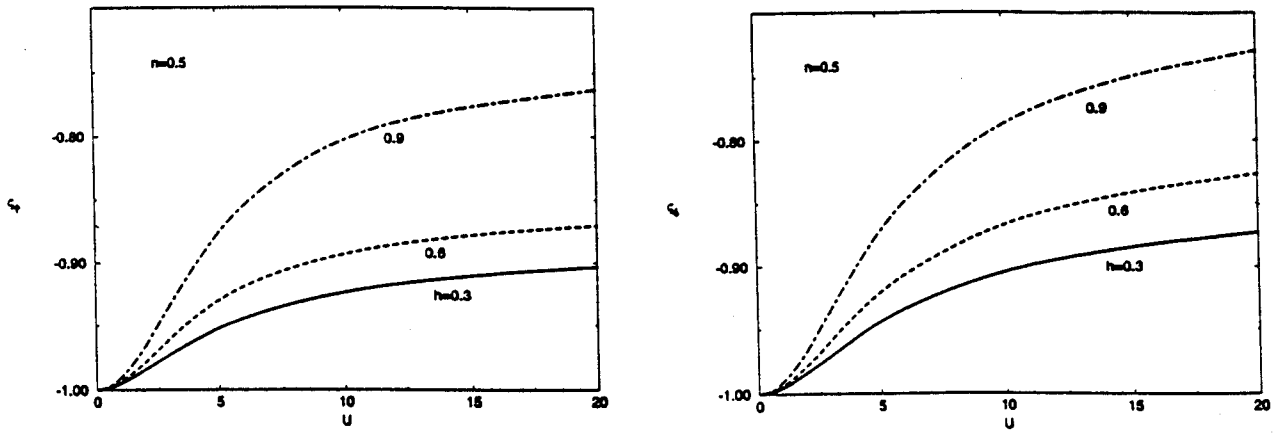

Figure 5.2: The critical exponents $\varsigma_{\downarrow}^{0}$ and $\varsigma_{\uparrow}^{0}$ as function of the on-site repulsion U for $n = 0.5$ and for various values of the magnetic field $h \equiv H/H_c$.

$$\begin{aligned}\bar{\varsigma}_{\downarrow} &= -3/2 + \frac{1}{2}\sum_{\alpha}\left[(\xi^{0}_{\alpha,c})^2 + (\xi^{1}_{\alpha,s})^2\right] \\ &+ \frac{1}{2}\sum_{\alpha}\left[(g^{0}_{\alpha;c,1})^2 - 2g^{0}_{\alpha;c,1}\xi^{0}_{\alpha,c}\right] \\ &+ \frac{1}{2}\left(-g^{1}_{c,1;s} + 1\right)^2. \end{aligned} \tag{5.22}$$

Importantly, for $U \gg t$ we have that $\epsilon_{c,1}(0) \to 0$. Since the leading term associated with the c-Yang-pairing channel has a smaller exponent than (5.21) and (5.22), the latter channel is for $U \gg t$ the dominant one. Moreover, we emphasize that at $n = 1$ the $c,1$ channel is not allowed and only the c-Yang-pairing channel exists.

Summarizing our results, we find for the spectral functions $B_{\sigma}(k,\omega)$, $A_{\sigma}^{LHB}(k,\omega)$ and $A_{\sigma}^{UHB}(k,\omega)$ the following asymptotic expressions near the critical points

$$\begin{aligned} &B_{\sigma}(\pm k_{F\sigma},\omega) \propto \omega^{\varsigma_{\sigma}^{0}}, && \omega \to 0^{-} \\ &B_{\uparrow}(\pm[2k_F + k_{F\downarrow}],\omega) \propto \omega^{\varsigma_{\uparrow}^{+}}, && \omega \to 0^{-}, \end{aligned} \tag{5.23}$$

$$\begin{aligned} &A_{\sigma}^{LHB}(\pm k_{F\sigma},\omega) \propto \omega^{\varsigma_{\sigma}^{0}}, && \omega \to 0^{+} \\ &A_{\uparrow}^{LHB}(\pm[2k_F + k_{F\downarrow}],\omega) \propto \omega^{\varsigma_{\uparrow}^{+}}, && \omega \to 0^{+} \end{aligned} \tag{5.24}$$

and

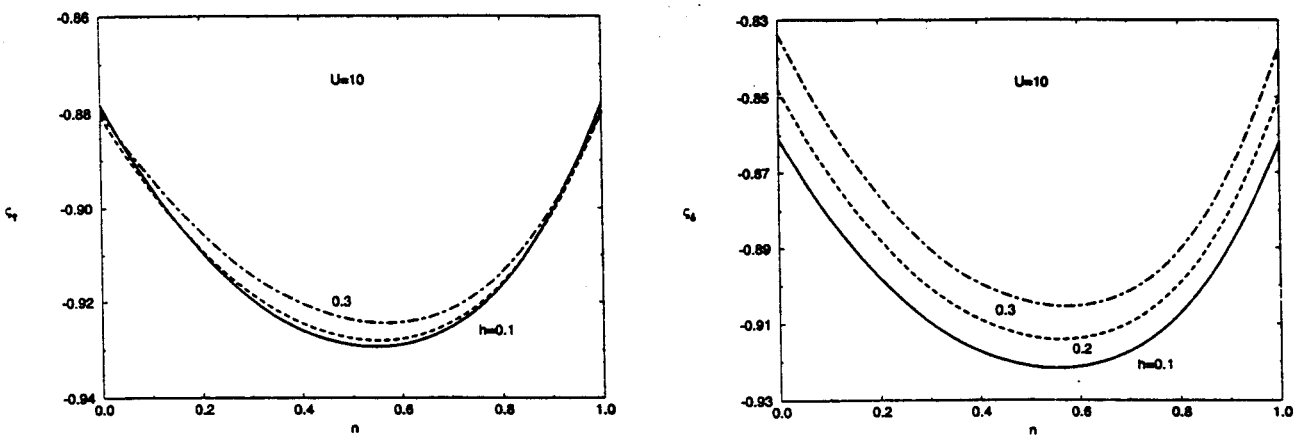

Figure 5.3: The critical exponents $\varsigma_{\downarrow}^{0}$ and $\varsigma_{\uparrow}^{0}$ as function of the electronic density n for $U = 10$ and various values of the magnetic field $h \equiv H/H_c$.

$$
\begin{aligned}
&A_{\sigma}^{UHB}(\pm[\pi - k_{F,-\sigma}],\omega) \propto (\omega - 2\epsilon_F)^{\varsigma_{-\sigma}^{0}}, && (\omega - 2\epsilon_F) \rightarrow 0^{+} \\
&A_{\downarrow}^{UHB}(\pm[\pi - 2k_F - k_{F\downarrow}],\omega) \propto (\omega - 2\epsilon_F)^{\varsigma_{\uparrow}^{+}}, && (\omega - 2\epsilon_F) \rightarrow 0^{+} \\
&A_{\sigma}^{UHB}(\pm k_{F\sigma},\omega) \propto (\omega - [2\epsilon_F + \epsilon_{c,1}(0)])^{\xi_{\sigma}}, && (\omega - [2\epsilon_F + \epsilon_{c,1}(0)]) \rightarrow 0^{+},
\end{aligned}
\tag{5.25}
$$

respectively. (We have defined the zero of energy at the Fermi level.)

The critical exponents (5.16)-(5.18), (5.21) and (5.22) are non-classical, depending on the on-site Coulomb repulsion U, electronic density n and applied magnetic field $h = H/H_c$. The critical exponents are linear combinations of the field dimensions, Eq. (4.91), and can be obtained numerically. The exponent ς_{σ}^{0} is plotted in Figs. 5.2, 5.3 and 5.4.

Let us consider the case of zero magnetic field. For $H \rightarrow 0$, we have that $r_{s,0} \rightarrow \infty$ and the coupled integral equations from which one obtains the dressed charge matrix [2, 5] can be solved by the Wiener-Hopf technique [2]. The dressed charge matrix reads in this limit

$$
Z_1 = \begin{bmatrix} \xi_0 & \xi_0/2 \\ 0 & 1/\sqrt{2} \end{bmatrix}. \tag{5.26}
$$

For densities $0 < n < 1$, the parameter ξ_0 is such that $\xi_0 \rightarrow \sqrt{2}$ as $U \rightarrow 0$ and $\xi_0 \rightarrow 1$ as $U \rightarrow \infty$ (see Fig. 5.5). For $n = 0$ and $n = 1$, the parameter ξ_0 reads $\xi_0 = \sqrt{2}$ at $U = 0$ and is given by $\xi_0 = 1$ for $U > 0$. Furthermore, in the zero magnetic field limit the $SU(2)$ spin symmetry implies that the critical exponents (5.16) and (5.18) are equal and read

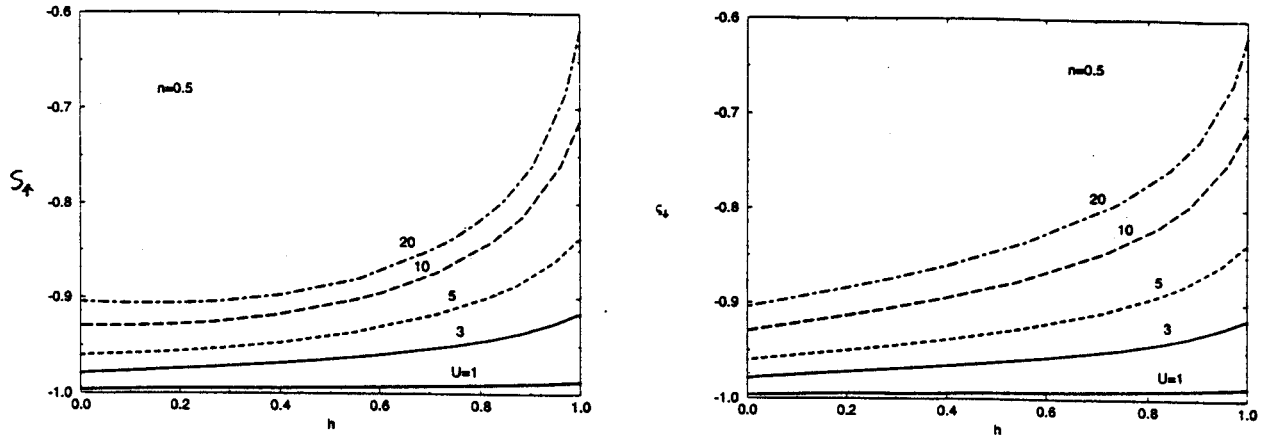

Figure 5.4: The critical exponents $\varsigma_{\downarrow}^{0}$ and $\varsigma_{\uparrow}^{0}$ as function of the magnetic field $h \equiv H/H_c$ for $n = 0.5$ and various values of the on-site repulsion U.

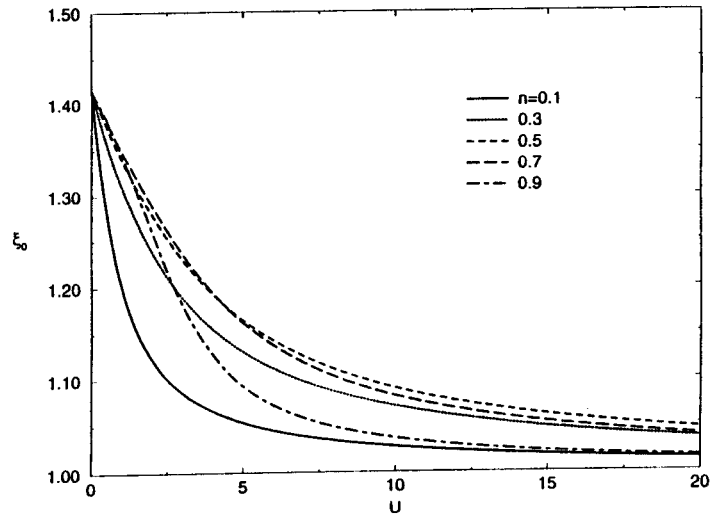

Figure 5.5: The parameter ξ_0 of Eq. (5.26) as function of U (in units t) for several values of the density n.

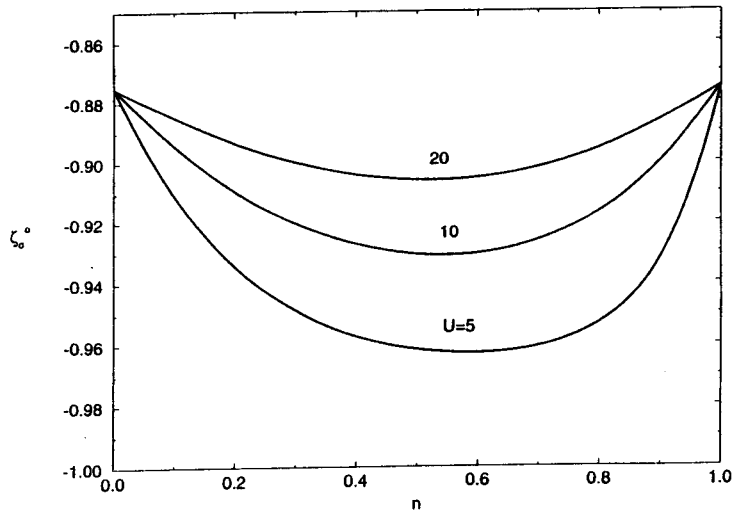

Figure 5.6: Critical exponent ς_σ^0 as function of the density n for several values of U (in units of t).

$$\varsigma_\uparrow^0 = \varsigma_\uparrow^0 = \varsigma_\sigma^0 = -2 + \left(\frac{1}{\xi_0} + \frac{\xi_0}{2}\right)^2 , \tag{5.27}$$

whereas the critical exponent (5.17) is given by

$$\varsigma_\uparrow^+ = \varsigma_\sigma^0 + \xi_0^2. \tag{5.28}$$

Thus, we confirm taht at $H = 0$ the exponent ς_σ^0 is the most divergent, with $\varsigma_\sigma^0 < \varsigma_\uparrow^+$.

For $U \to \infty$ the exponents (5.27),(5.28), (5.21) and (5.22) have the following values

$$\varsigma_\sigma^0 = -7/8 \tag{5.29}$$

$$\varsigma_\uparrow^+ = 1/8 \tag{5.30}$$

$$\bar{\varsigma}_\uparrow = \bar{\varsigma}_\downarrow = \bar{\varsigma}_\sigma = 1/8 . \tag{5.31}$$

The exponents (5.29), (5.30) and (5.31) are plotted in Figs. 5.6, 5.7 and 5.8, respectively. Note that the exponents ς_σ^0 and $\bar{\varsigma}_\sigma$ are such that $\varsigma_\sigma^0 < \bar{\varsigma}_\sigma$. This confirs that at $H = 0$ the channel corresponding to the creation of one c-Yang particle is more important than the $c, 1$ pseudoparticle channel, in what the UHB is concerned.

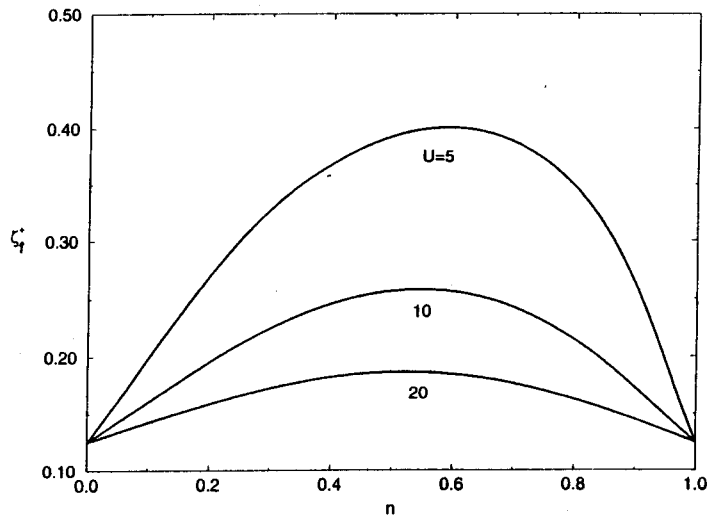

Figure 5.7: Critical exponent $\varsigma_{\uparrow}^{+}$ as function of the density n for several values of U (in units of t).

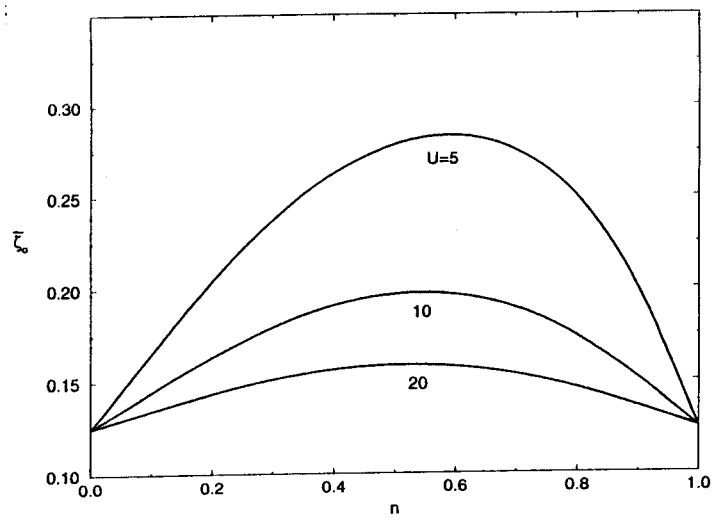

Figure 5.8: Critical exponent $\bar{\varsigma}_{\sigma}$ as function of the density n for several values of U (in units of t).

5.4 Phase-space restrictions of the one-electron spectral function

In this section we consider the phase-space restrictions of the one-electron spectral function for the whole parameter-space of the $1D$ Hubbard model. This study is not restricted to the threshold energies ω_0 and refers to the whole range of energies. However, in this section we do not take into account the effects of the matrix elements pseudomomentum dependence

It is not our goal to obtain the full closed-form expression of the one-electron spectral function, but rather to study the effects of the phase-space restrictions on the shape of that spectral function. Our analysis explains and provides further physical insight in what previous results obtained by other methods are concerned.

We consider the zero-magnetic field case and drop the spin index We evaluate $B(k,\omega)$ as the limit of $H \rightarrow 0$ of $2B_{\downarrow}(k,\omega)$. The dominant transitions involve the creation of one holon and one spinon at the $c,0$ and $s,0$ pseudo-Fermi surfaces respectively. On the other hand, we compute $A_{LHB}(k,\omega)$ from the $H \rightarrow 0$ limit of $2A_{\uparrow}^{LHB}(k,\omega)$. In this case the dominant transitions involve the creation of one $c,0$ pseudoparticle and one spinon at the $c,0$ and $s,0$ pseudo-Fermi surfaces,respectively . Finally we derive $A_{UHB}(k,\omega)$ by considering the $H \rightarrow 0$ limit of $2A_{\uparrow}^{UHB}(k,\omega)$. In this case there are two main contributions, (i) the c-Yang particle channel and (ii) the $c,1$ pseudoparticle channel. For the first channel, the dominant transitions involve the creation of one c-Yang particle, one holon and one spinon. For the second channel, the dominant transitions involve the creation of one $c,1$ pseudoparticle, one holon and one spinon. As we have seen, the critical exponent which controls the spectral function leading order term in the vicinity of the UHB bottom-edge energy is less divergent for the second channel than for first channel.

In order to study the spectral function in the whole domain of energy, we consider that all the above processes occur not only at the pseudoc-Fermi surfaces but in the whole accessible momentum space. Since the $\alpha,0$ pseudoparticle, $c,1$ pseudoparticle and c-Yang particle are one- and two-electron objects, multi-pseudoparticle processes contibute with almost no weight. At zero magnetic field the $s,0$ band is filled and there are no multi-spinon processes in $s,0$ band. Analogously, at half filling ($n=1$) the $c,0$ band is also filled and there are no multi-holon processes in the $c,0$ band.

The matrix elements $\langle f,N-1|c_{k\sigma}|GS,N\rangle$ and $\langle f,N+1|c_{k\sigma}^{\dagger}|GS,N\rangle$ are not in general known. For energies near the critical energy ω_0, Eq. (4.27), and critical momenta k_0, Eq. (4.33), these matrix elements show a singularity which controls the power-law behaviour predicted by CFT .

Away from the critical points, i.e. away from the pseudo-Fermi points of the $\epsilon_{\alpha,\gamma}^{0}$ bands, the contributions from the terms of order $j>1$ of the energy expansion (2.84) are irrelevant, since they are corrections of order $(1/L)^{j-1}$ relatively to

$\Delta E^{(1)}_{SO(4)}$ energy (2.85). Therefore, in the general case we can express the energy eigenvalues in terms of the $\epsilon^0_{\alpha,\gamma}$ bands only and omit the corrections from the f-functions.

We first consider the function $B(k,\omega)$. For densities $0 < n < 1$ there exist two degenerated final CRS's whose momenta differ from $\Delta k = \pm 4k_F$. The corresponding GS - CRS transitions involve a topological momentum shift of momentum $j2k_F$, with $j = \pm 1$ for each of the two above alternative CRS's. Each of these CRS's is associated with a family of final states generated by creating the holon and the spinon away from the pseudo-Fermi points of the $c,0$ and $s,0$ bands, respectively. The topological momentum shifts do not cost energy. One has also to consider the Umklapp processes which have momentum $i2\pi$ (with $i = 0, \pm 1, \pm 2, ...$). As the spectral function is an even function of the electronic momentum k, we will consider that $k \in [0, \pi[$.

The total momentum for removing one electron is thus given by

$$k \;=\; q_c + q_s + j2k_F + i2\pi \tag{5.32}$$

where q_c is the holon momentum in the $c,0$ band ($q_c \in [-2k_F, 2k_F]$) and q_s is the spinon momentum in the $s,0$ band ($q_s \in [-k_F, k_F]$). As we discuss in next section, if we take into account the matrix elements, we would find that both (i) for $U \gg t$ and all densities n and (ii) n close to 1 and all values of $U > U^*$, only states with the spinon at $q_c \approx \pm 2k_F$ contibute. This is because the matrix elements vanish in these limits for final states with spinons at $|q_c| < 2k_F$.

The phase-space restrictions on the function (5.3) follow from considering the creation of one holon and one spinon in the pseudomomentum domains, taking into account both the two final alternative family of states and the Umklapp processses. This leads to

$$\begin{aligned}
\tilde{B}_\sigma(k,\omega) &= \int_{-\infty}^{\infty} dq_c \int_{-\infty}^{\infty} dq_s \; \theta(2k_F - |q_c|)\theta(k_F - |q_s|)\delta(\omega - \epsilon^0_{c,0}(q_c) - \epsilon^0_{s,0}(q_s)) \\
&= \sum_{ij} \int_{-\infty}^{\infty} dq \; \theta(2k_F - |q|)\theta(k_F - |k - j2k_F - i2\pi - q|) \times \\
&\quad \times \delta(\omega - \epsilon^0_{c,0}(q) - \epsilon^0_{s,0}(k - j2k_F - i2\pi - q)).
\end{aligned} \tag{5.33}$$

This expression can be rewritten in terms of the following four integrals

$$\begin{aligned}
\tilde{B}_\sigma(k,\omega) &= \int_{Min(k+k_F, 2k_F)}^{2k_F} dq \; \delta(\omega - \epsilon^0_{c,0}(q) - \epsilon^0_{s,0}(k + 2k_F - q)) + \\
&+ \int_{Max(-2k_F, k+k_F-2\pi)}^{Max(-2k_F, k+3k_F-2\pi)} dq \; \delta(\omega - \epsilon^0_{c,0}(q) - \epsilon^0_{s,0}(k + 2k_F - 2\pi - q)) + \\
&+ \int_{Max(-2k_F, k-3k_F)}^{Min(2k_F, k-k_F)} dq \; \delta(\omega - \epsilon^0_{c,0}(q) - \epsilon^0_{s,0}(k - 2k_F - q)) +
\end{aligned}$$

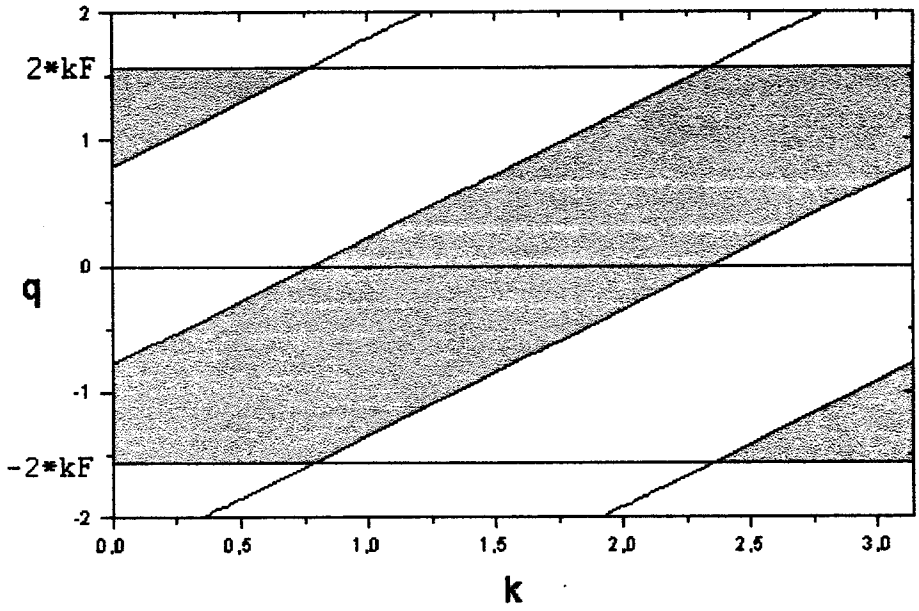

Figure 5.9: The shadowed areas are the regions of integration of the function $\tilde{B}(k,\omega)$ for density $n = 0.5$.

$$+ \int_{Min(k-3k_F+2\pi,2k_F)}^{2k_F} dq\ \delta(\omega - \epsilon^0_{c,0}(q) - \epsilon^0_{s,0}(k + 2k_F + 2\pi - q)) \tag{5.34}$$

which correspond to $(j = -1, i = 0)$, $(j = -1, i = +1)$, $(j = +1, i = 0)$ and $(j = +1, i = -1)$, respectively. For instance, these regions are plotted in a graphics of q versus k in Fig. 5.9 for electronic density $n = 0.5$. As the electronic density n increases the regions become bigger and superposition of regions appears. For some values of n one or several of the four integrals of Eq. (5.34) vanish.

As we have mentioned before, expressions (5.33) and (5.34) disregard the pseudomomentum dependence of the matrix elements. Therefore, these expressions only provide information on the phase-space restrictions effects on the spectral function. Note that the matrix elements may vanish for some final states, what further restricts the spectral-weight domains, as the example given above.

We now consider For densities $0 < n < 1$ there exist again two families of orthogonal states differing by a momentum $\Delta k = 4k_F$ One has also to consider the Umklapp processes momentum $i2\pi$ (with $i = 0, \pm 1, \pm 2, ...$). The momentum of the added electron is given by the expression

$$k = -q_c + q_s + j2k_F + i2\pi \tag{5.35}$$

where q_c is the momentum of the pseudoparticle in $c,0$ band and q_s is the spinon momentum, $q_s \in [-k_F, k_F]$. For simplicity, we consider the pseudo-Brillouin zone of the $c,0$ band as $[0, 2\pi[$ and thus one has that $q_c \in [-2k_F, 2\pi - 2k_F]$. The

phase-space restrictions on the function $A_{LHB}(k,\omega)$ result by considering all the final states associated with the above processes, what leads to

$$\begin{aligned}\tilde{A}_{LHB}(k,\omega) &= \int_{-2k_F}^{2\pi-2k_F} dq_c \int_{-\infty}^{\infty} dq_s\ \theta(k_F-|q_s|)\delta(\omega+\epsilon^0_{c,0}(q_c)-\epsilon^0_{s,0}(q_s)) \\ &= \sum_{ij}\int_{-2k_F}^{2\pi-2k_F} dq\ \theta(k_F-|k-j2k_F-i2\pi+q|)\times \\ &\quad \times\delta(\omega+\epsilon^0_{c,0}(q)-\epsilon^0_{s,0}(k-j2k_F-i2\pi+q)). \qquad (5.36)\end{aligned}$$

This function can be rewritten as

$$\begin{aligned}\tilde{A}_{LHB}(k,\omega) &= \int_{Max(-k-3k_F+2\pi,2k_F)}^{Max(Min(2\pi-2k_F,-k-k_F+2\pi),2k_F)} dq\ \delta(\omega+\epsilon^0_{c,0}(q)-\epsilon^0_{s,0}(k+2k_F-2\pi+q))+ \\ &+ \int_{2k_F}^{Max(Min(2\pi-2k_F,-k+3k_F),2k_F)} dq\ \delta(\omega+\epsilon^0_{c,0}(q)-\epsilon^0_{s,0}(k-2k_F+q))+ \\ &+ \int_{Min(-k+k_F+2\pi,2\pi-2k_F)}^{Min(2\pi-2k_F,-k+3k_F+2\pi)} dq\ \delta(\omega+\epsilon^0_{c,0}(q)-\epsilon^0_{s,0}(k-2k_F-2\pi+q))\ . \qquad (5.37)\end{aligned}$$

The three integrals of this expression correspond to $(j=-1,i=+1)$, $(j=+1,i=0)$, and $(j=+1,i=+1)$, respectively.

Finally, we consider the function $A_{UHB}(k,\omega)$. As we have seen before, for ω values in the vicinity of the UHB bottom-edge, there are two main channels of final states contributing to this function. The critical exponent of the expression obtained for the creation of one $c,1$ pseudoparticle is smaller than the exponent of the expression obtained for the creation of one c-Yang particle. Therefore, for simplicity, we consider only the latter channel, which at $n=1$ is the only one allowed. The momentum of the additional electron is given by

$$k = q_c+q_s+j2k_F+i2\pi-\pi \qquad (5.38)$$

where the momentum π is associated with the creation of the c-Yang particle. A detailed study of the processses which contribute to the c-Yang particle channel reveals that the functions $A_{UHB}(k,\omega)$ and $B(k,\omega)$ are related as follows

$$\tilde{A}_{UHB}(k,\omega-\epsilon_F) = \tilde{B}(k-\pi,-\omega+\epsilon_F). \qquad (5.39)$$

This relation is exact at $n=1$ and also is valid for $0<n<1$ if we restrict the final states to the the one holon, one spinon and one c-Yang particle processes consider above. The phase-space restrictions on the function $A_{UHB}(k,\omega)$ lead then to Eq. (5.39) with $\tilde{B}(k,\omega)$ given by Eq. (5.33).

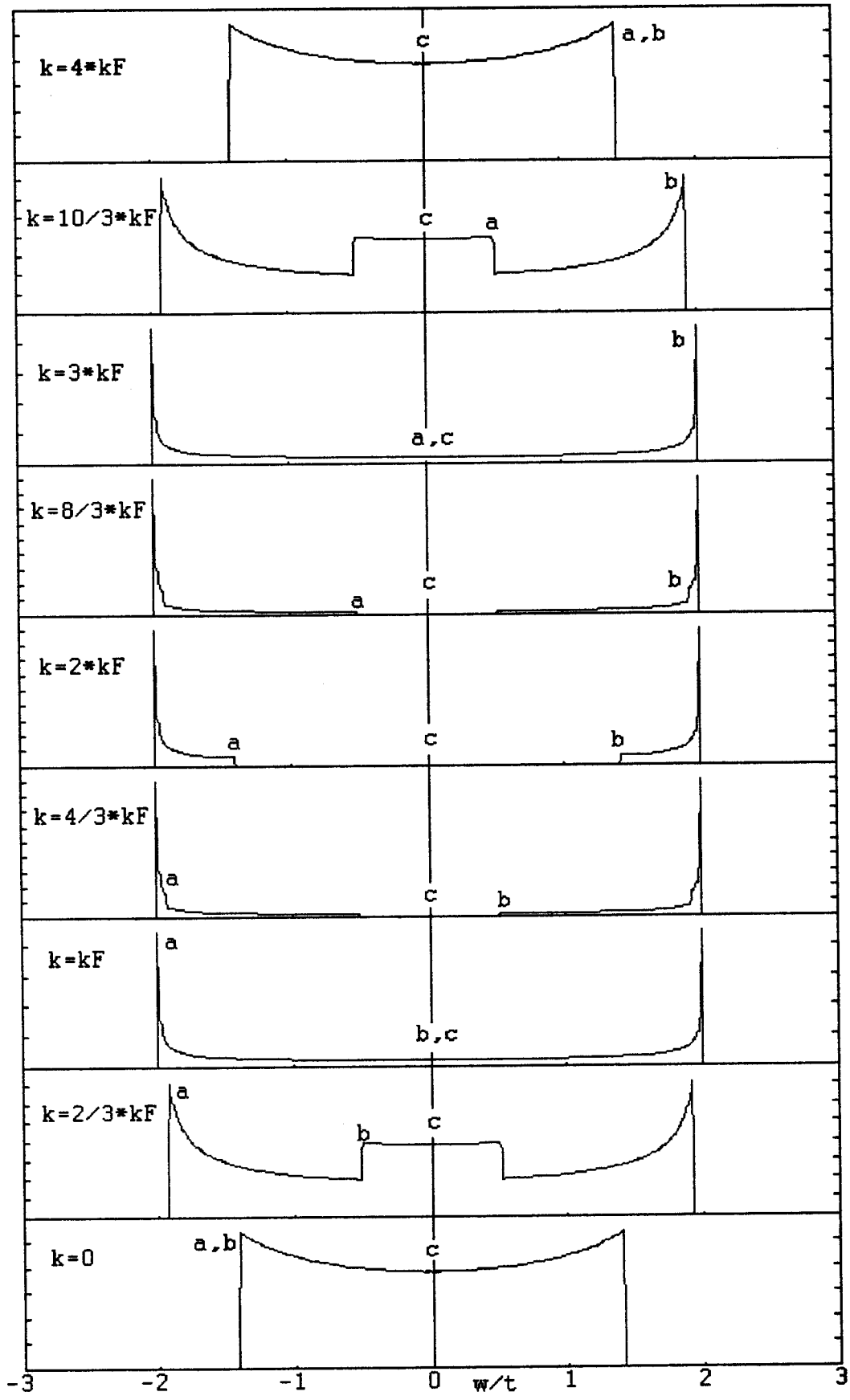

Figure 5.10: The functions $\tilde{B}(k,\omega)$ and $\tilde{A}_{LHB}(k,\omega)$ for $U=\infty$ and $n=0.5$ as function of ω/t for selected values of the momentum k.

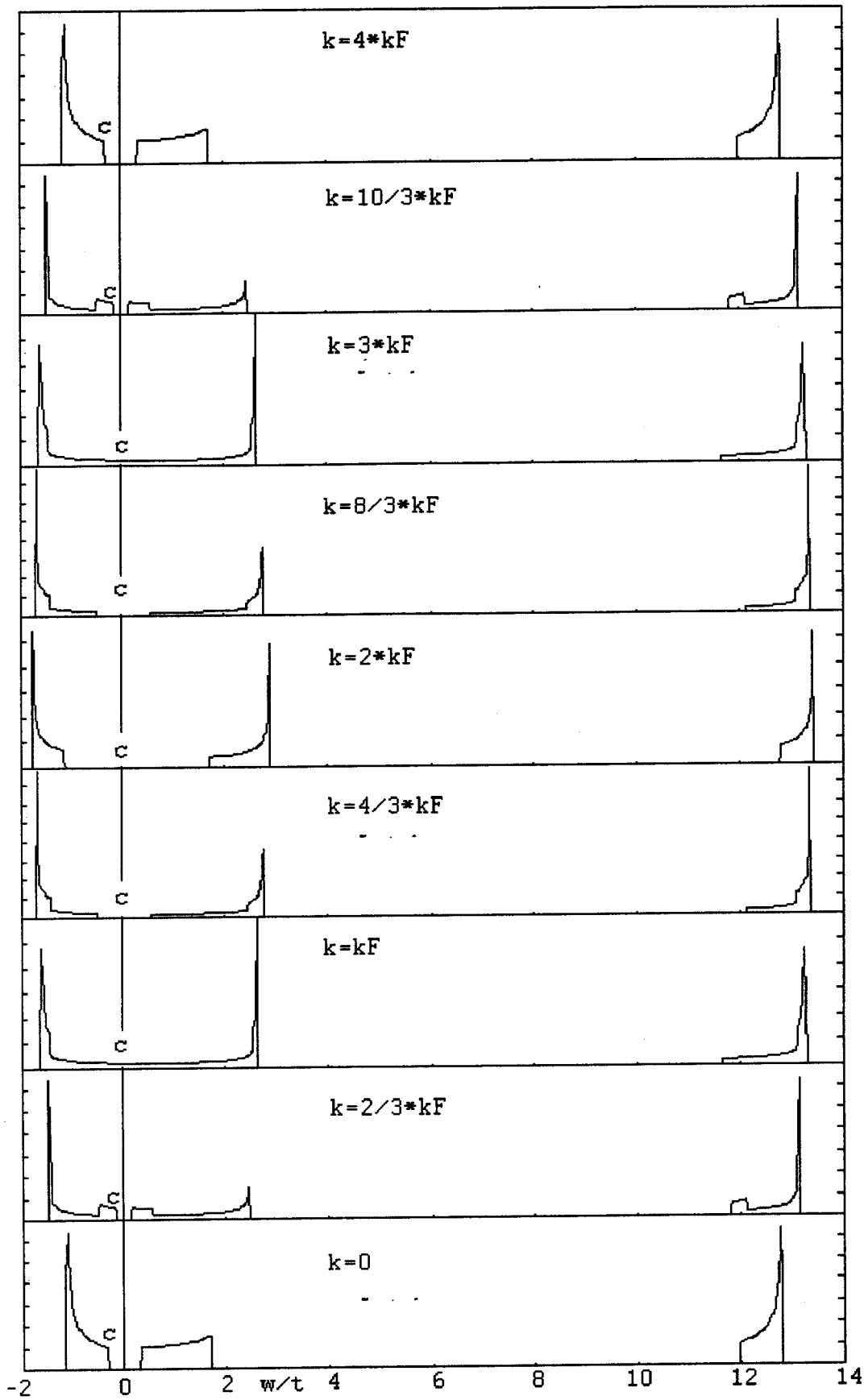

Figure 5.11: The functions $\tilde{B}(k,\omega)$, $\tilde{A}_{LHB}(k,\omega)$, and $\tilde{A}_{UHB}(k,\omega)$ for $U = 10t$ and $n = 0.5$ as function of ω/t for selected values of the momentum of k.

We have evaluated the functions $\tilde{B}(k,\omega)$, $\tilde{A}_{LHB}(k,\omega)$ and $\tilde{A}_{UHB}(k,\omega)$ numerically for $U=\infty$ and $n=0.5$ (Fig. 5.10) and for $U=10t$ and $n=0.5$ (Fig. 5.11). For $U=10t$ we used the $U\gg t$ expressions, Eqs. (2.89) and (2.90).

The spectral function is essentially given by the convolution of the $c,0$ holon band with the $s,0$ spinon band. Therefore, it is completely *incoherent*, in contrast to the FL theory. The use of the critical theory introduced in the previous chapter provides the matrix-element contributions, which lead to a LL type behaviour, as expected for a 1D fermionic system [22].

Combining the information of Figs. 5.9 with the pseudoparticle bands represented in Fig. 2.1, one can interpret the shape of the functions $\tilde{B}(k,\omega)$, $\tilde{A}_{LHB}(k,\omega)$ and $\tilde{A}_{UHB}(k,\omega)$ in terms of these pseudoparticle bands and identify the origin of the special points marked in Figs. 5.10 and 5.11.

We first analyze Fig. 5.10. The "a" and "b" points correspond to the holon band. There are two distinct holon bands which correspond to the two families of final states whose momentum differs by $\Delta k=\pm 4k_F$. The "c" point correspond to the spinon band, which remains at zero energy, since as $U\rightarrow\infty$ the spinon band becomes flat ($W_s=0$). Since in that limit $\epsilon^0_{c,0}(q)=-2t\cos(q)$ [see Eq. (2.89)], the holon bands have energy dispersion given by $\epsilon(k)=-2t\cos(k-k_F)$ and $\epsilon(k)=-2t\cos(k+k_F)$, respectively. This is in agreement with the results obtained by Penc *et al.* [9] using the Ogata-Shiba wavefunction [18]. They interpret the "b" point as the holon dispersion, what agrees with our result. However, they interpert the "a" point as a shadow band [23] coming from the spin fluctuations which diverge at $2k_F$, whereas we find that the "a" point also arises from the holon dispersion. The "duplication" of the holon dispersion is simply due to the *topological momentum shift mechanism*, which duplicates the number of final states

We now analyze the function plotted in Fig. 5.11. Apart from the holon bands, the main point is that the "c" point has now a dispersive band, since for finite U one has $W_s>O$. The "c" point corresponds to the spinon band, whose dispersion is given by $\epsilon(k)=-W_s\cos(k/n)$ for $k\in[0,k_F]\cup[3k_F,4k_F]$. Analogous results have been found by Penc *et al.* [9] for the spectral function of the Xiang and d'Ambrumenil model with XY exchange at half-filling and J finite ($J=0.4t$).

The overall conclusion of the study of this section, which considered the effects on the spectral function of the phase-space restrictions associated with the form of the pseudoparticle bands, is that the one-electron spectral function of the 1D Hubbard model exhibits both the holon and the spinon dispersion bands and that there are two holon bands dephased by $2k_F$ due to the topological momentum shift mechanism. In our discussion we have disregarded the pseudomomentum dependence of the matrix elements. These dependences are important in the vicinity of the critical points, leading to LL divergences and edges in the spectral function, as it was discussed in previous sections.

For $U \gg t$ or/and n in the vicinity of 1 the matrix elements are also important, since they strongly constrain the spinon pseudomomentum, which remains at $q_s \approx \pm k_F$.

5.5 Study of the density of states

In this section we consider again the effects of the matrix-element pseudomomentum dependences on the spectral function and density of states. We note that the correlation-function expressions obtained from the critical theory introduced in Chapter 4 are exact and take into account these matrix elements. On the other hand, that critical theory does not provide closed-form expressions for the matrix elements, the correlation-function expressions resulting from summations of many matrix elements. In this section we study the density of states $B(\omega)$, $A_{LHB}(\omega)$ and $A_{UHB}(\omega)$ defined in Eqs. (5.1) and (5.2) in terms of the one-particle spectral function. We will consider only the dominant contributions for the different parts of the density of states, as we have made for the study of the spectral function.

We start by considering the ω domains where there is significant spectral weight. We call ω_B the ω domain width of the function $B(\omega)$. This width is determined by the combined accessible phase-spaces for the holon and spinon and is given by

$$\omega_B \;=\; \left[\epsilon^0_{c,0}(2k_F) - \epsilon^0_{c,0}(0)\right] + W_s \;. \qquad (5.40)$$

where W_s is given by Eq. (2.91). At $n = 1$ the spectral width of the function $B(\omega)$ is exactly $4t$. Moreover, we find that for densities close to $n = 1$ and/or for large U and all values of n the matrix element $\langle f, N-1|c_{k\sigma}|GS, N\rangle$ is such that only final states where the spinon remains close to its pseudo-Fermi surface, $q_s = \pm k_F$, are finite. For large U this effect follows from the properties of the limit $U \rightarrow \infty$ wave function. Fortunately, in the limit $U \rightarrow \infty$ the BA wavefunction can be used directly in actual calculations. In the case of one-particle spectral function, the results of Refs. [8, 9] reveal that only states where the spinon remains close to its Fermi surface, i.e. $q_s \approx k_F$ or $q_s \approx -k_F$, contribute to that function. This effect follows from the matrix elements $\langle f, N-1|c_{k\sigma}|GS, N\rangle$ and $\langle f, N+1|c^{\dagger}_{k\sigma}|GS, N\rangle$ which vanish for final states where the spinon has pseudomomentum away from its pseudo-Fermi points. This effect survives for large U for all densities n, at least at order t^2/U. On the other hand, for smaller values of U this effect only survives for densities n close to half filling.

It follows that for both $U \gg t$ or for electronic densities in the vicinity of $n = 1$, W_s should be omitted in Eq. (5.40). From equation (2.89) we find for $U \gg t$

$$\omega_B \;=\; 2t\left[1 - \cos(n\pi)\right] - \frac{8t^2}{U}\ln 2\left[\sin(n\pi)\right]^2 , \qquad U \gg t$$

(5.41)

We denote by ω_{LHB} and ω_{UHB} the ω domains where there is significant spectral weight in the functions $A_{LHB}(\omega)$ and $A_{UHB}(\omega)$, respectively. The same type of considerations as for ω_B leads to

$$\omega_{LHB} = \left[\epsilon^0_{c,0}(\pi) - \epsilon^0_{c,0}(2k_F)\right] + W_s \, . \tag{5.42}$$

where W_s is given by Eq. (2.91). Again, in the strong coupling limit (or for densities close to half filling) the term W_s should be omitted and ω_{LHB} reads

$$\omega_{LHB} = 2t\left[1+\cos(n\pi)\right] + \frac{8t^2}{U}\ln 2\left[\sin(n\pi)\right]^2 , \qquad U \gg t \, . \tag{5.43}$$

On the other hand, consideration of the dominant contribution associated with the creation of one c-Yang particle, leads to

$$\omega_{UHB} = \omega_B \, . \tag{5.44}$$

Combining the ω location of the edges of the functions $B(\omega)$, $A_{LHB}(\omega)$ and $A_{UHB}(\omega)$ with the ω widths where these functions have significant spectral weight, we find that their domains are $\omega \in [-\omega_B, 0]$, $\omega \in [0, \omega_{LHB}]$ and $\omega \in [\omega_{LHB} + \Delta, \omega_{LHB} + \Delta + \omega_{UHB}]$, respectively. The parameter Δ is given by

$$\Delta = \frac{\Delta_c}{2} + \epsilon_F - W_s \tag{5.45}$$

where Δ_c and ϵ_F are the quantities alredady defined in Chapter 2. In the strong coupling limit (or for densities close to half-filling) W_s should be omitted and Δ is given by

$$\Delta = U - 2t\left[1-\cos(n\pi)\right] + \frac{8t^2}{U}\ln 2\left[\sin(n\pi)^2 + \left(1 - \frac{\sin(2\pi n)}{2\pi n}\right)\right] . \tag{5.46}$$

Due to the weakness of multi-pseudoparticle (or multi-pseudohole) processes, there is nearly no spectral weight for energies $\omega < -\omega_B$, $\omega \in [\omega_{LHB}, \omega_{LHB} + \Delta]$ and $\omega > \omega_{LHB} + \Delta + \omega_{UHB}$. Hence, Δ is a pseudo-gap between the LHB and the UHB, which becomes the Mott-Hubbard gap as $n \rightarrow 1$.

We have just clarified the question of the ω domains of the density of states $B(\omega)$, $A_{LHB}(\omega)$ and $A_{UHB}(\omega)$. We consider again the results of Chapter 4, in what critical exponents are concerned. The critical theory studied in that chapter provides the critical exponents which control the ω dependences of these density

of states at their ω domains edges. For $n < 1$ we find the following asymptotic behaviours

$$\begin{array}{ll} B(\omega) \propto \omega^{\nu}, & \text{for } \omega \rightarrow 0^{-}; \\ A_{LHB}(\omega) \propto \omega^{\nu}, & \text{for } \omega \rightarrow 0^{+}; \\ A_{UHB}(\omega) \propto (\omega - \omega_0)^{\nu}, & \text{for } (\omega - \omega_0) \rightarrow 0^{+}; \end{array} \tag{5.47}$$

where $\omega_0 = \omega_{LHB} + \Delta$ and $\nu = \varsigma_{\sigma}^{0} + 1$ and the exponent ς_{σ}^{0} is given by Eq. (5.27). At $H = 0$ the exponent $\nu \rightarrow 1/8$ as $U \rightarrow \infty$.

On the other hand, for densities close to half filling and $U \rightarrow \infty$, the use the generalized critical theory described in Chapter 4 and introduced in Ref. [24], leads to the following threshold behaviours

$$\begin{array}{ll} B(\omega) \propto (\omega + \omega_B)^{-3/16}, & \text{for } (\omega + \omega_B) \rightarrow 0^{+}; \\ A_{LHB}(\omega) \propto (\omega - \omega_{LHB})^{-3/16}, & \text{for } (\omega - \omega_{LHB}) \rightarrow 0^{-}; \\ A_{UHB}(\omega) \propto (\omega - (\omega_0 + \omega_{UHB})^{-3/16}, & \text{for } (\omega - (\omega_0 + \omega_{UHB})) \rightarrow 0^{-}. \end{array} \tag{5.48}$$

The divergences at these threshold energies occur when the holon (or the $c,0$ pseudoparticle) reaches the bottom-edge (or the top-edge) of the $c,0$ band.

At $n = 1$ the $c,0$ band is full for the GS. Moreover, states with one holon the $c,0$ band is quadratic and the problem cannot be treated within CFT. In Ref. [24] a theory of multicomponent problems with both linear and non-linear bands was introduced. As in the case of the $\gamma > 0$ pseudoparticles, it turns out that the general expresssions (4.87)-(4.88) and (4.90) also apply to $n = 1$.

The results for $A_{LHB}(\omega)$ and $A_{UHB}(\omega)$ are combined in a semi-qualitative sketch for the density of states in Fig. 5.12 for $n = 1$ and $n = 0.7$ and for $U = 0$ and $U = 12t$. The curves have the correct spectral weights, spectral widths and bottom- and top-edge ω threshold dependences. Thus, the ω interpolation for energies away of the edges is expected to be close to the true curves. The $n = 1$ exponents are given in Refs. [41, 40]. Upon doping, the UHB loses weight rapidly to the LHB and the singularity of the UHB bottom edge disappears, as illustrated in Fig. 5.12. Note that $A(\omega)$ vanishes at $\omega = 0$, in contrast to the $U = 0$ curve.

5.6 Concluding remarks

Our results on the density of states confirm the Luttinger-Liquid behaviour ω^{ν} at the Fermi surface [22, 25, 26, 27, 28], where the non-universal exponent ν depends on the on-site Coulomb repulsion U, electronic density n and applied magnetic field H. In particular, we find that $\nu \rightarrow 1/8$ at $H \rightarrow 0$ in the strong coupling limit $U \rightarrow \infty$, in agreement with previous theoretical results [8, 18, 29]. The supression of the Fermi surface is observed in photoemission experiments for quasi-one dimensional conductors [30, 31, 32, 33, 34, 35].

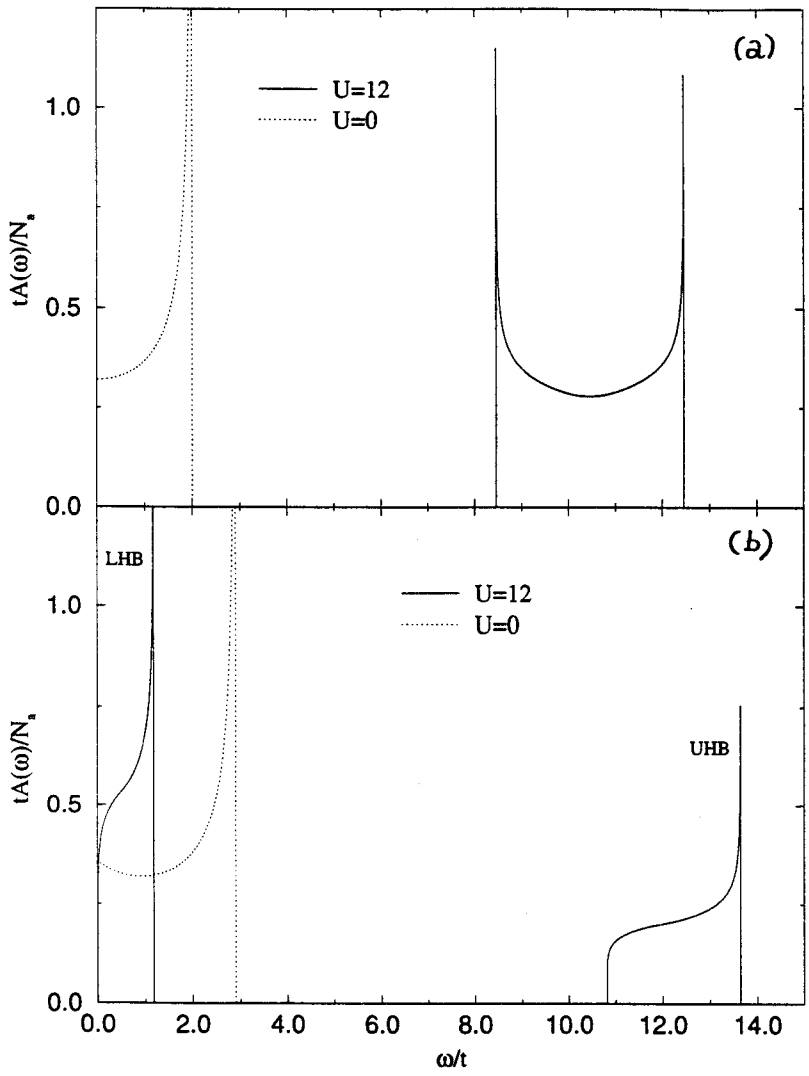

Figure 5.12: Sketch of $A(\omega)$ as function of ω/t for (a) $n = 1$ and (b) $n = 0.7$ and for $U = 0$ (dashed lines) and $U = 12t$ (solid lines). The initial GS energy is at $\omega = 0$. (N_a is the number of sites.)

Moreover, we find a pseudo-gap between the LHB and the UHB, in agreement with previous numerical studies [11, 20]. Our approach allows us to evaluate the threshold behaviour at finite energies ω_0 corresponding to the UHB, where we find again the behaviour $(\omega - \omega_0)^\nu$.

Thus, to complement the ARPES studies of Refs. [30, 36, 37, 38, 39], we propose inverse-photoemission studies, which can be directly compared with our theoretical predictions, namely the occurrence of a pseudo-gap for densities away from half-filling.

Bibliography

[1] N. Kawakami and A. Okiji, Phys. Rev. B **40**, 7066 (1989).

[2] F. Woynarovich, J. Phys. A: Math. Gen. **22**, 4243 (1989).

[3] H. J. Schulz, Phys. Rev. Lett. **64**, 2831 (1990).

[4] N. Kawakami and S.-K. Yang, Phys. Rev. Lett. **65**, 3063 (1990).

[5] H. Frahm and V. E. Korepin, Phys. Rev. B **42** 10553 (1990).

[6] S. Sorella and A. Parola, J. Phys.: Condens. Matter **4**, 3589 (1992).

[7] T. Momoi, Phys. Lett. A **195**, 351 (1994).

[8] K. Penc, F. Mila and H. Shiba, Phys. Rev. Lett. **75**, 894 (1995).

[9] K. Penc, K. Hallberg, F. Mila and H. Shiba, Phys. Rev. Lett. **77**, 1390 (1996).

[10] H. Eskes and A. M. Oleś, Phys. Rev. Lett. **73**, 1279 (1994).

[11] R. Preuss *et al.*, Phys. Rev. Lett. **73**, 732 (1994).

[12] J. Voit, Phys. Rev. B **47**, 6740 (1993).

[13] K. Schönhammer and V. Meden, Phys. Rev. B **47**, 16205 (1993).

[14] E. H. Lieb, and F. Y. Wu, Phys. Rev. Lett. **20**, 1445 (1968).

[15] F. H. L. Eßler and V. E. Korepin, Phys. Rev. Lett. **72**, 908 (1994).

[16] J. M. P. Carmelo, and N. M. R. Peres, Nuc. Phys. B **458**, 579 (1996).

[17] J. M. P. Carmelo and N. M. R. Peres, Phys. Rev. B **56**, 3717 (1997).

[18] M. Ogata and H. Shiba, Phys. Rev. B **41**, 2326 (1990).

[19] H. Eskes, M. B. J. Meinders and G. A. Sawatzky, Phys. Rev. Lett. **67**, 1035 (1991).

[20] M. B. J. Meinders, H. Eskes and G. A. Sawatzky, Phys. Rev. B **48**, 3916 (1993).

[21] J. M. P. Carmelo, P. Horsh and A. A. Ovchinnikov, Phys. Rev. B **46**, 14728 (1992).

[22] F. D. M. Haldane, J. Phys. C **14**, 2585 (1981).

[23] A. P. Kampf and J. R. Schrieffer, Phys. Rev. B **42**, 7967 (1990).

[24] J. M. P. Carmelo, J. M. E. Guerra, J. M. B. Lopes dos Santos and A. H. Castro Neto, Phys. Rev. Lett. **83**, 3892 (1999).

[25] S. Tomonaga, Prog. Theor. Phys. **5**, 544 (1950).

[26] J. M. Luttinger, J. Math. Phys. (N.Y.) **4**, 1154 (1963).

[27] D. C. Mattis and E. Lieb, J. Math. Phys. (N.Y.) **6**, 304 (1965).

[28] J. Sólyom, Adv. Phys. **28**, 201 (1979).

[29] M. Ogata, T. Sugiyama and H. Shiba, Phys. Rev. B **43**, 8401 (1991).

[30] B. Dardel *et al.*, Phys. Rev. Lett. **67**, 3144 (1991).

[31] Y. Hwu *et al.*, Phys. Rev. B **46**, 13624 (1992).

[32] B. Dardel *et al.*, Europhys. Lett. **19**, 525 (1992).

[33] C. Coluzza *et al.*, Phys. Rev. B **47**, 6625 (1993).

[34] B. Dardel *et al.*, Europhys. Lett. **24**, 687 (1993).

[35] M. Nakamura *et al.*, Phys. Rev. B **49**, 16191 (1994).

[36] C. Kim *et al.*, Phys. Rev. Lett. **77**, 4054 (1996).

[37] K. Kobayashi *et al.*, Phys. Rev. Lett. **80**, 3141 (1998).

[38] K. Kobayashi *et al.*, Phys. Rev. Lett. **82**, 803 (1999).

[39] J. D. Dendinger *et al.*, Phys. Rev. Lett. **82**, 2540 (1999).

[40] J. M. P. Carmelo, L. M. Martelo, T. Prosen and D. K. Campbell (submitted to Phys. Rev. Lett., 1999).

[41] J. M. P. Carmelo, J. M. E. Guerra and L. M. Martelo (preprint, 1999).

Chapter 6

Variational Wave Functions for the Hubbard Model

6.1 Introduction

For dimension $D > 1$ there is no available exact solution for the Hubbard model. Perturbative methods are limited to their own range of validity and exact diagonalizations are still restricted to small size systems.

The variational approach is an alternative way for studying ground state properties. Physical insight of the system can be obtained with an well-chosen variational wave function.

One of the main problems with variational wave functions is to know their quality. The energy criterion, which states that the variational energy is an upper bound of the exact ground state energy, is not enough to decide whether a certain variational wave function is qualitatively correct to describe a model within the region of parameters for which the variational wave function has been constructed. This is specially relevant when there are competing instabilities in the model. One needs to be careful in the construction of a variational wave function and a precise idea how the model behaves is very helpful. In view of this, it is important to compare variational results with results from different methods.

The advantages of using variational wave functions are that usually they are conceptually very clear and they can display essential features of the model without requiring heavy calculations.

6.2 Gutzwiller wave function

Gutzwiller [1, 2] introduced an ansatz for the ground state wave function of the Hubbard model given by

$$\psi_G = e^{-\eta \hat{D}} \psi_0 \tag{6.1}$$

where η is a variational parameter and $\psi_0 = \prod_{k<k_F,\sigma} \hat{c}^\dagger_{\mathbf{k},\sigma}|0\rangle$ is the exact ground state for $U = 0$, i.e., the Fermi sea filled up to the Fermi momentum k_F.

It is instructive to write ψ_0 as a superposition of eigenstates of the operator $\hat{D}$, the wave functions ϕ_D such that $\hat{D}\phi_D = D\phi_D$, and then apply the Gutzwiller projector

$$\begin{aligned} \psi_G &= e^{-\eta \hat{D}}[\phi_0 + \phi_1 + \phi_2 + \ldots] \\ &= \phi_0 + e^{-\eta D}\phi_1 + e^{-2\eta D}\phi_2 + \ldots \,. \end{aligned} \tag{6.2}$$

Therefore, configurations with D doubly occupied sites are mutiplied by a factor $e^{-\eta D}$, i.e. they are exponentially suppressed with D. This is the "way" how the Gutzwiller wave function, starting from the uncorrelated Fermi sea ψ_0, takes into account the correlation effects due to the on-site interaction U of the Hubbard model.

It is also instructive to express the Gutzwiller wave function in real space occupation number representation

$$\psi_G = \sum_{\{n_{i\sigma}\}} e^{-\eta \sum_i n_{i\uparrow} n_{i\downarrow}} f(\{n_{i\sigma}\})|\{n_{i\sigma}\}\rangle \tag{6.3}$$

where the Fermi surface does not show up explicitely but is hidden in the phase correlations of the complex amplitudes $f(\{n_{i\sigma}\})$. The Gutzwiller correlator $e^{-\eta \hat{D}}$ does not destroy these subtle phase correlations, it merely *reweights* all configurations with D doubly occupied sites by an overall factor $e^{-\eta D}$. Therefore one expects that for any finite value of η (equivalent to finite U) the Gutzwiller wave function will preserve the discontinuity at the Fermi surface in the single-particle momentum distribution function. We will show below that it represents always a conducting state for $\eta < \infty$. Only in the limit $\eta \to \infty$ one is left with a fully projected wave function where no doubly occupied sites are left over (see Eq. 6.2). In this limit, at half-filling, the single-particle momentum distribution function is constant: $\langle \hat{n}_{\mathbf{k}\sigma} \rangle = 1/2$.

The Gutzwiller wave function only in very rare cases can be treated exactly: for the one-dimensional Hubbard model [3] and for the one-dimensional $1/r$-hopping Hubbard model [4, 5]. Nevertheless, there exist at least reasonable approximations and straightforward numerical techniques: the Variational Monte Carlo [6].

We present now the systematic expansion for the Gutzwiller wave function in terms of powers of U/t. This expansion is based on standard many-body techniques. The ground state energy of the Gutzwiller wave function is obtained by minimization of the following expression

$$F_G(\eta) = \frac{\langle\psi_0|e^{-\eta\hat{D}}\hat{H}e^{-\eta\hat{D}}|\psi_0\rangle}{\langle\psi_0|e^{-2\eta\hat{D}}|\psi_0\rangle} \tag{6.4}$$

with respect to the variational parameter η. In the weak coupling limit, $U \ll t$, the variational parameter η is also small and the exponential can be expanded in powers of η. As the Fermi sea ψ_0 is a Slater determinant one can apply the Linked Cluster Theorem [7]. One gets the following expression for the kinetic term

$$T(\eta) = \sum_{\nu=0}^{\infty} \frac{(-\eta)^\nu}{\nu!}\langle\psi_0|\{\hat{D},...\{\hat{D},\hat{T}\},\}|\psi_0\rangle_C \tag{6.5}$$

where $\hat{D}$ appears ν times in the anticommutators and the index C denotes that, after using Wick's Theorem to evaluate expectation values, one has to sum only over diagrams with connected contractions. The expansion for the potential term yields

$$UD(\eta) = U\sum_{\nu=0}^{\infty} \frac{(-2\eta)^\nu}{\nu!}\langle\psi_0|\hat{D}^{\nu+1}|\psi_0\rangle_C. \tag{6.6}$$

Using the optimal parameter η_0 that minimizes expression (6.4), one can obtain not only the ground state energy but also expectation values of any quantity (momentum distribution function, n-particle correlation functions, etc). In fact, it has been used for evaluating the ground state energy [8, 9] and the momentum distribution function [10] of the $1D$ Hubbard model and equal-time correlation functions of both the $1D$ and $2D$ (square lattice) Hubbard model [11].

The first term of this expansion is just the energy for the Hubbard model in the Hartree-Fock approximation. This energy per site $\epsilon_{HF} = E_{HF}/L$ is given by

$$\begin{aligned}
\epsilon_{HF} &= \frac{1}{L}\langle\psi_0|\hat{T}|\psi_0\rangle + \frac{1}{L}\sum_i \langle\psi_0|\hat{n}_{i\uparrow}\hat{n}_{i\downarrow}|\psi_0\rangle\, U \\
&= \epsilon_0 + \frac{1}{L}\sum_i \langle\hat{n}_{i\uparrow}\rangle\langle\hat{n}_{i\downarrow}\rangle\, U \\
&= \epsilon_0 + \frac{1}{4}U \\
&= \epsilon_0 + \epsilon_1\left(\frac{U}{t}\right)
\end{aligned} \tag{6.7}$$

where ϵ_0 is the kinetic energy per site of the Fermi sea and $\epsilon_1 = 0.25t$.

Gutzwiller himself introduced an approximation to his wave function [2]. This approximation can be interpreted as a two-site cluster approximation, where the cluster is treated exactly but it is embedded in a mean-field environment [12, 13, 14, 15]. The ground state energy per site in the Gutzwiller approximation reads

$$\epsilon_{GA} = \begin{cases} \epsilon_0 \left(1 - \frac{U}{U_0}\right)^2 & \text{for } U \leq U_0 \\ 0 & \text{for } U > U_0 \end{cases} \tag{6.8}$$

where $U_0 = 8|\epsilon_0|$. At $U = U_0$ both the number of doubly occupied sites and the discontinuity at the Fermi surface of the single-particle momentum distribution function drop to zero. Therefore, as pointed out by Brinkman and Rice [16], the Gutzwiller approximation predicts a metal-insulator transition at $U = U_0$. They have also assumed that the effective electronic mass equals the reciprocal of the discontinuity of the momentum distribution as in a Fermi liquid. Thus the effective electronic mass becomes infinite at the metal-insulator transition. In this scenario the double occupancy appears as the order parameter of the metal-insulator transition.

For $U < U_0$ this approximation describes a paramagnetic conducting state. At $U = U_0$ the energy is zero, i.e., the energy of a paramagnetic insulating state. As remarked by Brinkman and Rice, a magnetically ordered insulating state will have a lower energy than the paramagnetic one and the transition from a paramagnetic conducting state to a magnetically ordered insulating state will occur for a value of U smaller than U_0.

In the limit of infinite dimensions, Metzner and Vollhardt using a suitable diagrammatic expansion for the Gutzwiller wave function were able to show that the "Gutzwiller approximation" becomes exact [17]. Starting from the limit of infinite dimensions, a systematic procedure to include $1/D$-corrections to the Gutzwiller approximation has also been introduced [18].

In the large U limit empty and doubly occupied sites are not distributed homogeneously over the system but rather tend to form *pairs*, a feature that is completely absent in the Gutzwiller wave function, as noticed some time ago [19]. There have been attempts to cure this defect by introducing further operators in the Gutzwiller wave function, which enhance the nearest correlations between empty and doubly occupied sites. In this way, it has been possible to produce much better variational energies in the strong coupling limit, as compared to the original Gutzwiller wave function, but unfortunately expectation values can only be evaluated by using certain approximations [20] or numerically [21]. Moreover, these wave functions do not represent an insulating ground state at half-filling, and therefore it is problematic to use them for the strong coupling limit.

6.3 "Dual" Gutzwiller wave function

In view of the shortcomings of the Gutzwiller wave function in the large U limit, an alternative variational wave function [22] has been introduced, which can be regarded as the strong coupling counterpart of the Gutzwiller wave function. It is defined as

$$\psi_B = e^{-\kappa \hat{T}} \psi_\infty \tag{6.9}$$

where ψ_∞ is the ground state of the Hubbard model for $U \to \infty$. In this chapter we are interested in studying the Hubbard model at half-filling ($n = 1$) and therefore we will essentially focus hereafter in this special case. At half-filling, the state ψ_∞ is the the ground state of the antiferromagnetic (AF) Heisenberg model. This state has exactly one electron per site: electrons are "localized" in the sites of the lattice and the state is an insulting one.

It is instructive to write ψ_∞ as a superposition of eigenstates of the kinetic operator $\hat{T}$, the wave functions $\psi_n (n = 0, 1, ...)$ such that $\hat{T}\psi_n = T_n \psi_n$ and then apply the kinetic projector (shifted by an irrelevant constant factor that cancels out when expectation values are evaluated)

$$\begin{aligned} \psi_B = &= e^{-\kappa(\hat{T}-T_0)}[\psi_0 + \psi_1 + \psi_2 + \ldots] \\ &= \psi_0 + e^{-\kappa(T_1-T_0)}\psi_1 + e^{-2\kappa(T_2-T_0)}\psi_2 + \ldots \ . \end{aligned} \tag{6.10}$$

As the parameter κ increases (which is equivalent to U decreasing) more and more electrons are delocalized and double occupancy is allowed. It appears in the system particle-hole pairs. This is the "way" how the the ψ_B wave function, starting from the state ψ_∞ takes into account the existence of doubly occupied sites due to a finite on-site interaction U.

It is also instructive to rewrite ψ_B in k-space occupation number representation, in perfect correspondence to the real space representation for ψ_G,

$$\psi_B = \sum_{\{n_{k\sigma}\}} e^{-\kappa \sum_{k,\sigma} \epsilon_k n_{k\sigma}} g(\{n_{k\sigma}\}) |\{n_{k\sigma}\}\rangle \tag{6.11}$$

Here $g(\{n_{k\sigma}\})$ are the coefficients of the antiferromagnetic ground state ψ_∞ in momentum space representation. The operator $e^{-\kappa \hat{T}}$ suppresses configurations with high kinetic energy. For small values of κ the spin correlations of the variational wave function ψ_B will resemble very much those of the Heisenberg antiferromagnet since the phase relations among the $g(\{n_{k\sigma}\})$ are not affected by the operator $e^{-\kappa \hat{T}}$. We will show below that the ψ_B describes an insulating state for $\kappa < \infty$. In the limit $\kappa \to \infty$ only the configuration with the lowest kinetic energy, the Fermi sea, survives (see Eq. 6.10). Thus ψ_B is the exact ground state not only for $U \to \infty$ but also in the limit $U \to 0$.

A complementary way to visualize the nature of ψ_B, at least for small κ, is to expand it in powers of κ,

$$\psi_B = \psi_\infty - \kappa \hat{T}\psi_\infty + \frac{\kappa^2}{2}\hat{T}^2\psi_\infty - \ldots \tag{6.12}$$

In the special case of nearest-neighbour hopping, $\hat{T}$ moves an electron from one site to a neighbouring one. Thus, particle-hole pairs appear on nearest neighbour

sites within the contribution $\sim \kappa$, while higher order contributions $\sim \kappa^n$ contain pairs separated by at most n steps. The presence of few and tightly bound pairs for small η characterizes well the ground state for large values of U. Therefore, the trial state ψ_B appears to be more natural in this limit than the Gutzwiller wave function supplemented by a correlation factor for particles and holes.

In contrast to ψ_0, the state ψ_∞ is in general not known. Exceptions are the one-dimensional case [23] and the case of bipartite lattices in the limit of infinite dimensions [24]. This renders practical calculations for ψ_B rather difficult. Exact results using ψ_B are available only for special particular cases: the one-dimensional $1/r$-hopping Hubbard model [5] and the limit of infinite dimensions [25].

We present now the systematic expansion for the wave function ψ_B in terms of powers of t/U. The ground state energy ψ_B is obtained by minimization of the following expression

$$F_B(\kappa) = \frac{\langle\psi_\infty|e^{-\kappa\hat{T}}\hat{H}e^{-\kappa\hat{T}}|\psi_\infty\rangle}{\langle\psi_\infty|e^{-2\kappa\hat{T}}|\psi_\infty\rangle} \tag{6.13}$$

with respect to the variational parameter κ. In the strong coupling limit, $U \gg t$, the variational parameter κ is small and the exponential can be expanded in powers of κ. As in general ψ_∞ is not a Slater determinant, one cannot apply the Linked Cluster Theorem. One gets for the kinetic term

$$T(\kappa) = \frac{\sum_{\nu=0}^{\infty} \frac{(-2\kappa)^\nu}{\nu!}\langle\psi_\infty|\hat{T}^{\nu+1}|\psi_\infty\rangle}{N} \tag{6.14}$$

and for the potential term one gets

$$UD(\kappa) = U\,\frac{\sum_{\nu=0}^{\infty} \frac{(-\kappa)^\nu}{\nu!}\langle\psi_\infty|\{\hat{T},...\{\hat{T},\hat{D}\},\}|\psi_\infty\rangle}{N} \tag{6.15}$$

where $\hat{T}$ appears ν times in the anticommutators and

$$N = \sum_{\nu=0}^{\infty} \frac{(-2\kappa)^\nu}{\nu!}\langle\psi_\infty|\hat{T}^\nu|\psi_\infty\rangle. \tag{6.16}$$

The state ψ_∞ has exactly one electron per site and it is straightforward to show that $T(\kappa)$ is zero for ν even, $D(\kappa)$ is zero for ν odd and N is zero for ν odd. The first term of this expansion gives the variational energy $E_B = 0$, ($T_0 = \langle\psi_\infty|\hat{T}|\psi_\infty\rangle = 0$ and $D_0 = \langle\psi_\infty|\hat{D}|\psi_\infty\rangle = 0$) which corresponds to the Heitler-London approximation [26] for the Hubbard model.

One can show that the leading order term in t/U gives a variational energy E_B identical to the ground state energy of the antiferromagnetic Heisenberg model [22]. Considering that the state ψ_∞ is normalized, one obtains for the kinetic term

$$T(\kappa) = -2\kappa \, \langle \psi_\infty | \hat{T}^2 | \psi_\infty \rangle + \mathcal{O}(\kappa^2) \tag{6.17}$$

and for the potential term

$$D(\kappa) = \frac{\kappa^2}{2} \, \langle \psi_\infty | \hat{T}^2 | \psi_\infty \rangle + \mathcal{O}(\kappa^2) \tag{6.18}$$

once $\langle \psi_\infty | \hat{T}\hat{D}\hat{T} | \psi_\infty \rangle = 1/2 \langle \psi_\infty | \hat{T}^2 | \psi_\infty \rangle$. Expression (6.13) becomes

$$F_B(\kappa) = (-2\kappa + \frac{k^2}{2}U) \, \langle \psi_\infty | \hat{T}^2 | \psi_\infty \rangle. \tag{6.19}$$

The optimal variational parameter in the leading order term reads $\kappa_0 = 2/U$. The state ψ_∞ has one-electron per site and the operator $\hat{T}^2$ can be written in terms of the spin-1/2 operators as [27]

$$\langle \psi_\infty | \hat{T}^2 | \psi_\infty \rangle = -2|t|^2 \sum_{\langle ij \rangle} \langle \psi_\infty | \left(\mathbf{S_i}.\mathbf{S_j} - \frac{1}{4} \right) | \psi_\infty \rangle. \tag{6.20}$$

And one finally gets

$$E_B = J \sum_{\langle ij \rangle} \langle \psi_\infty | \left(\mathbf{S_i}.\mathbf{S_j} - \frac{1}{4} \right) | \psi_\infty \rangle \tag{6.21}$$

where $J = 4|t|^2/U$ and the sum is over the pairs $\langle ij \rangle$.

In the limit of infinite dimensions and for bipartite lattices, ψ_∞ is simply the Néel state [24]. The wave function ψ_B can then be exactly solved in this special limit. For dimensions $D < \infty$ the Néel state is no more the exact ground state. However, if we are in the presence of a bipartite lattice that shows antiferromagnetic long-range order, one can use the Néel state as a mean-field approximation, once one is neglecting spin fluctuations but expecting to the keep the qualitative physics. This can be seen has the counterpart of the Gutzwiller approximation, in the sense that both become exact in the limit of infinite dimensions.

As we will show below that the ψ_B describes an insulating state for $\kappa < \infty$. For $\kappa = \infty$ the wave function ψ_B coincides with the Fermi sea (see Eq. 6.10) and therefore it describes a conducting state. So by its own the wavefunction ψ_B can predict a metal-insulating transition. This is somehow the counterpart of the Brinkman-Rice transition. For $\kappa = \infty$ we reach the "maximum" delocalization of electrons and the system becomes conducting, in a dual way with the Brinkman-Rice transtion where the effective electronic mass becomes infinite at the metal-insulator transition.

6.4 Charge stiffness

A criterion due to Kohn [28], based on the sensitivity of the ground state energy with respect to changes of boundary conditions, is particularly useful in order

to decided if a given wavefunction is a conducting or an insulating one, once it does not require any information about excited states. For the sake of simplicity we limit ourselves to the one-dimensional case (the generalization to arbitrary dimensions is straightforward). One considers a closed ring of length L threaded by a magnetic flux Φ. The flux has associate a vector potential $A = \Phi/L$ along the chain. The hopping matrix elements have to be multiplied by a phase factor, kown as the Peierls substitution (see Appendix A6), and the flux dependent kinetic energy reads

$$\hat{T}(\Phi) = -t \sum_{i,\sigma} \left(e^{i\Phi/L}\, \hat{c}^{\dagger}_{i\sigma} \hat{c}_{i+1,\sigma} + e^{-i\Phi/L}\, \hat{c}^{\dagger}_{i+1,\sigma} \hat{c}_{i,\sigma} \right) \tag{6.22}$$

while the potential term remains unchanged. It can be shown [28] that the real part of the zero-temperature conductivity is given by a singular part (corresponding to "free" acceleration of the charge carriers of the system) plus a regular part (corresponding to absortion in the system)

$$\sigma(\omega) = \pi D_c \delta(\omega) + \sigma_{reg}(\omega) \tag{6.23}$$

where D_c is the charge stiffness (or Drude weight) and is given by

$$D_c = L \left. \frac{d^2 E(\Phi)}{d\Phi^2} \right|_{\Phi=0} . \tag{6.24}$$

where $E(\Phi)$ is the ground state energy for a given flux Φ. The natural criterion that comes out is that the charge stiffness is *finite* for a conducting wavefunction while it *vanishes* for an insulating one.

We first consider the Gutzwiller wave function. The variational ground state energy for a given flux Φ is obtained by minimizing

$$F_G(\Phi, \eta) = \frac{\langle \psi_0(\Phi) | e^{-\eta \hat{D}} \hat{H}(\Phi) e^{-\eta \hat{D}} | \psi_0(\Phi) \rangle}{\langle \psi_0(\Phi) | e^{-2\eta \hat{D}} | \psi_0(\Phi) \rangle} \tag{6.25}$$

with respect to η. The result is $E_G(\Phi) = F_G(\Phi, \eta_0(\Phi))$ where $\eta_0(\Phi)$ denotes the optimal value of η for a given flux Φ. The second derivative of the variational energy with respect to Φ yields

$$\frac{d^2 E_G(\Phi)}{d\Phi^2} = \frac{\partial^2 F_G}{\partial \Phi^2} + 2 \frac{\partial^2 F_G}{\partial \Phi \partial \eta} \frac{d\eta}{d\Phi} + \frac{\partial^2 F_G}{\partial \eta^2} \left(\frac{d\eta}{d\Phi} \right)^2 \tag{6.26}$$

where we have already used the minimum condition $\partial F_G / \partial \eta = 0$. In the limit $\Phi \to 0$ the above equation simplifies further since $\eta_0(\Phi)$ is an even function, and therefore $\partial \eta_0 / \partial \Phi = 0$ at $\Phi = 0$. The charge stiffness of the Gutzwiller wave function is thus simply given by the first term of Eq. (6.26),

$$D_c = L \left. \frac{\partial^2 F_G(\Phi, \eta)}{\partial \Phi^2} \right|_{\Phi=0} . \tag{6.27}$$

In order to proceed, it is crucial to realize that the ground state $\psi_0(\Phi)$ of the non-interacting system does not depend on Φ as long as Φ is small enough. When a flux Φ is applied, the one-particle energy levels $\epsilon(k)$ are shifted to $\epsilon(k+\Phi/L)$, but levels will not cross if $\Phi \ll 1$. Therefore the second derivative with respect to Φ in Eq. (6.27) acts only on $\hat{H}(\Phi)$. Using the fact that $\partial^2\hat{H}(\Phi)/\partial\Phi^2 = -\hat{T}(\Phi)/L^2$ we obtain the final result

$$D_c = -\frac{1}{L}\langle\hat{T}\rangle\,. \tag{6.28}$$

The charge stiffness for the Gutzwiller wave function is proportional to the expectation value of the kinetic energy and therefore vanishes only in the limit of the completely projected state $\eta \to \infty$. This result has previously been obtained by Millis and Coppersmith using slightly different arguments [29].

We now consider the wave function ψ_B. As before we have to calculate the flux-dependent variational ground state energy $E_B(\Phi)$ which is obtained by minimizing

$$F_B(\Phi,\kappa) = \frac{\langle\psi_\infty|e^{-\kappa\hat{T}(\Phi)}\hat{H}(\Phi)e^{-\kappa\hat{T}(\Phi)}|\psi_\infty\rangle}{\langle\psi_\infty|e^{-2\kappa\hat{T}(\Phi)}|\psi_\infty\rangle} \tag{6.29}$$

with respect to κ. First of all, we notice that ψ_∞ does not depend on Φ, once in the limit $U \to \infty$ and at half-filling the Hubbard model can be mapped onto the antiferromagnetic Heisenberg model with exchange coupling $J = 4|t|^2/U$, and so the phase factor associated with Φ cancels out. Expanding all exponentials appearing in Eq.(6.29) in powers of $\hat{T}(\Phi)$ one is left with expectation values of the type

$$\langle\psi_\infty|\hat{T}^n(\Phi)\,\hat{D}\,\hat{T}^m(\Phi)|\psi_\infty\rangle \tag{6.30}$$

The wave function ψ_∞ is a superposition of states where each site is singly occupied (at half-filling). Acting with $\hat{T}(\Phi)$ on ψ_∞ moves an electron from one site to a neighbouring one, thus creating empty and doubly occupied sites in the system. Each move to the right (left) is associated with a phase factor $e^{i\Phi/L}(e^{-i\Phi/L})$. In order to have a non-vanishing matrix element (6.30) the total number of moves to the left and to the right must be the same, since in the end one has to reach again a state where each site is singly occupied. Therefore all phase factors cancel completely and the matrix elements are independent of Φ. Consequently $E_B(\Phi)$ is independent of Φ and the its charge stiffness is zero. Therefore the wave function ψ_B is an insulating one.

6.5 The Mott-Hubbard transition

The metal-insulator transition produced by electron correlations, i.e. the Mott transition [31], when treated within the framework of the Hubbard model is known

as the Mott-Hubbard transition. In this chapter, we are interested in studying the Mott-Hubbard transition at $T = 0K$ and at half-filling $n = 1$ using variational wavefunctions.

We give now a physical picture how the Hubbard model at half-filling embodies the Mott phenomenon. For $U \to \infty$ all sites are singly occupied and no free charge carriers are available: the system is insulating. For large but finite U holes and doubly occupied sites appear, but they are bound in pairs. The gain in kinetic energy is not favourable in comparison with the cost of the on-site Coulomb energy U associated with doubly occupied sites. Both the number and the size of these particle-hole pairs steadily increase with decreasing U and, correspondingly, the dielectric constant increases until it *diverges* at a critical value U_c. Below this value free "particles" (doubly occupied sites) and holes exist: the system is metallic. The gain in kinetic energy is now favourable in comparison with the Coulomb on-site energy cost.

A complementary picture, how the Hubbard model can exhibit the Mott transition at half-filling, starting from the limit $U \to 0$ is now given. For $U = 0$, electrons are only correlated due to the Pauli Exclusion Principle and the ground state of the system is just the Fermi sea, where one has exactly $1/4$ of doubly occupied sites and the same concentration of empty sites (holes). The left $1/2$ of the sites are single occupied. Holes are free charges carriers and so the Fermi sea is a conducting state. As the repulsive on-site interaction U increases, the number of double occupied sites decreases, and one begins to lose charge fluctuations. The holes are still free since $U < W$ (where W is the bandwidth), because the gain in kinetic energy is relatively favourable to the loss of Coulomb energy. When $U > W$ the cost in moving an electron is relatively high and holes and doubly occupied sites are no more frees (they tend to bind in pairs): the system becomes insulating. For $U = 0$ the single-particle momentum distribuition function $n_{\mathbf{k},\sigma}$ is equal to 1 for $k < k_F$ and zero for $k > k_F$, showing the characteristic jump of the Fermi sea. In order to eliminate double occupancy, as the interaction increases, one has to create electron-hole excitations (*excitons*) in the Fermi sea. In the limit $U \to \infty$ we have created all the excitons that the system can support and the single-particle momentum distribuition function becomes constant.

In a qualitative way, the critical value U_c at which the Mott-Hubbard transition occurs is expected to be of the order of the bandwidth W.

The Brinkman-Rice metal-insulator transition is obtained by taking in the metallic phase the Gutzwiller approximation energy E_{GA} for the Gutzwiller wave function and in the insulating phase the Heitler-London energy $E_{HL} = 0$. As the energies are not treated at the same level the obtained critical value U_0 is overestimated. The Mott-Hubbard transition described by the wave function ψ_B is obtained by comparing in the insulating phase the energy of the wave function ψ_B (e.g. by starting with the Néel state) with the Hartree-Fock energy E_{HF} in the metallic phase. Again, as the energies are not treated at the same foot the

obtained critical value is underestimeted.

It seems therefore natural to approach the problem of the Mott-Hubbard transition using both wave functions ψ_B and ψ_G, since these variational wave functions are constructed in a symmetric way with respect to each other. For small values of U the conducting wavefunction ψ_G is expected to have lower energy, whereas for large U the insulating wavefunction ψ_B will be energetically more favoured. The value U_c where both wave functions yield the same variational energy will then locate the Mott-Hubbard transition.

It is also worth mentioning the case when the Hubbard model is out of half-filling, $n < 1$. Besides the metal-insulator transition as function of U, there is also a transition as function of the band filling n. For the $1D$ Hubbard model, even for $U \to \infty$, it shows a conducting behaviour as it still has free charges carriers. For $U > U_c$ the increasing of electronic concentration induces a metal-insulator transition and when we reach the critical value $n_c = 1$ the system becomes insulating [33] (for the $1D$ case one has $U_c = 0$). In case of dimensions $D > 1$, the lack of exact solutions makes the problem of determine the phase diagram (U,n) a difficult task. Studies within the Unrestricted Hartree-Fock (UHF) approximation predict that the model exhibit the metal-insulator transition at a critical value of band filling $n_c < 1$, at least for strong U, where insulating antiferromagnetic and ferromagnetic states appear [34, 35, 36]. However it is well-known that the mean field UHF approximation exagerates the tendency towards broken symmetry states. Actually, numerical simulations for the $2D$ Hubbard model lead to conjecture a phase diagram identical to the one described above for the $1D$ case [36].

6.6 The limit of infinite dimensions

It was shown that there exists a non-trivial limit of infinite dimensions where the difficult tasks encountered in dealing with strongly correlated systems are greatly simplified [17]. Presently many properties are already known for the Hubbard model in infinite dimensions and the physical meaning of this limit as a dynamical mean-field theory for the finite dimensional case is essentially clear [30].

In the interesting case of two- and three-dimensional systems the variational wavefunctions ψ_G and ψ_B up to now could not be treated exactly. Fortunately, in the limit of infinite dimensions both variational wave functions can be treated exactly.

We consider two types of bipartite lattices: the hypercubic and the hyper-diamond lattices. The latter is the generalization of the $2D$ honeycomb and $3D$ diamond lattices to arbitrary dimensions. These lattices are unfrustrated and so they can show antiferromagnetic long-range order in the strong coupling limit. We consider the Hubbard Hamiltonian

$$\begin{aligned}\hat{H} &= \hat{T} + U\hat{D} \\ &= -t \sum_{<i,j>,\sigma} (c^{\dagger}_{i\sigma} c_{j\sigma} + h.c.) + U \sum_{i} \hat{n}_{i\uparrow}\, \hat{n}_{i\downarrow}\end{aligned} \tag{6.31}$$

where t is the hopping parameter, U is the repulsive on-site interaction, $c^{\dagger}_{i\sigma}(c_{i\sigma})$ are the Wannier electronic operators which create (anihilate) an electron at the site i with spin projection σ and $\hat{n}_{i\sigma} = c^{\dagger}_{i\sigma} c_{i,\sigma}$ counts the number of electrons in the site i with spin projection σ.

We first consider the hypercubic lattice. The wave function ψ_{∞} is simply the Néel state, which can be written in k representation as

$$\psi_{\infty} = \prod_{\mathbf{k},\sigma}{}' \frac{1}{\sqrt{2}} (\hat{c}^{\dagger}_{\mathbf{k}\sigma} + \sigma\, \hat{c}^{\dagger}_{\mathbf{k}+\mathbf{Q},\sigma})|0\rangle, \tag{6.32}$$

where $\mathbf{Q} = (\pi, \pi, \ldots, \pi)$ is the antiferromagnetic wave vector and the prime indicates that $\mathbf{k}$ belongs to the antiferromagnetic Brillouin zone. The application of the operator $e^{-\kappa \hat{T}}$ to the Néel state yields

$$\psi_B = \prod_{\mathbf{k},\sigma}{}' \frac{1}{\sqrt{2}} (e^{-\kappa\epsilon(\mathbf{k})} \hat{c}^{\dagger}_{\mathbf{k}\sigma} + \sigma\, e^{\kappa\epsilon(\mathbf{k})} \hat{c}^{\dagger}_{\mathbf{k}+\mathbf{Q},\sigma})|0\rangle \tag{6.33}$$

where $\epsilon(\mathbf{k})$ is the tight-binding spectrum. This equation has the same form as the conventional Unrestricted Hartree-Fock spin density wave (SDW) state although with different amplitudes.

Nevertheless, it should mention that in the insight behind each wave function is in general different. The Unrestricted Hartree-Fock spin density wave ψ_{UHF} is related to the Slater antiferromagnetic instability due to the nesting of the Fermi surface. Bipartitity of the lattice is needed to support this band antiferromagnetism. Starting from the uncorrelated Fermi sea this instability opens a charge gap in the spectrum for $U \geq U_m^{UHF}$ and it becomes more stable as U increases. The ground state changes from a paramgnetic conducting one to a spin density wave insulating one. For infinite U the spin density wave reaches saturation, becoming then the Néel state. The wave function ψ_B starting from the state ψ_{∞} generates charge fluctuations in a single-occupied site state (if we are at the half-filling case), which is not necesssary a magnetic ordered state. As U decreases charge fluctuations become more important and at a certain critical value of U the charge gap closes. The ground state changes from insulating state (magnetic ordered or not) to a conducting one. Only in the special limit of infinite dimensions and for bipartite lattices these two wavefunctions resemble more to each other.

Since in this special limit ψ_B is a single-particle wave function (Eq. 6.33), Wick's theorem can be applied and the energy per site $\epsilon_B = E_B/L$ reads

$$\epsilon_B = \frac{T}{L} + \frac{U}{4}(1 - m^2) \tag{6.34}$$

where

$$\frac{T}{L} = -\int_{-\infty}^{\infty} d\epsilon\, \rho(\epsilon)\, \epsilon\, \tanh(2\kappa\epsilon) \tag{6.35}$$

is the kinetic energy,

$$m = \int_{-\infty}^{\infty} d\epsilon\, \rho(\epsilon)\, \frac{1}{\cosh(2\kappa\epsilon)} \tag{6.36}$$

is the sublattice magnetization and $\rho(\epsilon)$ is the density of states. It is straightfoward to derive equations (6.35) and (6.36) for the hyperdiamond case. The details of the calculations are presented in Appendix B6.

We notice that all information about the symmetry and the dimensionality of the lattice is contained in the density of states. For the infinite dimensional case this quantity has been calculated either by envoking the central-limit theorem [17, 37] or by expanding the Fourier transform of $\rho(\epsilon)$ in powers of $1/D$ [38] (see Appendix C6). One has to keep in mind that a non-trivial limit is obtained only if the hopping parameter t is rescaled, as already observed by Metzner and Vollhardt [17]. With the choice $t = (2D)^{-1/2}t^*$ the density of states for the hypercubic lattice is found to be

$$\rho_{hc}(\epsilon) = \frac{1}{\sqrt{2\pi}\, t^*} \exp[-\epsilon^2/2t^{*2}]. \tag{6.37}$$

For the hyperdiamond lattice we choose the scaling $t = (D/2)^{-1/2}t^*$ and obtain

$$\rho_{hd}(\epsilon) = \frac{|\epsilon|}{2t^{*2}} \exp\left[-\epsilon^2/2t^{*2}\right]. \tag{6.38}$$

For large ϵ the two expressions are very similar, however they differ markedly in the limit $\epsilon \to 0$, where the density of states has a maximum for the hypercubic lattice and vanishes for the hyperdiamond lattice (Fig. 6.1).

The variational ground state energy for the wave function ψ_B is obtained by minimizing Eq.(6.34) with respect to κ. The results are shown in Figs. 6.2 and 6.3 together with the ground state energies of the Gutzwiller approximation [Eq. (6.8)], with $\varepsilon_0 = -\epsilon_0 = (2/\pi)^{1/2}t^*$ for the hypercubic lattice and $\varepsilon_0 = -\epsilon_0 = (\pi/2)^{1/2}t^*$ for the hyperdiamond lattice.

The critical value U_c is seen to be much lower than U_0. In our approach, the Brinkman-Rice transition does not occur. The insulating state ψ_B is energetically favoured with respect to ψ_G already below U_0, and in the entire region $U < \infty$ the double occupancy remains finite. Therefore, in our approach, the double occupancy cannot be taken as the order parameter of the metal-insulator transition.

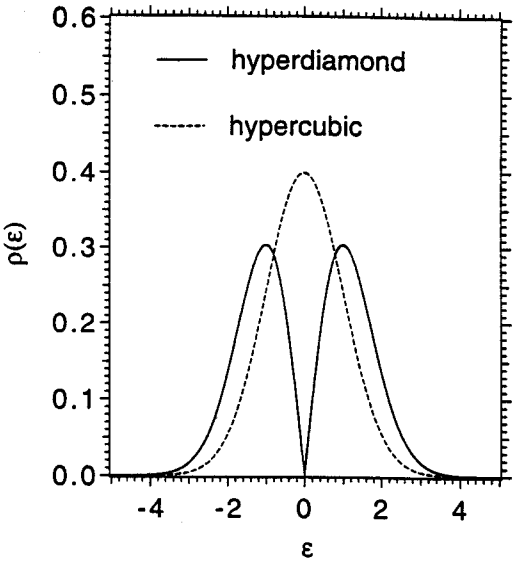

Figure 6.1: Density of states for the hypercubic lattice and for hyperdiamond lattice (the energy is in units of t).

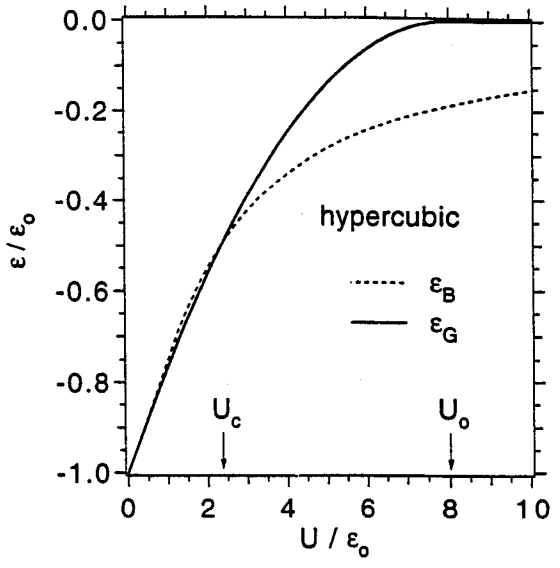

Figure 6.2: Variational ground state energies for the hypercubic lattice. The transition from the metallic (full line) to the insulating state (dashed line) is locate at U_c. The Brinkman-Rice transition is locate at U_0.

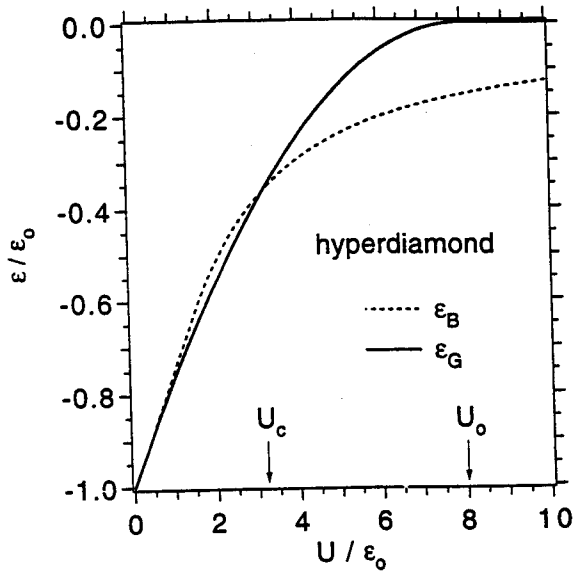

Figure 6.3: Variational ground state energies for the hyperdiamond lattice. The transition from the metallic (full line) to the insulating state (dashed line) is locate at U_c. The Brinkman-Rice transition is locate at U_0.

The critical values U_c obtained are quite similar in the two cases. The Mott-Hubbard transition is locate at the critical values $U_c \simeq 1.9\ t^* = 2.4|\epsilon_0|$ for hypercubic lattice and $U_c \simeq 4.0\ t^* = 3.2|\epsilon_0|$ for the hyperdiamond lattice. In fact, in both cases it corresponds to an effective bandwidth (see Fig. 6.1).

In order to eliminate the double occupancy as U increases we have to create electron-hole excitations (excitons). In the hypercubic case, the Fermi surface is relatively large (the "center of gravity" of the band ϵ_0 is relatively near the Fermi level) and relatively little energy is required to create these excitons. On the contrary, in the hyperdiamond case the density of states in the Fermi surface is zero (the corresponding "center of gravity" of the band ϵ_0 is relatively farer from the Fermi level) and the energy cost to create an exciton is relatively higher. Thus, one expects a critical value U_c relatively bigger for the hyperdiamond lattice than for the hypercubic lattice.

The charge stiffness D_c and the sublattice magnetization m for the hyperdiamond lattice are shown in Fig. 6.4. The Gutzwiller ansatz yields a finite charge stiffness below the value U_0, which may be identified with the critical point where the conducting solution is unstable with respect to the Mott phenomenon. With more refined methods this instability point is found to be shifted to slightly lower values [30, 37]. On the other hand the state ψ_B represents an antiferromagnetic insulator with a finite sublattice magnetization, which tends to zero as U approaches U_m from above. The value U_m lies below U_c. Inclusion of spin fluctuations in the Néel state will shift this point to the right, but it is not expected that it will eventually coincide with the Mott transition.

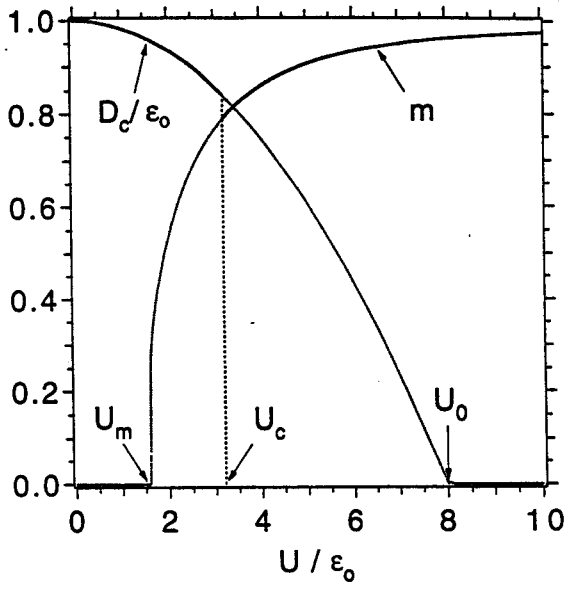

Figure 6.4: Charge stiffness D_c and the sublattice magnetization for the hyperdiamond lattice. The interpretation of the special values U_m, U_c, U_0 is given in the text.

Within our variational approach there is a single first-order transition at U_c with a jump both in the charge stiffness D_c and in the sublattice magnetization m order parameters.

The Slater instability in infinite dimensions can be studied within the Unrestricted Hartree-Fock approximation. The sublattice magnetization is given by $m = 2\Delta/U$, where Δ is the gap in the tight-band spectrum of the system by imposing a symmetry breaking and can be obtained as function of U by the usual gap equation [36]

$$\frac{1}{U} = \frac{1}{2}\int_{-\infty}^{\infty} d\epsilon\, \rho(\epsilon)\, \frac{1}{\sqrt{\epsilon^2+\Delta^2}}. \tag{6.39}$$

The system becomes unstable with respect to a spin density wave ground state at the critical value U_m, which is obtained making $\Delta = 0$ in the gap equation. We have obtained the critcal values $U_m^{UHF} = 0$ for the hypercubic lattice and $U_m^{UHF} = (4/\pi)|\epsilon_0| = 1.596\ t^*$ for the hyperdiamond lattice. The density of states at the Fermi surface for the hypercubic case is finite and the presence of a Slater instability for any finite value of U is expected. On the contrary, $\rho(\epsilon_F) = 0$ for the hyperdiamond case and the absence of nesting leads us to expect the Slater instability to occur at a finite value of U.

Therefore, the Mott-Hubbard transition is complete masked for the hypercubic lattice, while for the hyperdiamond lattice we have obtained that $U_m < U_c$. Thus, the critical value U_m locates the transition from a paramagnetic conducting state to an Slater-type insulating state (with small moments) followed by a continuous

crossover to an antiferromagnetic Heisenberg-type insulating state (with nearly saturated moments) around U_c.

This picture is qualitative in agreement with previous studies using quantum Monte Carlo and second-order perturbation theory for the hyperdiamond lattice, where it was found $U_m \simeq 2.3t^*$ for the antiferromagnetic Slater instability and $U_c \simeq 8.5t^*$ for the Mott-Hubbard transition [37].

6.7 Two-dimensional honeycomb lattice

The pure Mott transition is often masked by the an antiferromagnetic instability of the metallic phase. This is the case of the Hubbard model on the one-dimensional, square, cubic up to hypercubic lattices.

There exist ways for escaping the antiferromagnetic instability of the metallic phase, namely: (i) frustration introduced by the geometry of the lattice; (ii) the addition of long-range hopping terms, reducing the nesting of the Fermi surface; (iii) considering specific lattice symmetries which entail a vanishing density of states at the Fermi energy and therefore strongly reduce the tendency towards the opening of a spin density wave gap. This is the case of the honeycomb lattice considered in this section.

We consider the Hubbard Hamiltonian, Eq. 6.31, for $2D$ honeycomb lattice. The honeycomb lattice is bipartite and the two sublattices will be labeled by A and B. We consider the set of vectors $\{\mathbf{d}_\alpha : \alpha = 1,2,3\}$ which connect a site of sublattice A with its nearest neighbours, belonging the sublattice B. We choose these vectors in cartesian coordinates to be $\mathbf{d}_1 = (\sqrt{3}/2, -1/2)a$, $\mathbf{d}_2 = (-\sqrt{3}/2, -1/2)a$ and $\mathbf{d}_3 = (0,1)a$, where a is the distance between nearest neighbours. For each sublattice we define the respective Bloch operators through the Fourier transform

$$\begin{aligned} c^\dagger_{A,\mathbf{k}\sigma} &= \sqrt{\frac{2}{L}} \sum_{i \in A} e^{-i\mathbf{k}.\mathbf{r}_i} c^\dagger_{i\sigma} \\ c^\dagger_{B,\mathbf{k}\sigma} &= \sqrt{\frac{2}{L}} \sum_{j \in B} e^{-i\mathbf{k}.\mathbf{r}_j} c^\dagger_{j\sigma} \end{aligned} \tag{6.40}$$

where L is the total number of atoms and $\mathbf{r}_l$ is the position-vector of l-th atom. These operators partially diagonalize the kinetic term

$$\hat{T} = -t \sum_{\mathbf{k} \in BZ, \sigma} \left(F_\mathbf{k} c^\dagger_{A,\mathbf{k}\sigma} c_{B,\mathbf{k}\sigma} + h.c. \right) \tag{6.41}$$

with

$$F_\mathbf{k} = \sum_\alpha e^{-i\mathbf{k}.\mathbf{d}_\alpha} \tag{6.42}$$

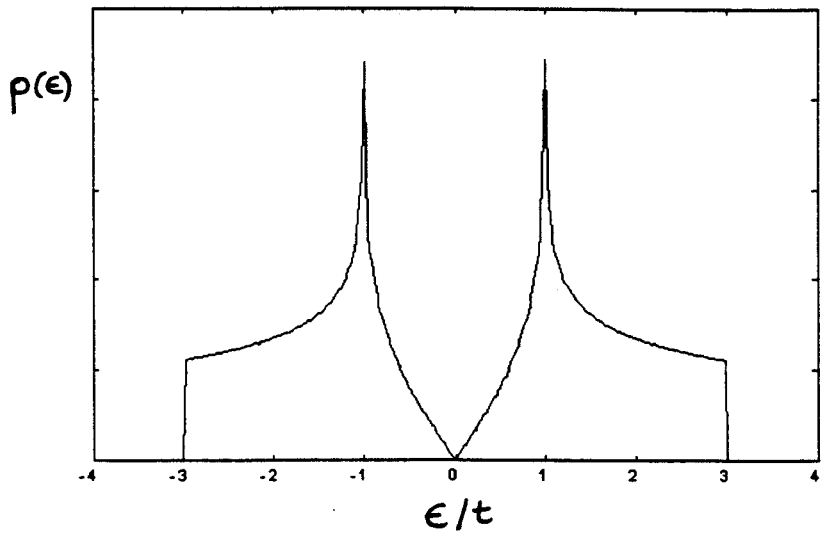

Figure 6.5: Density of states for the honeycomb lattice.

and BZ denotes the Brillouin zone. In order to diagonalize the Hamiltonian one has to make a canonical transformation defining the operators $c^{\dagger}_{p,\mathbf{k}\sigma} = u_{p,\mathbf{k}\sigma}c^{\dagger}_{A,\mathbf{k}\sigma} + v_{p,\mathbf{k}\sigma}c^{\dagger}_{B,\mathbf{k}\sigma}$. These operators should obey fermionic anticommuting relations and therefore the parameters of the canonical transformation should obey the relation $|u_{p,\mathbf{k}\sigma}|^2 + |v_{p,\mathbf{k}\sigma}|^2 = 1$. These operators are given by

$$\begin{aligned} c^{\dagger}_{-,\mathbf{k}\sigma} &= \frac{1}{\sqrt{2}}\left(\frac{|F_{\mathbf{k}}|}{F^{\star}_{\mathbf{k}}}c^{\dagger}_{A,\mathbf{k}\sigma} + c^{\dagger}_{B,\mathbf{k}\sigma}\right) \\ c^{\dagger}_{+,\mathbf{k}\sigma} &= \frac{1}{\sqrt{2}}\left(\frac{-|F_{\mathbf{k}}|}{F^{\star}_{\mathbf{k}}}c^{\dagger}_{A,\mathbf{k}\sigma} + c^{\dagger}_{B,\mathbf{k}\sigma}\right) \end{aligned} \tag{6.43}$$

and the Hamiltonian finally becomes

$$\hat{H} = \sum_{\mathbf{k}\in BZ,p,\sigma} \epsilon_p(\mathbf{k})c^{\dagger}_{p,\mathbf{k}\sigma}c_{p,\mathbf{k}\sigma} + U\,\hat{D} \tag{6.44}$$

where $p = -,+$ is the band index and refers to the lower (valence) and to the upper (conduction) bands, respectively. The dispersion relation has two branches given by

$$\epsilon_{\pm}(\mathbf{k}) = \pm\, t|F_{\mathbf{k}}|. \tag{6.45}$$

The honeycomb lattice density of states $\rho(\epsilon)$ is plotted in Fig. 6.5.

Up to now, the variational energies E_G and E_B have not been treated exactly for the two-dimensional honeycomb lattice. The variational procedure is here carried through using two approximative methods. In the first approach, we

expand E_G in powers of U/t and E_B in powers of t/U. In the second one, we use a "mean-field level" by adopting the exact solution in the limit of infinite dimensions for the two-dimensional honeycomb lattice.

The expansion of the Gutzwiller variational energy E_G in powers of U/t was presented in the Sec. 6.2. In order to make the weak coupling expansion we introduce the equal-time correlation functions

$$\begin{aligned} G_{ij} &= \langle\psi_0|c^\dagger_{i\sigma}c_{j\sigma}|\psi_0\rangle \\ \tilde{G}_{ij} &= \langle\psi_0|c_{i\sigma}c^\dagger_{j\sigma}|\psi_0\rangle \end{aligned} \tag{6.46}$$

which are related by $\tilde{G}_{ij} = \delta_{ij} - G_{ij}$. Due to symmetry we have the relations $G_{ij} = G_{ji}$ and $\tilde{G}_{ij} = \tilde{G}_{ji}$. These correlation functions at half-filling obey the following sum rules

$$\begin{aligned} \sum_k G_{ik}G_{kj} &= G_{ij} \\ \sum_k \tilde{G}_{ik}\tilde{G}_{kj} &= \tilde{G}_{ij} \\ \sum_k G_{ik}\tilde{G}_{kj} &= 0. \end{aligned} \tag{6.47}$$

Using the Fourier transform operators $c_{A,\mathbf{k}\sigma}$ and $c_{B,\mathbf{k}\sigma}$, one can write

$$G^{SS'}_{ij} = \frac{2}{L}\sum_{\mathbf{k}\in BZ} e^{i\mathbf{k}.\mathbf{r}_{ij}}\ \langle\psi_0|c^\dagger_{S,\mathbf{k}\sigma}c_{S',\mathbf{k}\sigma}|\psi_0\rangle \tag{6.48}$$

where $\mathbf{r}_{ij} = \mathbf{r}_i - \mathbf{r}_j$ and $S(S')$ denotes the sublattice to which the site $i(j)$ belongs. The equal-time correlation functions are given for sites belonging to the same sublattices by

$$\begin{aligned} G^{AA}_{ij} &= \frac{2}{L}\sum_{\mathbf{k}\in BZ} e^{i\mathbf{k}.\mathbf{r}_{ij}} \\ &= \delta_{\mathbf{r}_{ij},0} \end{aligned} \tag{6.49}$$

and for sites belonging to different sublattices by

$$G^{AB}_{ij} = \frac{2}{L}\sum_{\mathbf{k}\in BZ}\frac{F^*_{\mathbf{k}}}{|F_{\mathbf{k}}|}\, e^{i\mathbf{k}.\mathbf{r}_{ij}}. \tag{6.50}$$

At half-filling and due to the fact that the honeycomb lattice is a Bravais lattice with a basis of two atoms, the correlation function (6.46) is zero between different sites of the same sublattice and finite correlations appear for sites belonging

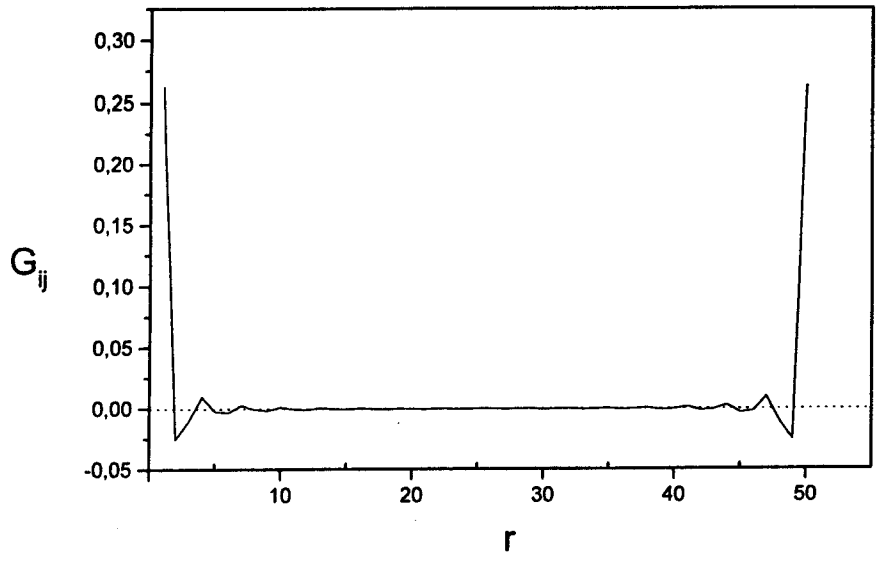

Figure 6.6: Equal-time correlation function between sites of different sublattices for the honeycomb lattice as function of the distance r (in units of the distance a between nearest neighbours).

to different sublattices. As expected these correlations decay quickly with the distance between sites (Fig. 6.6).

We are now able to expand the energy per site $\epsilon_G = E_G/L$ up to second-order in U/t. One obtains

$$\epsilon_G = \epsilon_0 + \epsilon_1 \frac{U}{t} + \epsilon_2 \left(\frac{U}{t}\right)^2 \tag{6.51}$$

where $\epsilon_0 = -1.5746t$, $\epsilon_1 = 0.25t$ and $\epsilon_2 = -9.685 \times 10^{-3}t$ (see Appendix D6 for details). The expansion of the variational energy E_B in powers of t/U was presented in Sec. 6.3. Using the results from quantum Monte Carlo simulations for the honeycomb lattice Heisenberg model [39], the energy per site ($\epsilon_B = E_B/L$) to leading order reads

$$\epsilon_B = -3.678t \left(\frac{t}{U}\right). \tag{6.52}$$

The results of both expansions are displayed in Fig. 6.7 as dashed lines. Although the two curves do not intersect, the distance between them reaches a minimum for U/t between 4 and 5 indicating the crossover between weak and strong coupling.

We turn now to the approximate calculation of E_G and E_B using the corresponding analytical solutions in the limit of infinite dimensions, where the two wavefunctions become exact. The Gutzwiller approximation energy per site is given by Eq. (6.8) whith $\epsilon_0 = -1.5746t$, the kinetic energy per site of the Fermi sea of the honeycomb lattice. The result of the Gutzwiller approximation agrees

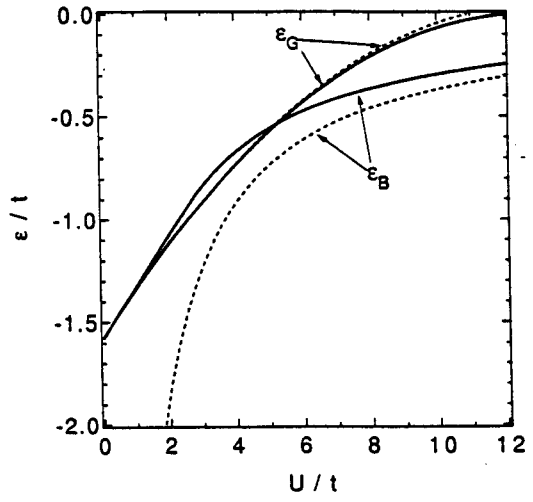

Figure 6.7: Variational ground state energies per site ϵ_G and ϵ_B for the honeycomb lattice obtained as discussed in text: weak and strong coupling expansions (dashed lines) and mean field approximation (full lines).

very well with the weak coupling expansion (see Fig. 6.7) . Comparison with Variational Monte Carlo (VMC) calculations (to be discussed below) shows that the weak coupling expansion is no more accurate for $U/t \gtrsim 4$.

For the honeycomb lattice, Monte Carlo simulations (and linear spin-wave theory) show that the staggered magnetization m is strongly reduced from its Néel value due to quantum fluctuations but it remains finite: $m = 0.44 \pm 0.06$ (taking the Néel staggered magnetization as unit) and that the system still exhibits long-range AF order [39]. Thus, by taking the Néel state as the ground state for the honeycomb lattice in the limit of strong coupling $U \to \infty$, we expect to keep the qualitative physics. If, for instance, the system did not show long-range magnetic order, the Néel state would certainly not be a good choice, and one should take another type of state, e.g. a spin-liquid state. The variational energy per site for the wave function ψ_B starting form the Néel state is given by Eq. (6.34) using for the density of states $\rho(\epsilon)$ that of the honeycomb lattice. Thus, we obtain an approximate solution for the energy of the variational wave function ψ_B which is displayed in Fig. 6.7 together with the result of the Gutzwiller approximation. The intersection of both curves at $U_c = 5.28t$ locates the Mott-Hubbard transition [40] in reasonable agreement with the value $U_c = (4.5 \pm 0.5)t$ obtained by quantum Monte Carlo simulations [41]. As for the infinite dimensional case, the Brinkman-Rice transition does not occur.

We plot the expression (6.13) of the wave function ψ_B starting form the Néel state for the honeycomb lattice: the function $F_{BN}(\kappa)$ (Fig. 6.8). The optimal variational parameter κ_0 as function of the interaction U is plotted in Fig. 6.9.

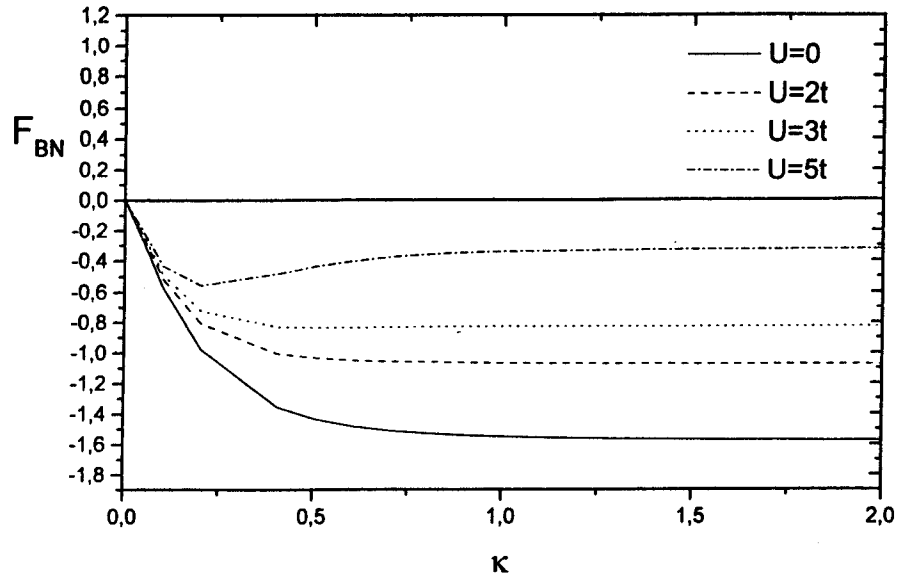

Figure 6.8: Function $F_{BN}(\kappa)$ (in units of t) for the honeycomb lattice as function of the variational parameter κ for several values of U, as explained in text.

It becomes *infinite* at the value $U_c = 2.8t$, locating the metal-insulator transition which was described in Sec. 6.3 as the counterpart of the Brinkman-Rice transition. In our approach, this transition also does not occur.

We address now the question of the Slater instability of the conducting phase for the honeycomb lattice.

We first evaluate the non-interacting linear staggered susceptibility χ_0. This can be achieved by applying to the system a staggered magnetic field h and taking at the end the limit $h \to 0$. The Hubbard Hamiltonian (Eq. 6.31) for $U = 0$ in the presence of the staggered field h and after Fourier transform reads

$$\hat{H} = -t \sum_{\mathbf{k}\in BZ,\sigma} \left(F_{\mathbf{k}} c^{\dagger}_{A,\mathbf{k}\sigma} c_{B,\mathbf{k}\sigma} + h.c. \right) + \sum_{\mathbf{k}\in BZ,\sigma} h\sigma \left(c^{\dagger}_{A,\mathbf{k}\sigma} c_{A,\mathbf{k}\sigma} - c^{\dagger}_{B,\mathbf{k}\sigma} c_{B,\mathbf{k}\sigma} \right)$$

where $\sigma = \uparrow, \downarrow$ becomes $\sigma = +, -$ when it is taken as a number. Considering the canonical transformation $c^{\dagger}_{p,\mathbf{k}\sigma} = u_{p,\mathbf{k}\sigma} c^{\dagger}_{A,\mathbf{k}\sigma} + v_{p,\mathbf{k}\sigma} c^{\dagger}_{B,\mathbf{k}\sigma}$, the parameters are now given by

$$\begin{aligned} u_{p,\mathbf{k}\sigma}(h) &= \left(\frac{|F_{\mathbf{k}}|^2}{2(|F_{\mathbf{k}}|^2 + h^2 + ph\sigma\sqrt{|F_{\mathbf{k}}|^2 + h^2})} \right)^{1/2} \left(\frac{-h\sigma - p\sqrt{|F_{\mathbf{k}}|^2 + h^2}}{F^{\star}_{\mathbf{k}}} \right) \\ v_{p,\mathbf{k}\sigma}(h) &= \left(\frac{|F_{\mathbf{k}}|^2}{2(|F_{\mathbf{k}}|^2 + h^2 + ph\sigma\sqrt{|F_{\mathbf{k}}|^2 + h^2})} \right)^{1/2} \end{aligned} \tag{6.53}$$

and the Hamiltonian reads

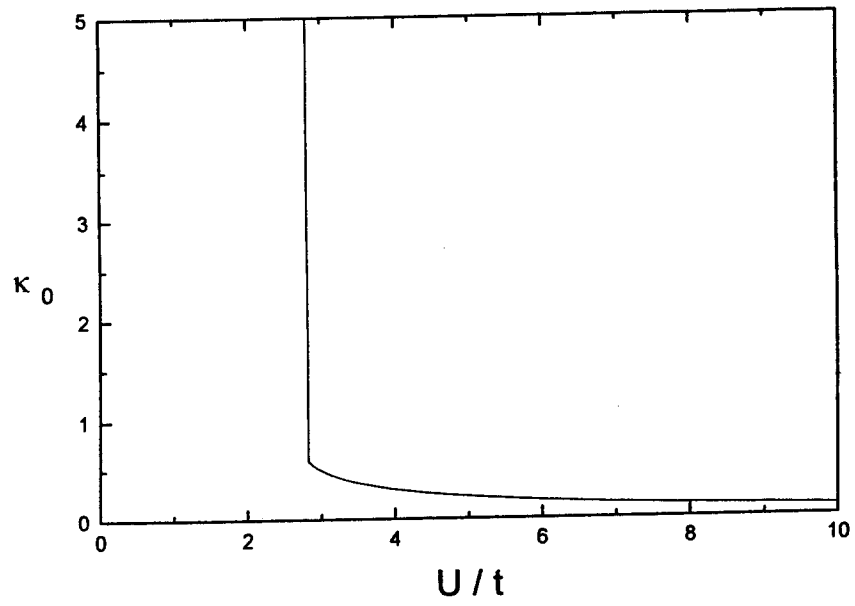

Figure 6.9: The optimal variational parameter k_0 for the honeycomb lattice as function of the interaction U.

$$\hat{H} = \sum_{p,\mathbf{k}\in BZ,\sigma} \epsilon_p(\mathbf{k},h) c^\dagger_{p,\mathbf{k}\sigma} c_{p,\mathbf{k}\sigma} + U\ \hat{D}, \tag{6.54}$$

where the dispersion relation has two branches given now by $\epsilon_\pm(\mathbf{k},h) = \pm t\sqrt{|F_\mathbf{k}|^2 + h^2}$. At half-filling, the ground state is given by filling up completely the valence band $(p=-1)$

$$\psi_0 = \prod_{\mathbf{k}\in BZ,\sigma} c^\dagger_{-,\mathbf{k}\sigma}|0\rangle. \tag{6.55}$$

The non-interacting linear staggered magnetization χ_0 is defined by

$$\chi_0 = \lim_{h\to 0} \frac{m}{h}, \tag{6.56}$$

where the staggered magnetization m is given by

$$\begin{aligned} m &= \Big[\sum_{i\in A} \langle\psi_0|(c^\dagger_{i\uparrow}c_{i\uparrow} - c^\dagger_{i\downarrow}c_{i\downarrow})|\psi_0\rangle - \sum_{i\in B} \langle\psi_0|(c^\dagger_{i\uparrow}c_{i\uparrow} - c^\dagger_{i\downarrow}c_{i\downarrow})|\psi_0\rangle\Big] \\ &= \sum_{\mathbf{k}\in BZ} \langle\psi_0|(c^\dagger_{A,\mathbf{k}\uparrow}c_{A,\mathbf{k}\uparrow} - c^\dagger_{A,\mathbf{k}\downarrow}c_{A,\mathbf{k}\downarrow}) - (c^\dagger_{B,\mathbf{k}\uparrow}c_{B,\mathbf{k}\uparrow} - c^\dagger_{B,\mathbf{k}\downarrow}c_{B,\mathbf{k}\downarrow})|\psi_0\rangle \end{aligned} \tag{6.57}$$

Using the canonical transformation defined above, after straightforward calculations, the non-interacting linear staggered magnetization χ_0 at half-filling is given by

$$\begin{aligned}\chi_0 &= \frac{1}{L}\sum_{\mathbf{k}\in BZ}\frac{1}{|\epsilon_{-,\mathbf{k}}|} \\ &= \int_{-\infty}^{0} d\epsilon\,\frac{\rho(\epsilon)}{|\epsilon|} \\ &= \frac{1}{2}\int_{-\infty}^{\infty} d\epsilon\,\frac{\rho(\epsilon)}{|\epsilon|}. \end{aligned} \tag{6.58}$$

This expression is in perfect correspondence with the one obtained for the square lattices using the Lindhard diagram [36]. At $U = 0$, the single-particle density of states of the honeycomb lattice is linear for energies around zero, $\rho(\epsilon) \sim |\epsilon|$ (see Fig. 6.5). For the particular case of half-filling, the density of states becomes zero at the Fermi level, and consequently there is no Fermi surface that could produce a magnetic instability in the limit $U \to 0$. Therefore, χ_0 does not diverges and the Slater instability will occur at a finite value of U. The honeycomb lattice is bipartite and therefore antiferromagnetic order is possible, but only at a finite value of U.

This can also be seen in a simple UHF approximation. The system becomes unstable with respect to a spin-wave density ground state at the critical value U_m which is given by the UHF gap equation for $\Delta = 0$ [see Eq. (6.39)]

$$\frac{1}{U_m} = \frac{1}{2}\int_{-\infty}^{\infty} d\epsilon\,\frac{\rho(\epsilon)}{|\epsilon|}. \tag{6.59}$$

One obtains the value $U_m^{UHF} = 2.23t$.

For finite interaction U the magnetic susceptibility $\chi(\mathbf{q})$ can be approximatively given within the Random Phase Approximation by the sum of particle-hole ladder diagrams as

$$\chi(\mathbf{q}) = \frac{2\chi_0(\mathbf{q})}{1 - U\chi_0(\mathbf{q})}. \tag{6.60}$$

The staggered susceptibility is given by taking $\mathbf{q} = \mathbf{Q}$. where $\mathbf{Q} = (\pi, \pi)$ is the AF wave vector. The critical value U at which the antiferromagnetic transition occurs is then given by $U_m = 1/\chi_0$. As χ_0 does not diverge for the honeycomb lattice U_m is finite. It is also coincident with the UHF value.

We investigate now the Slater instability within a variational procedure by studying the stability of the Gutzwiller wave function with respect to the formation of a spin density wave. For this purpose, we have considered the generalized Gutzwiller wave function

$$\psi_{GAF}(\Delta) = e^{-\eta\hat{D}}\psi_{UHF}(\Delta) \tag{6.61}$$

where $\psi_{UHF}(\Delta)$ is the ground state of the UHF solution for the ground state of the Hubbard model, i.e. a SDW state with the gap parameter Δ. For $\Delta = 0$ this

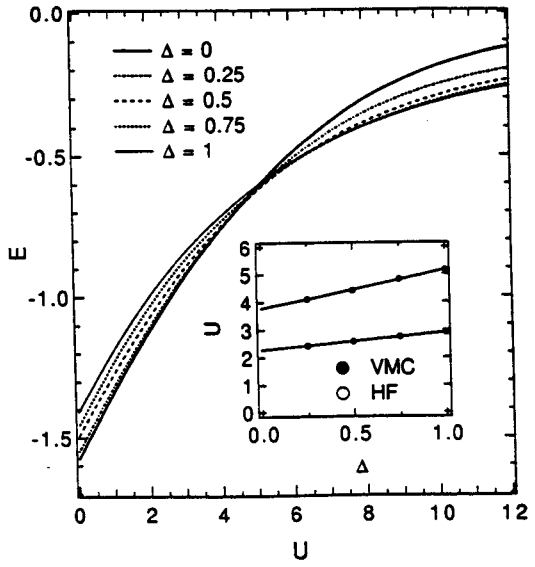

Figure 6.10: Variational Monte Carlo results for the honeycomb as explained in text (energies are plotted in units of t).

generalized wave function is the usual Gutzwiller wavefunction. Both the gap parameter Δ and the Gutzwiller parameter η have to be minimized in order to determine the variational energy.

Our results were obtained by VMC simulations (see Appendix E6) of systems containing up to 200 atoms. In a first step, η is optimized and we obtain the energy $E_{GAF}(U, \Delta)$ as a function of U/t for several values of Δ (Fig. 6.10). In order to determine the value U_m where the system opens a gap and the transition to the SDW phase occurs, we have plotted the values of U where $\Delta E = E_{GAF}(\Delta, U) - E_{GAF}(0, U)$ changes signal as function of Δ in the inset of Fig. 6.10. Extrapolating the data to $\Delta = 0$ yields $U_m = (3.7 \pm 0.1)t$.

For a chosen Δ and for each η we have made 10 different simulations. A simulation is made with 200 measurements. After 100 warming-up sweeps, each measurement is made every 4 Monte Carlo steps.

As an example of the output that one can obtain from a VMC simulation, we choose the case $\Delta = 0$ in a 10×10 unit cell lattice: Figs. 6.11, 6.12 and 6.13 show the optimal variational parameter η_0, the kinetic energy and double occupancy as function of U for the honeycomb lattice, respectively. As expected the optimal variational parameter η_0 increases as function of U from zero for $U = 0$ and tends to infinity as $U \to \infty$. The kinetic energy starts from the Fermi sea energy ϵ_0 and tends to zero as $U \to \infty$. The double occupancy starts from the Fermi sea value of $1/4$ and tends to zero as $U \to \infty$, remaining *finite* for $U < \infty$.

In order to study the finite size effects, we have repeated the procedure with η fixed to zero, i.e. the case where the wavefunction ψ_{GAF} reduces to the UHF wave function. The data obtained for a lattice of 8×8 unit cells shown in the inset of Fig.

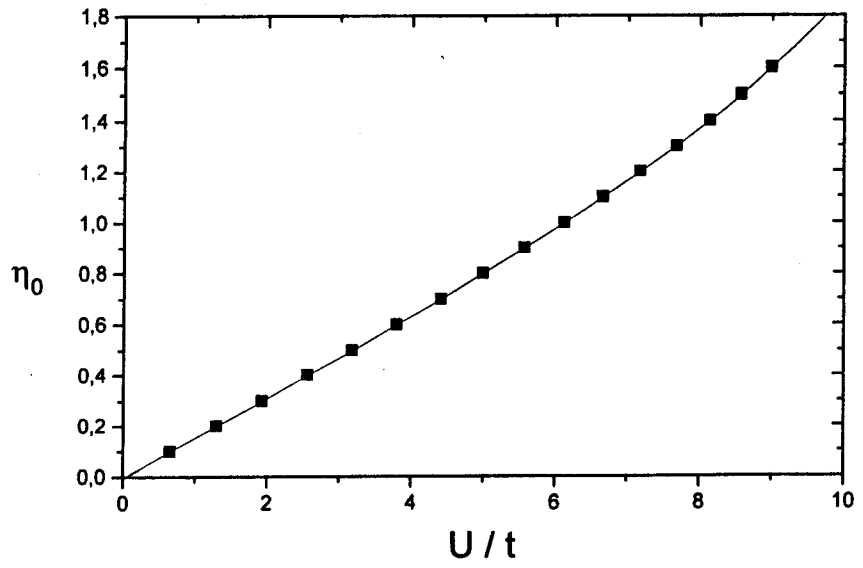

Figure 6.11: The optimal variational parameter η_0 as function of U obtained by VMC simulations in a 10×10 unit cell honeycomb lattice.

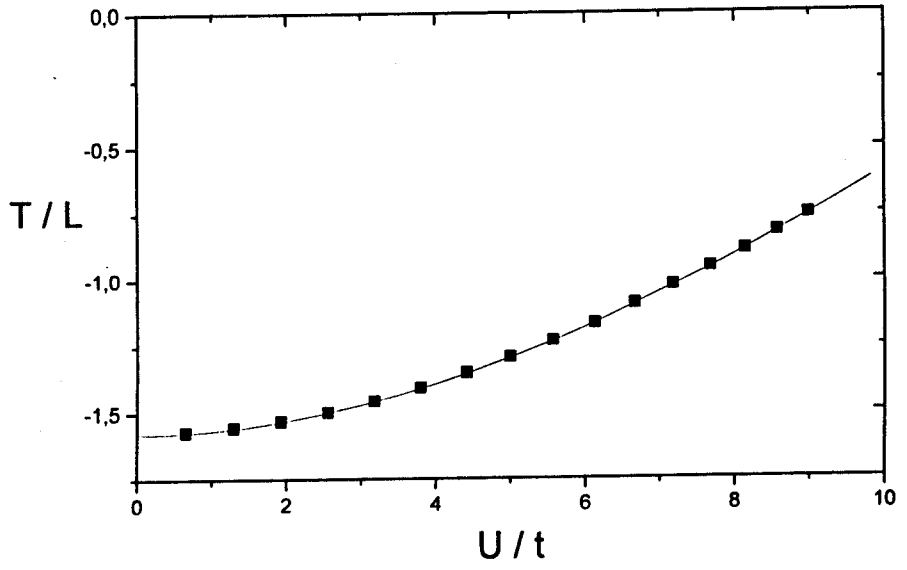

Figure 6.12: The kinetic energy per site (in units of t) as function of U obtained by VMC simulations in a 10×10 unit cell honeycomb lattice.

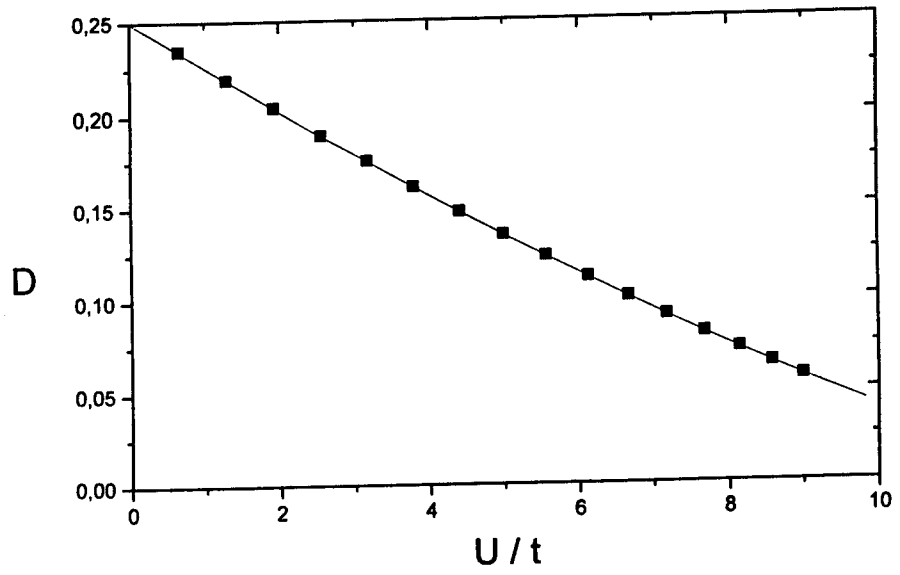

Figure 6.13: Double occupancy as function of U obtained by VMC simulations in a 10×10 unit cell honeycomb lattice.

6.10 extrapolate to $U_m^{UHF} = 2.27t$ which is very close to the infinite lattice value $U_m^{UHF} = 2.23t$ and so finite size effects are negligible. These effects should also be negligible for the correlated wavefunction ψ_{GAF}, once the Gutzwiller projector tends to "localize" electrons and so surface effects are expected to be smaller.

We have also calculated the local moment $\langle \hat{\mathbf{S}}_i^2 \rangle$. In a Slater scenario the local moment in the paramagnetic region remains that of the filled Fermi sea, i.e. $\langle \hat{\mathbf{S}}_i^2 \rangle = 3/8$. This has to be compared with the fully developed local moment $\langle \hat{\mathbf{S}}_i^2 \rangle = 3/4$ in the limit $U \to \infty$. Our VMC simulations yield a local moment $\langle \hat{\mathbf{S}}_i^2 \rangle = 0.5$ at the transition, exactly in between the two limiting values. This implies that we are dealing with a situation where neither the Slater nor the Heisenberg type description of the magnetic phase transition is appropriate.

The mean-field treatment of the wavefunctions ψ_G and ψ_B has allowed to estimate the critical value $U_c = 5.28t$ of the Mott-Hubbard transition for the $2D$ honeycomb at half-filling. Since quantum fluctuations are expected to be stronger for ψ_B than for ψ_G, this value is considered as an *upper bound.* Using the wavefunction ψ_{GAF}, the Slater instability within VMC simulations was found at the critical value $U_m = 3.7t$. As this wavefunction appears to overestimate the tendency towards antiferromagnetism [42], we expect this value to be a *lower bound* for the appearance of antiferromagnetism. Therefore, our results do not disagree with the possibility of a single transition where the opening of a charge gap due to the Mott phenomenon and the magnetic instability coincide. This would be in line with previous Monte Carlo simulations, which have been interpreted in terms of a single transition at $U_c = (4.5 \pm 0.5)\ t$ [41].

The present variational scheme predicts a first-order transition at U_c, in con-

tradiction to the general belief that the Mott-Hubbard transition is of second-order [43]. This is not surprising, as the two wave functions, although exact in the limits $U \to 0$ and $U \to \infty$, are not very accurate at intermediate U [5]. Therefore the important question of the critical behavior close to U_c requires other methods.

Further studies of the conducting phase would also be worth being pursued. At half-filling the Fermi surface of the honeycomb lattice is reduced to only *two points* and so the system, at this particular filling, is expected to show deviations from the simple Fermi liquid behaviour. In fact, strong deviations have been obtained by perturbative methods [44].

6.8 Scenario for the half-filling Hubbard model

A phase diagram (U,T) is sketched for the Hubbard model at half-filling (Fig. 6.14).

We first consider the line $T = 0$. Following the previous studies, on the infinite dimensional hypercubic and hyperdiamond lattices and on the $2D$ honeycomb lattice, the Hubbard model is expected to exhibit a Mott transition at the critical value $U_c \sim W$, where W is the bandwidth. However, this transition is often masked by a Slater instability of the Fermi surface at a critical value U_m. For the one-dimensional, square, cubic up to hypercubic lattices, which have a nested Fermi surface, one has $U_m = 0$. The Slater instability can appear at a finite value U_m for lattices which have a "special geometry" as discussed before. This is, for instance, the case of the $2D$ honeycomb lattice. Considering that with increasing U the Slater instability occurs before the Mott transition, the critical value U_c does not locate the metal-insulator transition but the smooth crossover between a Slater insulator to an antiferromagnetic Heisenberg insulator.

We consider now the case $T \neq 0$. For finite temperatures the antiferromagnetic order is destroyed in two dimensions due to thermal fluctuations. In three dimensions one expects long-range antiferromagnetic order up to a critical temperature. Above this temperature one can still distinguish a metallic from an insulating phase according to the T-dependence of the electrical conductivity. The Slater insulating state is expected to be stabilized with increasing U, while the Heisenberg insulating state is governed by the energy scale t^2/U. As the energy scale for the Slater instability is much smaller than that for the Mott transition [30], the critical value U_c is also expected to mark the point where the critical temperature has a maximum and at higher temperatures a Mott-Hubbard transition from a paramagnetic conducting state to a non-magnetic insulating state occurs. Thus we expect a phase diagram as in Fig. 6.14.

This scenario is in agreement with the phase diagram experimentally observed for the typical example of a strongly correlated system: the $(V_{1-x}M_x)_2O_3$ (Fig. 6.15) and with recent strong coupling expansion for the $1D$ Hubbard model [45]

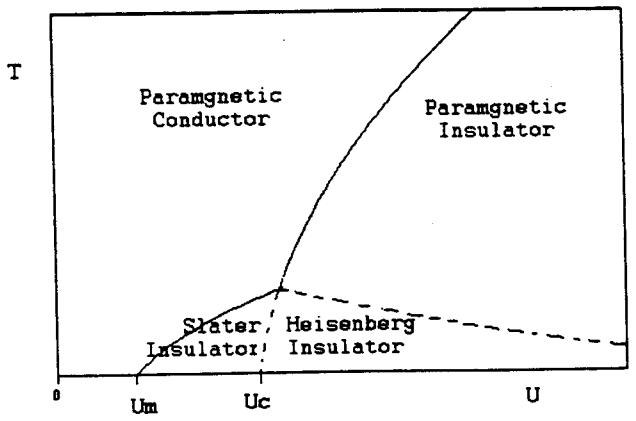

Figure 6.14: Sketch of the phase diagram (U,T) for the Hubbard Model at half-filling.

(in this case the AF phase shows short-range order). The pressure applied to $(V_{1-x}M_x)_2O_3$ reduces the distances between the sites of the material and so that the hopping parameter t increaser. As we take t as the unit of energy, the increase of pressure can be seen as an effective decrease of the on-site repulsion U of the Hubbard model.

6.9 Future work: inclusion of spin fluctuations

Up to now the wave function ψ_B for bipartite lattices has been treated on a mean-field level, since we have taken for ψ_∞ the Néel state. As the dimension decreases ψ_∞, the ground state of the antiferromagnetic Heisenberg model, is no more the Néel state. At $D = 1$ the spin fluctuations are large enough to destroy the long-range order and the ground state is that of a spin liquid.

In order to take into account spin fluctuations we choose the ansatz

$$\psi_{SF} = e^{-\kappa \hat{T}}\ e^{-\sum_{ij} f_{ij}(S_i^+ S_j^- + S_i^- S_j^+)}\ |N> \tag{6.62}$$

where S_i^α are spin-1/2 operators and κ and f_{ij} are variational parameters. $|N>$ denotes the Néel state. One starts from a state which is only exact for $D = \infty$ and for $U = \infty$.

We will set all variational parameters f_{ij} equal to a constant λ and and use as "spin fluctuation operator" the total spin operator

$$\psi_{SF} = e^{-\kappa \hat{T}}\ e^{-\lambda \hat{\mathbf{S}}^2}\ |N> \tag{6.63}$$

where $\hat{\mathbf{S}}^2 = \sum_{ij}[S_i^z S_j^z + 1/2(S_i^+ S_j^- + S_i^- S_j^+)]$. Expanding the Néel state as a sum of eigenstates of the operator $\hat{\mathbf{S}}^2$ (with $S_z = 0$)

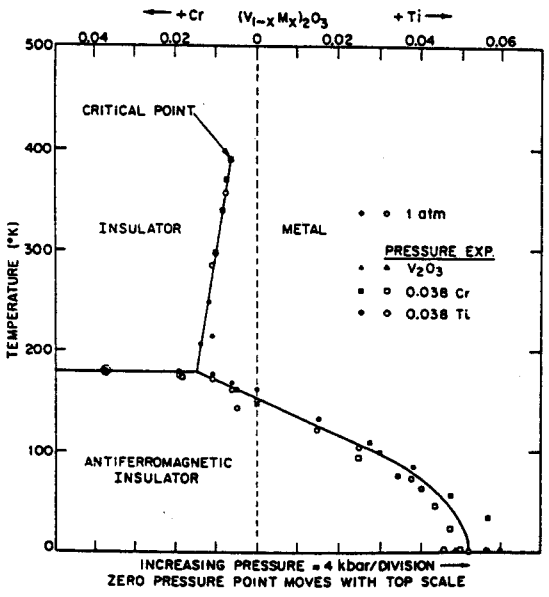

Figure 6.15: Pressure-temperature phase diagram for the $(V_{1-x}M_x)_2O_3$ coumpond doped with concentration x of Cr or Ti (from Ref. [32]).

$$|N>=\sum_{S=0}^{S_{max}} \alpha(S)|S, S_z=0> \ . \tag{6.64}$$

We see that the "spin fluctuation operator" transforms the Néel state more and more into a singlet state as λ increases. Thus, one expects $\lambda = 0$ for $D = \infty$ and $\lambda = \infty$ for $D = 1$.

Appendix A6

In this appendix the Peierls substitution is presented. The hopping parameter between any two sites of the lattice labeled by the vectors $\mathbf{R}$ and $\mathbf{R}'$ is given in the Wannier representation by

$$\begin{aligned} t_{\mathbf{R},\mathbf{R}'} &= \langle \mathbf{R}|\hat{T}(\mathbf{p})|\mathbf{R}'\rangle \\ &= \frac{\hbar^2}{2m}\int d\mathbf{r}\ \varphi^{\star}(\mathbf{r}-\mathbf{R})\left(\frac{\nabla}{i}\right)^2\varphi(\mathbf{r}-\mathbf{R}') \\ &= \frac{\hbar^2}{2m}\int d\mathbf{r}\ \varphi^{\star}_{\mathbf{A}}(\mathbf{r}-\mathbf{R})e^{i\theta(\mathbf{r}-\mathbf{R})}\left(\frac{\nabla}{i}\right)^2 e^{-i\theta(\mathbf{r}-\mathbf{R}')}\varphi_{\mathbf{A}}(\mathbf{r}-\mathbf{R}') \\ &= \frac{\hbar^2}{2m}\int d\mathbf{r}\ \varphi^{\star}_{\mathbf{A}}(\mathbf{r}-\mathbf{R})e^{i\theta(\mathbf{R}-\mathbf{R}')}\left(\frac{\nabla}{i}-\nabla\theta(\mathbf{r}-\mathbf{R}')\right)^2\varphi_{\mathbf{A}}(\mathbf{r}-\mathbf{R}') \end{aligned}$$

where $\varphi_{\mathbf{A}}(\mathbf{r}-\mathbf{R}) = e^{i\theta(\mathbf{r}-\mathbf{R})}\varphi(\mathbf{r}-\mathbf{R})$ are the Wannier functions in the presence of a magnetic field. This is shown below.

The eigenstates for the Hamiltonian of non-interacting electrons in the presence of a periodic lattice potential $V(\mathbf{r}+\mathbf{R}) = V(\mathbf{r})$, where $\mathbf{R}$ is a Bravais vector of the lattice, are the Bloch functions $\psi_{n,\mathbf{k}}(\mathbf{r})$ [46]. The band index n is going to be omitted hereafter. It is straightforward to show that the eigenstates of this system in the presence of the potential vector $\mathbf{A}(\mathbf{r})$ (associate to the applied magnetic field) are given by

$$\psi^{\mathbf{A}}_{\mathbf{k}}(\mathbf{r}) = e^{i\theta(\mathbf{r}-\mathbf{R})}\psi_{\mathbf{k}}(\mathbf{r}) \tag{A6.1}$$

where we have chosen the gauge

$$\nabla\theta(\mathbf{r}-\mathbf{R}) = \frac{e}{\hbar c}\mathbf{A}(\mathbf{r}) \tag{A6.2}$$

which implies

$$\theta(\mathbf{r}-\mathbf{R}) = \frac{e}{\hbar c}\int_{\mathbf{R}}^{\mathbf{r}} d\mathbf{r}'\ \mathbf{A}(\mathbf{r}'). \tag{A6.3}$$

The Wannier functions are given in terms of the Bloch functions by [46]

$$\varphi(\mathbf{r}-\mathbf{R}) = \frac{1}{v_0}\int d\mathbf{k}\ e^{-i\mathbf{k}.\mathbf{R}}\psi_{\mathbf{k}}(\mathbf{r}) \tag{A6.4}$$

where v_0 is the volume of the first Brillouin zone and the integral is over this zone. Thus it follows the relation

$$\varphi_{\mathbf{A}}(\mathbf{r}-\mathbf{R}) = e^{i\theta(\mathbf{r}-\mathbf{R})}\varphi(\mathbf{r}-\mathbf{R}). \tag{A6.5}$$

The hopping parameter is then

$$
\begin{aligned}
t_{\mathbf{R},\mathbf{R}'} &= e^{i\theta(\mathbf{R}-\mathbf{R}')} \int d\mathbf{r}\ \varphi^{\star}_{\mathbf{A}}(\mathbf{r}-\mathbf{R}) \frac{\hbar^2}{2m} \left(\frac{\nabla}{i} - \frac{e}{\hbar c}\mathbf{A}(\mathbf{r}) \right)^2 \varphi_{\mathbf{A}}(\mathbf{r}-\mathbf{R}') \\
&= e^{i\theta(\mathbf{R}-\mathbf{R}')} \langle \mathbf{R}(\mathbf{A}) | \hat{T}(\mathbf{A}) | \mathbf{R}'(\mathbf{A}) \rangle \\
&= e^{i\theta(\mathbf{R}-\mathbf{R}')} t_{\mathbf{R},\mathbf{R}'}(\mathbf{A}) \qquad \text{(A6.6)}
\end{aligned}
$$

where $t_{\mathbf{R},\mathbf{R}'}(\mathbf{A})$ is the hopping parameter in the presence of a magnetic field. The Peierls substitution is then given by

$$
t_{\mathbf{R},\mathbf{R}'}(\mathbf{A}) = e^{-i\frac{e}{\hbar c}\int_{\mathbf{R}'}^{\mathbf{R}} d\mathbf{r}'\ \mathbf{A}(\mathbf{r}')}\ t_{\mathbf{R},\mathbf{R}'} \qquad \text{(A6.7)}
$$

For simplicity, we consider that the applied magnetic field is such that the potential vector $\mathbf{A}(\mathbf{r})$ only affects one direction (of size L) of the system. If now it is assumed that $\mathbf{A}(\mathbf{r})$ is *approximatively constant* in the domain $\mathbf{R}-\mathbf{R}'$, one finally has

$$
t_{\mathbf{R},\mathbf{R}'}(\mathbf{A}) = e^{\pm i\frac{e}{\hbar c}\frac{\Phi}{L}\cdot|\mathbf{R}-\mathbf{R}'|} t_{\mathbf{R},\mathbf{R}'} \qquad \text{(A6.8)}
$$

where Φ is the magnetic flux. The on-site electronic repulsion parameter U, which in the Wannier representation is given by

$$
U = \int d\mathbf{r} \int d\mathbf{r}'\ \varphi^{\star}(\mathbf{r}-\mathbf{R})\varphi^{\star}(\mathbf{r}'-\mathbf{R}) \frac{e^2}{|\mathbf{r}-\mathbf{r}'|} \varphi(\mathbf{r}'-\mathbf{R})\varphi(\mathbf{r}-\mathbf{R}) \qquad \text{(A6.9)}
$$

is not affected by the magnetic field.

Appendix B6

In this appendix we present the calculation of the variational energy of the wave function ψ_B starting from the Néel state for two types of bipartite lattices: the "D-cubic lattices" (square, cubic, up to hypercubic) and the "D-diamond lattices" (honeycomb, diamond, up to hyperdiamond), which coordination numbers are $z = 2D$ and $z = D + 1$, respectively.

We first consider the Hubbard Hamiltonian (6.31) for "D-cubic lattices". Transforming the Wannier states into Bloch waves, through the Fourier transform of the electronic operators, one diagonalizes the kinetic term and the dispersion relation is given by

$$\epsilon(\mathbf{k}) = -2t \sum_{\alpha=1}^{D} \cos(k_\alpha) \tag{B6.1}$$

where k_α are the projections of the vector $\mathbf{k}$ onto the basis vectors of the unit cell. Since $\epsilon(\mathbf{k}+\mathbf{Q}) = -\epsilon(\mathbf{k})$, where $\mathbf{Q} = (\pi, ..., \pi)$, the kinetic energy can be written as

$$\hat{T} = \sum_{\mathbf{k},\sigma}{}' \epsilon(\mathbf{k}) \; (\hat{c}^\dagger_{\mathbf{k}\sigma}\hat{c}_{\mathbf{k}\sigma} - \hat{c}^\dagger_{\mathbf{k}+\mathbf{Q},\sigma}\hat{c}_{\mathbf{k}+\mathbf{Q},\sigma}) \tag{B6.2}$$

where the prime on the sum indicates that $\mathbf{k}$ belongs the antiferromagnetic Brillouin zone. The wavefunction ψ_B is given by Eq. (6.33) and the evaluation of the expectation value of the kinetic energy per site is straightforward

$$\begin{aligned}
\frac{T}{L} &= \frac{1}{L}\sum_{\mathbf{k},\sigma}{}' \epsilon(\mathbf{k}) \; \frac{\langle\psi_B|(\hat{c}^\dagger_{\mathbf{k}\sigma}\hat{c}_{\mathbf{k}\sigma} - \hat{c}^\dagger_{\mathbf{k}+\mathbf{Q},\sigma}\hat{c}_{\mathbf{k}+\mathbf{Q},\sigma}|\psi_B\rangle}{\langle\psi_B|\psi_B\rangle} \\
&= -\frac{1}{L}\sum_{\mathbf{k},\sigma}{}' \epsilon(\mathbf{k}) \tanh(2\kappa\epsilon(\mathbf{k})) \\
&= -\int_{-\infty}^{\infty} d\epsilon \; \rho(\epsilon)\epsilon \tanh(2\kappa\epsilon).
\end{aligned} \tag{B6.3}$$

We evaluate now the expectation value of the potential energy. Since in this case the wave function ψ_B is a single-particle wave function, Wick's theorem can be applied. For this state one has $\langle\hat{n}_{i\uparrow}\hat{n}_{i\downarrow}\rangle = \langle\hat{n}_{i\uparrow}\rangle\langle\hat{n}_{i\downarrow}\rangle$ and thus

$$U\langle\hat{D}\rangle = U\sum_i \langle n_{i\uparrow}\rangle \; \langle n_{i\downarrow}\rangle. \tag{B6.4}$$

In this special case, the wavefunction ψ_B is nothing else than a SDW with different amplitudes and as usual for a SDW we make

$$\langle\hat{n}_{i\sigma}\rangle = \frac{1}{2}(1 + \sigma(-1)^i m) \tag{B6.5}$$

where the factor $(-1)^i = +1(-1)$ for $i \in A(B)$, respectively. The expectation value of the potential energy per site is then given by

$$\frac{U\langle\hat{D}\rangle}{L} = \frac{U}{4}(1-m^2) \tag{B6.6}$$

where the sublattice magnetization m is given by

$$\begin{aligned} m &= \frac{1}{L}\sum_i (-1)^i \langle \hat{n}_{i\uparrow} - \hat{n}_{i\downarrow}\rangle \\ &= \frac{1}{L}\sum_{\mathbf{k},\sigma}{}' \sigma \, \langle \hat{c}^\dagger_{\mathbf{k}\sigma}\hat{c}_{\mathbf{k}+\mathbf{Q},\sigma} - \hat{c}^\dagger_{\mathbf{k}+\mathbf{Q},\sigma}\hat{c}_{\mathbf{k}\sigma}\rangle \\ &= \frac{1}{L}\sum_{\mathbf{k}}{}' \frac{2}{\cosh(2\kappa\epsilon(\mathbf{k}))} \\ &= \int_{-\infty}^{\infty} d\epsilon \rho(\epsilon) \frac{1}{\cosh(2\kappa\epsilon)}. \end{aligned} \tag{B6.7}$$

We consider now the "D-diamond" lattices. By Fourier transform of the Wannier operators into Bloch waves, we define the operators $\hat{c}^\dagger_{A,\mathbf{k}\sigma}$ and $\hat{c}^\dagger_{B,\mathbf{k}\sigma}$ for each sublattice. This gives a partially diagonalized kinetic term. The full diagonalization is made by a canonical transformation defining the operators $\hat{c}^\dagger_{p,\mathbf{k}\sigma} = u_{p,\mathbf{k}\sigma}\hat{c}^\dagger_{A,\mathbf{k}\sigma} + v_{p,\mathbf{k}\sigma}\hat{c}^\dagger_{B,\mathbf{k}\sigma}$ and one has

$$\hat{H} = \sum_{p,\mathbf{k}\in BZ,\sigma} \epsilon_p(\mathbf{k}) \, \hat{c}^\dagger_{p,\mathbf{k}\sigma}\hat{c}_{\mathbf{k},p,\sigma} + U \sum_i \hat{n}_{i\uparrow}\,\hat{n}_{i\downarrow} \tag{B6.8}$$

where $p = -, +$ and

$$\epsilon_\pm(\mathbf{k}) = \pm t\sqrt{\left(1 + \sum_{\alpha=1}^{D}\cos(k_\alpha)\right)^2 + \left(\sum_{\alpha=1}^{D}\sin(k_\alpha)\right)^2} \tag{B6.9}$$

where k_α are the projections of the vector $\mathbf{k}$ onto the basis vectors of the unit cell. The kinetic energy operator is written as

$$\hat{T} = \sum_{\mathbf{k}\in BZ,\sigma} \epsilon_-(\mathbf{k}) \, (\hat{c}^\dagger_{-,\mathbf{k}\sigma}c_{-,\mathbf{k}\sigma} - \hat{c}^\dagger_{+,\mathbf{k}\sigma}c_{+,\mathbf{k}\sigma}) \tag{B6.10}$$

and the Néel state as

$$\psi_\infty = \prod_{\mathbf{k}\in BZ,\sigma} \frac{1}{\sqrt{2}} \, (\hat{c}^\dagger_{-,\mathbf{k}\sigma} + \sigma \, \hat{c}^\dagger_{+,\mathbf{k}\sigma})|0\rangle. \tag{B6.11}$$

The wave function ψ_B is then given by

$$\psi_B = \prod_{\mathbf{k}\in BZ,\sigma} \frac{1}{\sqrt{2}} \, (e^{-\kappa\epsilon_-(\mathbf{k})}\hat{c}^\dagger_{-,\mathbf{k}\sigma} + \sigma \, e^{\kappa\epsilon_-(\mathbf{k})}\hat{c}^\dagger_{+,\mathbf{k}\sigma})|0\rangle. \tag{B6.12}$$

For D-diamond lattices, calculations are analogous and one has the same expressions for the kinetic energy (Eq. B6.3) and for the sublattice magnetization (Eq. B6.7).

Appendix C6

In this appendix we calculate the density of states for hypercubic and hyperdiamond lattices in the limit of infinite dimensions following the method of Müller-Hartmann [38]. The density of states is defined as

$$\begin{aligned}\rho(\epsilon) &= \int_{BZ} \left(\frac{dk}{2\pi}\right)^d \delta(\epsilon - \epsilon_{\mathbf{k}}) \\ &= \int_{BZ} \left(\frac{dk}{2\pi}\right)^d \int_{-\infty}^{\infty} \frac{d\xi}{2\pi}\, e^{i\xi(\epsilon-\epsilon_{\mathbf{k}})} \end{aligned} \tag{C6.1}$$

We first consider the hypercubic lattices, which dispersion is additive (Eq. B6.1). Therefore we find

$$\begin{aligned}\rho_{hc}(\epsilon) &= \int_{-\infty}^{\infty} \frac{d\xi}{2\pi}\, e^{i\xi\epsilon} \left[\int_{-\pi}^{\pi} \frac{dk}{2\pi}\, e^{2i\xi t\cos\, k}\right]^D \\ &= \int_{-\infty}^{\infty} \frac{d\xi}{2\pi}\, e^{i\xi\epsilon}\, [J_0(2\xi t)]^D. \end{aligned} \tag{C6.2}$$

For small arguments the Bessel function can be expanded: $J_0(x) \simeq 1 - x^2/4 \simeq \exp(-x^2/4)$. Using this expansion in the above equation we get

$$\rho_{hc}(\epsilon) = \frac{1}{\sqrt{\pi D}\; 2t} \exp[-(\epsilon/\sqrt{D}\; 2t)^2]. \tag{C6.3}$$

This expression was first obtained by Metzner and Vollhardt [17], who remarked that while the on-site repulsion parameter U remains well defined in infinite dimensions, the hopping parameter t must be conveniently rescaled for one has a non-trivial model. Using the scaling $t^\star = \sqrt{2D}\; t$, one obtains the non-trivial density of states in the limit $D = \infty$ (what justifies the expansion of the above Bessel function) for the hypercubic lattice, Eq. (6.37).

We consider now the hyperdiamond lattice, which has a unit cell with two atoms. Therefore, the dispersion has two branches, Eq. (B6.9). For $\epsilon > 0$ the density of states per site can be written as

$$\rho_{hd}(\epsilon) = \frac{1}{2}\int dx \int dy \int \left(\frac{dk}{2\pi}\right)^D \delta(x - \sum_\alpha \cos\, k_\alpha)\, \delta(y - \sum_\alpha \sin\, k_\alpha)\, \delta(\epsilon - t\sqrt{(1+x)^2 + y^2}). \tag{C6.4}$$

Introducing the representation

$$\delta(x - x_0) = \int \frac{d\xi}{2\pi} e^{i\xi(x-x_0)} \tag{C6.5}$$

we again obtain an expression where the k-integration can be factorized

$$\rho_{hd}(\epsilon) = \frac{1}{2}\int dx \int dy\, \delta(\epsilon - t\sqrt{(1+x)^2+y^2}) \int \frac{d\xi}{2\pi}\int \frac{d\eta}{2\pi}\, e^{i\xi x}\, e^{i\eta y}\, I^D \quad \text{(C6.6)}$$

where

$$I = \int_{-\pi}^{\pi} \frac{dk}{2\pi}\, e^{-i(\xi cos\ k + \eta \sin\ k)} = J_0(\sqrt{\xi^2+\eta^2}). \quad \text{(C6.7)}$$

For large D the leading contribution comes again from small arguments of the Bessel function

$$J_0(\sqrt{\xi^2+\eta^2}) \simeq 1 - \frac{1}{4}(\xi^2+\eta^2) \simeq e^{-\frac{1}{4}(\xi^2+\eta^2)}. \quad \text{(C6.8)}$$

It is then straightforward to perform the remaining integrals, giving

$$\rho_{hd}(\epsilon) = \frac{1}{2}\int dx \int dy\, \delta(\epsilon - t\sqrt{(1+x)^2+y^2})\, \frac{1}{\pi D}\, e^{-(x^2+y^2)/D}. \quad \text{(C6.9)}$$

In the limit $D \to \infty$ we obtain

$$\rho_{hd}(\epsilon) = \frac{1}{D\, t^2}\, \epsilon\, e^{-\frac{\epsilon^2}{Dt^2}}. \quad \text{(C6.10)}$$

Using the scaling $t = (D/2)^{-1/2} t^*$, we obtained for the hyperdiamond density of states given by Eq. (6.38) For $\epsilon < 0$ one simply uses the electron-hole symmetry, $\rho(\epsilon) = \rho(-\epsilon)$.

Appendix D6

In this appendix the systematic expansion in the weak coupling limit ($U \ll t$) for the Gutzwiller wave functionin terms of U/t is presented. The energy of the ground state given by the Gutzwiller wave functionis obtained by minimization of the following expression

$$F_G(\eta) = \frac{\langle\psi_0|e^{-\eta\hat{D}}\hat{H}e^{-\eta\hat{D}}|\psi_0\rangle}{\langle\psi_0|e^{-2\eta\hat{D}}|\psi_0\rangle} \tag{D6.1}$$

with respect to the variational parameter η. In the weak coupling limit the variational parameter η is also small and the exponential is expanded in powers of η. As the Fermi sea ψ_0 is a Slater determinant one can apply the Linked Cluster Theorem to get the following expression for the kinetic term

$$\begin{aligned} T(\eta) &= -t\sum_{\nu=0}^{\infty}\frac{(-\eta)^\nu}{\nu!}\langle\psi_0|\{\hat{D},...\{\hat{D},\hat{T}\},\}|\psi_0\rangle_C \\ &= -t\sum_{\nu=0}^{\infty}\frac{(-\eta)^\nu}{\nu!}T_\nu \end{aligned} \tag{D6.2}$$

where $\hat{D}$ appears ν times in the anticomutators and for the potential term

$$\begin{aligned} UD(\eta) &= U\sum_{\nu=0}^{\infty}\frac{(-2\eta)^\nu}{\nu!}\langle\psi_0|\hat{D}^{\nu+1}|\psi_0\rangle_C \\ &= U\sum_{\nu=0}^{\infty}\frac{(-2\eta)^\nu}{\nu!}D_\nu \end{aligned} \tag{D6.3}$$

respectively. One uses standard expansion techniques to get the expansion up to desired order. As seen in text, one introduces the equal-time correlation functions G_{ij} ($\tilde{G_{ij}}$) (Eq. 6.46).

For the honeycomb lattice, which is a bipartite lattice with two atoms per unit cell, one gets for the parameters of the expansion

$$\begin{aligned} T_0 &= \langle\psi_0|\hat{T}|\psi_0\rangle_C \\ &= -t\sum_{<ij>,\sigma}(G_{ij}+G_{ji}) \\ &= -t\,L\,p_0 \end{aligned}$$

$$T_1 = \langle\psi_0|\{\hat{D},\hat{T}\}|\psi_0\rangle_C$$

$$
\begin{aligned}
&= -2t \sum_{<ik>i\in A,j\in R} \langle\psi_0|c^\dagger_{j\uparrow}c_{j\uparrow}c^\dagger_{j\downarrow}c_{j\downarrow}(c^\dagger_{i\sigma}c_{k\sigma}+h.c.)|\psi_0\rangle \\
&= 4t \sum_{<ik>i\in A,j\in R} (\tilde{G}_{ji}G_{jj}G_{jk}+\tilde{G}_{jk}G_{jj}G_{ji}) \\
&= 0
\end{aligned}
$$

$$
\begin{aligned}
T_2 &= \langle\psi_0|\{\hat{D},\{\hat{D},\hat{T}\}\}|\psi_0\rangle_C \\
&= -32t \sum_{<ik>i\in A,j\in R,l\in R} G_{ij}G^3_{jl}G_{lk} + \\
&\quad +16t \sum_{<ik>i\in A,j\in R} (G^3_{ij}G_{jk}+G_{ij}G^3_{jk}) - \\
&\quad -8t \sum_{<ik>i\in A} G^3_{ik} - 2t \sum_{<ik>i\in A} G_{ik} \\
&= -t\,\frac{L}{2}\,p_2. \qquad \text{(D6.4)}
\end{aligned}
$$

$$
\begin{aligned}
D_0 &= \langle\psi_0|\hat{D}|\psi_0\rangle_C \\
&= 1/4\ L \\
\\
D_1 &= \langle\psi_0|\hat{D}^2|\psi_0\rangle_C \\
&= \sum_{i,j\in R} G^4_{ij} \\
&= L\ q_1 \\
\\
D_2 &= \langle\psi_0|\hat{D}^3|\psi_0\rangle_C \\
&= L\ q_2, \qquad \text{(D6.5)}
\end{aligned}
$$

where R means that the site runs over the two sublattices A and B. The expression for Gutzwiller variational energy per site $F_G(\eta)/L$ becomes

$$
F_G(\eta)/L = -p_0 t + \frac{1}{4}U - 2\eta q_1 U - \frac{\eta^2}{4}p_2 t + 2\eta^2 q_2 U \qquad \text{(D6.6)}
$$

after minimization we get for the optimal variational parameter η_0, in the weak coupling limit ($U/t \ll 1$), the solution

$$
\begin{aligned}
\eta_0 &= \frac{-4q_1(U/t)}{p_2 t\,[1-(8q_2/p_2)(U/t)]} \\
&= \frac{-4q_1}{p_2}\left(\frac{U}{t}\right) + \mathcal{O}\left(\frac{U}{t}\right) \qquad \text{(D6.7)}
\end{aligned}
$$

which confirms that the variational increases with U/t ($q_1 > 0$ and $p_2 < 0$ for the honeycomb lattice). The Gutzwiller wave function energy per site is then given by

$$\begin{aligned} \epsilon_G &= -p_0 t + \frac{1}{4} t \left(\frac{U}{t}\right) + \frac{4q_1^2}{p_2} t \left(\frac{U}{t}\right)^2 \\ &= \epsilon_0 + \epsilon_1 \left(\frac{U}{t}\right) + \epsilon_2 \left(\frac{U}{t}\right)^2 . \end{aligned} \tag{D6.8}$$

Therefore, in order to obtain the energy up to second-order in U/t, one has to evaluate the kinetic energy up to second-order in the variational parameter η and the potential energy up to first-order in the variational parameter η.

The values of p_0, q_1 and p_2 were evaluated numerically for a honeycomb lattice with 50×50 unit cells and we have that: $\epsilon_0 = -1.5746t$, $\epsilon_1 = 0.25t$ and $\epsilon_2 = -9.6845 \times 10^{-3} t$.

Appendix E6

In this appendix the Variational Monte Carlo procedure is presented. Our aim is to calculate the expectation value of a given operator using a Gutzwiller-type wave function

$$\langle \hat{O} \rangle = \frac{\langle \phi | e^{-\eta \hat{D}} \hat{O} e^{-\eta \hat{D}} | \phi \rangle}{\langle \phi | e^{-2\eta \hat{D}} | \phi \rangle} \tag{E61}$$

where ϕ can be, in principle, any wave function. Monte Carlo numerical techniques are based on the Hubbard-Stratonovich transformation [47]

$$e^{\frac{1}{2}\hat{A}^2} = \sqrt{2\pi} \int_{-\infty}^{\infty} d\phi \; e^{(-\frac{1}{2}\phi^2 - \phi \hat{A})}. \tag{E62}$$

For the particular case of the Gutzwiller projector and noticing that $n_{i\sigma} = 0, 1$ for the Hubbard model, this transformation takes the particular form

$$e^{-\eta \hat{n}_{i\uparrow} \hat{n}_{i\downarrow}} = \frac{1}{2} e^{-\frac{\eta}{2}\hat{n}_i} \sum_{s_i = \pm 1} e^{-\eta^* \hat{S}_i s_i} \tag{E63}$$

where $\hat{n}_i = \hat{n}_{i\uparrow} + \hat{n}_{i\downarrow}$, $\hat{S}_i = \hat{n}_{i\uparrow} - \hat{n}_{i\downarrow}$, s_i are auxiliar Ising spins and $\cosh(\eta^*) = \exp(\eta/2)$.

The expectation value (Eq. E61) is then given by

$$\langle \hat{O} \rangle = \frac{\sum_{\{s_i^L = \pm 1, s_i^R = \pm 1\}} \langle s^L | \hat{O} | s^R \rangle}{\sum_{\{s_i^L = \pm 1, s_i^R = \pm 1\}} \langle s^L | s^R \rangle} \tag{E64}$$

where we have to distinguish between "left" and "right" auxiliar Ising spins

$$|s^p\rangle = e^{-\eta^* \sum_{i=1}^{L} \hat{S}_i s_i^p} |\phi\rangle \tag{E65}$$

with $p = L, R$. The expectation value is the trace over the 4^L configurations of the s_i^p Ising spins. Thus, it can be obtained as in a classical Monte Carlo procedure. The expectation value (Eq. E61) in the Monte Carlo algorithm is given by

$$\langle \hat{O} \rangle \approx \frac{1}{M} \sum_{m=1}^{M} \langle \hat{O} \rangle (\{s_m\}) \tag{E66}$$

where

$$\langle \hat{O} \rangle (\{s_m\}) = \frac{\langle s^L | \hat{O} | s^R \rangle}{\langle s^L | s^R \rangle} \tag{E67}$$

and $\{s_m\}$ is a particular configuration of the auxiliar Ising spins. The Monte Carlo algorithm generate M configurations $\{s_m\}$ of the auxiliar Ising spins s_i^p with probablility distribution $w(\{s_m\}) = \langle s^L | s^R \rangle$. The number of Monte Carlo steps equals M.

The energy of the Hubbard model for a given configuration $\{s_m\}$ is given by

$$\langle \hat{H} \rangle (\{s_m\}) = \frac{\langle s^L | \left(-t \sum_{<i,j>,\sigma} (c^\dagger_{i\sigma} c_{j\sigma} + h.c.) + U \sum_i n_{i\uparrow} n_{i\downarrow} \right) | s^R \rangle}{\langle s^L | s^R \rangle} \quad \text{(E68)}$$

If the wave function ϕ is a single-particle state then Wick's Theorem applies and we have

$$\langle \hat{H} \rangle (\{s_m\}) = -t \sum_{<i,j>,\sigma} (g_{i,j,\sigma}(\{s_m\}) + h.c.) + U \sum_i g_{i,i,\uparrow}(\{s_m\}) g_{i,i,\downarrow}(\{s_m\}) \quad \text{(E69)}$$

where the Green's function is given by

$$g_{i,j,\sigma}(\{s_m\}) = \frac{\langle s^L | c^\dagger_{i\sigma} c_{j\sigma} | s^R \rangle}{\langle s^L | s^R \rangle}. \quad \text{(E610)}$$

Starting from an initial configuration $\{s\}$, a Monte Carlo step creates a new configuration $\{s'\}$ by changing the sign of just one auxiliar Ising spin: $s^p_l \to -s^p_l$. One evaluates then the ratio of the probabilities of each configuration

$$\begin{aligned} r &= w(\{s'\})/w(\{s\}) \\ &= \left[1 + (e^{2\eta^* s^p_l} - 1) g_{l,l,\uparrow}(\{s\})\right] \left[1 + (e^{-2\eta^* s^p_l} - 1) g_{l,l,\downarrow}(\{s\})\right] \end{aligned} \quad \text{(E611)}$$

If r is greater then a random number generated at each step the new configuration is not accepted. Otherwise, the new configuration is accepted and the Green's function should be actualized according to

$$\begin{aligned} g_{i,j,\uparrow}(\{s'\}) &= g_{i,j,\uparrow}(\{s\}) - \\ &- \frac{Q(\sigma s^p_l)}{R_\sigma(s,p,l)} g_{i,l,\sigma}(\{s\}) g_{l,j,\sigma}(\{s\}) + \\ &+ \frac{Q(\sigma s^p_l)}{R_\sigma(s,p,l)} g_{i,j,\sigma}(\{s\}) [\delta_{il}\delta_{pL} + \delta_{jl}\delta_{pR}] \end{aligned} \quad \text{(E612)}$$

where

$$R_\sigma(s,p,l) = 1 + Q(\sigma s^p_l) g_{l,l,\sigma}(\{s\}) \quad \text{(E613)}$$

with $Q(x) = e^{\eta x}(1 + \sqrt{1 - e^\eta})^{2x} - 1$.

Bibliography

[1] M. C. Gutzwiller, Phys. Rev. Lett. **10**, 159 (1963).

[2] M. C. Gutzwiller, Phys. Rev. **134**, A923 (1964); *ibid.*, **137**, A1726 (1965).

[3] W. Metzner, and D. Vollhardt, Phys. Rev. Lett. **59**, 121 (1987); *ibid.*, Phys. Rev. B **37**, 7382 (1988), Erratum Phys. Rev. B **39**, 12339 (1989).

[4] F. Gebhard, and A. Girndt, Z. Phys. B **93**, 455 (1994).

[5] M. Dzierzawa, D. Baeriswyl, and M. di Stasio, Phys. Rev. B **51**, 1993 (1995).

[6] H. Yokoyama, and H. Shiba, J. Phys. Soc. Japan. **56**, 1490 (1987); *ibid.*, **56**, 3582 (1987).

[7] P. Horsch, and P. Fulde, Z. Phys. B **36**, 23 (1979).

[8] P. Horsch, Phys. Rev. B **24**, 7351 (1981).

[9] D. Baeriswyl, and K. Maki, Phys. Rev. B **31**, 6633 (1985).

[10] D. Baeriswyl, J. Carmelo, and K. Maki, Synthetic Metals **21**, 271 (1987).

[11] J. Carmelo, M. Dzierzawa, X. Zotos, and D. Baeriswyl, Phys. Rev. B **43**, 598 (1991).

[12] T. Ogawa, K. Kanda, and T. Matsubara, Prog. Theo. Phys. **53**, 614 (1975).

[13] H. Razafimandimby, Z. Phys. B **49**, 33 (1982).

[14] D. Vollhardt, Rev. Mod. Phys. **56**, 99 (1984).

[15] P. Fazekas, *Electron Correlation and Magnetism* (World Scientific, 1999).

[16] W. F. Brinkman, and T. M. Rice, Phys. Rev. B **2**, 4302 (1970).

[17] W. Metzner, and D. Vollhardt, Phys. Rev. Lett. **62**, 324 (1989).

[18] F. Gebhard, Phys. Rev. B **41**, 9452 (1990).

[19] T. Kaplan, P. Horsch, and P. Fulde, Phys. Rev. Lett. **49**, 889 (1982).

[20] P. Fazekas, and K. Penc, Int. J. Mod. Phys. B **2**, 1021 (1988).

[21] H. Yokoyama, and H. Shiba, J. Phys. Soc. Japan **59**, 3669 (1990).

[22] D. Baeriswyl, in *Nonlinearity in Condensed Matter* (edited by A. R. Bishop *et al.*, Springer Series in Solid State Sciences **69**, p. 183, 1987).

[23] H. A. Bethe, Z. Phys. **71**, 205 (1931).

[24] T. Kennedy, E. H. Lieb, and B. S. Shastry, Phys. Rev. Lett. **61**, 2582 (1988).

[25] M. Dzierzawa, D. Baeriswyl, and L. M. Martelo, Helv. Phys. Acta **70**, 124 (1997).

[26] W. Heitler, and F. London, Z. Phys. , 455 (1927).

[27] V. J. Emery, Phys. Rev. B **14**, 2989 (1976).

[28] W. Kohn, Phys. Rev. **133**, A171 (1964).

[29] A. J. Millis, and S. N. Coppersmith, Phys. Rev. B **43**, 13770 (1991).

[30] A. Georges, G. Kotliar, W. Krauth, and M. J. Rozenberg, Rev. Mod. Phys. **68**, 13 (1996).

[31] N. F. Mott, Proc. Phys. Soc. **A62**, 416 (1949); *ibid.*, *Metal-Insulator Transitions*, (Taylor and Francis, London 1990).

[32] D. B. McWhan *et al.*, Phys. Rev. Lett. **27**, 941 (1971); D. B. McWhan *et al.*, Phys. Rev. B **7**, 9224 (1973).

[33] E. H. Lieb, and F. Y. Wu, Phys. Rev. Lett. **20**, 1445 (1968).

[34] D. R. Penn, Phys. Rev. **142**, 350 (1966).

[35] M. Rasetti, *The Hubbard Model, Recent Results*, (World Scientific, 1991).

[36] J. E. Hirsch, Phys. Rev. B **31**, 4403 (1985).

[37] G. Santoro, M. Airoldi, S. Sorella, and E. Tosatti, Phys. Rev. B **47**, 16 216 (1993).

[38] E. Müller-Hartmann, Z. Phys. B **74**, 507 (1989).

[39] J. D. Reger, J. A. Riera, and A. P. Young, J. Phys.: Cond. Matter **1**, 1855 (1989).

[40] L. M. Martelo, M. Dzierzawa, L. Siffert, and D. Baeriswyl, Z. Phys. B **103**, 335 (1997).

[41] S. Sorella, and E. Tosatti, Europhys. Lett. **19**, 699 (1992).

[42] E. Jeckelmann, and D. Baeriswyl, Synth. Met. **65**, 211 (1994).

[43] M. Imada, J. Phys. Soc. Japan **64**, 2954 (1995).

[44] J. González, F. Guinea, and M. A. H. Vozmediano, Phys. Rev. Lett. **77**, 3589 (1996).

[45] S. Pairault, D. Sénéchal, and A.-M. S. Tremblay, Phys. Rev. Lett. **80**, 5389 (1998).

[46] N. W. Ashcroft and N. Mermin, *Solid State Physics*, (Saunders College Publishing, Fort Worth, 1976).

[47] J. E. Hirsch, Phys. Rev. B **28**, 4059 (1983).

Chapter 7

Dielectric Susceptiblity for Interacting Electrons

7.1 Introduction

The Hubbard model (and generalized versions of its) is one of the simplest model to study the Mott transition and to gain some insight to the metal-insulator transition induced by electronic correlations. The Hubbard model at half filling exhibits a metal-insulator transition as function of the on-site Coulomb repulsion at a critical value U_c. For $U > U_c$ holes and doubly occupied sites are bound in pairs. Therefore, the model has *dielectric dipoles.* These dipoles are ramdomly distributed in the system and thus the macroscopic polarization of the system is zero. An external applied electric field would induces an orientation of these dipoles creating a finite polarization in the system. The number and the size of these dipoles increase as U decreases and thus the dielectric constant increases until it *diverges* at the critical value U_c, where the dipoles are "broken" and free charge carriers appear in the system.

The divergence of the dielectric susceptibilty at the metal-insulator transition is observed experimentally, e.g. in the phosphorus-doped silicon $Si : P$ [1] (Fig. 7.1). Essentially, the doping process introduces an excess of electrons and one expects a Mott transition at some critical concentration n_c. It should be mentioned that the transition is a continuous second-order one at $T \neq 0$ and so it is not a pure Mott transition. In fact, dopants induce disorder in the system and the transition will be, in part, of the Andersson-type [2].

7.2 Dielectric susceptibility

The definition of the macroscopic polarization of a system is not as straightforward as one could believed at first sight and is still a field of some controversy.

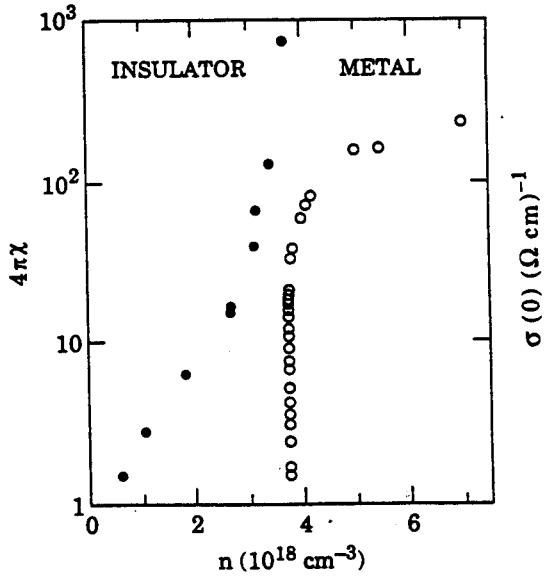

Figure 7.1: Divergence of the dielectric susceptiblibilty (solid points) and the vanishing of the static conductivity (open points) at the metal-insulator transition of Silicon doped with a concentration n of Phosphorus. Data are extrapolated to $T = 0$ (after reference [1]).

Nevertheless, progress has been made recently towards a quantum theory of polarization, and, correspondingly, of the dielectric susceptibility [3, 4, 5].

We are interested in the dielectric susceptibilty due to the conduction electrons (ions will be taken at fixed positions). The wave vector and frequency dependent electronic dielectric susceptibility $\chi(\mathbf{q}, \omega)$ can be evaluated for a system of interacting electrons within several approximative methods, such as the semi-classical Thomas-Fermi approach or the the Lindhard approach (equivalent to a Random Phase Approximation) [6, 7, 8, 9]. Here, we develop a quite general method for evaluating the dielectric constant $\chi_0 = \chi(\mathbf{q} = 0, \omega = 0)$ for interacting electronic systems .

For the sake of simplicity, we consider the Hamiltonian of N interacting electrons on a one-dimensionlattice,submitted to an external applied electric field

$$\hat{H} = \hat{H}_0 + \hat{H}_{int}(t) \tag{7.1}$$

where

$$\hat{H}_0 = \sum_{i=1}^{N} \frac{\hat{p}_i^2}{2m} + \hat{V} + \hat{U} \tag{7.2}$$

consists of three parts, the kinetic energy (with the electron mass m), a periodic potential $\hat{V}$ and the electron-electron interaction $\hat{U}$, and

$$\hat{H}_{int}(t) = -L\ \hat{P}.F(\hat{x},t) \tag{7.3}$$

describes the coupling between the polarization $\hat{P}$ and the external electric field $F(\hat{x},t)$ (L the size of the system, which coincides with the number of sites of the system if one takes for lattice constant $a = 1$).

The electronic polarization (dipole per unit of length) is given by

$$\hat{P} = \lim_{L\to\infty} \frac{e}{L}\langle X\rangle \tag{7.4}$$

where e is the electron charge. The expectation value $\langle X\rangle$ depends crucially on the boundary conditons imposed on the system [5]. For open boundary conditions, one defines the operator $\hat{X}$ as

$$\hat{X} = \sum_{i=1}^{N} \hat{x}_i. \tag{7.5}$$

For Born-von Kármán periodic boundary conditions the operator $\hat{x}$ is ill-defined and the expectation value $\langle X\rangle$ is given by an "electron-in-broth"-type formula [11, 5]

$$\langle X\rangle = \frac{L}{2\pi}\ Im\ \log\langle\psi_0|e^{i\frac{2\pi}{L}\hat{X}}|\psi_0\rangle \tag{7.6}$$

where ψ_0 is the ground state of the system and $\hat{X}$ is the operator defined by Eq.(7.5).

We choose open boundary conditions. A small spatially uniform electric field is now adiabatically turned on. The corresponding electric potential is then given by

$$\Phi(\hat{x},t) = \frac{V_0}{L}\ \hat{x}\ f(t)e^{\eta t} \tag{7.7}$$

where the parameter V_0 is such that $V_0/L \ll 1$ and $\eta \to 0^+$. The Hamiltonian (7.1) becomes

$$\hat{H} = \sum_{i=1}^{N} \frac{\hat{p}_i^2}{2m} + \hat{V} + \hat{U} + \frac{eV_0}{L}\sum_{i=1}^{N} \hat{x}_i f(t)e^{\eta t} \tag{7.8}$$

In linear response theory [12] one has

$$\langle\psi_0|\hat{x}_{i_H}(t)|\psi_0\rangle = \langle\phi_0|\hat{x}_{i_H}(t)|\phi_0\rangle + \frac{1}{i\hbar}\int_{-\infty}^{t} dt'\ \langle\phi_0|\left[\hat{x}_{i_H}(t), \hat{H}_{int_H}(t')\right]|\phi_0\rangle \tag{7.9}$$

where ψ_0 is the exact ground state of the perturbed Hamiltonian $\hat{H}$, ϕ_0 is the exact ground state of the unperturbed Hamiltonian $\hat{H}_0$ and

$$\hat{x}_H(t) = e^{i\hat{H}_0 t/\hbar}\hat{x}e^{-i\hat{H}_0 t/\hbar}. \tag{7.10}$$

Noticing that $\langle\phi_0|\hat{x}_{i_H}(t)|\phi_0\rangle = 0$, making the Fourier transform as usual to the frequency space, using the eigenstates of the unperturbed Hamiltonian $\hat{H}_0|\phi_l\rangle = E_l|\phi_l\rangle$, we arrive at

$$\begin{aligned}\langle\psi_0|\hat{x}_{i_H}|\psi_0\rangle_{(\omega)} &= -e\sum_{l\neq 0}\sum_{j=1}^{N}\left[\frac{1}{E_0 - E_l + \hbar\omega + i\eta}\langle\phi_0|\hat{x}_i|\phi_l\rangle\langle\phi_l|\hat{x}_j|\phi_0\rangle + \right.\\ &\left. + \frac{1}{E_0 - E_l - \hbar\omega - i\eta}\langle\phi_0|\hat{x}_j|\phi_l\rangle\langle\phi_l|\hat{x}_i|\phi_0\rangle\right]\cdot\\ &\cdot\left[-\frac{V_0}{L}f(\omega)\right]\end{aligned} \tag{7.11}$$

This yields the macroscopic polarization [Eq. (7.4)],

$$\begin{aligned}P(\omega) &= \lim_{L\to\infty}\frac{e}{L}\sum_{i=1}^{N}\langle\hat{x}_i(\omega)\rangle\\ &= \chi(\omega)E(\omega).\end{aligned} \tag{7.12}$$

with the frequency dependent dielectric susceptibility

$$\begin{aligned}\chi(\omega) &= -\lim_{L\to\infty}\frac{e^2}{L}\sum_{l\neq 0}\sum_{i,j=1}^{N}\left[\frac{1}{E_0 - E_l + \hbar\omega + i\eta}\langle\phi_0|\hat{x}_i|\phi_l\rangle\langle\phi_l|\hat{x}_j|\phi_0\rangle + \right.\\ &\left. + \frac{1}{E_0 - E_l - \hbar\omega - i\eta}\langle\phi_0|\hat{x}_j|\phi_l\rangle\langle\phi_l|\hat{x}_i|\phi_0\rangle\right].\end{aligned} \tag{7.13}$$

The real and imaginary parts read

$$Re\chi(\omega) = -\lim_{L\to\infty}\frac{e^2}{L}\sum_{l\neq 0}\sum_{i,j=1}^{N}\left[\mathcal{P}\frac{1}{E_0 - E_l + \hbar\omega} + \mathcal{P}\frac{1}{E_0 - E_l - \hbar\omega}\right]\langle\phi_0|\hat{x}_i|\phi_l\rangle\langle\phi_l|\hat{x}_j|\phi_0\rangle \tag{7.14}$$

$$Im\chi(\omega) = \lim_{L\to\infty}\frac{e^2\pi}{L}\sum_{l\neq 0}\sum_{i,j=1}^{N}\left[\delta(E_0 - E_l + \hbar\omega) - \delta(E_0 - E_l - \hbar\omega)\right]\langle\phi_0|\hat{x}_i|\phi_l\rangle\langle\phi_l|\hat{x}_j|\phi_0\rangle. \tag{7.15}$$

We show now that the static susceptibility $\chi_0 = Re\chi(0)$ can be also obtained on the basis of the ground state energy in a static electric field. To show this, we consider a small static spatially uniform electric field defined by the potential

$$\Phi(\hat{x}) = \frac{V_0}{L}\hat{x}. \tag{7.16}$$

The Hamiltonian (7.1) becomes

$$\hat{H}(V_0) = \sum_{i=1}^{N} \frac{\hat{p}_i^2}{2m} + \hat{V} + \hat{U} + \frac{eV_0}{L}\sum_{i=1}^{N} \hat{x}_i. \tag{7.17}$$

The derivative of the ground state energy $E_0(V_0)$ with respect to V_0 yields the polarization

$$\begin{aligned} \frac{dE_0(V_0)}{dV_0} &= \langle\phi_0(V_0)|\frac{\partial\hat{H}(V_0)}{\partial V_0}|\phi_0(V_0)\rangle \\ &= \frac{e}{L}\langle\phi_0(V_0)|\sum_{i=1}^{N}\hat{x}_i|\phi_0(V_0)\rangle \qquad (7.18) \\ &= \frac{e}{L}\langle\hat{X}\rangle_0 \qquad (7.19) \end{aligned}$$

In second-order perturbation theory we have

$$E_0(V_0) = E_0(0) + \langle\phi_0|\hat{H}_{int}(V_0)|\phi_0\rangle + \sum_{l\neq 0}\frac{|\langle\phi_0|\hat{H}_{int}(V_0)|\phi_l\rangle|^2}{E_0 - E_l}. \tag{7.20}$$

Considering the above equation as the expansion in powers of V_0, we have for the first derivative

$$\left.\frac{dE_0(V_0)}{dV_0}\right|_{V_0=0} = \frac{e}{L}\langle\phi_0|\sum_{i=1}^{N}\hat{x}_i|\phi_0\rangle, \tag{7.21}$$

in agreement with the previous equation (7.18), and for the second derivative

$$\left.\frac{d^2E_0(V_0)}{dV_0^2}\right|_{V_0=0} = 2\left(\frac{e}{L}\right)^2\sum_{l\neq 0}\frac{|\langle\phi_0|\sum_{i=1}^{N}\hat{x}_i|\phi_l\rangle|^2}{E_0 - E_l}. \tag{7.22}$$

Comparing now Eq.(7.13) for $\omega = 0$ and Eq.(7.22) we arrive to the main result for the dielectric constant

$$\chi_0 = -\lim_{L\to\infty}\frac{1}{L}\left.\frac{d^2E_0(F)}{dF^2}\right|_{F=0} \tag{7.23}$$

where $E_0(F)$ is the ground state energy in the the presence of an external electric field $F = V_0/L$.

This result can be interpretated as a Stark effect. The electric field deforms the electronic wave function such that it induces a polarization $P \sim \chi F$. This

contributes to the energy E of the system, $E \sim P.F \sim \chi F^2$, and the response dielectric constant χ is essentially given by the second derivative of the energy with respect to the applied electric field.

We now turn to the description of the Mott metal-insulator transition. It can be shown [10] that the real part of the zero-temperature electronic conductivity has two components, a singular part (corresponding to "free" acceleration of the charge carriers) and a regular part (corresponding to absortion)

$$\sigma(\omega) = \pi D_c \delta(\omega) + \sigma_{reg}(\omega) \tag{7.24}$$

where D_c is the charge stiffness (or Drude weight), given by

$$D_c = L \left. \frac{d^2 E_0(\Phi)}{d\Phi^2} \right|_{\Phi=0} . \tag{7.25}$$

$E_0(\Phi)$ is the ground state energy and Φ is the flux due to an external magnetic field applied to the system. Kohn's criterion states that the charge stiffness is finite for an ideal conducting system ($U < U_c$) while it is zero for an insulating one ($U > U_c$). If, in fact, the charge stiffness is the order parameter for the Mott metal-insulator transition, one expects, at zero-temperature, that $D_c = 0$ at the Mott transition ($U = U_c$), if the Mott transition is continuous. The dielectric constant, given by Eq.(7.23), will be finite in the insulating phase ($U > U_c$) increase with decreasing U and diverge at the Mott transition ($U = U_c$). This view is in line with a classical phase transition where, e.g. the parameter driving the transition is the temperature. If one considers, for instance, the classical Heisenberg ferromagnet, the order parameter is the magnetization of the system, which starts from a maximum value at $T = 0$, decreases in the ferromagnetic phase down to zero at the ferromagnetic-paramagnetic transition ($T = T_c$) and is zero in the paramagnetic phase ($T > T_c$). The magnetic susceptibility of the system is divergent at the ferromagnetic-paramagnetic transition temperature T_c and decreases in the paramagnetic region as temperature increases.

7.3 Application to the $1D$ dimerized model

The one-dimensional dimerized model is given by the following Hamiltonian

$$\hat{H} = - \sum_{i \ even,\sigma} \left(t_1 c^\dagger_{i\sigma} c^\dagger_{i\sigma} + h.c. \right) - \sum_{i \ odd,\sigma} \left(t_2 c^\dagger_{i\sigma} c^\dagger_{i\sigma} + h.c. \right) \tag{7.26}$$

where $c^\dagger_{i\sigma}(c_{i\sigma})$ are the electronic operators that create (anihilate) an electron at site i with spin projection σ. The different hoppings parameters t_1 and t_2 between even/odd sites can be considered as the effect of the electron-phonon interaction giving rise to dimerization.

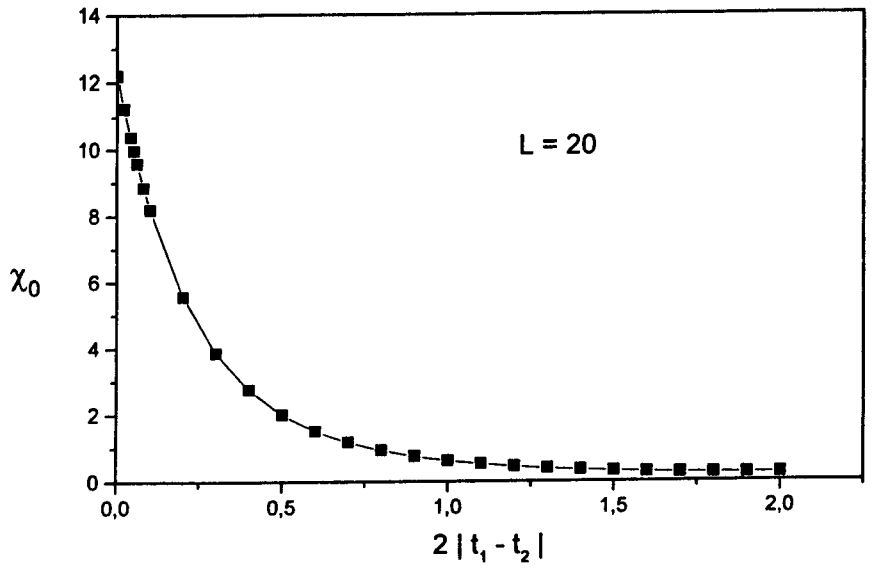

Figure 7.2: Dielectric constant (in arbitrary units) for the dimerized model (with $t_1 = 1$) as function of $2 \mid t_1 - t_2 \mid$ for a the system of size $L = 20$.

Considering periodic boundary conditions, in the thermodynamic limit the one-particle dispersion has two branches given by

$$\epsilon(k) = \pm\sqrt{t_1^2 + t_2^2 + 2t_1 t_2 \cos(2ka)} \tag{7.27}$$

where $2a$ is the lattice constant. The one-particle spectrum has a gap given by $\Delta = 2 \mid t_1 - t_2 \mid$. For $t_1 = t_2$ the model reduces to the simple tight-binding model, which is conducting for electronic densities $0 < n < 2$. For $t_1 \neq t_2$ the spectrum has a finite gap $\Delta > 0$. Therefore, at the half-filling case ($n = 1$) the model exhibits a metal-insulator transition at the critical value $\Delta_c = 0$.

We now consider the dimerized model with open boundary conditions and in the presence of an external uniform electric field F

$$\hat{H} = -\sum_{i\ even,\sigma} \left(t_1 c_{i\sigma}^{\dagger} c_{i\sigma}^{\dagger} + h.c.\right) - \sum_{i\ odd,\sigma} \left(t_2 c_{i\sigma}^{\dagger} c_{i\sigma}^{\dagger} + h.c.\right) + e\ F \sum_{i=1,\sigma}^{L} x_i\ c_{i\sigma}^{\dagger} c_{i\sigma} \tag{7.28}$$

where L is the number of sites. One has taken $t_1 = 1$ and the electron charge $e = 1$. The model was solved by exact numerical diagonalization. At half-filling, the number of electrons N equals the number of sites L and the ground state energy is given by

$$E_0(F) = 2 \sum_{n=1}^{L/2} E_n(F) \tag{7.29}$$

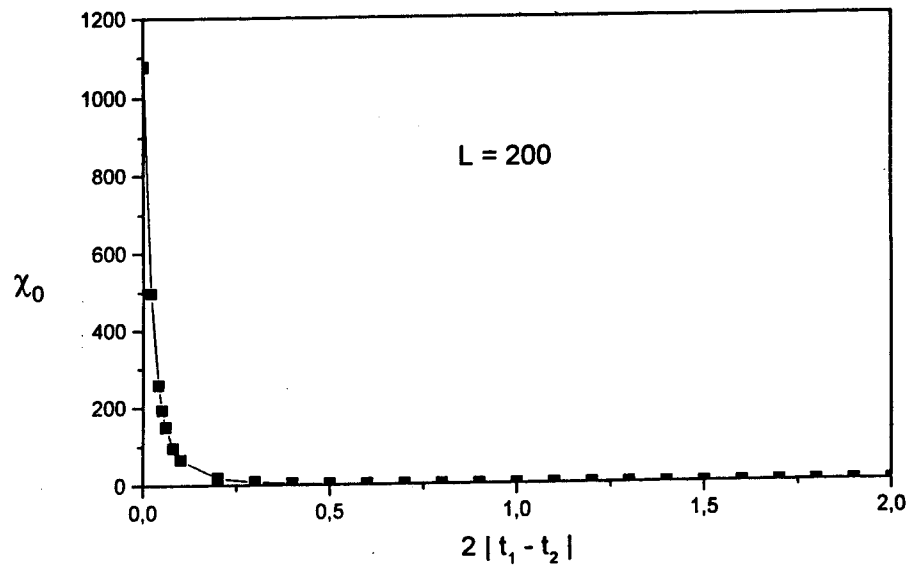

Figure 7.3: Dielectric constant (in arbitrary units) for the dimerized model (with $t_1 = 1$) as function of $2 \mid t_1 - t_2 \mid$ for a system of size $L = 200$.

where $E_n(F)$ are the one-particle eigenenergies of the system in the presence of the electric field ($E_1 < E_2 < ... < E_L$).

The dielectric constant is given by Eq.(7.23). In order to obtain the second derivative, a six-point formula was used: $\chi_0 = 1/L^2[10E_0(-F) - 15E_0(0) - 4E_0(F) + 14E_0(2F) - 6E_0(3F) + E_0(4F)]$ and to accuratetly determine the value of χ_0 at zero-field, for each value of $\mid t_1 - t_2 \mid$ and L, the electric field values were taken from $F = 10^{-3}$ down to $F = 10^{-7}$ (in arbitrary units).

The dielectric constant as function of $2 \mid t_1 - t_2 \mid$ is plotted for systems of size $L = 20$ and $L = 200$ in Figs. 7.2-7.3, respectively, and for different values of the system size L in Fig. 7.4.

In order to study the behaviour of the dielectric constant as function of the system size L, χ_0 is plotted for $2 \mid t_1 - t_2 \mid = 0$ and for $2 \mid t_1 - t_2 \mid = 0.5$ in Figs. 7.5-7.6, respectively, and for different values of $2 \mid t_1 - t_2 \mid$ in Fig. 7.7.

As expected, at the half-filling case, the dielectric constant diverges for $t_1 = t_2$, i.e, in the conducting phase, while it remains finite for $t_1 \neq t_2$, i.e, in the insulating phase, decreasing down to zero as the difference between the hopping parameters increases up to infinity.

We evaluate now the charge stiffness for the dimerized model. One considers periodic boundary conditions in order to apply Kohn's method. For evaluting the charge stiffness, one applies an external magnetic field following Kohn's method and makes the Peierls substitution in the hopping parameters of the Hamiltonian (7.26): $t_1 \rightarrow e^{\pm i\Phi/L} t_1$ and $t_2 \rightarrow e^{\pm i\Phi/L} t_2$. The lower band of the one-particle spectrum becomes

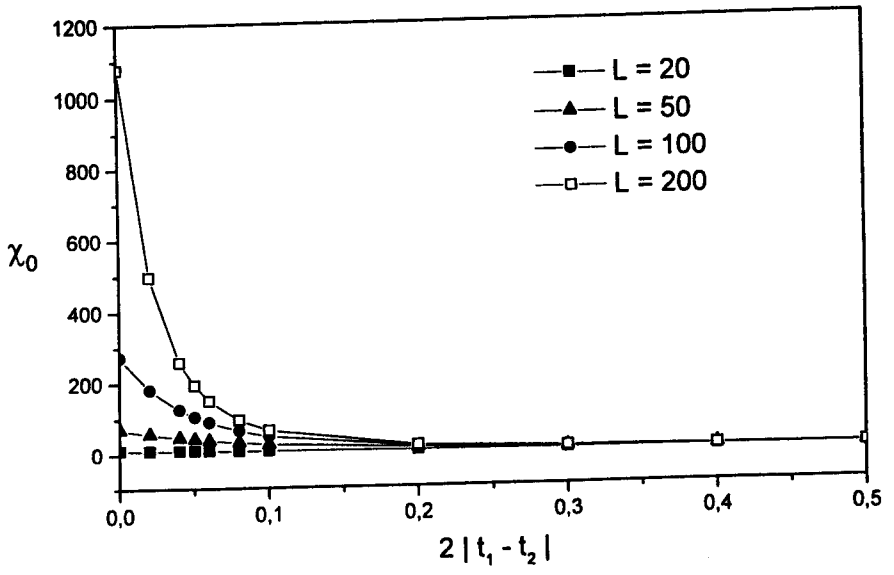

Figure 7.4: Dielectric constant (in arbitrary units) for the dimerized model (with $t_1 = 1$) as function of $2 \mid t_1 - t_2 \mid$ for different values of the system size L.

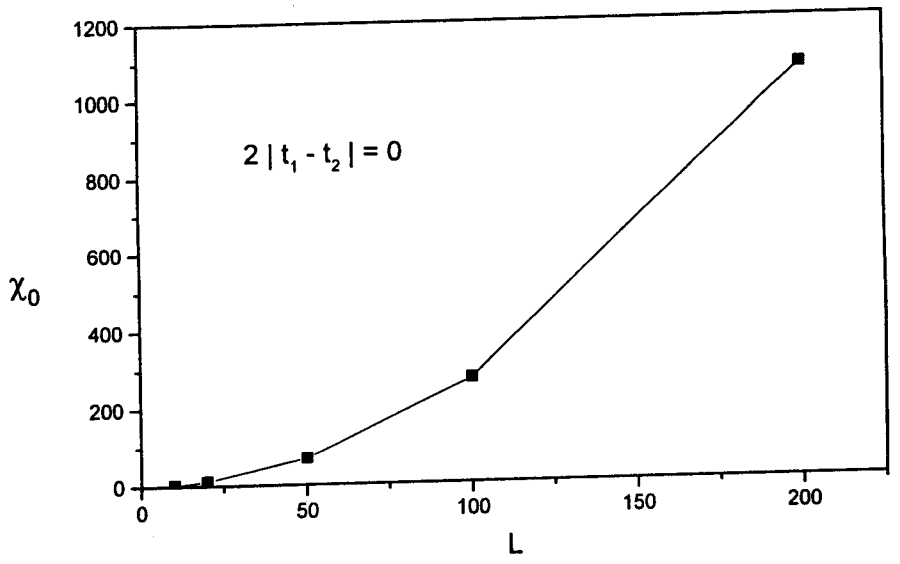

Figure 7.5: Dielectric constant (in arbitrary units) for the dimerized model (with $t_1 = 1$) as function of the system size L for $2 \mid t_1 - t_2 \mid = 0$.

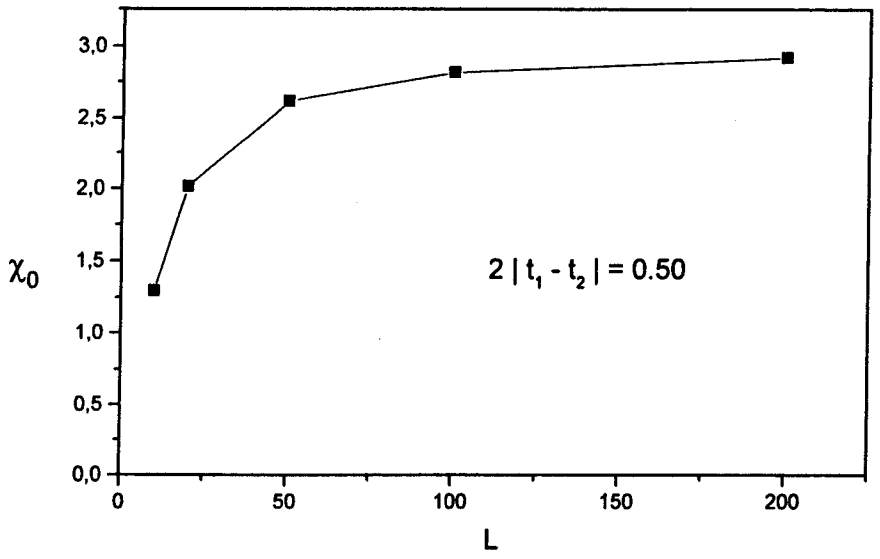

Figure 7.6: Dielectric constant (in arbitrary units) for the dimerized model (with $t_1 = 1$) as function of the system size L for $2 \mid t_1 - t_2 \mid = 0.5$.

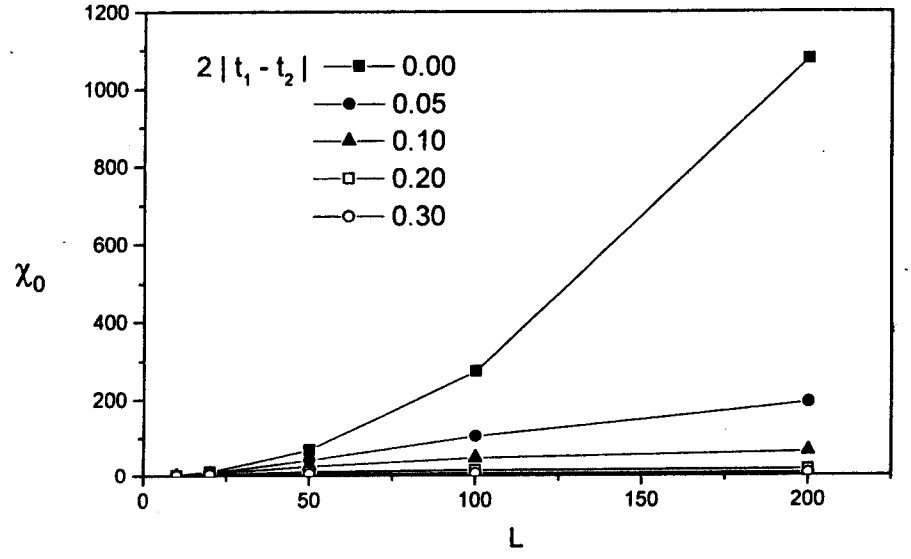

Figure 7.7: Dielectric constant (in arbitrary units) for the dimerized model (with $t_1 = 1$) as function of the system size L for different values of $2 \mid t_1 - t_2 \mid$.

$$\epsilon(k,\Phi) = -\sqrt{t_1^2 + t_2^2 + 2t_1 t_2 \cos\left(2(k+\Phi/L)\right)} \tag{7.30}$$

where a was considered the length unit. The charge stiffness as function of the electronic density is given by

$$\begin{aligned} D_c &= L \left.\frac{d^2 E_0(\Phi)}{d\Phi^2}\right|_{\Phi=0} \\ &= L \sum_{k\leq k_F,\sigma} \left.\frac{\partial^2 \epsilon(k,\Phi)}{\partial\Phi^2}\right|_{\Phi=0} \\ &= \frac{2L^2}{\pi}\int_0^{k_F} dk \left.\frac{\partial^2\epsilon(k,\Phi)}{\partial\Phi^2}\right|_{\Phi=0} \\ &= \frac{4}{\pi}\frac{t_1 t_2 \sin(n\pi)}{\sqrt{t_1^2+t_2^2+2t_1t_2\cos(n\pi)}} \end{aligned} \tag{7.31}$$

where k_F is the Fermi momentum and is given by $2k_F = n\pi$. Therefore, at half filling ($n = 1$), the charge stiffness is finite for $\Delta = 0$ ($t_1 = t_2$) and equals $D_c = 4t/\pi$, whereas $D_c = 0$ for $\Delta > 0$ ($t_1 \neq t_2$).

Thus, the $1D$ dimerized model at half filling has a conducting phase for $\Delta = 0$ characterized by a finite charge stiffness and for $\Delta > 0$ it has an insulating phase, which is characterized by a dielectric constant diverging for $\Delta_c \to 0$ and decreasing with increasing Δ.

Bibliography

[1] T. F. Rohsenbaum *et al.*, Phys. Rev. B **27**, 7509 (1983).

[2] D. Belitz, and T. R. Kirkpatrick, Rev. Mod. Phys. **66**, 261 (1994).

[3] R. Resta, M. Posternak, and A. Baldereschi, Phys. Rev. Lett. **70**, 1010 (1993).

[4] R. Resta, Rev. Mod. Phys. **66**, 899 (1994) and references therein.

[5] R. Resta, cond-mat/9802004 (1998).

[6] N. W. Ashcroft and N. Mermin, *Solid State Physics*, (Saunders College Publishing, Fort Worth, 1976).

[7] D. Pines and P. Nozières, *The Theory of Quantum Liquids: Normal Fermi Liquids*, (Addison-Wesley, Second Edition, 1989).

[8] G. D. Mahan, *Many Particle Physics*, (Plenum Press, New York, Second Edition, 1990).

[9] A. A. Abrikosov, L. P. Gorkov, and I. E. Dzyaloshinski, *Methods of Quantum Field Theory in Statistical Physics*, (Dover Publications, New York, 1975).

[10] W. Kohn, Phys. Rev. **133**, A171 (1964).

[11] A. Selloni, P. Carnevali, R. Car, and M. Parrinello, Phys. Rev. Lett. **59**, 823 (1987).

[12] A. L. Fetter and J. D. Walecka, *Quantum Theory of Many-Particle Systems*, (McGraw-Hill, New York, 1971).

Chapter 8

Conclusions

In this thesis we studied of the one-particle spectral and transport properties of the Hubbard model, by means of exact and variational methods. Our main motivations for these studies were, (i) the renewed interst on the one-electron spectral properties of quasi-one-dimensional materials [1, 2, 3, 4] and (ii) the general understanding of the metal-insulator transition mechanisms, which are particularly important for the theory of high-temperature superconductors [5, 6].

The use of the $SO(4)$ symmetry of the Hubbard model enabled us to demonstrate the absence of s-wave η-pairing superconductivity in the Hubbard model for a bipartite lattice in any dimension.

In this thesis we have also used the pseudoparticle picture developed in Ref. [7] to write down explicit expressions for the total of $2L + 4$ independent conservation laws. Moreover, we exhibited the utility of the conservation laws expressed in terms of the pseudoparticle operators by calculating, through a suitable multicomponent CFT, the critical exponents for the threshold behaviour of the one-electron spectral function at the UHB finite energies. Interestingly, we found a LL power-law behaviour for the density of states at the bottom edge of the UHB. This reveals that the low-energy LL behaviour also can appear around finite-energy edges.

The critical exponents were expressed in terms of conformal dimensions associated with GS - CRS transitions. The CRS's are generalized GS's which correspond to sub-canonical ensemble Hilbert subspaces, i.e. subspaces spanned by all the states of constant α, γ pseudoparticle charge and current numbers, $N_{\alpha,\gamma}$ and $J_{\alpha,\gamma}$, respectively, and α-Yang particle numbers, $\mathcal{N}_\alpha$. This set of states includes the CRS and the tower of states obtained from it by α, γ pseudoparticle-pseudohole processes. We emphasize that only for CRS's involving a small yet finite density of $\alpha, \gamma > 0$ pseudoparticles is the critical theory conformal invariant. On the other hand, the CFT's presented here refer to CRS's with both vanishing and finite α-Yang particles.

The low-energy multicomponent CFT's studied in this thesis refer to a quantum problem constructed by adding to the 1D Hubbard model "chemical poten-

tial" α, γ pseudoparticle charge conservation-law terms. Fortunately, the symmetries associated with these conservation laws allow the evaluation of finite-energy expressions for the 1D Hubbard model correlation functions from the corresponding low-energy expressions obtained from the multicomponent CFT's.

These CFT's are associated with the α, γ Virasoro algebras. The generators of these algebras were expressed in the pseudoparticle basis and obey the expected commutation relations. The complete critical theory is a product of the α, γ-occupied-band Virasoro algebras, all these algebras having conformal anomaly $C_{\alpha,\gamma} = 1$.

The multicomponent CFT's correspond to low-energies $(\omega - \omega_0)$ and small momenta $(k - k_0)$. Here ω_0 and k_0 are particular values of the 1D Hubbard model excitation energies and momenta which correspond to GS - CRS transitions. Therfore, for each CRS there is a energy ω_0 and a momentum k_0 value. We note that these CFT's were already known for CRS's with $\omega_0 = 0$ and k_0 finite or zero [8].

Our investigation on the one-electron spectral properties of the 1D Hubbard model included the effects of phase-space restrictions on the one-particle spectral function. Our study paid particular attention to zero magnetic field $H = 0$, electronic densities $o < n < 1$ and large U. As expected for a 1D interacting electronic system, we have found that the spectral function is completely incoherent. This incoherence follows, in part, from the fact that the one-electron spectral function involves the convolution of the holon and the spinon excitation bands. That function exhibits characteristic peaks, whose location in the (k, ω) space corresponds two lines. The shapes of these lines are directly determined by the shape of the holon and spinon bands. The associated divergences are controlled by matrix elements. As was observed for $U \rightarrow \infty$ [9], we found that there are two lines of holon peaks, i.e. there is a duplication of the holon band. Moreover, we have shown that this effect follows from two families of final states associated with the topological momentum shift mechanism. This disagrees with the shadow-band interpretation of Ref. [9].

In the case of the one-particle density of states our results confirm the LL behaviour, ω^{ν}, at the Fermi surface [10, 11, 12, 13, 14]. The non-universal exponent ν depends on the on-site Coulomb repulsion U, electronic density n and magnetic field H. In particular, we find at $H = 0$ that $\nu \rightarrow 1/8$ as $U \rightarrow \infty$, in agreement with previous theoretical results [15, 16, 17]. The supression of the density of states at the Fermi surface is observed in photoemission experiments for quasi-one dimensional conductors [18, 19, 20, 21, 22, 23].

Furthermore, we find a pseudo-gap between the LHB and the UHB, in agreement with previous numerical studies [24, 25]. This result was obtained from the study of the one-electron spectral weight distribution. The ω domains of the LHB and UHB were derived from the analysis of the transitions which originates these bands. Our approach allows us to evaluate the threshold behaviour at finite

energy $\omega_0 = 2\epsilon_F$, where we find again the power-law behaviour $(\omega - \omega_0)^\nu$. On the other hand, the critical theory introduced in Ref. [26] reveals that at $n = 1$ the UHB bottom edge shows, instead, a non-LL divergence [27].

Importantly, several recent analyses of the ARPES results mentioned in Chapter 1, agree with theoretical predictions based on the 1D Hubbard model in what the LHB is concerned [1, 2, 3, 4, 18]. Following the results presented in Ref. [27], our study extends these LHB analyses to the UHB. Thus, to complement the ARPES studies of Refs. [1, 2, 3, 4, 18], we propose inverse-photoemission studies, which can be directly compared with our theoretical predictions, including the occurrence of the pseudo-gap for densities away from half-filling. As future work, using our approach, we suggest the study of the spectral properties at finite magnetic fields.

In what concerns the transport properties, we have presented a variational study of the Hubbard model at half filling, by means of two types of wave functions. The first one was introduced many years ago by Gutzwiller (ψ_G) and describes a metallic phase (or rather, a zero-gap semiconductor). The second type of variational wave function (ψ_B) referred to the GS of the Heisenberg model and descibes an antiferromagnetic insulator. We have considered the Hubbard model in the 2D honeycomb lattice and both in the hypercubic and hyperdiamond lattices. We have obtained that for small U the first wave function has lower energy, whereas for large U the second wave function is prefered. Within this variational scheme a transition between a paramagnetic metal and an antiferromagnetic insulator occurs for $U \sim W$, where W is the band width.

The special value of U, in the limit of dimensions $D \to \infty$, found in this way should not be identified with the true metal-insulator transition. This is because the metallic phase close to this point is expected to be unstable with respect to a SDW. Therefore, the true transition will be shifted to lower values of U and assume the character of a Slater-type magnetic instability, presumably at $U = 0$ for the hypercubic lattice, but at a finite value of U for hyperdiamond. This band antiferromagnetism is expected to be stabilized with increasing U, whereas the antiferromagnetism in the insulating phase will be governed by the energy scale t^2/U. Therefore, we expect that the special value of U calculated here not only marks the crossover between a SDW and a Heisenberg antiferromagnet, but also corresponds to the point where the critical temperature has a maximum, and where at still higher temperatures a Mott transition between a paramagnetic metal and a non-magnetic insulator occurs. More refined variational calculations will be necessary to substantiate this conclusion.

We also analyzed the case of the half-filled honeycomb lattice. On the one hand, the Gutzwiller wave function, ψ_G, has lower energy at small U, whereas, on the other hand, the complementary insulating wave function, ψ_B, is preferred for large U. A mean-field treatment for both wave functions has allowed to estimate the critical value U_c forhe Mott-Hubbard transition, which reads $U_c \approx 5.3t$. Since

fluctuations are expected to be stronger for ψ_B than for ψ_G, we consider this value as an upper bound. We have also studied the magnetic instability of the Gutzwiller wave function and found a critical value $U_m \approx 3.7t$. The Gutzwiller ansatz appears to overestimate the tendency towards antiferromagnetism [29], and therefore we expect this value to be a lower bound for the appearance of antiferromagnetism. Therefore our results do not disagree with the possibility of a single transition where the opening of a charge gap due to the Mott phenomenon and the magnetic instability coincide. This would be in line with previous Monte Carlo simulations, which have been interpreted in terms of a single transition at $U_c = (4.5 \pm 0.5)t$ [30].

The present variational scheme predicts a first-order transition at U_c, in contradiction to the general belief that the Mott-Hubbard transition is of second-order [31]. This is not surprising, as the two wave functions, although exact in the limits $U \to 0$ and $U \to \infty$, are not very accurate at intermediate values of U. Therefore, the important question of the critical behaviour close to U_c requires other methods. Further studies of the "metallic" phase would also be worth being pursued, as strong deviations from simple FL behavior have been obtained by perturbative methods [32].

A quite general method to evaluate the dielectric susceptibilty for interacting eletronic was discussed. This constant is expected to be a good quantity to describe the insulating phase since it diverges at the metal-insulator transition. We have studied the 1D dimerized model and we have found that the Drude peak is non-zero in the conducting phase and zero in the insulating phase. As expected, the dielectric constant diverges at the metal-insulator transition.

As an overall conclusion, although the Hubbard model is formally a simple model, very rich physics can be extracted from it and it is a good starting point for the description of electronic correlations in a discrete lattice.

Bibliography

[1] C. Kim *et al.*, Phys. Rev. Lett. **77**, 4054 (1996).

[2] K. Kobayashi *et al.*, Phys. Rev. Lett. **80**, 3141 (1998).

[3] K. Kobayashi *et al.*, Phys. Rev. Lett. **82**, 803 (1999).

[4] J. D. Dendinger *et al.*, Phys. Rev. Lett. **82**, 2540 (1999).

[5] P. W. Anderson, in *Frontiers and Borderlines in Many-Particle Physics*, (edited by R. A. Broglia, and J. R. Schrieffer, North-Holland, Amsterdam, p. 1, 1988).

[6] E. Dagotto, Rev. Mod. Phys. **66**, 763 (1994).

[7] J. M. P. Carmelo and N. M. R. Peres, Phys. Rev. B **56**, 3717 (1997).

[8] W. Metzner and Carlo Di Castro. Phys. Rev. B **47**, 16107 (1993).

[9] K. Penc, K. Hallberg, F. Mila and H. Shiba, Phys. Rev. Lett. **77**, 1390 (1996).

[10] F. D. M. Haldane, J. Phys. C **14**, 2585 (1981).

[11] S. Tomonaga, Prog. Theor. Phys. **5**, 544 (1950).

[12] J. M. Luttinger, J. Math. Phys. (N.Y.) **4**, 1154 (1963).

[13] D. C. Mattis and E. Lieb, J. Math. Phys. (N.Y.) **6**, 304 (1965).

[14] J. Sólyom, Adv. Phys. **28**, 201 (1979).

[15] K. Penc, F. Mila and H. Shiba, Phys. Rev. Lett. **75**, 894 (1995).

[16] M. Ogata and H. Shiba, Phys. Rev. B **41**, 2326 (1990).

[17] M. Ogata, T. Sugiyama and H. Shiba, Phys. Rev. B **43**, 8401 (1991).

[18] B. Dardel *et al.*, Phys. Rev. Lett. **67**, 3144 (1991).

[19] Y. Hwu *et al.*, Phys. Rev. B **46**, 13624 (1992).

[20] B. Dardel *et al.*, Europhys. Lett. **19**, 525 (1992).

[21] C. Coluzza *et al.*, Phys. Rev. B **47**, 6625 (1993).

[22] B. Dardel *et al.*, Europhys. Lett. **24**, 687 (1993).

[23] M. Nakamura *et al.*, Phys. Rev. B **49**, 16191 (1994).

[24] R. Preuss *et al.*, Phys. Rev. Lett. **73**, 732 (1994).

[25] M. B. J. Meinders, H. Eskes and G. A. Sawatzky, Phys. Rev. B **48**, 3916 (1993).

[26] J. M. P. Carmelo, J. M. E. Guerra, J. M. B. Lopes dos Santos and A. H. Castro Neto, Phys. Rev. Lett. **83**, 3892 (1999).

[27] J. M. P. Carmelo, L. M. Martelo, T. Prosen and D. K. Campbell (submitted to Phys. Rev. Lett., 1999).

[28] J. M. P. Carmelo, J. M. E. Guerra and L. M. Martelo (preprint, 1999).

[29] E. Jeckelmann, and D. Baeriswyl, Synth. Met. **65**, 211 (1994).

[30] S. Sorella, and E. Tosatti, Europhys. Lett. **19**, 699 (1992).

[31] M. Imada, J. Phys. Soc. Japan **64**, 2954 (1995).

[32] J. González, F. Guinea, and M. A. H. Vozmediano, Phys. Rev. Lett. **77**, 3589 (1996).